Western Graduate&PostdoctoralStudies

Western University
Scholarship@Western

Electronic Thesis and Dissertation Repository

7-8-2020 10:30 AM

Regulation of Glucagon Secretion and Trafficking by Proteins in the Glucagon Interactome

Farzad Asadi Jomnani, *The University of Western Ontario*

Supervisor: Dhanvantari, Savita, *The University of Western Ontario*

A thesis submitted in partial fulfillment of the requirements for the Doctor of Philosophy degree in Pathology and Laboratory Medicine

© Farzad Asadi Jomnani 2020

Follow this and additional works at: https://ir.lib.uwo.ca/etd

Part of the Diseases Commons

Recommended Citation

Asadi Jomnani, Farzad, "Regulation of Glucagon Secretion and Trafficking by Proteins in the Glucagon Interactome" (2020). *Electronic Thesis and Dissertation Repository*. 7074.
https://ir.lib.uwo.ca/etd/7074

This Dissertation/Thesis is brought to you for free and open access by Scholarship@Western. It has been accepted for inclusion in Electronic Thesis and Dissertation Repository by an authorized administrator of Scholarship@Western. For more information, please contact wlswadmin@uwo.ca.

Abstract

Patients with diabetes exhibit hyperglucagonemia, or excess glucagon secretion. The glucagonocentric hypothesis of diabetes states that hyperglucagonemia, rather than hypoinsulinemia, may be the underlying mechanism of hyperglycemia of diabetes. Thus, uncovering mechanisms that regulate glucagon secretion from pancreatic α-cells is crucial for developing treatments for hyperglycemia. One clue to the regulation of glucagon secretion may lie in the proteins that interact with glucagon in α-cell's secretory pathway, primarily within the secretory granule. The purpose of my work was to identify proteins that interact with glucagon within the secretory granule and characterize a candidate protein within this network that regulates the intracellular trafficking of glucagon to control its secretion.

To identify secretory granule proteins that interact with glucagon, I purified secretory granules from α-TC1-6 cells. I then used affinity purification using tagged glucagon to isolate protein complexes that interact with glucagon, and identified these proteins through liquid chromatography/mass spectrometry. In this way, I identified a glucagon "interactome" within the α-cell secretory granule. I found that components of the interactome changed in response to different glucose concentrations, and to treatment with the paracrine inhibitors insulin and GABA.

Next, I characterized the function of one interactome protein, the neuronal cytoskeletal protein stathmin-2, in glucagon secretion. Through overexpression and siRNA-mediated silencing of stathmin-2 in α-TC1-6 cells, I showed that stathmin-2 is a tonic inhibitor of glucagon secretion. Using confocal high-resolution immunofluorescence microscopy, I found that stathmin-2 exerts its regulatory role by trafficking of glucagon to the endolysosomal system.

Finally, I examined how the trafficking role of stathmin-2 is altered in the hyperglucagonemia of diabetes. Using isolated islets from a mouse model of diabetes, I showed that the increase in cellular glucagon was accompanied by a reduction in stathmin-2 levels. Confocal microscopy analysis indicated that, in diabetes, there is a switch from the anterograde trafficking of glucagon towards the lysosome to retrograde

trafficking towards secretory granules, possibility mediated by the endosomal protein Rab7.

In summary, my thesis describes the discovery of a regulatory mechanism for glucagon secretion from α-cells that may operate in hyperglucagonemia. These findings have clinical application for treatment of hyperglycemia of diabetes.

Keywords

Keywords: glucagon, secretory granule, glucagon secretion. proteomics, stathmin-2, diabetes, endolysosome

Summary for Lay Audience

People with diabetes have an abnormal amount of a hormone called “glucagon” in their blood, which seriously increases blood sugar. Glucagon is released from a cell called “alpha cell”, which is in the gland of the pancreas. My research was to discover some proteins within a special structure in alpha cells called “secretory granule” that control the release of glucagon. I found that the type and numbers of proteins within the secretory granule changed when I exposed alpha cells to suppressors of glucagon secretion (insulin or GABA). This would mean that those proteins are candidates for decreasing glucagon secretion (stathmin-2 being one of the proteins). I found that both glucagon and stathmin-2 are located within the secretory granule of a mouse’s pancreas in a close distance from each other. By using a genetic technique, I removed stathmin-2 from the alpha cell and found that cells released a lot of glucagon. On the other hand, when alpha cells produced a lot of stathmin-2, they did not secrete glucagon. There is a structure within alpha cells called “endolysosome”. I found that when there is a lot of stathmin-2 within the alpha cell, it directs glucagon into the endolysosome, where it is destroyed. However, when there is a lack of stathmin-2 in alpha cells, glucagon is not destroyed in the endolysosome. These mean that stathmin-2 controls glucagon secretion through endolysosome. I then proposed that, in diabetes, glucagon is not destroyed in the endolysosome. This is the reason for high glucagon secretion from the pancreas. To test this idea, I found that, in diabetic mice, there was very little stathmin-2 versus lots of glucagon in its pancreas. Then, by using advanced microscopic studies, I found that both glucagon and stathmin-2 were not destroyed in the endolysosome of alpha cells in the diabetic mouse. I found that stathmin-2 collected into a structure called “late endosome”, and at the same time, alpha cells showed an increase in glucagon secretion. Therefore, stathmin-2 is a novel molecule that can control glucagon secretion. In future studies, it could be used to decrease high blood sugar in people with diabetes.

Acknowledgments

To my supervisor, Dr. Savita Dhanvantari, I would like to express my sincere gratitude for your continuous support, advice, encouragement, and immense knowledge for conducting this hot-topic project. Your guidance, critical thoughts, and constructive criticism have been always tremendous sources of advice for me to learn the concept of this novel project. I had very pleasant academic journey at your lab to conduct the experiments by using advanced imaging and molecular techniques. I enjoyed the great privilege of working in a scientific and friendly environment with a united research team. Your guidance, help and support opened many doors for me.

I would like to thank my advisory committee members: Dr. Chandan Chakraborty who has been always a great scientific source when I had questions and a priceless support for my scientific progress, Dr. Rennian Wang for her tremendous knowledge and endless scientific support on interpretation of findings, logical thinking of results and providing many feedback, insightful discussions and suggestions, which have been absolutely invaluable, and Dr. Jimmy Dikeakos for his deep knowledge, and providing very helpful comments.

To Dr. Edith Arany, thank you for your help, support, positive attitude and letting me to have a memorable collaboration with your lab.

I acknowledge our former chair of program, Dr. Chandan Chakraborty, and current chair, Dr. Zia Khan, for their positive attitude, providing a unique environment through weekly presentation, and being always ready to help.

To my labmates, Rebecca, Maya, and Ahmed, it rocks that I have such friends, thank you for being very kind friends, and having a very close friendship, which will absolutely stay forever.

Thanks to the students who worked with our lab, Derek, Nabeel, Tina, Alissa, Nithin, and Melissa; your good relationship made a warm environment to work well and having amazing productive time.

I am very grateful to my friends Brenda Strutt and Sandra Katherine Szlapinski at Lawson Health Research Institute for her help and bringing positive energy every day.

I would like to express my gratitude to Tracey Koning, at Department of Pathology, for her positive attitude and all provided help and supports.

I am very grateful to Susan Underhill for her help and assist in organizing thesis exam.

To all individuals at Department of Pathology and Laboratory Medicine and Lawson Health Research Institute, thank you for making a pleasant and memorable time.

Thanks to financial supporters of my project: Natural Sciences and Engineering Research Council of Canada (NSERC), The Ontario Graduate Scholarship (OGS), Dean's Award-Schulich School of Medicine & Dentistry, Western University, Dr. Frederick Winnett Luney Graduate Scholarship, Lawson Health Research Institute, and collaborative program on Molecular Imaging.

To my Parents, thank you for your all support and encouragement, it has been always a tremendous motivation for me.

To my family, Parvaneh and Katayoun, I would like to express my heartful thanks for your patience, continuous support and providing a warm and lovely family environment, I love you!

List of Abbreviations

ACC, acetyl-CoA carboxylase

ACO2, aconitate hydratase, mitochondrial

AMPA, α-amino-3-hydroxy-5-methyl-4-isoxazolepropionic acid

AMPK, 5' AMP-activated protein kinase

ARFGEF2, Brefeldin A-inhibited guanine nucleotide-exchange protein 2

ARFRP1, ADP-ribosylation factor-related protein 1

AT2, alpha-tubulin 2

ATP5F1A, ATP synthase F1 subunit alpha

ATP6V0C, V-type proton ATPase 16 kDa proteolipid subunit

BAT, brown adipose tissue

BIG3, Brefeldin A-inhibited guanine nucleotide exchange protein 3

BSA, bovine serum albumin

BSA, bovine serum albumin

BSN, Bassoon

cAMP, adenosine 3',5'-cyclic monophosphate

CD63, CD63 antigen

ChgA, chromogranin A

ChgB, chromogranin B

CPE, carboxypeptidase E

CRAC, Ca^{2+}-release-activated channel

CREB, cAMP response element-binding (CREB) protein

Cys, cysteine

Ddit3, DNA damage-inducible transcript 3 protein

DMEM, Dulbecco's modified eagle's medium

DTT, dithiothreitol

EEA1, early endosome antigen 1

EGFP, enhanced green fluorescent protein

Epac, exchange proteins activated directly by cyclic AMP

EPS, extracellular polysaccharides

ER, endoplasmic reticulum

ERC1, ELKS/Rab6-interacting/CAST family member 1

ERK, extracellular-signal-regulated kinase

EXO1, exonuclease 1

FAM20C, extracellular serine/threonine protein kinase FAM20C

Fc, crystalizable fragment

FFAR, free fatty acid receptor

FGF21, Fibroblast Growth Factor 21

FITC, fluorescein isothiocyanate

FoxA2, forkhead transcription factor A2

FXYD2, FXYD domain-containing ion transport regulator 2

GABA, gamma-aminobutyric acid

GCG, glucagon

Gcgr, glucagon receptor

$Gcgr^{-/-}$, glucagon receptor null (mouse)

GFP, green fluorescent protein

GIP, glucose-dependent insulinotropic factor (gastric inhibitory polypeptide)

GIRK, G-protein coupled inwardly rectifying K^+

GLP-1, glucagon-like peptide 1

GLP-2, glucagon-like peptide 2

GLUT, glucose transporter

GRP78, 78-kDa glucose-regulated protein

GRPP, glicentin-related polypeptide

HBSS, Hank's buffered salt solution

HFD, high-fat diet

HG, high glucose

HM13, minor histocompatibility antigen H13

HRP, horseradish peroxidase

Hspa5, heat shock protein a5 (Endoplasmic reticulum chaperone Bip)

IgG, immunoglobulin G

INS, insulin

IP-1, intervening peptide 1

IP-2, intervening peptide 2

$K\text{-}_{ATP}$, ATP-sensitive K^+-channel

KCIP-1, 14-3-3 protein zeta/delta

KD, knocked down

Ki-67, Proliferation marker protein Ki-67

KRB, Krebs-Ringer buffer

LALS, large angle light scattering

Lamp2A, Lysosome-associated membrane protein 2

LC-MS/MS, liquid chromatography–mass spectrometry

LG, low glucose

M6PR, mannose-6-phosphate receptor

MAP2, microtubule-associated protein 2

MDH1, malate dehydrogenase 1

MEM, minimal essential medium

METAP2, methionine aminopeptidase 2

MIA3, transport and Golgi organization protein 1 homolog

MPGF, major proglucagon-derived fragment

mTORC1, mammalian target of rapamycin-1

MYH9, myosin-9

NA, numerical aperture

NENF, neudesin

NMDA, N-methyl-D-aspartate

NOD mouse, Non-obese diabetic mouse

OE, overexpressed

OXM, oxyntomodulin

PAIP2B, polyadenylate-binding protein-interacting protein 2B

PAM, peptidylglycine alpha-amidating monooxygenase

PC, phosphatidylcholine

PC1/3, prohormone convertase 1/3

PC2, prohormone convertase 2

PCC, Pearson's correlation coefficient

PCL0, polycomb protein Pcl

PCLO, Piccolo

PCR, polymerase chain reaction

PCSK2, proprotein convertase subtilisin/kexin type 2

PDI, protein disulfide-isomerase

PEPCK, phosphoenolpyruvate carboxykinase

PFA, paraformaldehyde

PGDP, proglucagon-derived peptide

PGP, glycerol-3-phosphate phosphatase

PI, phosphatidylinositol

PKA, protein kinase A

PKM, pyruvate kinase PKM

PMSF, phenylmethylsulfonyl fluoride

PNS, post-nuclear supernatant

POMC, pro-opiomelanocortin

PPAR-α, peroxisome proliferator-activated receptor-α

PPG, pre-proglucagon

PPP1R13B, apoptosis-stimulating of p53 protein 1

PRD, Proline rich domain

PRDX2, peroxiredoxin-2

PROM1, prominin-1

proSAAS, proprotein convertase subtilisin/kexin type 1 inhibitor

PVDF membrane, polyvinylidene fluoride membrane

Rab, Ras-related protein (such as Rab3, Rab7, Rab11)

RER, rough endoplasmic reticulum

RILP, Rab7 interacting lysosomal protein

RIMS, regulating synaptic membrane exocytosis protein

RIPA buffer, Radioimmunoprecipitation assay buffer

ROI, region of interest

RP, reserve pool

RPH3a1, Rabphilin-3A

RRP, readily releasable pool

SALS, small angle light scattering

SAR1B, GTP-binding protein SAR1b

SCFD1, Sec1 family domain-containing protein 1

SCG10, Superior cervical ganglion-10 protein

SDS-PAGE, sodium dodecyl sulfate polyacrylamide gel electrophoresis

Sec22b, vesicle-trafficking protein SEC22b

SERCA, sarcoendoplasmic reticulum calcium transport ATPase

SET, Protein SET

SG, secretory granule

SgII, secretogranin II

SGLT, sodium-dependent glucose transporter (such as SGLT1, SGLT2)

SgVII, secretogranin VII

siRNA, small interfering RNA

Slc30A/ZnT8, solute carrier 30 (A)/ zinc transporter (8)

SLD, stathmin-like domain

SLDN, N-terminal region of SLD

SNAP, soluble NSF attachment protein

SNARE, Soluble N–ethylmaleimide sensitive factor (NSF) attachment protein receptor

SOC, store-operated current

SST, somatostatin

SSTR2, somatostatin receptor 2

STIM1, stromal interaction molecule 1

Stmn1, stathmin-1

Stmn2, stathmin-2

STX, syntaxin-4

STZ, Streptozotocin

SYT, Synaptotagmin

SYTL5, synaptotagmin-like protein 5, SYTL5

T1D, type 1 diabetes mellitus

T2D, type 2 diabetes mellitus

TBR, tubulin binding repeats

TBS-T, tris-buffered saline-Tween 20

TEM, transmission electron microscopy

TGN, trans-Golgi network

TM9SF3, transmembrane 9 superfamily member 3

TMEM24, transmembrane protein 24

TOMM22, mitochondrial import receptor subunit TOM22 homolog

UCP1, uncoupler protein 1

VAMP2, vesicle-associated membrane protein-2

VAMP4, vesicle-associated membrane protein-4

VDCC, voltage-dependent Ca^{2+} channels

VGLUT2, vesicular glutamate transporter 2

VPS45, Vacuolar protein sorting-associated protein 45

VTI1B, Vesicle transport through interaction with t-SNAREs homolog 1B

WT, wild-type

α-COP, coatomer subunit alpha

1Xbp1, X-box-binding protein

5-HT_{1f} R, 5-hydroxytryptamine (1f) receptor

Table of Contents

Abstract i

Summary for Lay Audience iii

Acknowledgments iv

List of Abbreviations vi

Table of Contents xv

List of Tables xxi

List of Figures xxii

Chapter 1 1

1.1 Introduction 1

1.2 Glucagon and its general function in metabolism 2

1.2.1 Glucagon and glucose metabolism 2

1.2.2 Glucagon and lipid metabolism 3

1.2.3 Glucagon and metabolism of protein and amino acids 4

1.2.4 Glucagon and energy metabolism 5

1.3 The glucagonocentric hypothesis of diabetes 6

1.4 Understanding the mechanisms and consequences of hyperglucagonemia 8

1.4.1 Intrinsic mechanism of glucagon secretion 8

1.5 Paracrine and autocrine regulation of glucagon secretion 11

1.5.1 Released factors from β-cells 11

1.5.2 Released factors from α-cells 14

1.5.3 Released factors from δ-cells 15

1.5.4 Cross-talk among β and δ and α-cells and glucagon secretion 16

1.6 Chronic inflammation and diabetes 18

1.7 GLP-1: Intra-islet or intestinal? 19

1.8 Biogenesis of the regulated secretory pathway 21
1.8.1 Molecular mechanisms of sorting glucagon into secretory granule 21
1.8.2 Secretory granule exocytosis 24
1.8.3 Diabetes and alterations in dynamics of secretory granules 27
1.9 Pancreatic islet protein reference map 27
1.9.1 Islet proteomics and glucagon secretion 28
1.9.2 The state-of-the-art secretory granule proteomics 30
1.10 Endolysosomal system of islet cells in diabetic condition 31
1.10.1 Alterations in endolysosmal enzyme activities in islet cells 32
1.10.2 Degradation of glucagon in endolysosomal system 32
1.11 Aims and rationale of the study 33
1.12 References 34
Chapter 2 56
2. Plasticity in the Glucagon Interactome Reveals Novel Proteins that Regulate Glucagon Secretion in α-TC1-6 Cells 56
2.1 Abstract 57
2.2 Introduction 58
2.3 Materials and methods 59
2.3.1 Gene construct and plasmid preparation 59
2.3.2 Extraction and enrichment of secretory granules 60
2.3.3 Immunoblotting for organelle-specific markers 61
2.3.4 Nanoscale flow cytometry 61
2.3.5 Proteomic analysis of secretory granule proteins associated with glucagon 62
2.3.6 Immunoprecipitation-immunoblotting of proteins associated with glucagon 64

2.3.7 Histone H4 assay 64
2.3.8 Immunofluorescence microscopy 64
2.3.9 siRNA-mediated depletion of targeted proteins 65
2.3.10 Glucagon measurement 66
2.3.11 Glucagon secretion and cell glucagon content in response to nutritional and paracrine effectors 66
2.3.12 Statistical analysis 67
2.4 Results 67
2.4.1 Secretory granule enrichment 67
2.4.2 Confirmation of the enriched secretory granules 67
2.4.3 Proteomic analysis of proteins that are associated with glucagon within α-cell secretory granules 68
2.4.4 GRP78 interacts with glucagon and co-localizes to glucagon-positive secretory granules 69
2.4.5 GABA induces histone H4 interaction and co-localization with glucagon 71
2.4.6 The glucagon interactome changes in response to glucose, GABA and insulin 73
2.4.7 The dynamic glucagon interactome reveals novel proteins that regulate glucagon secretion 79
2.4.8 Alterations in glucagon secretion and cell glucagon content in response to nutritional and paracrine effectors 81
2.5 Discussion 82
2.6 References 88
2.7 Supplementary Figures 96
2.8 Supplementary Tables 101
Chapter 3 123
3. Stathmin-2 Mediates Glucagon Secretion from Pancreatic α-cells 123

3.1 Abstract 124

3.2 Introduction 125

3.3 Materials and methods 126

3.3.1 Cell culture 126

3.3.2 Gene construct and plasmid preparation 127

3.3.3 Gene silencing experiments 127

3.3.4 Immunoblotting 128

3.3.5 Immunofluorescence confocal microscopy 129

3.3.6 Immunoelectron microscopy 131

3.3.7 Primary islet culture 132

3.3.8 Statistical analysis 133

3.4 Results 133

3.4.1 Stathmin-2 localizes to the α-cell secretory pathway in mouse pancreatic islets 136

3.4.2 Effects of depletion and overexpression of Stmn2 on glucagon secretion 140

3.4.3 Stmn2 directs glucagon into early endosomes 142

3.4.4 Stmn2 overexpression increases glucagon presence in the late endosome/lysosome compartment 144

3.5 Discussion 146

3.6 References 152

Chapter 4 159

4. Mediation of Glucagon Trafficking from the Endolysosomal System Towards the Secretory Pathway by Stathmin-2 in Diabetic α-Cells 159

4.1 Abstract 160

4.2 Introduction 162

4.3 Materials and methods 164

4.3.1 Animals 164

4.3.2 Preparation of pancreas tissue sections for confocal immunofluorescence 165

4.3.3 Double immunogold labeling transmission electron microscopy 166

4.3.4 Proglucagon and stathmin-2 gene expression 167

4.3.5 Primary islet culture 168

4.4 Results 170

4.4.1 Induction of diabetes in C57BL/6 mice 170

4.4.2 Glucagon and Stmn2 co-localize in islets of diabetic and non-diabetic mice 171

4.4.3 STZ-induced diabetes increases glucagon levels and reduces Stmn2 levels in α-cells 174

4.4.4 Both glucagon and Stmn2 are localized within secretory granules of α-cells 177

4.4.5 Arginine stimulates parallel increases in glucagon and Stmn2 secretion 179

4.4.6 Trafficking of glucagon and Stmn2 to the lysosome is inhibited in islets from STZ-induced diabetic mice: 180

4.4.7 STZ-induced diabetes increased the localization of Stmn2 in late endosomes 183

4.4.8 Glucagon and Stmn2 do not localize within the early endosome 188

4.4.9 Glucagon is not present in recycling endosome 190

4.5 Discussion 196

4.6 References 200

Chapter 5 208

5. Discussion and Future Directions 208

5.1 Glucagon interactome in secretory granules of α-cells and its plasticity 208

5.2 Stmn2 modulates glucagon secretion through the endolysosomal system in non-diabetic α-cells 214

5.3 Stmn2 plays a role in glucagon hypersecretion through intracellular glucagon trafficking towards endolysosomal system in diabetic α-cells 216

5.4 Summary 217

5.5 Future Directions 219

5.6 References 220

6. Appendices 228

7. Curriculum Vitae 229

List of Tables

Table 2-1. A- Sub-groups of proteins categorized as “structural molecules” in the glucagon interactome under conditions of 25 mM glucose. 77

Table 2-2. B - Sub-groups of proteins categorized as “structural molecules” in the glucagon interactome under conditions of 5.5 mM glucose. 79

List of Figures

Figure 1-1. V-shape curve of glucagon secretion in response to glucose in dispersed human non-diabetic α-cells (black line)..... 9

Figure 1-2. Glucagon secretion from intact mouse islets. 10

Figure 1-3. Cross-talk among α, β, and δ-cells towards inhibition of glucagon secretion 17

Figure 1-4. Cleavage processing of proglucagon in α-cells..... 23

Figure 1-5. Kinetic model for trafficking of secretory granules in α-cells. 26

Figure 2-1. The glucagon interactome in secretory granules of α-TC1-6 cells. 69

Figure 2-2. Glucagon and GRP78 directly interact and are localized within secretory granules in α-TC1-6 cells..... 71

Figure 2-3. GABA induces direct interaction between glucagon and histone H4 within secretory granules in α-TC1-6 cells. 73

Figure 2-4. The glucagon interactome is altered in response to paracrine effectors in 25 mM glucose..... 74

Figure 2-5. The glucagon interactome is altered in response to paracrine effectors in 5.5 mM glucose. 76

Figure 2-6. Glucagon secretion and cell content are regulated by a subset of interactome proteins..... 81

Figure 3-1. Stathmin-2 localizes to secretory granules in α-TC1-6 cells. 136

Figure 3-2. Stathmin-2 is present in α-cells, but not β-cells, in murine pancreatic islets. 137

Figure 3-3. Glucagon and Stmn2 are present within secretory granules of pancreatic α-cells. 139

Figure 3-4. Silencing Stathmin-2 increased glucagon secretion and overexpression of stathmin-2 suppressed glucagon secretion in α-TC1-6 cells. 141

Figure 3-5. Stathmin-2 modulates glucagon trafficking through early endosomes..... 143

Figure 3-6. Overexpression of Stathmin-2 increases the presence of glucagon in late endosomes..... 145

Figure 3-7. Proposed pathways by which stathmin-2 modulates glucagon secretion from α-TC1-6 cells. ……150

Figure 4-1. Streptozotocin (STZ) induced diabetes in C57BL/6 mice.. 170

Figure 4-2. Stathmin-2 colocalizes with glucagon but not insulin in both non-diabetic and STZ-induced diabetic mice. 172

Figure 4-3. Imbalanced ratios of stathmin-2 and glucagon in islets of STZ-induced diabetic mice.. 176

Figure 4-4. Expression of Stmn2 and Gcg mRNA levels were determined in islets of non-diabetic (n=4) and diabetic (n=4) mice by RT-qPCR.. 177

Figure 4-5. The presence of stathmin-2 and glucagon within secretory granules of α-cells. 178

Figure 4-6. Parallel alterations in secretion of glucagon and Stmn2 from α-cells in both non-diabetic and diabetic mice. 180

Figure 4-7. The localization of Stmn2 and glucagon in lysosomes of α-cells is inhibited in diabetes.. 183

Figure 4-8. Diabetes enhanced colocalization of Stmn2 with late endosome in α-cells. 187

Figure 4-9. Glucagon and stathmin-2 are not localized in early endosomes in α-cells. . 190

Figure 4-10. Glucagon is not localized in recycling endosome of α-cells. ± SEM. Each dot represents a mean of 9-15 images per mouse. 195

Figure 5-1. Predicted proteins in the first shell of interacting proteins with glucagon within the glucagon interactome.. 211

Figure 5-2. Schematic structure of Stmn2 in comparison with other members of the stathmin family.. 215

Figure 5-3. Rab7 mediates late endosomal cargos towards lysosome (for degradation) or plasma membrane (for secretion)..... 217

Figure 5-4. Late endosomal re-routing of glucagon and Stmn2 from lysosome towards secretory pathway in diabetic α-cells.. 219

List of Supplementary Figures

Supplementary Figure 2-1. Proglucagon gene knock down in α-TC1-6 cells ……..96

Supplementary Figure 2-2. Immunoblotting assessment of enrichment in the extracted secretory granules. ……97

Supplementary Figure 2-3. Nano-scale flow cytometry of the enriched secretory granules ……..…… 98

Supplementary Figure 2-4. siRNA mediated gene silencing of target proteins in the secretory granules. ……...…….99

Supplementary Figure 2-5. Alterations in glucagon secretion and cell glucagon content of α-TC1-6 cells in response to nutritional and paracrine effectors…….100

List of Supplementary Tables

Supplementary Table 2-1. Reagents and resources……....101

Supplementary Table 2-2. List of proteins that interact the with Fc segment alone under conditions of 25 mM glucose…….…….109

Supplementary Table 2-3. List of proteins that interact the with Fc segment alone under conditions of 5.5 mM glucose……..……111

Supplementary Table 2-4. Profile of the histone, cytoskeletal and ribosomal proteins contained within the glucagon interactome when α-TC1-6 cells were incubated for 24h in media containing 25 mM or 5.5 mM glucose……..……112

Supplementary Table 2-5. Profile of the histone, cytoskeletal and ribosomal proteins within the glucagon interactome of α-TC1-6 in media containing 25 mM glucose……114

Supplementary Table 2-6. Profile of the histone, cytoskeletal and ribosomal proteins within the glucagon interactome of α-TC1-6 in media containing 5.5 mM……117

Supplementary Table 2-7. Functional categories of the proteins within the glucagon interactome in the context of 25 mM glucose. ……..…….120

Supplementary Table 2-8. Functional categories of proteins within the glucagon interactome in the context of 5.5 mM glucose. ……...……121

Chapter 1

1.1 Introduction

Diabetes as a widespread disease affects around half a billion people worldwide and is mainly categorized to type 1 and type 2 diabetes (1). Based on World Health Organization projections, diabetes will be affecting around 2 billion people by 2040, which would have a severe impact on global health. According to the Public Health Agency of Canada (www.canada.ca/en/public-health), diabetes affected 3.4 million Canadians in 2015 (9.3% of the population). Based on this report, the prevalence was 1 in 300 for younger people (≤ 19 years old) and 1 in 10 for those over 20 years of age. The prevalence of diabetes in Canada is predicted to grow to 5 million (12.1% of the population) by 2025, a 44% increase compared to 2015 (2).

The β-cell of pancreatic islet secretes insulin, which reduces high blood glucose levels and the α-cell secretes glucagon that counteracts insulin actions and increases blood glucose levels. Thus, euglycemia is achieved when there is a fine balance between functions of these two hormones. However, diabetes disrupts this balance, resulting in fasting hyperglycemia that is characteristic of diabetes (3–5). Preclinical and clinical findings in all diabetic models and clinical cases of diabetes also show a level of hyperglucagonemia, even in well-controlled diabetes (6). In particular, people with type 2 diabetes have fasting hyperglucagonemia and defects in postprandial glucagon suppression (4). This hyperglucagonemia exacerbates the pathological consequences of diabetes such as hyperglycemia, hyperaminoacidemia, obesity, and cardiovascular diseases. Therefore, the impact of consistent hyperglucagonemia in diabetes has brought up questions up on how hyperglucagonemia exacerbates the pathophysiology of diabetes, and the development of potential pharmacological interventions targeting hyperglucagonemia for the treatment of diabetes (4,7). Uncovering the molecular mechanisms of glucagon secretion and action as the key to understanding the pathogenesis of hyperglucagonemia has been a relatively recent focus in diabetes

research. In fact, some recent findings have suggested that glucagon secretion should also be a main target for the treatment of diabetes(4,8).

In this Introduction, I have first described the physiological actions of glucagon. I then discuss the role of glucagon in the development and pathophysiology of diabetes. I have specifically focused on hyperglucagonemia as the underlying mechanism of hyperglycemia in diabetes. I have reviewed the current literature on the cellular pathways governing normal and abnormal glucagon secretion, and emphasized what the latest proteomic studies have revealed on the alterations in the α-cell secretory pathway in relation to diabetes. This provided a rationale for my study to interrogate a protein within the secretory granule, which regulate glucagon secretion.

1.2 Glucagon and its general function in metabolism

Glucagon, a 29 amino acid peptide, is a product of the post-translational processing of proglucagon by the enzyme prohormone convertase 2 (PC2) within the secretory pathway of pancreatic α-cells(9–11). Glucagon is then stored within secretory granules and secreted in response to nutritional, hormonal and neural factors. It is the major glucose counter-regulatory hormone, and also functions in lipid and protein metabolism and energy expenditure. In a general view, glucagon increases hepatic gluconeogenesis and glycogenolysis and by this means regulates glycemia. In terms of lipid metabolism, it increases lipolysis and ketogenesis. Regarding protein metabolism, it increases both ureagenesis and uptake of amino acids by the liver. In addition, by reducing the level of food intake and increasing energy expenditure it participates in energy metabolism (12).

1.2.1 Glucagon and glucose metabolism

Glucagon is the major glucose counter-regulatory hormone. In healthy individuals, following an overnight fast, blood glucose levels fall to 3.8 mmol/L, which potently stimulates glucagon secretion to increase blood glucose level towards its normal range (4-5.4 mol/L). Then, when blood glucose levels reach above the normal level, glucagon secretion will be suppressed (13–15). Glucagon exerts it actions by binding to the glucagon receptor, a class B seven- transmembrane G-protein coupled receptor that is highly expressed in the liver. It is also present in the central nervous system, kidney,

gastrointestinal tract and pancreas. Following the binding of glucagon with its receptor, it triggers Gαs-coupled proteins, which activates downstream adenylate cyclase, and production of cAMP. The increased level of cAMP activates both protein kinase A (PKA) and cAMP response element-binding (CREB) protein. CREB enhances gluconeogenesis through increasing transcription of both glucose 6-phosphatase and phosphoenolpyruvate carboxykinase (PEPCK). At the same time, PKA activates fructose 2, 6-bisphosphatease and inactivates phospho-fructokinase 2, increasing levels of fructose 6-phosphate and potentiation of gluconeogenesis and suppression of glycolysis. PKA also increases fructose 1,6-bisphosphate and decreases pyruvate levels, which consequently suppresses glycolysis. In addition, PKA activates phosphorylase kinase that results in glycogenolysis and improved levels of glucose 1-phosphate and simultaneously suppression of glycogen synthase (16).

However, in the absence of glucagon action, the counter-regulation of glucose metabolism still occurs. Inducing glucagon deficiency by either blocking glucagon action through anti-glucagon antibodies or deleting the glucagon receptor in mice did not result in hypoglycemia. In the absence of glucagon, glucose counter-regulation can occur through the glucocorticoid hormone cortisol, (17), and through the actions of the catecholamines, norepinephrine and epinephrine (18,19).Taken together, all of these hormones target the liver to release glucose, with catecholamines, especially epinephrine, playing a redundant role in glucose counter-regulation(19).

1.2.2 Glucagon and lipid metabolism

In hepatocytes, glucagon reduces hepatic fatty acid biosynthesis and simultaneously increases fatty acid oxidation. Glucagon receptor signaling through cAMP results in inhibition of acetyl-CoA carboxylase (ACC), prevention of malonyl-CoA formation and suppression of fatty acid biosynthesis; 2) increases the AMP/ATP ratio, which activates 5' AMP-activated protein kinase (AMPK), inhibits ACC and suppresses fatty acid biosynthesis and enhancing β-oxidation of fatty acids; and 3) activates CREB, peroxisome proliferator-activated receptor-α (PPAR-α) and forkhead transcription factor A2 (FoxA2), which enhance transcription of target genes controlling β-oxidation (20).

Triggering fatty acid oxidation is a protective mechanism that provides energy for the fight-or-flight response. However, whether glucagon exerts its lipolytic actions directly on human adipose tissue is a matter of some debate. Even though glucagon induces lipolysis in rodent adipose tissue, there are ambiguities about its role in human adipose tissue (20). In vitro experiments show that glucagon increases lipolysis in human adipocytes at both physiological (3 ng/kg) and pharmacological (0.5 – 1 mg) doses (21,22). However, physiological concentrations of glucagon did not affect lipolysis in both healthy people and people with type 1 diabetes (23). In a recently published review article, it was extensively discussed that pharmacological levels of glucagon (in the range of 6×10^{-11} – 10^{-8} M) has lipolytic effects on rat, bird, rabbit and human adipocytes *in vitro*, but that physiological concentrations of glucagon (1-40 pM) did not increase lipolysis in human adipocytes (20). These controversies about a direct effect of glucagon on adipocytes also extend to detection of the glucagon receptor on adipocytes. While following treatment of rat adipocytes with glucagon there was an increased level of *Gcgr* mRNA, alteration at the protein level was not shown for the receptor (24). In fact, determination of glucagon receptor in adipocytes is severely hampered by a lack of a specific antibody (25). Thus, further molecular research on glucagon action in adipocytes awaits another technique for detecting the glucagon receptor.

1.2.3 Glucagon and metabolism of protein and amino acids

Glucagon plays crucial roles in amino acids and protein metabolism. In neuroendocrine of glucagonoma, all affected people show hypoaminoacidemia (26). In contrast, there is a marked hyperaminoacidemia following total pancreatectomy (27). These effects are mirrored in experimental animal models, as direct administration of glucagon decreased blood amino acid levels and increased hepatic ureagenesis (26,28,29), and blocking glucagon action with anti-glucagon receptor antibodies or silencing of the *Gcgr* gene increased amino acid levels. Blocking the hepatic glucagon receptor also brought about α-cell proliferation (30–32), prompting the description of a hepatic-α-cell axis (32).

Mechanistically, glucagon receptor signaling through cAMP in hepatocytes increases the transcription of genes encoding amino acid transporters and enzymes involved in ureagenesis (16), thereby promoting amino acid clearance and metabolism.

Interestingly, blocking the hepatic glucagon receptor results not only in hyperaminoacidemia, but also α-cell hyperplasia. Kim et al (2017) showed that after blocking glucagon action on mouse hepatocytes, there was an increase in expression of *slc38a5*, which encodes the neutral amino acid transporter in α-cells. When *slc38a5* was depleted, blocking glucagon action on liver had a very mild effect on α-cell proliferation (33), indicating that specific amino acids that were transported by SLC38A5, such as glutamine, functioned in α-cell hyperplasia. Glutamine may promote α-cell hyperplasia through activation of the nutrient sensor mammalian target of rapamycin complex 1 (mTORC1), since blocking mTORC1 by rapamycin suppresses both induction of slc38a5 and α-cell proliferation (34). Other signaling processes may also mediate the effects of glutamine on α-cell proliferation (35). Additionally, Dean et al (2017) showed that serum of the *Gcgr-/-* mouse enhanced expression of a proliferation marker, Ki67, in α-cells. They treated intact mouse islets with the serum of $Gcgr^{-/-}$ or $Gcgr^{+/+}$ mouse, and then dispersed the islets and prepared primary cell culture. Further analysis showed that serum fraction of <10 KDa had proliferative effect on α-cells, which contained amino acids, in particular glutamine (32).

Altogether, these findings suggest a crucial role for glucagon in amino acids and protein homeostasis.

1.2.4 Glucagon and energy metabolism

In healthy individuals, it was shown that glucagon administration brings about an increase oxygen consumption and weight loss; however, there are controversies about its effect in non-diabetic animal models(36,37). Mechanistically, it is proposed that glucagon increases energy expenditure through its receptor on brown adipose tissue (BAT). Glucagon's acute effect on energy expenditure through BAT immediately appears following its administration, with a rapid up-regulation of FGF21 in BAT of mice and humans (38), increases in oxygen consumption and changes in the expression of genes linked to thermogenesis and mitochondrial function in *ex vivo* BAT of mice (39). However, depletion of GCGR in BAT does not affect whole body energy expenditure, suggesting a BAT-independent pathway for glucagon's effect on energy expenditure. In humans, glucagon can also mediate its effects on energy expenditure by increasing blood

cortisol levels (40), which results in higher energy expenditure through increasing the levels of BAT UCP1 at both the gene and protein levels (41,42).

1.3 The glucagonocentric hypothesis of diabetes

The increased blood glucose levels in diabetes is attributed to β-cell dysfunction (defective insulin secretion) and insulin resistance in peripheral tissues. The pathogenesis of diabetes, which includes decreased glucose utilization, increased lipolysis, increased proteolysis, increased hepatic glycogenolysis, increased ketogenesis and decreased glycogen synthesis, has historically been attributed to a lack of insulin (43). In the 1970s, new findings about role of glucagon in metabolism and energy homeostasis led to the discovery of other mechanisms based on the action of glucagon that could be responsible for the pathogenesis of diabetes. These findings that led an α-cell research team to propose a novel theory on pathogenesis of diabetes.

In 1975, Roger Unger and Lelio Orci proposed the "bi-hormonal theory of abnormalities in diabetes", which profoundly changed views on pathophysiology of diabetes (41). Based on this theory, people with diabetes suffer from both a lack of insulin and excessive glucagon. They described that some diabetes abnormalities are due to lack of insulin, such as decreased glucose utilization, increased lipolysis and increased proteolysis, while some other abnormalities such as increased hepatic glycogenolysis, increased hepatic gluconeogenesis, increased ketogenesis and decreased glycogen synthesis are caused by excess glucagon levels (44).

Over the next several decades, further research by Unger's group and other researchers revealed more biological effects of glucagon on the pathogenesis of diabetes. In 2012, Unger and Cherrington proposed a "glucagonocentric hypothesis of abnormalities in diabetes" to describe the pathogenesis of diabetes (3). This hypothesis states that blockade of glucagon action will reduce hyperglycemia even in case of insulin deficiency. It was shown that glucagon receptor knockout mice (*Gcgr*$^{-/-}$) were resistant to STZ-induced diabetes (45) and normalization of hyperglucagonemia in rodent models of uncontrolled diabetes reversed ketosis (3,44,46), decreased hepatic glucose production

and mitigated hyperglycemia (3). Thus, hyperglucagonemia plays a crucial, and perhaps the primary, role in the development of diabetic hyperglycemia (47).

There is a range of relative to absolute hyperglucagonemia in diabetes, which contributes to both fasting and postprandial hyperglycemia. People with diabetes always have at least a relative hyperglucagonemia; however, in patients with type 2 diabetes often there is an absolute hyperglucagonemia. In this state, a carbohydrate meal or glucose load does not suppress glucagon secretion; instead it paradoxically increases glucagon secretion, thus reflecting a degree of α-cell dysfunction. Furthermore, in the presence of hyperglucagonemia, a protein meal often exacerbates glucagon secretion regardless of blood glucose concentrations. Malfunctioning of α-cells can be due to resistance of α-cells to insulin, postprandial disturbance in interaction between glucagon and insulin, defect in glucose-induced suppression of glucagon secretion, malfunctioning β-cells or reduced numbers of β-cells, and lack of GLP-1(48,49), all of which lead to exacerbation of hyperglycemia. Therefore, combating hyperglucagonemia has been spotlighted in diabetes research over the past few years.

There are two strategies to combat hyperglucagonemia: *1)* blocking glucagon action at target organs; or *2)* inhibition of glucagon secretion from α-cells. Blocking glucagon action can be achieved through: *i)* glucagon receptor antagonists, in particular small molecule antagonists, which can allosterically or competitively inhibit glucagon action (50); *ii)* Glucagon receptor neutralizing antibody (51); and *iii)* Antisense oligonucleotides against the glucagon receptor (52). However, many of the compounds that target the glucagon receptor have been discontinued at different phases of clinical trials, since they only have short-term beneficial effects towards reducing blood glucose levels. Their long-term administration can be accompanied by the following consequences : *i)* severe α-cell hyperplasia (20,30,53,54); *ii)* elevation of hepatic and serum transaminases (20,29,55); *iii)* increased risk of hypoglycemia (55–57); *iv)* increased hepatic glycogen storage (16); *v)* increased risk of hyperlipidemia; (58); and *vi)* increased body weight (54,57,59).

1.4 Understanding the mechanisms and consequences of hyperglucagonemia

In order to understand the mechanisms that underlie hyperglucagonemia, we should know about the cellular and molecular mechanisms thar regulate glucagon secretion. These mechanisms have not been as widely studied as insulin secretion from β-cells, as a result, there are conflicting hypotheses.

Inhibition of glucagon secretion from α-cells is a long-standing puzzle in islet biology. In fact, there is no single factor to govern glucagon secretion or alter its secretion rate. Glucagon secretion is simultaneously under the control of nutritional, neural and hormonal factors, which interact with each other to making a complex set of pathways for governing glucagon secretion (60). The following three theories have been proposed as governing mechanisms for glucagon secretion from α-cells; *i)* Intrinsic mechanism, *ii)* Paracrine mechanisms and *iii)* Extrinsic mechanism (which is not going to be discussed here).

1.4.1 Intrinsic mechanism of glucagon secretion

This hypothesis states that glucose is the key regulator of glucagon secretion from the α-cell. One argument in favour of this hypothesis is that glucagon secretion from isolated non-diabetic α-cells can respond directly to glucose in the absence of paracrine inputs.

A) Pattern of glucagon secretion from dispersed α-cells and intact islets

1) Glucagon secretion from dispersed α-cells: Isolated non-diabetic mouse pancreatic α-cells, clonal hamster In-R1-G9 cells(14,61), and non-diabetic human dispersed α-cells(62) show a bimodal V-shaped curve in response to increasing glucose concentrations. Increasing glucose concentrations from 1 to ~7 mM suppresses glucagon secretion in a dose-dependent manner. On the other hand, increasing glucose concentrations from 7-20 mM increases glucagon secretion dose-dependently (Figure 1-1). This profile of secretion suggests that α-cells are equipped with intrinsic mechanism for regulating glucagon secretion which are effective in the range of 1-7 mM of glucose, and these mechanisms are ineffective at higher glucose concentrations. It is noteworthy to

mention that in this context, there is an argument as to whether if glucose- regulated glucagon secretion in isolated α-cells follow a V shape curve or a dose pattern. A dose dependent increase in glucagon secretion was shown in FACS sorted rat α-cells(63).

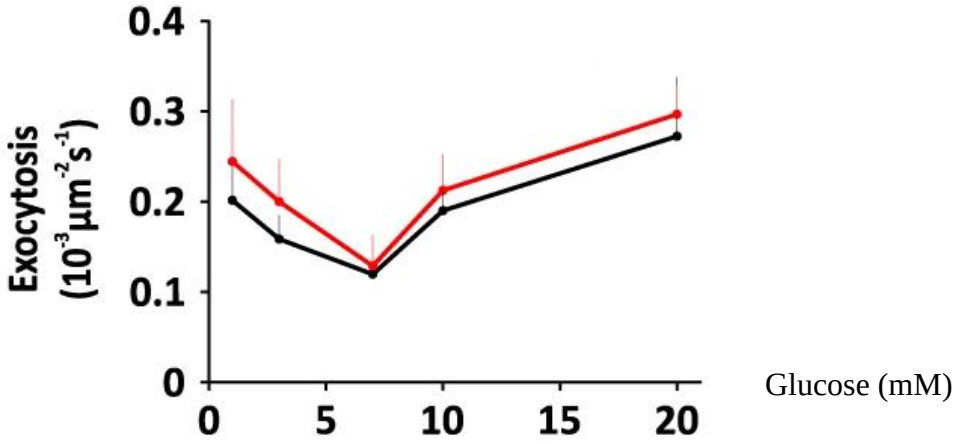

Figure 1-1. V-shape curve of glucagon secretion in response to glucose in dispersed human non-diabetic α-cells (black line). Red line denotes response of islets from patients with T2D, which is discussed in the related section in 1.6.3. The Figure was extracted from reference 62 under the Creative Commons Attribution License (http://creativecommons.org/Licenses/by/4.0/).

2) Glucagon secretion from α-cells within intact islets: It was shown that increasing glucose concentration from 1 to 7 mM dose dependently decreases glucagon secretion from mouse α-cells within intact islets (64) and human intact islets (62). However, by increasing glucose concentration from 7 mM to 20 mM glucagon secretion remains low (Figure 1- 2). A U shape curve was shown for glucagon secretion when glucose concentration gradually increased up to 30 mM (61). In other words, 7-20 mM glucose suppresses glucagon secretion when α-cells are located in their normal anatomical positions within the islet and subject to paracrine regulation from other islet cells.

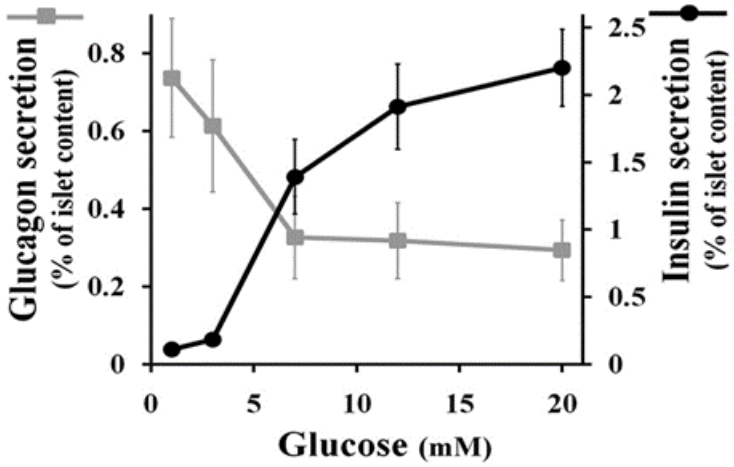

Figure 1-2. Glucagon secretion from intact mouse islets. The Figure was extracted from reference 64 under the license of https://www.asbmb.org/journals-news/editorial-policies.

B) Mechanisms of glucose-regulated glucagon secretion: Human α-cells transport glucose into the cell via the glucose transporter GLUT1 and sodium-dependent glucose transporters SGLT1 and SGLT2. Glucose then has direct effects on glucagon secretion via the following mechanisms:

1) Effect of glucose on K_{ATP} channel conductance: Glucose is subsequently metabolized to generate ATP which binds to and closes KATP channels at the plasma membrane. (65) As a result, voltage-dependent Ca^{2+} channels close, which decreases Ca^{2+} influx into the cytosol, thus reducing SNARE protein-mediated docking and fusion of secretory granules to the plasma membrane (66).

2) Effect of glucose on store-operated current (SOC): While α-cells have potent voltage-dependent Ca2+ channels, SOC through Orai1 Ca^{2+}-release-activated channel (CRAC) also plays an important role in regulation of glucagon secretion from α-cells(67). Under low glucose conditions, the Ca^{2+} depletion of the ER causes the translocation of stromal interaction molecule 1 (STIM1) from the ER to the subplasmalemmal junctions leading to clustering with Orai1, resulting in SOC activation. It is believed that SOC plays a central role in glucose inhibition of glucagon secretion and epinephrine-stimulated

glucagon secretion(68). It is mentioned that α-cells have a low membrane conductance, which confers high sensitivity to SOC-induced current(14). In contrast, exposure of α-cells to high glucose conditions and subsequent high ATP levels activate the sarcoendoplasmic reticulum calcium transport ATPase (SERCA) pump, which results in Ca^{2+} sequestration from the cytoplasm into the ER. Filling the store with Ca^{2+} inhibits the translocation of STIM1, turns off CRAC channel subunit, reduces VDCC activity and suppresses glucagon secretion (68,69).

3) Effect of glucose on cytosolic levels of cAMP: When high glucose levels strongly suppress glucagon secretion, there is only a moderate (or temporary) reduction in the cytoplasmic Ca^{2+} levels, suggesting the presence of an alternate regulator for glucagon secretion. Low glucose levels regulate glucagon secretion through increasing cytoplasmic levels of cAMP, which activates the Epac signaling pathway, stimulating L-type Ca^{2+} channels and increasing glucagon secretion. Furthermore, it was emphasized that increased cAMP is accompanied by mobilization of secretory granules into the "readily releasable pool", which potentiates glucagon secretion. High glucose levels lower cytoplasmic levels of cAMP, resulting in PKA-mediated inhibition of N-type or P/Q type Ca^{2+} channel and suppression of glucagon secretion (66,70).

1.5 Paracrine and autocrine regulation of glucagon secretion

1.5.1 Released factors from β-cells

1) Insulin: Insulin plays a key role in the paracrine regulation of glucagon secretion. Insulin binds to its receptor on the α-cell and suppresses glucagon secretion through several mechanisms. Insulin receptor signaling through PI3 kinase reduces K_{ATP}-channel activity, causing plasma membrane hyperpolarization and reduced activity of the P/Q type Ca^{2+} channel which results in reduced glucagon secretion (71). Insulin receptor activation also results in the translocation of $GABA_A$ receptors from the cytoplasm to the plasma membrane which activates GABA signaling pathway towards suppression of glucagon secretion(72). In fact, all of these findings demonstrate that insulin directly suppresses glucagon secretion from α-cells (73).

In addition to direct effects on the α-cell, insulin can also inhibit glucagon secretion through promoting the secretion of somatostatin from δ-cells. Although initial work failed to find the insulin receptor on δ-cells (74), it has recently been shown that insulin binds to its receptor on δ-cells and stimulates somatostatin secretion. Then somatostatin binds to its receptor on α-cells and potently inhibits glucagon secretion (75) (discussed below).

2) Gamma amino butyric acid (GABA): GABA is a potent suppressor of glucagon secretion from α-cells (76,77). Activating the $GABA_A$ receptor in α-cells results in Cl^- influx into the cells which hyperpolarizes the membrane and reduces glucagon secretion (78). As well, there is coordination between insulin and GABAA receptor activity, as insulin action leads to the translocation of $GABA_A$ receptor to the cell membrane(79). In addition, GABA also inhibits mTOR activity to suppress α-cell proliferation. In type 1 diabetes, due to destruction of β-cells, the amount of secreted GABA is also reduced, resulting in the activation of mTOR and cell proliferation(80). It has been shown that activation of $GABA_A$ receptor may trans-differentiate adult α- cells to β-like cells(81–83), in a way that cell secretory granules will pack insulin and respond to glucose.

3) Serotonin: In human islets, serotonin can suppress glucagon secretion in two ways: through a stimulatory autocrine effect on β-cells to increase insulin secretion and by this way indirectly suppress glucagon secretion, or by a direct paracrine effect on α-cells (84,85). Direct effects are mediated by activation of the serotonin receptor, $5\text{-}HT_{1F}R$, on α-cells, which reduces intracellular cAMP to suppress glucagon secretion. In patients with long-standing T2D, the proportion of α-cells expressing $5\text{-}HT_{1F}R$ is decreased, suggesting that reduced serotonin action on α-cells may play a role in hyperglucagonemia of diabetes. In STZ-treated mice, administration of the $5\text{-}HT_{1F}R$ agonist LY344864 alleviated hyperglucagonemia and hyperglycemia. However, insulin-induced hypoglycemia was worsened, suggesting that the effects of serotonin are glucose-independent. (84). Therefore, while α-cell $HT_{1F}R$ may be a potential target for the treatment of hyperglucagonemia, it may not be an ideal target.

4) Amylin: Amylin, a 39 amino acid peptide, is a major component of the islet amyloid deposit in patients with type 2 diabetes. It is co-released with insulin in response to nutritional stimuli (86) and is an inhibitor of glucagon secretion. Exogenous administration of amylin and its agonists potently and profoundly suppresses glucagon secretion in intact animals or subjects (87). However, there are controversies about underlying mechanism of Amylin's effect on glucagon secretion. Some researchers proposed that Amylin just suppresses glucagon secretion *in vivo,* and does not have effect on glucagon secretion in isolated islets and perfused pancreas (88). On the other hand, some other researchers oppose this idea and believe that Amylin binds to its receptor on α-cells and its action suppresses glucagon secretion in both *in vitro* and *in vivo* conditions (89). As another proposed mechanism, amylin modulates vagus nerve signals in pancreas, which inhibits post-meal glucagon secretion (90).

5) Adenosine: There are some controversies about the source of adenosine. One hypothesis states that the ATP that is co-secreted with insulin is converted to adenosine in the interstitial matrix of islet (91). However, there are species-related variations in expression of 5'-ectonucleotidase (92). Adenosine may also be secreted directly with insulin. Pharmacological concentrations of adenosine may stimulate glucagon secretion (92), but physiologically, adenosine secreted from β-cells has an inhibitory effect on glucagon secretion (93). The effects of adenosine are mediated by the adenosine A1 receptor (Adora1), in which activation is coupled to opening of K_{ATP} channels, hyperpolarization of the cell membrane and prevention of granule exocytosis. In NOD mice, human autoantibody-positive and people with long-term T1D, α-cells gradually lose Adora1 expression, suggesting that the hyperglucagonemia of diabetes is associated with a loss of adenosine action (93).

6) Zn^{2+}: The Zn^{2+} transporter, *Slc30A/*ZnT8, is a causative gene for T2D, and ZnT8 is located in the secretory granule membrane of both α-and β-cells. There is a direct relationship between expression of the proglucagon gene and *Slc30A* in α-cells (94). However, there are conflicting findings about the effects of Zn^{2+} on glucagon secretion (94). There are reports that, in isolated mouse islets and α-cells, Zn^{2+} administration decreases glucagon secretion (95), or has no effect (96). In contrast, treatment of isolated

human islets with similar concentrations of Zn^{2+} enhanced glucagon secretion (97). The reason for these discordant results is not clear; it may be that exogenously administered Zn^{2+} or Zn^{2+} secreted from the β-cell does not have a direct role in glucagon secretion in normal physiology. Interestingly, in mice lacking *Slc30A*/ZnT8 specifically in α-cells, there is a heightened secretory response to 1 mM glucose (98), and overexpression of ZnT8 specifically in α-cells restricted glucagon secretion in response to 1 mM glucose (99), suggesting paracrine regulation by Zn^{2+}.

1.5.2 Released factors from α-cells

1) Acetylcholine: In addition to cholinergic innervation of islets from parasympathetic nerve endings, a cholinergic system is also contained within α-cells: the vesicular acetylcholine transporter is present on α-cells, and choline acetyltransferase co-localizes with glucagon in human pancreatic islets (131). Acetylcholine is secreted upon low glucose stimulation, whereby it acts on M3 muscarinic receptors on β-cells and sensitizes β-cells for insulin secretion (100). Acetylcholine has an important role in minimizing blood glucose volatility and potentially aids in survival of β-cells (100,101). Therefore, α-cells are equipped with a unique cholinergic-based system that responds to daily variations in blood glucose.

2) Glutamate: The α-cell contains its own glutaminergic system that regulates glucagon secretion in an autocrine manner. α-cells express the vesicular glutamate transporter, VGLUT2, on secretory granules, enabling the transport and storage of glutamate within the α-cell secretory granules. Both metabotropic and ionotropic glutamate receptors are present on α-cells, but only ionotropic AMPA/kainite receptor activation was coupled to glucagon secretion (102,103). Following α-cell exposure to low glucose, a glutamate feedback loop is activated, which further increases the glucagon secretory response to low glucose. In this way, the α-cell glutaminergic system guarantees that enough glucagon is secreted in case of need, which prevents blood glucose volatility(34,102,104). As well, the secreted glutamate may also activate α-amino-3-hydroxy-5-methyl-4-isoxazolepropionic acid (AMPA) receptors on β and δ-cells , thus participating in an intra-islet glutaminergic system that finely controls glucose homeostasis(105). In both patients with diabetes and diabetic mice, glutamate levels are

significantly increased. It was proposed that glutamate takes a role in development of diabetes through exaggerated activation of N-methyl-D-aspartate (NMDA) receptors in β-cells that may result in dysfunction and apoptosis of β-cells(106).

3) Glucagon: Secreted glucagon from α-cells can stimulate its secretion through an autocrine effect. It has been shown that glucagon stimulates glucagon secretion from the rat and mouse isolated α-cells in an autocrine manner through glucagon receptor-stimulated cAMP signaling (107). Both biosynthesis and secretion of glucagon in human and mouse α-cells is augmented due to the autocrine effect of glucagon. Thus, targeting autocrine and paracrine effectors of glucagon secretion, including glucagon, has been proposed as therapeutic strategies in patients with diabetes(108).

4) Other α-cell proteins: The role of proteins, in particular proteins of secretory granule, may be new factors that regulate the secretion of glucagon from α-cells. It was shown that brefeldin A-inhibited guanine nucleotide exchange protein 3 (BIG3) is a conserved secretory granule protein in α-cells, and negatively regulates glucagon secretion (109). Li et al (2015) showed that levels of glucagon within the secretory granule were increased in different animal models of diabetes, in pancreatic islets and isolated α-cells, which may contribute to higher glucagon secretion in diabetes. Therefore, the α-cell secretory granule itself may contain other proteins that play a role in the regulation of glucagon secretion.

1.5.3 Released factors from δ-cells

Somatostatin is a well-known inhibitor of glucagon secretion. Somatostatin binds to its receptor, SSTR2, on α-cells, activates adenylate cyclase and generates cAMP. In the downstream process, cAMP activates the serine/threonine protein phosphatase calcineurin, which results in de-priming of the secretory granule (14). Notably, secretion of somatostatin and inhibition of glucagon secretion potently occurs at 3mM glucose, while this level of glucose does not have stimulatory effect on insulin secretion, indicating that the α-cell response to low glucose may be mediated by somatostatin (110).

Circulating and pancreatic somatostatin, together with SST mRNA, are elevated in diabetes. However, expression of SSTR2 on α-cells is decreased in T2D, which makes α-cells resistant to somatostatin; together with α-cell insulin resistance, this could be a reason for paradoxical high glucagon secretion in hyperglycemic condition of diabetes(62).

1.5.4 Cross-talk among β and δ and α-cells and glucagon secretion

In gross histology, rodents' islets are composed of β-cells in the core and non-β-cells in the periphery. However, in human islets, non-β-cells are intermingled within β-cells(111) and appear to be organized as "superclusters" of islets(112). Recently, Briant et al (2018) applied optogenetic techniques to study temporal and spatial cross-talk among mouse islet cells (Figure 1-3). By this approach, they demonstrated that, under high glucose conditions, insulin secreted from β-cells suppresses glucagon secretion through insulin receptor signaling , and through actions on δ-cells mediated by gap junctions (113). As shown in Figure 1-3, high glucose levels stimulate glycolysis in β-cells to generate ATP, which closes K_{ATP} channels, causing membrane depolarization, Ca^{2+} influx through the voltage-dependent Ca^{2+} channels (VDCC), and insulin secretion (113). Additionally, following Ca^{2+} influx into the β-cells, this Ca^{2+} is transported via gap junction proteins into δ-cells, causing depolarization of the δ-cell membrane and initiating Ca^{2+} influx into the cell through the VDCCs, which results in somatostatin secretion (113). At the same time, entrance of glucose into the δ-cell and generation of ATP could activate δ-cells through the K_{ATP} channels to release somatostatin (as mentioned in section 1.3.1)(114). Somatostatin then binds to SSTR2 on α-cells, triggering Gαi and activating G-protein coupled inwardly rectifying K^+ (GIRK) channels, hyperpolarizing the α-cell membrane and suppressing glucagon secretion(113).

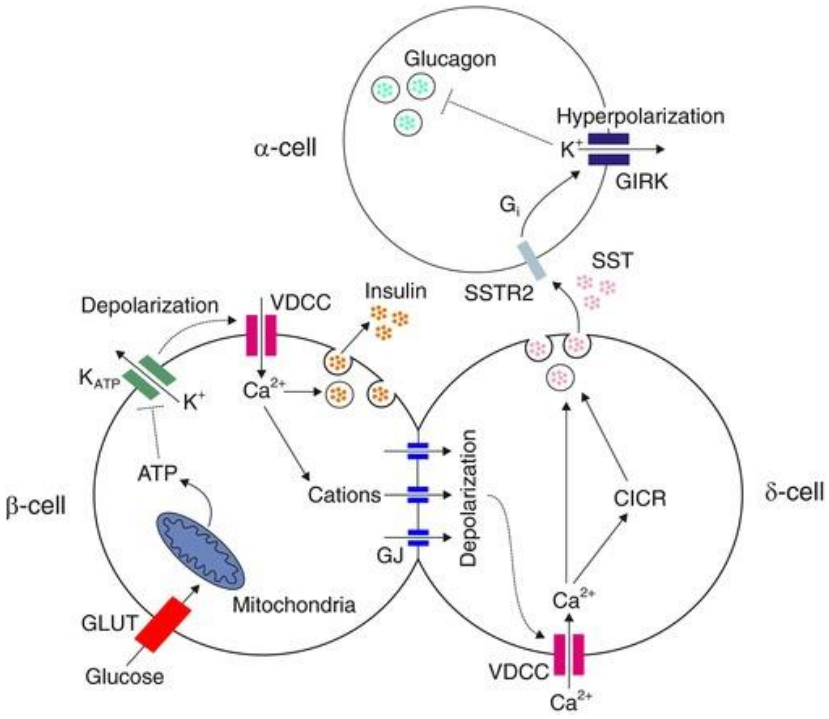

Figure 1-3. Cross-talk among α, β, and δ-cells towards inhibition of glucagon secretion. The Figure was extracted from reference 113 under the Creative Commons Attribution License (http://creativecommons.org/Licenses/by/4.0/).

It has been shown that eliminating insulin receptor on δ-cells completely abolishes the glucagonostatic effect of insulin, which proposes an indirect glucagonostatic effect for insulin through cell-cell junction. Additionally, the ability of insulin to inhibit glucagon secretion was lost when either SSTR2 or the sodium-glucose co-transporter 2 (SGLT2) were blocked. (75).Thus these findings highlight a central role for δ-cells in the context of intra-islet regulation of glucagon secretion, and may have implications for designing drugs for the treatment of hyperglucagonemia of diabetes. Glucagon may also play a role in the intra-islet regulation of insulin secretion. In a mouse specifically engineered to investigate intra-islet regulation, selectively shutting off glucagon secretion resulted in impairment of the insulin secretory response to glucose, resulting in hyperglycemia and glucose intolerance. Furthermore, it was demonstrated that these actions of glucagon were mediated through the GLP-1 receptor on β-cells (115). Further studies confirmed

insulinotropic role of glucagon through the β-cell GLP-1 receptor, in a way that in the fed state, glucagon cooperates with insulin towards glucose homeostasis instead of counteracting insulin's action (116).

In case of diabetes, α-cells do not respond to elevated levels of glucose in a physiological way, instead paradoxically secreting higher amounts of glucagon. The loss of response to hyperglycemia may be due to either β-cell secretory defects or α-cell insulin or somatostatin resistance (117,118). In spite of these proposed mechanisms, the underlying events of paradoxical glucagon hypersecretion in hyperglycemic condition has not been fully uncovered.

1.6 Chronic inflammation and diabetes

In the pancreatic islet of people with diabetes, in particular type 2 diabetes, there is a remarkable reduction in the beta cell population due to the presence of a chronic inflammation. This chronic inflammation is due to an increased levels of cytokines and chemokines that affect whole islets (119). In fact, activation of immune system in islets, triggers proinflammatory response and release of cytokines. Cytokines will be secreted by both innate immune cells and all parenchymal cells of islets(120). It was shown that in both human and rodent animal models there is an increase in macrophage infiltration in islets, which produces and secretes Interleukin-1 (IL-1). To this end, IL-1β plays a master role in development of inflammation within islets in a way that in the downstream induces expression of some proinflammatory factors (such as IL-6, IL-8, IL-1β, CXCL1, CCL2, and TNF-α)(119). These inflammatory factors bring about ER stress, oxidative stress, dysfunction of mitochondria, and apoptosis, which result in cell dysfunction. Furthermore, these adverse effects trigger up-regulation of more inflammatory mediators (such as CCL2, CXCL1, iNOS and Fas), which amplify inflammatory response, and exacerbate loss of β-cells (121). In addition, long-term exposure of islets to glucose induces Fas expression and increases secretion of IL-1β from resident immune cells within islets. This phenomenon activates amyloid system in islets, which results in initiation of inflammation. Thus, inflammation, brings about dysfunction in the cell-cell interaction within islets through inducing malfunction in β-cells, which will be resulted in dysfunction of δ and α-cells.

1.7 GLP-1: Intra-islet or intestinal?

In addition to the pancreatic α-cell, proglucagon is also expressed in the intestinal L cell, where it is post-translationally processed to glucagon-like peptide (GLP)-1 and GLP-2. GLP-1 is an incretin hormone, secreted following meal ingestion and stimulates insulin secretion in a glucose-dependent manner. GLP-1 also suppresses glucagon secretion in both healthy people and people with type 2 diabetes (122), leading to the development of GLP-1 receptor agonists for the treatment of T2D. The glucagonostatic actions of GLP-1, the glucagonotropic actions of GLP-2 (123,124) and another incretin, glucose-dependent insulinotropic polypeptide (GIP) (125,126) all regulate post-prandial blood glucose levels. This balance is disrupted in diabetes, in particular type 2 diabetes, which results in dysregulated glucagon secretion and hyperglucagonemia (126).

It has been believed that proglucagon processing to GLP-1 does not occur in pancreatic α-cells under normal circumstances, due to the relative lack of the processing enzyme PC1/3 (127). However, this hypothesis has been very recently overturned by a study showing that there is a substantial subpopulation of α-cells (40%) within the non-diabetic human pancreatic islets that potently secretes GLP-1(128), and that this subpopulation increases in T2D. It has previously been shown that, when α-cells encounter metabolic stress, such as in both T1D and T2D and hyperplasia, the abundance and activity of PC1/3 increases, cleaving proglucagon to generate GLP-1 (129,130). Therefore, the α-cell has a degree of plasticity which allows it to respond to sustained metabolic stress (131).

It has been postulated that islet-derived GLP-1 may act on β-cells to promote β- cell regeneration and thus ameliorate hyperglycemia and loss of β-cell mass By considering generation of GLP-1 in both gut and islet, there is a debate on which source of GLP-1 suppresses glucagon secretion from pancreatic α-cells. Chambers et al (2017) generated a *Gcg* knockout mouse and then by reactivation of *Gcg* in L-cells or α-cells, showed that islet-generated GLP-1 was primarily responsible for glucose homeostasis by promoting glucose-stimulated insulin secretion and suppressing glucagon secretion (118). The gut-

derived GLP-1 binds to its receptor on local afferent vagal nerve terminals, which ultimately signals for satiety, delaying gastric emptying and suppression of hepatic glucose release (129,132).

How GLP-1 exerts its actions on α-cells is a matter of debate. The search for a GLP-1 receptor on α-cells has been hampered by a lack of a reliable GLP-1 receptor antibody (127,133). However, GLP-1 appears to mildly reduce action potentials in the α-cell membrane at 1 mM glucose in isolated mouse α-cells, and this effect is blocked by the GLP-1R antagonist exendin (9-39), therefore suggesting the presence of GLP-1R, perhaps at a very low density, on a small proportion of α-cells (122).

It is known that GLP-1 acts on α-cells to trigger signaling through cAMP, which stimulates PKA-dependent activation of N-type Ca^{2+} channels, blocking Ca^{2+} influx and suppressing glucagon secretion. Notably, GLP-1 inhibits glucagon secretion in both basal status and in case of diabetes. It is noteworthy to mention that the low level of GLP-1R expression is crucial for GLP-1 inhibitory effect on glucagon secretion (134). It has also been shown that GLP-1R may be expressed on rat δ-cells, which, when activated, stimulates somatostatin secretion, which results in suppression of glucagon secretion from α-cells (127,135). However, this area needs further future research through designing a δ-cell-specific GLP-1R knockout.

As I have discussed so far, glucagon secretion from the pancreatic α-cell is regulated by multiple inputs from outside and within the α-cell. However, the entire picture of how glucagon secretion is regulated is far from clear (71). All of the factors I have thus far discussed ultimately converge on components of the regulated secretory pathway in the α-cell. In particular, the secretory granule, which stores mature glucagon, is the compartment that responds to factors that either stimulate or inhibit glucagon secretion. In the next section, I will outline the regulated secretory pathway of the α-cell, and propose that proteins contained within the secretory granule can regulate glucagon secretion.

1.8 Biogenesis of the regulated secretory pathway

The α-cell secretory pathway begins with the synthesis of proglucagon in the endoplasmic reticulum. It is then transported through the Golgi to the trans-Golgi network (TGN). Budding immature secretory granules from the TGN contain proglucagon, its processing enzymes and many other proteins (136). Two models have been proposed as underlying mechanisms for secretory granule biogenesis: “sorting for entry” and “sorting by retention”(137).

1.8.1 Molecular mechanisms of sorting glucagon into secretory granule

Based on the sorting for entry model, nascent granule budding occurs in a specific site on TGN, which contains sorting receptors and allows proteins with specific sorting signals to be directed into secretory granules. The sorting by retention model suggests that all protein components of the TGN are contained within the nascent secretory granule, which then matures by budding off constitutively-secreted proteins. Currently, it is not clear which of these models operate in α-cells, but it is generally believed that granule biogenesis is governed by the natural entity of the prohormone and its synthesis rate(136). Storage and concentration of proteins within secretory granule take place within the dense core portion of secretory granules (137).

Advocators of the TGN-based sorting model have been striving to find a governor sorting receptor in the TGN, and sorting signals within prohormones that interact with sorting receptors. It has been proposed that membrane-bound form of the processing enzyme carboxypeptidase E (CPE) can be a prohormone sorting receptor (138–141). It was shown that ablation of CPE disturbed regulated secretion of proopiomelanocortin (POMC), proenkephalin and proinsulin in related cell lines and the CPE ^{fat} mouse model, in which CPE is degraded within the pituitary (140,141). Sorting signals can take the form of amphipathic loops, such as for POMC (142) or proinsulin (140), or amphipathic alpha helices, as is the case for the N-terminal region of prosomatostatin, and in the C-terminal regions of PC1/3, PC2, PC5/6a, and CPE (143). These signals may also interact

directly with membrane lipids, in particular with lipid raft regions, to be sorted into secretory granules (143).

In pancreatic β-cells, there is evidence to support the "sorting-by-retention" theory of secretory granule biogenesis,, as the protein composition of immature secretory granules is altered during the process of granule maturation (144). In this context, proinsulin and the enzymes involved in the post-translational processing to mature insulin are retained within the secretory granule, while other proteins designated for constitutive secretion are removed (144).

By considering all of these findings, it is more likely that both "sorting for entry" and "sorting by retention" mechanisms operate in the sorting of prohormones into secretory granules. In this scenario, prohormones could be sorted into secretory granules by means of sorting signals, followed by retention within the granule as maturation of secretory granules takes place. The maturation process involves alterations in the components and composition of the secretory granule, by removal of constitutively-secreted proteins, acidification of the granule milieu, and exclusion of water to condense the intragranular environment.

The cellular events underlying the sorting of proglucagon to secretory granules have not been fully elucidated, and studying this mechanism is complicated by the multi-step processing of proglucagon. The processing of proglucagon in the α-cell is largely governed by the prohormone convertase (PC) family of enzymes. Proglucagon processing begins with cleavage of proglucagon at K70R71, which yields glicentin and major proglucagon fragment (MPGF) (Figure 1- 4)(145). This site is accessible to a number of processing enzymes and is likely cleaved by furin or PC1/3 in the absence of PC2 (148). This event occurs early in the secretory pathway, either in the TGN or immature secretory granule. Subsequent cleavage of glicentin by PC2 at K31R32 results in the production of mature glucagon. This cleavage event likely occurs within the mature secretory granule since the acidic pH and millimolar calcium level of secretory granules is optimal for PC2 activity (9,10,146,147). Thus, the sorting of proglucagon into the

secretory granule is vital for the generation of active glucagon, and storage within granules assures a robust secretory response in case of physiological need.

Previous work from the Dhanvantari lab has investigated some mechanisms of proglucagon sorting into the secretory granule by searching for sorting receptors and sorting signals. Using the α-cell line α–TC1-6, it was shown that siRNA-mediated knockdown of CPE increased constitutive secretion of glucagon (141), thereby suggesting that CPE may play a role in directing proglucagon to secretory granules(141). However, the processing of proglucagon to glucagon remained unchanged, and therefore these results are not clear. The search for sorting signals provided more clarity on the mechanisms of proglucagon sorting. Using Fc-tagged proglucagon-derived peptides that could be detected by immunoprecipitation and immunofluorescence microscopy, two dipolar α-helices containing hydrophobic patches with three charged residues within the sequences play roles as sorting signals. One amphipathic α-helix was located within the amino acid sequence of glucagon (SDYSKYLDSRRAQDFVQWLMN), and one within GLP-1(SDVSSYLEGQAAKEFLAWLVK) (145). Interestingly, Fc-glicentin could be sorted to secretory granules, but Fc-MPGF was not, indicating that proglucagon processing occurs after sorting to secretory granules.

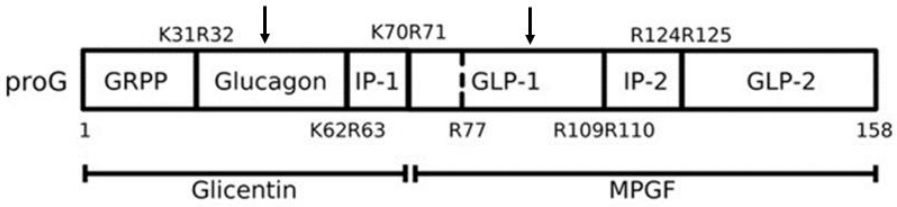

Figure 1-4. Cleavage processing of proglucagon in α-cells. Arrows depict sorting signals. The Figure was extracted from reference 145 under the license of https://www.asbmb.org/journals-news/editorial-policies.

As discussed above, this proglucagon processing profile changes in diabetes. In human α-cells co-presence of GLP-1 and PC1/3 was shown in both healthy individuals and patients with type 2 diabetes (148). As well, it was shown that high glucose condition

induced expression of PC1/3 and GLP-1 in primary culture of rat islets and also α-cell line models (149). In addition, it was shown that the diabetes-related pro-inflammatory cytokine, IL-6, caused an increase in the production of both GLP-1 and glucagon as well as expression of PC1/3 in primary culture of both human and mouse islets (150). Also, db/db (151), and ob/ob (152) showed the same expression pattern for PC1/3 , GLP-1 and glucagon. However, the NOD type 1 diabetic mouse did not show expression of GLP-1 and PC1/3 in α-cells(151). Thus, the presence of PC1/3 and GLP-1 and other processed fragments of MPGF (GLP-2 and IP-2) within the secretory granules of diabetic α-cells is a subject of ongoing research.

1.8.2 Secretory granule exocytosis

After proglucagon processing and granule maturation, glucagon is stored in the granule until a stimulus triggers exocytosis. Releasing stored glucagon from the large dense-core secretory granules in α-cells needs coupling of stimulus and secretion. The electrically excitable membrane of the α-cell is active with action potentials below the range of 4-5 mM glucose (153). Glucagon secretion could be in a Ca^{2+} dependent or independent manner.

A) Ca^{2+} dependent pathway of glucagon secretion: it was shown that a set of channels were clustered within the membrane of α-cells, which generate action potentials in the absence or low levels of glucose. Activation of K_{ATP} channels in low glucose condition brings about a level of membrane voltage that opens T-type Ca^{2+} channels. Influx of Ca^{2+} depolarizes the membrane to a level that opens Na^{+} channels and then N-type Ca^{2+} channels (non L-type, presumably P/Q type), which bring about glucagon secretion. At this step, L-type Ca^{2+} channels are also opened, but do not play a role in glucagon secretion (maybe due to spatial isolation). On the other hand, in high glucose condition, generation of ATP increases ATP/ADP ratio, which inhibits K_{ATP} channels and depolarizes the cell membrane (through L-type Ca^{2+} channels) at a level that it inactivates those mentioned channels in generation of action potentials, and consequently, suppresses electrical activity, Ca^{2+} influx and glucagon secretion. As it was discussed in 1.3.1, there is also a K_{ATP} -independent mechanism for inhibition of glucagon secretion from α-cells.

Based on this mechanism, high glucose condition inhibits glucagon secretion through suppression of SOC and preventing Ca^{2+} entry(153,154).

B) Ca^{2+}-independent pathway of glucagon secretion: This alternative theory expresses that in the context of high glucose concentration (e.g. 12 mM), K_{ATP} channels do not play a role in suppression of glucagon secretion. Accordingly, high glucose condition suppresses secretory granule trafficking or inhibits glucagon exocytosis in non-diabetic α-cells, which results in suppression of glucagon secretion. (155,156).

Based on experimental evidence from isolated mouse islets, a kinetic model of the exocytotic behaviour of secretory granules in α-cells under low glucose conditions has been derived (140). This model predicts the relationship between intracellular Ca^{2+} levels and granule dynamics and mobilization (Figure 1- 5). A reserve pool of secretory granules within the cytoplasm resupplies the primed pool in a reversible equilibrium rate. Priming occurs as a result of sequential Ca^{2+} binding events. Following binding with three Ca^{2+}, granules fuse with the plasma membrane in a non-reversible manner, which forms the fused pool and results in glucagon exocytosis (157).

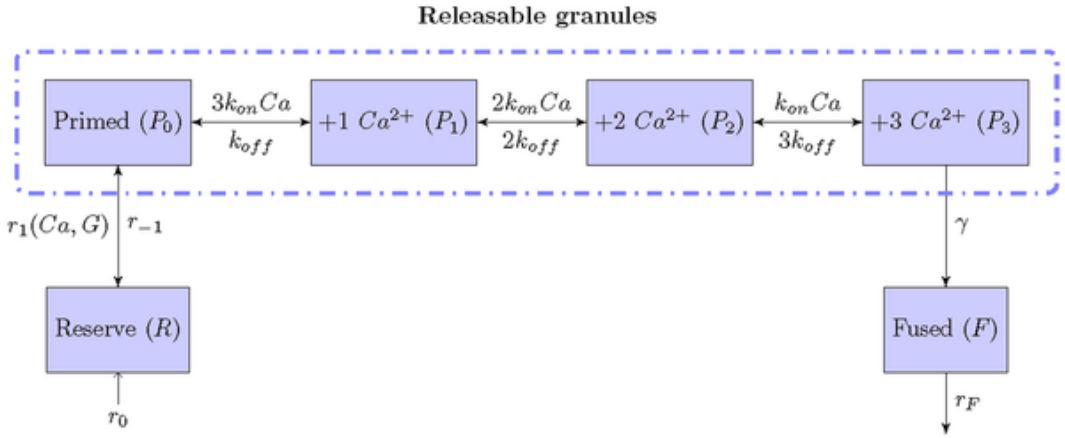

Figure 1-5. Kinetic model for trafficking of secretory granules in α-cells. R(reserve pool); P0(primed pool); F (fused pool); r1(forward resupply rate); r-1(backward resupply rate); Kon(binding rate); Koff (unbinding rate); γ (fusion rate); r0(granule formation); rF(granule release). The Figure was extracted from reference 157 according to the Creative Commons Attribution License (http://creativecommons.org/Licenses/by/4.0/).

It was quantitatively shown that in the presence of 1mM glucose, the mouse α-cell contains ~4400 secretory granules, of which ~140 are docked. This means that the reserve pool is large, and can resupply the primed pool to maintain euglycemia over extended periods of time. On the other hand, in the presence of 16.7 mM glucose numbers of the docked secretory granules increase to ~310 (157). By increasing exposure of α-cells to glucose from 1 to 16.7 mM, the levels of secreted glucagon will be reduced from ~40 to ~20 pg/islet/h (158).

It is believed that α-cells are highly sensitive to small changes in Ca^{2+} (159). The Ca^{2+} dependence of glucagon granule exocytosis is due to the actions of synaptotagmin VII (160), a major Ca^{2+}-responsive component of the SNARE complex of exocytotic proteins (62,161). This complex contains two subsets of proteins; *i)* the t-SNAREs syntaxin 1A and SNAP-25, located in the plasma membrane; and *ii)* the v-SNAREs VAMP2 and synaptotagmin VII, which are located in the granule membrane. Under low glucose conditions, SNAP-25 and syntaxin 1A are translocated to the plasma membrane. SNAP-25 itself may play a role in the transportation of granules from the RP to the RRP, and then mediates their fusion with plasma membrane via interaction with syntaxin 1A(157,159). Then, C2 domain of synaptotagmin VII binds to syntaxin 1A and forms the SNARE complex to prime the secretory granules for exocytosis (159) in a mechanism similar to that in β-cells (162,163). .

1.8.3 Diabetes and alterations in dynamics of secretory granules

It was shown that α-cells of patients with T2D show normal action potentials and Ca^{2+} entry into the cell; nonetheless, secretory granules remained close to the plasma membrane for a longer period of time compared to non-diabetic α-cells, and exocytosis is impaired (62). As mentioned above in section 1.3.1, the secretory behavior of dispersed α-cells from patients with T2D is similar to that of non-diabetic dispersed α-cells, which implies that paracrine effectors are determinants for the normal dynamics of glucagon secretory granules (108).

One very recent study has shown that α-cells in intact islets from patients with T2D were resistant to the effects of somatostatin due to a reduction in the expression of SSTR2. (62). SSTR2 is associated with L-type Ca^{2+} channels, and is linked with G_{i2} proteins; the binding of somatostatin activates the serine/threonine protein phosphatase calcineurin and prevents exocytosis through depriming secretory granules (164). Accordingly, it was mentioned that all paracrine effectors (insulin, somatostatin and GABA) suppress glucagon secretion through reducing priming, but not docking of secretory granules (62). These results suggest that reductions in paracrine regulation disrupt the depriming of secretory granules in diabetic α-cells, thus increasing secretory granule exocytosis, leading to glucagon hypersecretion.

Therefore, in this section I have outlined how properties of the α-cell secretory granule may be determinants of glucagon secretion, and how their alterations are linked to hyperglucagonemia of diabetes. While it is known that granule contents and composition are modified during normal granule maturation, a more complete picture of granule remodeling and heterogeneity in normal islet cell physiology and in diabetes is required, and can be provided by islet proteomics and single cell transcriptomics.

1.9 Pancreatic islet protein reference map

Development of proteomic techniques coupled with bioinformatic analysis has provided a means to discover a wide range of low expression proteins within the pancreatic islet that may provide a greater understanding of the mechanisms of glucagon secretion. Specifically, this strategy has enabled the discovery of protein networks in organelles that

may regulate islet hormone secretion, such as the rough endoplasmic reticulum (RER), Golgi, mitochondria and secretory granules. In particular, secretory granule proteomics has revealed some novel protein networks involved in proinsulin processing, insulin secretory granule maturation, secretory granule trafficking and exocytosis and degradation of proteins in the β-cell. Such an approach may also reveal new networks that govern glucagon secretion and their dysregulation in diabetes.

1.9.1 Islet proteomics and glucagon secretion

In a proteomics study on normal human islets, it was proposed that there is correlation between changes in islet protein profile and functional performance of islets, in particular insulin secretion (165,166). Importantly, islet proteomics shows dynamic alterations in secretory protein networks in response to changes in microenvironmental conditions, in particular those networks governing granule trafficking and exocytosis. After incubation of mouse islets for 24h in medium containing 5.6 mM versus 16.7 mM glucose, comparative analysis showed an increase in proteins related to glucose catabolism, cellular stress and cytoskeletal proteins, and a concomitant reduction in proteins related to vesicle trafficking (e.g. VAMP2, SERCA complex, synaptotagmin-like protein 4, Rab3b) under high glucose conditions. Accordingly, these alterations were accompanied by reduction in insulin secretion(167), thus identifying metabolic and structural changes that impact the β-cell secretory pathway in response to changes in prevailing glucose concentrations in a long-term cumulative incubation.

In rodent models of diabetes, islet proteome studies have revealed interactions between metabolic, structural and secretory protein networks. Proteomic analysis of islets from the MKR mouse (insulin resistance), Zucker diabetic fatty rat (leptin receptor mutation), HFD diabetic mouse (diet-induced obesity and diabetes) and STZ-treated mice (chemically-induced T1D) all showed differential regulation for expression of proteins involved in the redox system, chaperone activity, cytoskeleton, and vesicle trafficking (166,168). Furthermore, there is downregulation of proteins involved in insulin exocytosis in insulin-resistant pre-diabetes (169), demonstrating substantial alterations in islet secretory protein networks prior to the onset of diabetes.

Importantly, islet proteomics of diabetic db/db mice revealed potentially new proteins in β-cells that may have roles in ER-Golgi vesicle transport, granule trafficking, and signaling through PI3K-AKT and ERK1/2 pathways, such as: CD63 antigen (CD63), Neudesin (NENF), Glycerol-3-phosphate phosphatase (PGP), Minor histocompatibility antigen H13(HM13), Polyadenylate-binding protein-interacting protein 2B (PAIP2B), Pyruvate kinase PKM (PKM; isotopes M1 and M2), Prominin-1 (PROM1), Mitochondrial import receptor subunit TOM22 homolog (TOMM22), Protein SET (SET), Apoptosis-stimulating of p53 protein 1 (PPP1R13B), and Methionine aminopeptidase 2 (METAP2). The METAP2 has been introduced as a therapeutic target for the treatment of diabetes and obesity(170).

Islet proteomics can also show how diabetes-induced derangements in β-cell secretory networks can be restored by normalizing glucose conditions. Adaptation of islets from diabetic db/db mice to euglycemic conditions brought about a non-diabetic mouse islet proteomics profile in terms of both expression and phosphorylation of proteins involved in ER-Golgi vesicular transport (Transport and Golgi organization protein 1 homolog, MIA3; Coatomer subunit alpha, α-COP; GTP-binding protein SAR1b ;SAR1B), post-Golgi vesicular transport (Vesicle-associated membrane protein 4, VAMP4; ADP-ribosylation factor-related protein 1, ARFRP1; Vesicle transport through interaction with t-SNAREs homolog 1B , VTI1B; Brefeldin A-inhibited guanine nucleotide-exchange protein 2, ARFGEF2), secretory granule trafficking (Ras-related protein Rab-3B ,Rab3b; Ras-related protein Rab-27A, Rab27a; Rabphilin-3A, RPH3a1; Microtubule-associated protein 2, MAP2; Polycomb protein Pcl, PCL0; Myosin-9, MYH9; Vesicle-trafficking protein SEC22b, Sec22b), and exocytosis (Synaptotagmin-like protein 5, SYTL5; Synaptotagmin-7, SYT7; Synaptotagmin-10, SYT10; Exonuclease 1, EXO1; Syntaxin-4 , STX4a; Syntaxin-18, STX18; Regulating synaptic membrane exocytosis protein 2, RIMS2) (171). In this context, post-translational alterations such as phosphorylation and sialylation were particularly important (170) and revealed a role for the Golgi protein kinase FAM20C, which targets secretory proteins (e.g. BIG3), in trafficking and secretory granule biogenesis (171). Meanwhile, such alterations could be restored following treatment (for example in rat diabetic islets) with EPS (a hypoglycemic fungal extracellular polysaccharides) or Imidazoline (cationic surfactant with an insulinotropic

effect) (166). These types of experiments have revealed some new proteins involved in insulin secretion that could be novel targets for pharmaceutical treatment of diabetes.

1.9.2 The state-of-the-art secretory granule proteomics

Recent advances in the isolation and purification of secretory granules have enabled accurate coverage in the proteomic analysis of the granule compartment. Secretory granule proteomics complement islet proteomics through; 1) uncovering genuine protein components of secretory granules (172), and 2) unveiling alterations in protein components of secretory granules in diabetes. Diabetes alters the protein components of the secretory granule responsible for secretory granule trafficking, docking and exocytosis. For instance, in islets from patients with T2D, islet proteomics revealed down-regulation in a network of proteins that function in granule docking, fusion and exocytosis, such as the SNARE proteins SNAP25, Syntaxin-1A, Syntaxin-binding protein 1(STXBP1), Synaptotagmin-1(SYT1), Synaptotagmin-7 (SYT7) and the Rab family of GTPases, Rab-3A, Rab-3B and Rab-3C, and new proteins that may function in this network, such as Regulating synaptic membrane exocytosis protein 1 (RIMS1) and RIMS2 and the presynaptic scaffold proteins Piccolo (PCLO) and Bassoon (BSN) (173).

Uncovered proteins in proteomic analysis of secretory granules can be categorized into three groups; 1) Proteins annotated as secretory granule proteins, 2) proteins annotated to have multiple localizations, and 3) proteins annotated as immature secretory granules or contaminants.

Annotated secretory granule proteins can be subcategorized as *a)* secretory granule proteins (e.g. INS-1E cell proteins of CPE, PC2,VAPM2, VAMP3, chromogranins) , *b)* islet cell protein, but not related to any organelle (e.g. INS-1E cell proteins of tubulin beta-2A chain, Annexin A11 , Kinesin-1 heavy chain) and *c)* non-islet cell proteins (e.g. INS-1E cell proteins of neuronal differentiation-related gene protein, and Proprotein convertase subtilisin/kexin type 1 inhibitor, proSAAS) (172). Importantly, this subcategorization could have clinical application in terms of introducing novel targets for the treatment of diabetes. Proteomics of INS-1E secretory granules revealed the presence of some membrane proteins within the granules (such as ARFRP1, ADP-ribosylation

factor-related protein 1;SCFD1, Sec1 family domain-containing protein 1; syntaxin12, STX12, syntaxin5, STX5; VPS45, Vacuolar protein sorting-associated protein 45, and ATP6V0C, V-type proton ATPase 16 kDa proteolipid subunit) that could play a role in the secretory granule biogenesis, maturation, trafficking and exocytosis (174). For instance, ATP6V0C is a subunit of vacuolar ATPase and regulates the acidification of the secretory granule over the maturation process. The presence of SNARE proteins within the secretory granule proposes their roles in the fusion step of exocytosis. The presence of related proteins to immature secretory granules (such as STX12, VTI1A, STX6 and VAMP4) within the secretory granule proposes homotypic fusion of immature secretory granule, which is an important step in the maturation process (174). In this context, the presence of transmembrane protein (such as Transmembrane 9 superfamily member 3, TM9SF3, a nine-transmembrane protein) implies a role for transmembrane proteins in secretory granule biogenesis, and their potential involvement in maturation, trafficking, and exocytosis.

Annotated proteins with multiple localizations imply that other intracellular compartments may interact with secretory granules and therefore have inputs into the secretory pathway. For instance, proteomic analysis of granules isolated from INS-1E cells revealed the presence of the endosomal proteins syntaxin 7 and VAMP 8 (172). In islets from diabetic mice, a lysosomal protein, Rab7 interacting lysosomal protein (RILP) is overexpressed, and plays a role in the maturation of secretory granules through cross-talk with lysosomes (175). As well, the presence of endosomal and lysosomal proteins in secretory granules indicates cross-talk between these two subcellular compartments, and may reveal new mechanisms of regulation of islet hormone secretion, and ultimately novel therapeutic candidates for treatment of diabetes (176,177).

1.10 Endolysosomal system of islet cells in diabetic condition

There is relationship between diabetes and lysosomal functions, in a way that alterations in lysosomal activities take part in physiopathology of diabetes.

1.10.1 Alterations in endolysosmal enzyme activities in islet cells

Alterations in the lysosomal enzyme activities have been reported in the liver, kidney, heart, saliva, brain and plasma of people with diabetes. While there is no published document to show activities of lysosomal system in α-cells, relationship between normal activities of lysosomes and insulin secretion from β-cells has been documented (178). In the β-cell, lysosomal enzyme of glucan-1,4-α-glucosidase has a direct relationship with glucose-stimulated insulin secretion from β-cells. Importantly, significant levels of abnormalities were shown in activities of lysosomal enzymes in islets of diabetic GK rats. While glucan-1,4-α-glucosidase and acid α –glucosidase showed higher activities, acid phosphatase, N-acetyl-β-D-glucosaminidase, cathepsin D, and β-glucuronidase showed diminished activities (178). Further to aberrant enzyme activities of lysosomal system in diabetes, there is uncontrolled lysosomal degradation of proinsulin/insulin in diabetic condition (179).While uncontrolled degradation of insulin in endolysosomal system participates in pathogenesis of type 2 diabetes, there is a question about implication of this aberrant system for diabetic α-cells and its potential role in glucagon hypersecretion and the hyperglucagonemia of diabetes.

1.10.2 Degradation of glucagon in endolysosomal system

In terms of glucagon degradation in α-cells, it has been shown that glucagon is taken up by α-cells after secretion and then directed into the lysosome. Within the lysosome, glucagon is dissociated from its receptor and then undergoes degradation (180). illustrating the capability of the α-cell to degrade glucagon through the endolysosomal system. Degradation of the endocytosed glucagon is governed by the rate of fusion between endocytic vesicles and lysosomes. This fusion event is a rate limiting step for the degradation of endocytic vesicle contents in the lysosome and could be altered in response to changes in microenvironmental conditions. For instance, α-cells simultaneously internalize several receptor-bound islet hormones, which may saturate the endolysosomal system and consequently inhibit glucagon degradation (180).

In a parallel finding on β-cells, it was proposed that insulin also will be taken up after secretion by β-cells and then undergo degradation in the lysosomal system (181). In

diabetes, aberrant insulin degradation in β-cells has been proposed as underlying mechanism for β-cell failure in type 2 diabetes (179). Importantly, in the context of diabetes, there is no published document to show status of glucagon degradation within endosomal/lysosomal system of α-cells.

1.11 Aims and rationale of the study

Based on the glucagoncentric hypothesis of diabetes, hyperglycemia of diabetes would be due to hyperglucagonemia instead of hypoinsulinemia. Several theories have been proposed to address underlying mechanisms of glucagon hypersecretion from α-cells. While some researchers have focused on glucose-regulated glucagon secretion from α-cells and alterations in its signaling processes in diabetes, some other researchers targeted paracrine effectors as major determinants in glucagon secretion and their disturbances in diabetes. Additionally, protein components of the regulated secretory pathway also regulate glucagon secretion from α-cells. In this context, our laboratory has already shown that alterations in ambient glucose levels alters levels of proteins in the regulated secretory pathway in α-cells. The prevailing hypothesis is that dissecting the cellular mechanisms of glucagon trafficking in the α-cell may reveal novel proteins, or networks of proteins, that function in glucagon secretion, and provide explanations for the hyperglucagonemia of diabetes.

Mapping of the α-cell secretory granule proteome under different microenvironmental inputs, such as glucose or insulin, would likely provide answers to our questions regarding the regulation of glucagon secretion in normal physiology, and in the pathobiology of diabetes. It may also reveal novel inputs to secretory granules, new cellular pathways by which glucagon secretion is regulated, and new insights into the development of hyperglucagonemia.

The specific aims of my thesis are:

1) To determine the glucagon interactome in the secretory granules of α-cells and its potential plasticity in response to microenvironmental conditions.

2) To identify and characterize a protein within the interactome that modulates glucagon secretion in normal α-cells by regulating its intracellular trafficking.

3) To determine how the interactome protein-mediated trafficking of glucagon is altered in the hyperglucagonemia of diabetes.

1.12 References

1. International Diabetes Federation. The global impact of diabetes. *Int Diabetes Fed* (2019) Available at: https://idf.org/aboutdiabetes/what-is-diabetes.html

2. Houlden RL. 2018 clinical practice guidelines -Introduction- diabetes Canada clinical practice guidelines expert committee. *Can J Diabetes* (2018) **42**:S1–S5. doi:10.1016/j.jcjd.2017.10.001

3. Unger RH, Cherrington AD. Glucagonocentric restructuring of diabetes: A pathophysiologic and therapeutic makeover. *J Clin Invest* (2012) **122**:4–12. doi:10.1172/JCI60016

4. Hædersdal S, Lund A, Knop FK, Vilsbøll T. The role of glucagon in the pathophysiology and treatment of type 2 diabetes. *Mayo Clin Proc* (2018) **93**:217–239. doi:10.1016/j.mayocp.2017.12.003

5. Ojha A, Ojha U, Mohammed R, Chandrashekar A, Ojha H. Current perspective on the role of insulin and glucagon in the pathogenesis and treatment of type 2 diabetes mellitus. *Clin Pharmacol Adv Appl* (2019) **11**:57–65. doi:10.2147/CPAA.S202614

6. Kawamori D, Katakami N, Takahara M, Miyashita K, Sakamoto F, Yasuda T, et al. Dysregulated plasma glucagon levels in Japanese young adult type 1 diabetes patients. *J Diabetes Investig* (2019) **10**:62–66. doi:10.1111/jdi.12862

7. Ceriello A, Genovese S, Mannucci E, Gronda E. Glucagon and heart in type 2

diabetes: New perspectives. *Cardiovasc Diabetol* (2016) **15**:1–7. doi:10.1186/s12933-016-0440-3

8. Li XC, Zhuo JL. Current insights and new perspectives on the roles of hyperglucagonemia in non insulin-dependent type 2 diabetes. *Curr Hypertens Rep* (2013) **15**:522–30. doi:10.1007/s11906-013-0383-y

9. Rouille Y, Westermark G, Martin SK, Steiner DF. Proglucagon is processed to glucagon by prohormone convertase PC2 in alpha TC1-6 cells. *Proc Natl Acad Sci* (1994) **91**:3242–3246. doi:10.1073/pnas.91.8.3242

10. Dhanvantari S, Seidah NG, Brubaker PL. Role of prohormone convertases in the tissue-specific processing of proglucagon. *Mol Endocrinol* (1996) **10**:342–355. doi:10.1210/me.10.4.342

11. Rouillé Y, Bianchi M, Irminger JC, Halban PA. Role of the prohormone convertase PC2 in the processing of proglucagon to glucagon. *FEBS Lett* (1997) **413**:119–123. doi:10.1016/S0014-5793(97)00892-2

12. Scott R V, Bloom SR. Peptides problem or solution : The strange story of glucagon. *Peptides* (2018) **100**:36–41. doi:10.1016/j.peptides.2017.11.013

13. Dunning BE, Foley JE, Ahrén B. Alpha cell function in health and disease: Influence of glucagon-like peptide-1. *Diabetologia* (2005) **48**:1700–1713. doi:10.1007/s00125-005-1878-0

14. Gylfe E. Glucose control of glucagon secretion—‘There’s a brand-new gimmick every year.’ *Ups J Med Sci* (2016) **9734**:1–13. doi:10.3109/03009734.2016.1154905

15. Knudsen J, Hamilton A, Ramracheya R, Tarasov A, Brereton M, Haythorne E, et al. Dysregulation of glucagon secretion by hyperglycemia-induced sodium-dependent reduction of ATP production. *Cell Metab* (2018)1–13. doi:10.1016/j.cmet.2018.10.003

16. Janah L, Kjeldsen S, Galsgaard KD, Winther-Sørensen M, Stojanovska E, Pedersen J, et al. Glucagon receptor signaling and glucagon resistance. *Int J Mol Sci* (2019) **20**: doi:10.3390/ijms20133314

17. Thiessen SE. Gunst J, Van den Berghe G. Role of glucagon in protein catabolism. *Curr Opin Crit Care* (2018) **24**:228–234. doi:10.1097/MCC.0000000000000509

18. Gerich J, Cryer P, Rizza R. Hormonal mechanisms in acute glucose counterregulation: The relative roles of glucagon, epinephrine, norepinephrine, growth hormone, and cortisol. *Metabolism* (1980) **29**:1164–1175. doi:10.1016/0026-0495(80)90026-8

19. Cryer PE, Tse TF, Clutter WE SS. Roles of glucagon and epinephrine in hypoglycemic and nonhypoglycemic glucose counterregulation in humans. *Am J Physiol* (1984) **247**:E198-205.

20. Galsgaard KD, Pedersen J, Knop FK, Holst JJ, Albrechtsen NJW. Glucagon receptor signaling and lipid metabolism. *Front Physiol* (2019) **10**:1–11. doi:10.3389/fphys.2019.00413

21. Perea A , Clemente F, Martinell J , Villanueva-Peñacarrillo ML , Valverde I.. Physiological effect of glucagon in human isolated adipocytes. *Horm Metab Res* (1995) **27**:372–375. doi:10.1055/s-2007-979981

22. Richter WO, Robl H, Schwandt P. Human glucagon and vasoactive intestinal polypeptide (VIP) stimulate free fatty acid release from human adipose tissue in vitro. *Peptides* (1989) **10**:333–335. doi:10.1016/0196-9781(89)90039-9

23. Højbjerg Gravholt C, Møller N, Jensen MD, Christiansen JS, Schmitz O. Physiological levels of glucagon do not influence lipolysis in abdominal adipose tissue as assessed by microdialysis. *J Clin Endocrinol Metab* (2001) **86**:2085–2089. doi:10.1210/jc.86.5.2085

24. Svoboda M, Tastenoy M, Vertongen P, Robberecht P. Relative quantitative analysis of glucagon receptor mRNA in rat tissues. *Mol Cell Endocrinol* (1994)

105:131–137. doi:10.1016/0303-7207(94)90162-7

25. van der Woning B, De Boeck G, Blanchetot C, Bobkov V, Klarenbeek A, Saunders M. DNA immunization combined with scFv phage display identi fi es antagonistic GCGR speci fi c antibodies and reveals new epitopes on the small extracellular loops. *MAbs* (2016) **8**:1126–1135. doi:10.1080/19420862.2016.1189050

26. Watanabe C, Seino Y, Miyahira H, Yamamoto M, Fukami A, Ozaki N, et al. Remodeling of hepatic metabolism and hyperaminoacidemia in mice deficient in proglucagon-derived peptides. *Diabetes* (2012) **61**:74–84. doi:10.2337/db11-0739

27. Boden G, Master RW, Rezvani IJ, Palmer JP, Lobe TE, Owen OE. Glucagon deficiency and hyperaminoacidemia after total pancreatectomy. *J Clin Invest* (1980) **65**:706–716. doi:10.1172/JCI109717

28. Charlton MR, Adey DB, Nair KS. Evidence for a catabolic role of glucagon during an amino acid load. *J Clin Invest* (1996) **98**:90–99. doi:10.1172/JCI118782

29. Solloway MJ, Madjidi A, Gu C, Eastham-Anderson J, Clarke HJ, Kljavin N, Zavala-Solorio J, Kates L, Friedman B, Brauer M, et al. Glucagon couples hepatic amino acid catabolism to mTOR-dependent regulation of α-cell mass. *Cell Rep* (2015) **12**:495–510. doi:10.1016/j.celrep.2015.06.034

30. Wei R, Gu L, Yang J, Yang K, Liu J, Le Y, et al. Antagonistic glucagon receptor antibody promotes α-cell proliferation and increases β-cell mass in diabetic mice. *iScience* (2019) **16**:326–339. doi:10.1016/j.isci.2019.05.030

31. Li M, Dean2 ED, Zhao L, Nicholson WE, Powers AC, Chen W. Glucagon receptor inactivation leads to α-cell hyperplasia in zebrafish. *J Endocrinol* (2015) **227**:93–103. doi:10.1016/j.physbeh.2017.03.040

32. Dean ED, Li M, Prasad N, Wisniewski SN, Von A, Spaeth J, Maddison L, et al. Interrupted glucagon signaling reveals hepatic-α-cell axis and role for L-glutamine in α-cell proliferation. *Cell Metab* (2017) **25**:1362–1373.

doi:10.1016/j.cmet.2017.05.011.

33. Kim J, Okamoto H, Huang ZJ, Anguiano G, Chen S, Liu Q, et al. Amino acid transporter Slc38a5 controls glucagon receptor inhibition-induced pancreatic α cell hyperplasia in mice. *Cell Metab* (2017) **25**:1348-1361.e8. doi:10.1016/j.cmet.2017.05.006

34. Hayashi Y, Seino Y. Regulation of amino acid metabolism and α-cell proliferation by glucagon. *J Diabetes Investig* (2018) **9**:464–472. doi:10.1111/jdi.12797

35. Indiveri C. Glutamine transport and mitochondrial metabolism in cancer cell growth. *Front Oncol* (2017) **7**:1–9. doi:10.3389/fonc.2017.00306

36. Chan EK, Mackey MA, Snover DC, Schneider PD, Rucker RD, Eugene Allen C, et al. Suppression of weight gain by glucagon in obese Zucker rats. *Exp Mol Pathol* (1984) **40**:320–327. doi:10.1016/0014-4800(84)90049-2

37. Heppner KM, Habegger KM, Day J, Pfluger PT, Perez-Tilve D, Ward B, et al. Glucagon regulation of energy metabolism. *Physiol Behav* (2010) **100**:545–548. doi:10.1016/j.physbeh.2010.03.019

38. Kim T, Nason S, Holleman C, Pepin M, Wilson L, Berryhill TF, et al. Glucagon receptor signaling regulates energy metabolism via hepatic farnesoid X receptor and fibroblast growth factor 21. *Diabetes* (2018) **67**:1773–1782. doi:10.2337/db17-1502

39. Beaudry JL, Kaur KD, Varin EM, Baggio LL, Cao X, Mulvihill EE. The brown adipose tissue glucagon receptor is functional but not essential for control of energy homeostasis in mice. *Mol Metab* (2019) **22**:37–48. doi:10.1016/j.molmet.2019.01.011

40. Kleinert M, Sachs S, Habegger KM, Hofmann SM, Müller TD. Glucagon regulation of energy expenditure. *Int J Mol Sci* (2019) **20**:5407.

41. Ramage LE, Akyol M, Fletcher AM, Morton NM, Walker BR, Stimson RH, et al.

Glucocorticoids acutely increase brown adipose tissue activity in humans , revealing species- specific differences in UCP-1 regulation. *Cell Metab* (2016) **24**:130–141. doi:10.1016/j.cmet.2016.06.011

42. Salem V, Coello C, Thomas DB, Chambers ES, Comninos AN, Buckley A, et al. Glucagon increases energy expenditure independently of brown adipose tissue activation in humans. *Diabetes, Obes Metab* (2016) **1**:72–81. doi:10.1111/dom.12585

43. Banting FG, Best CH, Collip JB, Campbell WR, Fletcher AA. Pancreatic extracts in the treatment of diabetes mellitus. 1922. *Indian J Med Res* (2007) **125**:141–146. doi:10.2337/diab.5.1.69

44. Dobbs AR, Sakurai H, Sasaki H, Faloona G, Valverde I, Baetens D, et al. Glucagon : Role in the hyperglycemia of diabetes mellitus. *Science (80-)* (1975) **187**:544–547.

45. Lee Y, Wang MY, Du XQ, Charron MJ, Unger RH. Glucagon receptor knockout prevents insulin-deficient type 1 diabetes in mice. *Diabetes* (2011) **60**:391–397. doi:10.2337/db10-0426

46. Meek TH, Dorfman MD, Matsen ME, Fischer JD, Cubelo A, Kumar MR, et al. Evidence that in uncontrolled diabetes, hyperglucagonemia is required for ketosis but not for increased hepatic glucose production or hyperglycemia. *Diabetes* (2015) **64**:2376–2387. doi:10.2337/db14-1562

47. Holst JJ, Holland W, Gromada J, Lee Y, Unger RH, Yan H, et al. Insulin and glucagon: Partners for life. *Endocrinology* (2017) **158**:696–701. doi:10.1210/en.2016-1748

48. Godoy-matos AF. The role of glucagon on type 2 diabetes at a glance. *Diabetol Metab Syndr* (2014) **6**:4–8.

49. Dunning BE, Gerich JE. The role of alpha -cell dysregulation in fasting and postprandial hyperglycemia in type 2 diabetes and therapeutic implications.

Endocr Rev (2007) **28**:253–283. doi:10.1210/er.2006-0026

50. Pearson MJ, Unger RH, Holland WL. Clinical trials, triumphs, and tribulations of glucagon receptor antagonists. *Diabetes Care* (2016) **39**:1075–1077. doi:10.2337/dci15-0033

51. Okamoto H, Cavino K, Na E, Krumm E, Kim SY, Cheng X, et al. Glucagon receptor inhibition normalizes blood glucose in severe insulin-resistant mice. *Proc Natl Acad Sci U S A* (2017) **114**:2753–2758. doi:10.1073/pnas.1621069114

52. Liang Y, Osborne MC, Monia BP, Bhanot S, Gaarde WA, Reed C. Reduction in glucagon receptor expression by an antisense oligonucleotide ameliorates diabetic syndrome in db/db mice. *Diabetes* (2004) **53**:410–417. doi:10.2337/diabetes.53.2.410

53. Pettus J, Reeds D, Cavaiola TS, Boeder S, Levin M, Tobin G, et al. Effect of a glucagon receptor antibody (REMD-477) in type 1 diabetes: A randomized controlled trial. *Diabetes, Obes Metab* (2018) **20**:1302–1305. doi:10.1111/dom.13202

54. Kazierad DJ, Bergman A, Tan B, Erion DM, Somayaji V, Lee DS, et al. Effects of multiple ascending doses of the glucagon receptor antagonist PF-06291874 in patients with type 2 diabetes mellitus. *Diabetes, Obes Metab* (2016) **18**:795–802. doi:10.1111/dom.12672

55. Kazda CM, Ding Y, Kelly RP, Garhyan P, Shi C, Lim CN, et al. Evaluation of efficacy and safety of the glucagon receptor antagonist LY2409021 in patients with type 2 diabetes: 12-and 24-week phase 2 studies. *Diabetes Care* (2016) **39**:1241–1249. doi:10.2337/dc15-1643

56. Kazierad DJ, Chidsey K, Somayaji VR, Bergman AJ, Calle RA. Efficacy and safety of the glucagon receptor antagonist PF-06291874: A 12-week, randomized, dose-response study in patients with type 2 diabetes mellitus on background metformin therapy. *Diabetes, Obes Metab* (2018) **20**:2608–2616.

doi:10.1111/dom.13440

57. Vajda EG, Logan D, Lasseter K, Armas D, Plotkin DJ, Pipkin JD, et al. Pharmacokinetics and pharmacodynamics of single and multiple doses of the glucagon receptor antagonist LGD-6972 in healthy subjects and subjects with type 2 diabetes mellitus. *Diabetes, Obes Metab* (2017) **19**:24–32. doi:10.1111/dom.12752

58. Guan HP, Yang X, Lu K, Wang SP, Castro-Perez JM, Previs S, et al. Glucagon receptor antagonism induces increased cholesterol absorption. *J Lipid Res* (2015) **56**:2183–2195. doi:10.1194/jlr.M060897

59. Nunez DJ, D'Alessio D. Glucagon receptor as a drug target: A witches' brew of eye of newt (peptides) and toe of frog (receptors). *Diabetes, Obes Metab* (2018) **20**:233–237. doi:10.1111/dom.13102

60. Grøndahl MF, Keating DJ, Vilsbøll T, Knop FK. Current therapies that modify glucagon secretion: What is the therapeutic effect of such modifications? *Curr Diab Rep* (2017) **17**: doi:10.1007/s11892-017-0967-z

61. Salehi A, Vieira E, Gylfe E. Paradoxical stimulation of glucagon secretion by high glucose concentrations. *Diabetes* (2006) **55**:2318–2323. doi:10.2337/db06-0080

62. Omar-Hmeadi M, Lund P-E, Gandasi NR, Anders Tengholm SB. Paracrine control of alpha-cell glucagon exocytosis is compromised in human type-2 diabetes. *Nat Commun* (2020) **11**:1896. doi:10.1038/s41467-020-15717-8

63. Olsen HL, Theander S, Bokvist K, Buschard K, Wollheim CB, Gromada J. Glucose stimulates glucagon release in single rat α-cells by mechanisms that mirror the stimulus-secretion coupling in β-cells. *Endocrinology* (2005) **146**:4861–4870. doi:10.1210/en.2005-0800

64. Le Marchand SJ, Piston DW. Glucose suppression of glucagon secretion: Metabolic and calcium responses from α-cells in intact mouse pancreatic islets. *J Biol Chem* (2010) **285**:14389–14398. doi:10.1074/jbc.M109.069195

65. Zhang Q, Ramracheya R, Lahmann C, Tarasov A, Bengtsson M, Braha O, et al. Role of KATP channels in glucose-regulated glucagon secretion and impaired counterregulation in type 2 diabetes. *Cell Metab* (2013) **18**:871–882. doi:10.1016/j.cmet.2013.10.014

66. Yu Q, Shuai H, Ahooghalandari P, Gylfe E, Tengholm A. Glucose controls glucagon secretion by directly modulating cAMP in alpha cells. *Diabetologia* (2019) **62**:1212–1224. doi:10.1007/s00125-019-4857-6

67. Klec C, Ziomek G, Pichler M, Malli R, Graier WF. Calcium signaling in ß-cell physiology and pathology : A revisit. *IInt J Mol Sci* (2019) **20**:6110.

68. Tian G, Tepikin A V, Tengholm A, Gylfe E. cAMP Induces Stromal Interaction Molecule 1 (STIM1) Puncta but neither Orai1 Protein Clustering nor Store-operated Ca 2 ⁺ Entry (SOCE) in Islet Cells *. *J Biol Chem* (2012) **287**:9862–9872. doi:10.1074/jbc.M111.292854

69. Watts M, Sherman A. Modeling the pancreatic α-cell: Dual mechanisms of glucose suppression of glucagon secretion. *Biophys J* (2014) **106**:741–751. doi:10.1016/j.bpj.2013.11.4504

70. Honzawa N, Fujimoto K, Kitamura T. Cell autonomous dysfunction and insulin resistance in pancreatic α cells. *Int J Mol Sci* (2019) **20**: doi:10.3390/ijms20153699

71. Gromada J, Franklin I, Wollheim CB. Alpha-cells of the endocrine pancreas: 35 years of research but the enigma remains. *Endocr Rev* (2007) **28**:84–116. doi:10.1210/er.2006-0007

72. Quesada I, Tudurí E, Ripoll C, Nadal A. Physiology of the pancreatic alpha-cell and glucagon secretion: role in glucose homeostasis and diabetes. *J Endocrinol* (2008) **199**:5–19. doi:10.1677/JOE-08-0290

73. Kawamori D, Kulkarni RN. Insulin modulation of glucagon secretion: the role of insulin and other factors in the regulation of glucagon secretion. *Islets* (2009) **1**:276–279. doi:10.4161/isl.1.3.9967

74. Hauge-Evans AC, Anderson RL, Persaud SJ, Jones PM. Delta cell secretory responses to insulin secretagogues are not mediated indirectly by insulin. *Diabetologia* (2012) **55**:1995–2004. doi:10.1007/s00125-012-2546-9

75. Vergari E, Knudsen JG, Ramracheya R, Salehi A, Zhang Q, Adam J, et al. Insulin inhibits glucagon release by SGLT2-induced stimulation of somatostatin secretion. *Nat Commun* (2019) **10**:1–11. doi:10.1038/s41467-018-08193-8

76. Wendt A, Birnir B, Buschard K, Gromada J, Salehi A, Sewing S, et al. Glucose inhibition of glucagon secretion from rat α-cells is mediated by GABA released from neighboring β-cells. *Diabetes* (2004) **53**:1038–1045. doi:10.2337/diabetes.53.4.1038

77. Li C, Liu C, Nissim I, Chen J, Chen P, Doliba N, et al. Regulation of glucagon secretion in normal and diabetic human islets by gamma-hydroxybutyrate and glycine. *J Biol Chem* (2013) **288**:3938–3951. doi:10.1074/jbc.M112.385682

78. Rorsman P, Berggren P, Bokvist K, Ericson H, Möhler H, Ostenson C et al. Glucose-inhibition of glucagon secretion involves activation of GABAA-receptor chloride channels. *Nature* (1989) **341**:233–236. doi:10.1038/341233a0

79. Xu E, Kumar M, Zhang Y, Ju W, Obata T, Zhang N, Liu S, Wendt A, Deng S, Ebina Y, et al. Intra-islet insulin suppresses glucagon release via GABA-GABAA receptor system. *Cell Metab* (2006) **3**:47–58. doi:10.1016/j.cmet.2005.11.015

80. Feng AL, Xiang Y, Gui L, Kaltsidis G, Feng Q, Lu W. Paracrine GABA and insulin regulate pancreatic alpha cell proliferation in a mouse model of type 1 diabetes. *Diabetologia* (2017) **60**:1033–1042. doi:10.1007/s00125-017-4239-x

81. Li J., Casteels T, Frogne T, Ingvorsen C, Honore C, Courtney M. et al. Artemisinins target GABAA receptor signaling and impair α cell identity. *Cell* (2017) **168**:86-100.e15. doi:10.1016/j.cell.2016.11.010

82. Weir GC, Bonner-Weir S. GABA signaling stimulates β- cell regeneration in diabetic mice. *Cell* (2017) **168**:7–9. doi:10.1016/j.cell.2016.12.006

83. Ben-Othman N, Vieira A, Courtney M, Record F, Gjernes E, Avolio F, et al. Long-term GABA administration induces alpha cell-mediated beta-like cell neogenesis. *Cell* (2017) **168**:73-85.e11. doi:10.1016/j.cell.2016.11.002

84. Woalder. Human beta cells produce and release serotonin to inhibit glucagon secretion from alpha cells. *Cell Rep* (2016) **17**:3281–3291. doi:10.1016/j.celrep.2016.11.072

85. Bennet H, Balhuizen A, Medina A, Dekker Nitert M, Ottosson Laakso E, Essén S, et al. Altered serotonin (5-HT) 1D and 2A receptor expression may contribute to defective insulin and glucagon secretion in human type 2 diabetes. *Peptides* (2015) **71**:113–120. doi:10.1016/j.peptides.2015.07.008

86. Ludvik B, Thomaseth K, Nolan JJ, Clodi M, Prager R, Pacini G. Inverse relation between amylin and glucagon secretion in healthy and diabetic human subjects. *Eur J Clin Invest* (2003) **33**:316–322. doi:10.1046/j.1365-2362.2003.01142.x

87. Young A. Inhibition of glucagon secretion. *Adv Pharmacol* (2005) **52**:151–71. doi:10.1016/S1054-3589(05)52008-8

88. Fineman MS, Koda JE, Shen LZ, Strobel SA, Maggs DG, Weyer C, et al. The human amylin analog, pramlintide, corrects postprandial hyperglucagonemia in patients with type 1 diabetes. *Metabolism* (2002) **51**:636–641. doi:10.1053/meta.2002.32022

89. Gedulin BR, Jodka CM, Herrmann K, Young AA. Role of endogenous amylin in glucagon secretion and gastric emptying in rats demonstrated with the selective antagonist, AC187. *Regul Pept* (2006) **137**:121–127. doi:10.1016/j.regpep.2006.06.004

90. Zhang X-X, Pan Y-H, Huang Y-M, Zhao H-L. Neuroendocrine hormone amylin in diabetes. *World J Diabetes* (2016) **7**:189. doi:10.4239/wjd.v7.i9.189

91. Novak I. Purinergic receptors in the endocrine and exocrine pancreas. *Purinergic Signal* (2008) **4**:237–253. doi:10.1007/s11302-007-9087-6

92. Yang GK, Squires PE, Tian F, Kieffer TJ, Kwok YN, Dale N. Glucose decreases extracellular adenosine levels in isolated mouse and rat pancreatic islets. *Islets* (2012) **4**:64–70. doi:10.4161/isl.4.1.19037

93. Yip L, Taylor C, Whiting CC, Fathman CG. Diminished adenosine a1 receptor expression in pancreatic a-cells may contribute to the patholog y of type 1 diabetes. *Diabetes* (2013) **62**:4208–4219. doi:10.2337/db13-0614

94. Ishihara H, Wollheim CB. Is zinc an intra-islet regulator of glucagon secretion? *Diabetol Int* (2016) **7**:106–110. doi:10.1007/s13340-016-0259-x

95. Franklin, I., Gromada, J., Gjinovci A., Theander, S. WCB. Beta cell secretory products activate alpha cell ATP-dependent potassium channels to inhibit glucagon release. *Diabetes* (2005) **54**:1808–1815.

96. Ravier MA, Rutter GA. Glucose or insulin, but not zinc ions, inhibit glucagon secretion from mouse pancreatic [alpha]-cells. *Diabetes* (2005) **54**:1789–1797. doi:10.2337/diabetes.54.6.1789

97. Ramracheya R, Ward C, Shigeto M, Walker JN, Amisten S, Zhang Q, et al. Membrane potential-dependent inactivation of voltage-gated ion channels in α-cells inhibits glucagon secretion from human islets. *Diabetes* (2010) **59**:2198–2208. doi:10.2337/db09-1505

98. Solomou A, Philippe E, Chabosseau P, Migrenne-li S, Gaitan J, Lang J, et al. Over-expression of Slc30a8 / ZnT8 selectively in the mouse α cell impairs glucagon release and responses to hypoglycemia. *Nutr Metab (Lond)* (2016) **13**:46. doi:10.1186/s12986-016-0104-z

99. Solomou A, Meur G, Bellomo E, Hodson DJ, Tomas A, Li SM, et al. The Zinc transporter Slc30a8/ZnT8 is required in a subpopulation of pancreatic α-cells for hypoglycemia-induced glucagon secretion. *J Biol Chem* (2015) **290**:21432–21442. doi:10.1074/jbc.M115.645291

100. Rodriguez-diaz R, Dando R, Jacques-silva MC, Fachado A, Molina J, Abdulreda

M, et al. Alpha cells secrete acetylcholine as a non-neuronal paracrine signal priming human beta cell function. *Nat Med* (2012) **17**:888–892. doi:10.1038/nm.2371.Alpha

101. Wessler I, Kirkpatrick CJ. Acetylcholine beyond neurons: The non-neuronal cholinergic system in humans. *Br J Pharmacol* (2008) **154**:1558–1571. doi:10.1038/bjp.2008.185

102. Hayashi M, Yamada H, Uehara S, Morimoto R, Muroyama A, Yatsushiro S, et al. Secretory granule-mediated co-secretion of L-glutamate and glucagon triggers glutamatergic signal transmission in islets of Langerhans. *J Biol Chem* (2003) **278**:1966–1974. doi:10.1074/jbc.M206758200

103. Gaisano HY, Leung YM. Pancreatic islet α-cell commands itself: Secrete more glucagon! *Cell Metab* (2008) **7**:474–475. doi:10.1016/j.cmet.2008.05.003

104. Cabrera O, Jacques-Silva MC, Speier S, Yang SN, Köhler M, Fachado A, et al. Glutamate is a positive autocrine signal for glucagon release. *Cell Metab* (2008) **503**:371–376. doi:10.1038/nature12598.DNMT1-interacting

105. Otter S, Lammert E. Exciting times for pancreatic islets: Glutamate signaling in endocrine cells. *Trends Endocrinol Metab* (2016) **27**:177–188. doi:10.1016/j.tem.2015.12.004

106. Huang XT, Li C, Peng XP, Guo J, Yue SJ, Liu W, et al. An excessive increase in glutamate contributes to glucose-toxicity in β-cells via activation of pancreatic NMDA receptors in rodent diabetes. *Sci Rep* (2017) **7**:1–14. doi:10.1038/srep44120

107. Ma X, Zhang Y, Gromada J, Sewing S, Berggren PO, Buschard K, et al. Glucagon stimulates exocytosis in mouse and rat pancreatic α-cells by binding to glucagon receptors. *Mol Endocrinol* (2005) **19**:198–212. doi:10.1210/me.2004-0059

108. Caicedo A. Paracrine and autocrine interactions in the human islet: more than meets the eye. *Semin Cell Dev Biol* (2012) **76**:211–220. doi:10.1007/s11103-011-

9767-z.Plastid

109. Li H, Liu T, Lim J, Gounko N V, Hong W, Han W. Increased biogenesis of glucagon-containing secretory granules and glucagon secretion in BIG3-knockout mice. *Mol Metab* (2015) **4**:246–242. doi:10.1016/j.molmet.2015.01.001

110. Rutter GA. Regulating glucagon secretion : Somatostatin in the spotlight. *Diabetes* (2009) **58**:299–301. doi:10.2337/db08-1534

111. Arrojo e Drigo R, Ali Y, Diez J, Srinivasan DK, Berggren PO, Boehm BO. New insights into the architecture of the islet of Langerhans: a focused cross-species assessment. *Diabetologia* (2015) **58**:2218–2228. doi:10.1007/s00125-015-3699-0

112. Bonner-Weir S, Sullivan BA, Weir GC. Human islet morphology revisited: human and rodent islets are not So different after all. *J Histochem Cytochem* (2015) **63**:604–612. doi:10.1369/0022155415570969

113. Briant LJB, Reinbothe TM, Spiliotis I, Miranda C, Rodriguez BRP. δ -cells and β -cells are electrically coupled and regulate α -cell activity via somatostatin. *J Physiol* (2018) **2**:197–215. doi:10.1113/JP274581

114. Braun M, Ramracheya R, Amisten S. Somatostatin release , electrical activity , membrane currents and exocytosis in human pancreatic delta cells. *Diabetologia* (2009) **52**:1566–1578. doi:10.1007/s00125-009-1382-z

115. Zhu L, Doliba NM, Wess J, Zhu L, Dattaroy D, Pham J, et al. Intraislet glucagon signaling is critical for maintaining glucose homeostasis. *JCI Insight* (2019) **4**:e127994.

116. Capozzi ME, Wait JB, Koech J, Gordon AN, Coch RW, Svendsen B, Finan B, D'Alessio DA, Campbell JE. Glucagon lowers glycemia when β cells are active. *JCI Insight* (2019) **4**: doi:10.1172/jci.insight.129954

117. Færch K, Vistisen D, Pacini G, Torekov SS, Johansen NB, Witte DR, et al. Insulin resistance is accompanied by increased fasting glucagon and delayed glucagon

suppression in individuals with normal and impaired glucose regulation. *Diabetes* (2016) **65**:3473–3481. doi:10.2337/db16-0240

118. Kellard JA, Rorsman NJG, Hill TG, Armour SL, Van De Bunt M, Rorsman P, et al. Reduced somatostatin signalling leads to hypersecretion of glucagon in mice fed a high fat diet. *bioRxiv* (2020) doi:10.1101/2020.04.07.028258.

119. Böni-Schnetzler M, Meier DT. Islet inflammation in type 2 diabetes. *Semin Immunopathol* (2019) **41**:501–513. doi:10.1007/s00281-019-00745-4

120. Donath MY, Dinarello CA, Mandrup-Poulsen T. Targeting innate immune mediators in type 1 and type 2 diabetes. *Nat Rev Immunol* (2019) **19**:734–746. doi:10.1038/s41577-019-0213-9

121. Imai Y, Dobrian AD, Morris MA, Nadle JL. Islet inflammation: A unifying target for diabetes treatment. *Trends Endocrinol Metab* (2013) **24**:351–360. doi:10.1038/jid.2014.371

122. Hare KJ, Knop FK, Asmar M, Madsbad S, Deacon CF, Holst JJ, et al. Preserved inhibitory potency of GLP-1 on glucagon secretion in type 2 diabetes mellitus. *J Clin Endocrinol Metab* (2009) **94**:4679–4687. doi:10.1210/jc.2009-0921

123. Meier JJ, Nauck MA, Pott A, Heinze KAI, Goetze O, Bulut K, et al. Glucagon-like peptide 2 stimulates glucagon secretion, enhances lipid absorption, and inhibits gastric acid secretion in humans. *Gastroenterology* (2006) **130**:44–54. doi:10.1053/j.gastro.2005.10.004

124. Meier JJ, Gallwitz B, Siepmann N, Holst JJ, Deacon CF, Schmidt WE, et al. Gastric inhibitory polypeptide (GIP) dose-dependently stimulates glucagon secretion in healthy human subjects at euglycaemia. *Diabetologia* (2003) **46**:798–801. doi:10.1007/s00125-003-1103-y

125. Christensen M, Vedtofte L, Holst JJ, Vilsbøll T, Knop FK. Glucose-dependent insulinotropic polypeptide: A bifunctional glucose-dependent regulator of glucagon and insulin secretion in humans. *Diabetes* (2011) **60**:3103–3109.

doi:10.2337/db11-0979

126. Lund A, Vilsboll T, Bagger JI, Holst JJ, Knop FK. The separate and combined impact of the intestinal hormones, GIP, GLP-1, and GLP-2, on glucagon secretion in type 2 diabetes. *Am J Physiol - Endocrinol Metab* (2011) **300**:1038–1046. doi:10.1152/ajpendo.00665.2010

127. Fava GE, Dong EW, Wu H. Intra-islet glucagon-like peptide-1. *J Diabetes Complicat* (2017) **30**:1651–1658. doi:10.1016/j.jdiacomp.2016.05.016.INTRA-ISLET

128. Campbell SA, Golec D, Hubert M, Johnson J, Salamon N, Barr A, et al. Human islets contain a subpopulation of glucagon-like peptide-1 secreting α cells that is increased in type 2 diabetes. *Mol Metab* (2020)101014. doi:10.1016/j.molmet.2020.101014

129. Chambers AP, Sorrell JE, Haller A, Roelofs K, Hutch CR, Kim KS, et al. The Role of Pancreatic Preproglucagon in Glucose Homeostasis in Mice. *Cell Metab* (2017) **25**:927-934.e3. doi:10.1016/j.cmet.2017.02.008

130. Marc Y. Donath RB. GLP-1 effects on islets: hormonal, neuronal, or paracrine? *Diabetes Care* (2013) **36**:S145–S148. doi:10.2337/dcS13-2015

131. Habener JF, Stanojevic V. α -cell role in β -cell generation and regeneration. *Islets* (2012) **4**:188–198.

132. Habener JF, Stanojevic V. Pancreas and not gut mediates the GLP-1-induced glucoincretin effect. *Cell Metab* (2017) **25**:757–758. doi:10.1016/j.cmet.2017.03.020

133. Holst J, Christensen M, Lund A, De Heer J, Svendsen B, Kielgast U, et al. Regulation of glucagon secretion by incretins. *Diabetes, Obes Metab* (2011) **13**:89–94. doi:10.1111/j.1463-1326.2011.01452.x

134. De Marinis YZ, Salehi A, Ward CE, Zhang Q, Abdulkader F, Bengtsson M, et al.

GLP-1 inhibits and adrenaline stimulates glucagon release by differential modulation of N- and L-type Ca2+ channel-dependent exocytosis. *Cell Metab* (2010) **11**:543–553. doi:10.1016/j.cmet.2010.04.007

135. J de Heer, C Rasmussen, D H Coy JJH. Glucagon-like peptide-1, but not glucose-dependent insulinotropic peptide, inhibits glucagon secretion via somatostatin (receptor subtype 2) in the perfused rat pancreas. *Diabetologia* (2008) **51**:2263–70. doi:10.1007/s00125-008-1149-y

136. Tooze S. Biogenesis of secretory granules in the trans-Golgi network of neuroendocrine and endocrine cells. *Biochim Biophys Acta* (1998) **1404**:231–244. doi:10.1016/s0167-4889(98)00059-7

137. Malosio ML, Giordano T, Laslop A, Meldolesi J. Dense-core granules: a specific hallmark of the neuronal/neurosecretory cell phenotype. *J Cell Sci* (2004) **117**:743–749. doi:10.1242/jcs.00934

138. Cool DR, Normant E, Shen FS, Chen HC, Pannell L, Zhang Y, et al. Carboxypeptidase E is a regulated secretory pathway sorting receptor: Genetic obliteration leads to endocrine disorders in Cpe(fat) mice. *Cell* (1997) **88**:73–83. doi:10.1016/S0092-8674(00)81860-7

139. Irminger JC, Verchere CB, Meyer K, Halban PA. Proinsulin targeting to the regulated pathway is not impaired in carboxypeptidase E-deficient Cpe(fat)/Cpe(fat) mice. *J Biol Chem* (1997) **272**:27532–27534. doi:10.1074/jbc.272.44.27532

140. Dhanvantari S, Shen F-S, Adams T, Snell CR, Zhang C, Mackin RB, et al. Disruption of a receptor-mediated mechanism for intracellular sorting of proinsulin in familial hyperproinsulinemia. *Mol Endocrinol* (2003) **17**:1856–1867. doi:10.1210/me.2002-0380

141. McGirr R, Guizzetti L, Dhanvanta ri S. The sorting of proglucagon to secretory granules is mediated by carboxypeptidase E and intrinsic sorting signals. *J*

Endocrinol (2013) **217**:229–40. doi:10.1530/JOE-12-0468

142. Cool DR, Fenger M, Snell CR, Loh YP. Identification of the sorting signal motif within pro-opiomelanocortin for the regulated secretory pathway. *J Biol Chem* (1995) **270**:8723–8729. doi:10.1074/jbc.270.15.8723

143. Zhang CF, Dhanvantari S, Lou H, Loh YP. Sorting of carboxypeptidase E to the regulated secretory pathway requires interaction of its transmembrane domain with lipid rafts. *Biochem J* (2003) **369**:453–460. doi:10.1042/BJ20020827

144. Arvan P, Halban PA. Sorting ourselves out: Seeking consensus on trafficking in the beta-cell. *Traffic* (2004) **5**:53–61. doi:10.1111/j.1600-0854.2004.00152.x

145. Guizzetti L, McGirr R, Dhanvantari S. Two dipolar alpha-helices within hormone-encoding regions of proglucagon are sorting signals to the regulated secretory pathway. *J Biol Chem* (2014) **289**:14968–14980. doi:10.1074/jbc.M114.563684

146. Dey A, Lipkind GM, Rouillé Y, Norrbom C, Stein J, Zhang C, Carroll R, Steiner DF. Significance of prohormone convertase 2, PC2, mediated initial cleavage at the proglucagon interdomain site, Lys70-Arg71, to generate glucagon. *Endocrinology* (2005) **146**:713–727. doi:10.1210/en.2004-1118

147. Furuta M, Zhou A, Webb G, Carroll R, Ravazzola M, Orci L, et al. Severe defect in proglucagon processing in islet alpha-cells of prohormone convertase 2 null mice. *J Biol Chem* (2001) **276**:27197–27202. doi:10.1074/jbc.M103362200

148. Marchetti P, Lupi R, Bugliani M, Kirkpatrick CL, Sebastiani G, Grieco FA, et al. A local glucagon-like peptide 1 (GLP-1) system in human pancreatic islets. *Diabetologia* (2012) **55**:3262–3272. doi:10.1007/s00125-012-2716-9

149. Whalley NM, Pritchard LE, Smith DM, White A. Processing of proglucagon to GLP-1 in pancreatic alpha cells: Is this a paracrine mechanism enabling GLP-1 to act on beta cells? *J Endocrinol* (2011) **211**:99–106. doi:10.1530/JOE-11-0094

150. Ellingsgaard H, Hauselmann I, Schuler B, Habib AM, Baggio LL, Meier DT, et

al. Interleukin-6 enhances insulin secretion by increasing glucagon-like peptide-1 secretion from L cells and alpha cells. *Nat Med* (2011) **17**:1481–1489. doi:10.1038/nm.2513.Interleukin-6

151. O'Malley TJ, Fava GE, Zhang Y, Fonseca VA, Wu H. Progressive change of intra-islet GLP-1 production during diabetes development. *Diabetes Metab Res Rev* (2014) **30**:661–668. doi:10.1002/dmrr.2534

152. Kilimnik G, Kim A, Steiner DF, Friedman TC, Hara M. Intraislet production of GLP-1 by activation of prohormone convertase 1/3 in pancreatic α-cells in mouse models of -cell regeneration. *Islets* (2010) **2**:149–155. doi:10.4161/isl.2.3.11396

153. Rorsman P, Braun M, Zhang Q. Regulation of calcium in pancreatic α- and β-cells in health and disease. *Cell Calcium* (2012) **51**:300–308. doi:10.1016/j.ceca.2011.11.006

154. Quesada I, Tudurí E, Ripoll C, Nadal Á. Physiology of the pancreatic α-cell and glucagon secretion: Role in glucose homeostasis and diabetes. *J Endocrinol* (2008) **199**:5–19. doi:10.1677/JOE-08-0290

155. Le Marchand SJ, Piston DW. Glucose decouples intracellular Ca2+ activity from glucagon secretion in mouse pancreatic islet alpha-cells. *PLoS One* (2012) **7**:1–10. doi:10.1371/journal.pone.0047084

156. Hughes JW, Ustione A, Lavagnino Z, Piston DW. Regulation of islet glucagon secretion: Beyond calcium. *Diabetes, Obes Metab* (2018) **20**:127–136. doi:10.1111/dom.13381

157. González-Vélez V, Dupont G, Gil A, González A, Quesada I. Model for glucagon secretion by pancreatic α-cells. *PLoS One* (2012) **7**:e32282. doi:10.1371/journal.pone.0032282

158. Salau C, James DJ, Greaves J, Chamberlain LH. Plasma membrane targeting of exocytic SNARE proteins. *Biochim Biophys Acta* (2004) **1693**:81–89. doi:10.1016/j.bbamcr.2004.05.008

159. Andersson SA, Pedersen MG, Vikman J, Eliasson L. Glucose-dependent docking and SNARE protein-mediated exocytosis in mouse pancreatic alpha-cell. *Mol Genomic Physiol* (2011) **462**:443–454. doi:10.1007/s00424-011-0979-5

160. Gustavsson N, Wei S, Hoang DN, Lao Y, Zhang Q, Radda GK, et al. Synaptotagmin-7 is a principal Ca 2 + sensor for Ca 2 + -induced glucagon exocytosis in pancreas. *J Physiol* (2009) **587**:1169–1178. doi:10.1113/jphysiol.2008.168005

161. Gerber SH, Sudhof TC. Molecular determinants of regulated exocytosis. *Diabetes* (2002) **51 (Suppl**:3–11. doi:10.2337/diabetes.51.2007.S3

162. Jewell JL, Oh E, Thurmond DC. Exocytosis mechanisms underlying insulin release and glucose uptake : conserved roles for Munc18c and syntaxin 4. *Am J Physiol Regul Integr Comp Physiol* (2010) **298**:R517–R531. doi:10.1152/ajpregu.00597.2009.

163. Gandasi NR, Yin P, Riz M, Chibalina M V, Cortese G, Lund P, et al. Ca 2 + channel clustering with insulin-containing granules is disturbed in type 2 diabetes. *J Clin Invest* (2017) **127**:2353–2364.

164. Gromada J1, Høy M, Buschard K, Salehi A RP. Somatostatin inhibits exocytosis in rat pancreatic alpha-cells by G(i2)-dependent activation of calcineurin and depriming of secretory granules. *J Physiol* (2001) **535**:519–532. doi:10.1111/j.1469-7793.2001.00519.x

165. Metz TO, Jacobs JM, Gritsenko MA, Fontès G, Qian WJ, Camp DG, et al. Characterization of the human pancreatic islet proteome by two dimensional LC/MS/MS. *J Proteome Res* (2006) **5**:3345–3354. doi:10.1021/pr060322n

166. Zhou JY, Dann GP, Liew CW, Smith RD, Kulkarni RN, Qian WJ. Unraveling pancreatic islet biology by quantitative proteomics. *Expert Rev Proteomics* (2011) **8**:495–504. doi:10.1586/epr.11.39.Unraveling

167. Waanders LF, Chwalek K, Monetti M, Kumar C, Lammert E, Mann M.

Quantitative proteomic analysis of single pancreatic islets. *ProcNatlAcadSci USA* (2009) **106**:18902–18907. doi:0908351106 [pii]\n10.1073/pnas.0908351106

168. Xie X, Li S, Liu S, Lu Y, Shen P, Ji Ji. Proteomic analysis of mouse islets after multiple low-dose streptozotocin injection. *Biochim Biophys Acta* (2008) **1784**:276–284.

169. Ouaamari A El, Zhou J, Liew CW, Shirakawa J, Dirice E, Gedeon N, Kahraman S, Jesus DF De, Kim J, Clauss TRW, et al. Compensatory islet response to insulin resistance revealed by quantitative proteomics. *J Proteome Res* (2015) **14**:3111–3122. doi:10.1021/acs.jproteome.5b00587.Compensatory

170. Kang T, Boland BB, Jensen P, Alarcon C, Nawrocki A, Grimsby JS, et al. Characterization of signaling pathways associated with pancreatic β-cell adaptive flexibility in compensation of obesity-linked diabetes in db/db mice. *Mol Cell Proteomics* (2020) doi:10.1074/mcp.RA119.001882

171. Kang T, Boland BB, Alarcon C, Grimsby JS, Rhodes CJ, Larsen MR. Proteomic analysis of restored insulin production and trafficking in obese diabetic mouse pancreatic islets following euglycemia. *J Proteome Res* (2019) **18**:3245–3258. doi:10.1021/acs.jproteome.9b00160

172. Schvartz D, Brunner Y, Couté Y, Foti M, Wollheim CB, Sanchez JC. Improved characterization of the insulin secretory granule proteomes. *J Proteomics* (2012) **75**:4620–4631. doi:10.1016/j.jprot.2012.04.023

173. Nikhil R. Gandasi PY, Omar-Hmeadi M, Laakso EO, Petter Vikman SB. Glucose-dependent granule docking limits insulin secretion and is decreased in human type 2 diabetes. *Cell Metab* (2018) **27**:470-478.e4. doi:10.1016/j.cmet.2017.12.017

174. Li M, Du W, Zhou M, Zheng L, Song E, Hou J. Proteomic analysis of insulin secretory granules in INS-1 cells by protein correlation profiling. *Biophys Reports* (2018) **4**:329–338. doi:10.1007/s41048-018-0061-3

175. Zhou Y, Liu Z, Zhang S, Zhuang R, Liu H, Liu X et al. RILP restricts insulin

secretion through mediating lysosomal degradation of proinsulin. *Diabetes* (2020) **69**:67–82. doi:10.2337/db19-0086

176. Pinheiro-Machado E, Sandberg TOM, Pihl C, Hägglund PM, Marzec MT. In silico approach to predict pancreatic β-cells classically secreted proteins. *Biosci Rep* (2020) **40**:1–13. doi:10.1042/BSR20193708

177. Brunner Y, Couté Y, Iezzi M, Foti M, Fukuda M, Hochstrasser DF, Wollheim CB, Sanchez J-C. Proteomics analysis of insulin secretory granules. *Mol Cell Proteomics* (2007) **6**:1007–17. doi:10.1074/mcp.M600443-MCP200

178. Salehi A, Henningsson R, Mosén H, Östenson CG, Efendic S, Lundquist I. Dysfunction of the islet lysosomal system conveys impairment of glucose-induced insulin release in the diabetic GK rat. *Endocrinology* (1999) **140**:3045–3053. doi:10.1210/endo.140.7.6862

179. Pasquier A, Vivot K, Erbs E, Spiegelhalter C, Zhang Z, Aubert V et al. Lysosomal degradation of newly formed insulin granules contributes to β cell failure in diabetes. *Nat Commun* (2019) **10**:1–14. doi:10.1038/s41467-019-11170-4

180. Amherdt M, Patel YC, Orci L. Binding and internalization of somatostatin, insulin, and glucagon by cultured rat islet cells. *J Clin Invest* (1989) **84**:412–417. doi:10.1172/JCI114181

181. Wang M, Li J, Lim GE, Johnson JD. Is dynamic autocrine insulin signaling possible? A mathematical model predicts picomolar concentrations of extracellular monomeric insulin within human pancreatic islets. *PLoS One* (2013) **8**:1–10. doi:10.1371/journal.pone.0064860

Chapter 2

Statement of Copyright

This chapter was reformatted from its original published paper in Frontiers in Endocrinology under the Creative Commons Attribution 4.0 International License (https://creativecommons.org/licenses/by/4.0/).

The citation for its original work is as follows:

Asadi F, Dhanvantari S. (2019) Plasticity in the Glucagon Interactome Reveals Novel Proteins That Regulate Glucagon Secretion in α-TC1-6 Cells. Front Endocrinol (Lausanne). 9:792. doi: 10.3389/fendo.2018.00792. eCollection 2018.

2. Plasticity in the Glucagon Interactome Reveals Novel Proteins that Regulate Glucagon Secretion in α-TC1-6 Cells

2.1 Abstract

Glucagon is stored within the secretory granules of pancreatic α-cells until stimuli trigger its release. The α-cell secretory responses to the stimuli vary widely, possibly due to differences in experimental models or microenvironmental conditions. We hypothesized that the response of the α-cell to various stimuli could be due to plasticity in the network of proteins that interact with glucagon within α-cell secretory granules. We used tagged glucagon with Fc to pull out glucagon from the enriched preparation of secretory granules in α-TC1-6 cells. Isolation of secretory granules was validated by immunoisolation with Fc-glucagon and immunoblotting for organelle-specific proteins. Then, enriched secretory granules were used for affinity purification with Fc-glucagon followed by liquid chromatography/tandem mass spectrometry to identify secretory granule proteins that interact with glucagon. Proteomic analyses revealed a network of proteins containing glucose regulated protein 78 KDa, GRP78, and histone H4. The interaction between glucagon and the ER stress protein GRP78 and histone H4 was confirmed through co-immunoprecipitation of secretory granule lysates, and colocalization immunofluorescence confocal microscopy. Composition of the protein networks was altered at different glucose levels (25 mM vs 5.5 mM) and in response to the paracrine inhibitors of glucagon secretion, GABA and insulin. siRNA-mediated silencing of a subset of these proteins revealed their involvement in glucagon secretion in α-TC1-6 cells. Therefore, results indicate a novel and dynamic glucagon interactome within α-TC1-6 cell secretory granules. We suggest that variations in the α-cell secretory response to stimuli may be governed by plasticity in the glucagon "interactome".

Keywords: glucagon, α-cell, proteomics, co-immunoprecipitation, confocal microscopy, glucagon interactome, glucagon secretion

2.2 Introduction

Glucagon is the major glucose counter-regulatory hormone, and maintains euglycemia by enhancing hepatic gluconeogenesis and glycogenolysis (1). However, both type 1 and type 2 diabetes are characterized by varying levels of hyperglucagonemia (2), which paradoxically exacerbates the hyperglycemia of diabetes (3, 4). More recently, it has been shown that glucagon may be an amino acid regulatory hormone, suggesting a link between hepatic amino acid metabolism and hyperglucagonemia (5). In pancreatic α-cells, glucagon secretion is tightly regulated by nutritional, hormonal, and neural effectors to maintain normal glucose homeostasis. However, in diabetes, this tight coupling is disrupted (6), resulting in dysfunctional glucagon secretion, which may be a factor in the development of type 2 diabetes (7). This abnormal glucagon secretion has led to strategies (8) to control glucagon action to ameliorate the hyperglycemia of diabetes, such as administering glucagon receptor antagonists or neutralizing antibodies against the glucagon receptor (9, 10). Although effective in the short term, this strategy tends to increase α-cell mass and worsen α-cell dysfunction over the long term (6). Therefore, a preferable strategy may be to control the secretion, rather than the action, of glucagon for improved glycemic control in diabetes.

In the context of the pancreatic islet, there is some debate as to whether glucagon secretion is primarily regulated by the paracrine influence of the β-cell, or through intrinsic factors (11, 12). Both insulin and GABA secreted from the β-cell strongly inhibit glucagon secretion, as does somatostatin (13, 14). However, these actions are dependent on prevailing glucose concentrations; at 5 mM glucose, both glucagon and insulin secretion are maximally suppressed (11), suggesting that intrinsic factors may exert an equally prominent influence on glucagon secretion. Some proposed mechanisms of intrinsic regulation of glucagon secretion include glucose metabolic-induced changes in Ca^{2+} and K^{+} membrane conductances or intracellular Ca^{2+} oscillations (15, 16). Intrinsic factors can also include proteins involved in the intracellular trafficking of glucagon. We have previously shown that prolonged culture of α-TC1-6 cells in medium containing 25 mM glucose resulted in the up-regulation of components of the regulated secretory pathway (17), notably proteins associated with secretory granules, such as SNARE

exocytotic proteins and granins. There may be direct interactions between granule proteins, such as chromogranin A and carboxypeptidase E, to ensure proper trafficking of glucagon into secretory granules (18), and distinct sorting signals within glucagon may mediate these interactions (19). Therefore, proteins within the α-cell secretory granules that directly interact with glucagon may provide additional clues for the regulation of glucagon secretion.

In order to identify networks of secretory granule proteins that interact with glucagon, we have continued to use the α-TC1-6 cell line, as this is a well-established cell line in which to study the intrinsic regulation of glucagon secretion (20). This cell line has been extensively used to study glucagon secretory pathway (17, 21) due to its resemblance to the normal pancreatic α-cell in terms of proglucagon processing (22) and response to insulin and somatostatin and nutritional effectors (12, 17). Our work has revealed a novel glucagon "interactome" that exhibits plasticity in response to glucose, insulin and GABA, and contains some novel glucagon-interacting proteins that may regulate glucagon secretion in α-TC1-6 cells.

2.3 Materials and methods

Sources for all reagents, assays, and software packages are listed in Supplementary Table 2-1.

2.3.1 Gene construct and plasmid preparation

We designed a glucagon fusion construct [Fc-glucagon –pcDNA3.1(+)] as follows: the amino acid sequence of glucagon derived from human proglucagon (GenScript, USA; http://www.genscript.com) was fused to the 3′ end of cDNA encoding the CH2/CH3 domain of mouse IgG-2b (Fc), preceded by a 28 amino acid signal peptide as described previously (19). As a negative control for all transfections, proteomics, immunofluorescence microscopy, and co-immunoprecipitation experiments, we also designed a Fc-pcDNA3.1(+) construct. DNA sequences were confirmed at the London Regional Genomics Facility, Western University.

2.3.2 Extraction and enrichment of secretory granules

Wild type α-TC1-6 cells (a kind gift from C. Bruce Verchere, Vancouver, BC) were cultured in DMEM containing 25 mM glucose, L-glutamine, 15% horse serum, and 2.5% fetal bovine serum, as described previously (17, 23). Based on the ATCC product sheet, the base cell culture medium for α-TC1-6 cells is low glucose (5.5 mM) Dulbecco's Modified Eagle's Medium (DMEM); however, for glucagon secretion (glucagon hypersecretion) studies, high glucose DMEM (16.7 or 25 mM) has been traditionally used to prepare α-TC-6 cells for downstream experiments (17, 24). Cells were grown to 90% confluency and transfected with Fc alone or Fc-glucagon using Lipofectamine 2000. To determine changes in granule size, mass, and proteome, cells were transiently transfected with Fc-glucagon or Fc-alone and then incubated with or without GABA (25 μM), insulin (100 pM), or GABA (25 μM) plus insulin (100 pM) in either 25 or 5.5 mM glucose prior to the granule enrichment procedure. To account for all potential modulators of glucagon secretion, including the possibility of autocrine regulation of glucagon secretion (25, 26) we chose long-term cumulative incubation that has previously been used by our team (17) and other investigators (23) for secretion studies in α-TC1-6 cells.

At the end of the incubation period, granules were extracted as previously published (27) with some modifications. Briefly, cells were detached using 5 mM EDTA in PBS (pH 7.4) containing cOmplete Mini Protease Inhibitor Cocktail (Supplementary Table 1) on ice, centrifuged and resuspended in ice-cold homogenization buffer (20 mM Tris-HCl pH7.4, 0.5 mM EDTA, 0.5 mM EGTA, 250 mM sucrose, 1 mM DTT, cOmplete Mini Protease Inhibitor Cocktail, and 5 μg/mL Aprotinin). The cells were passed 10 times through a 21G needle and again 10 times through a 25G needle. The resulting lysates were centrifuged to obtain a post-nuclear supernatant (PNS). The nuclear fraction was washed seven times in ice-cold homogenization buffer and stored at −80°C. The PNS was centrifuged at 5,400 × g for 15 min at 4°C to obtain a post-mitochondrial supernatant, which then was spun at 25,000 × g for 20 min, and the resultant pellet was washed five times at 4°C. Enrichment was confirmed through immunoblotting for organelle-specific markers as described below.

2.3.3 Immunoblotting for organelle-specific markers

The enriched preparations of secretory granules from α-TC1-6 cells were lysed using non-ionic lysis buffer (50 mM Tris pH 7.4, 150 mM NaCl, 1% Triton X-100 plus cOmplete Mini Protease Inhibitor Cocktail, and 5 μg/mL Aprotinin). Proteins were resolved by 4–12% NuPAGE, transferred to a PVDF membrane and probed with the following antibodies (Supplementary Table 1): vesicle-associated membrane protein 2 (VAMP2) for mature secretory granules; calreticulin for the endoplasmic reticulum; TGN46 for the trans-Golgi network; and Lamin B1 for the nuclear envelope. Immunoreactive bands were visualized using HRP-conjugated goat anti-rabbit secondary antibody and Clarity Western ECL substrate. Images were acquired on a BioRad ChemiDoc Imaging System. Total cell extracts were used as positive controls.

2.3.4 Nanoscale flow cytometry

Secretory granule preparation

We used nano-scale flow cytometry (A50-Micro nanoscale flow cytometer; Apogee FlowSystems Inc.) to confirm enrichment of the secretory granules and to determine the size distribution of the granules. α-TC1-6 cells were transfected with Fc-glucagon or Fc alone, and secretory granules were extracted as described above. Granules were fixed in freshly prepared 2% PFA (pH 7.4), permeabilized with 0.5% saponin at room temperature, centrifuged at 25,000 × g for 20 min at 4°C and washed three times in 0.1% saponin in PBS. Fc-containing granules were labeled with FITC-IgG (1:250 dilution in 0.1% saponin in 1% BSA/PBS) in the dark for 1 h, and diluted 200X in 0.1% saponin.

Size calibration

Secretory granules of non-transfected cells were used for size calibration. ApogeeMix beads were used to establish sizing gates along the Y axis—large angle light scattering (LALS) vs. X-axis- small angle light scattering (SALS) plot. The microparticle mixture contained plastic spheres with diameters of 180, 240, 300, 590, 880, and 1,300 nm with refractive indexes of 1.43 and 110 nm, and 500 nm green fluorescent beads with

refractive index of 1.59. Based on the manufacturer's default settings, the calibrated gates of the size distribution were 110, 179, 235, 304, 585, and 880 nm, which were used to categorize subpopulations of the enriched secretory granules.

Nano-flow analysis

To count the numbers of Fc-glucagon+ granules, fluorescence of FITC excitation (L488) was gated and the numbers of Fc-glucagon+ granules were counted at 110, 179, 235, 304, 585, and 880 nm within the LALS vs. L488 plot. To get the LALS vs. L488 plot, its gate was normalized for the following isotypes: secretory granules of non-transfected cells, secretory granules of Fc-transfected cells, FITC-IgG and diluent. This method resulted in size distributions of the granules that were positive for Fc-glucagon, specifically. All experiments were done in three biological samples and values were expressed as percent distribution of gated granules.

2.3.5 Proteomic analysis of secretory granule proteins associated with glucagon

Granule lysate preparation

α-TC1-6 cells were transfected by Fc-glucagon and treated with effectors (GABA, insulin and GABA plus insulin) in media containing 25 or 5.5 mM glucose as described above. To identify non-specific interactors, we used the Fc construct in untreated conditions. Secretory granules were extracted as described above, and lysed in a non-ionic lysis buffer.

Affinity purification

Fc or Fc-glucagon was purified from the granule lysate by immunoprecipitation as we have done previously (19). Briefly, a slurry of Protein A-Sepharose beads (Supplementary Table 1) was mixed 1:1 with the granule lysate and rotated overnight at 4°C. The mixture was then centrifuged at 500 × g for 2 min at 4°C and the pellet was washed twice with 50 mM Tris (pH 7.5) and once with pre-urea wash buffer (50 mM Tris pH 8.5, 1 mM EGTA, 75 mM KCl). Fc or Fc-glucagon was eluted with two volumes of

urea elution buffer (7 M urea in 20 mM Tris buffer pH 7.5 plus 100 mM NaCl). This step was repeated twice more and the supernatants were collected and pooled. The pooled supernatant was mixed with acetone in a 1:4 ratio and kept at −20°C overnight, then centrifuged at 16,000 × g for 15 min at 4°C. The pellet was air-dried for proteomic analysis.

Proteomic analysis

Protein identification was conducted using LC-MS/MS according to the protocols of the Western University Mass Spectrometry Laboratory (https://www.schulich.uwo.ca/lrpc/bmsl/protocols/index.html). Briefly, the air-dried pellet was reconstituted in 50 mM NH_4CO_3, and proteins were reduced in 200 mM dithiothreitol (DTT), alkylated in freshly prepared 1M iodoacetamide and digested with trypsin for 18 h at 37°C with occasional shaking. Tryptic peptides were acidified using formic acid (0.25; v/v), loaded onto a Hypersep C18 column, washed, and eluted in 50% acetonitrile. The eluent was dried down in a speed vacuum and reconstituted in acetonitrile. Each experimental condition was done in three biological replicates. Peptide sequences were identified using the mouse database and further analyzed for protein categorization through PANTHER GO (http://www.Pantherdb.org), determination of subcellular locations and activity using http://www.uniport.org, and functional protein-protein interaction clustering through http://string-db.org. To predict protein-protein interactions using string, clustering of proteins was done based on strength of data support in the context of all active interaction sources. The minimum interaction score was set at median of 0.4 and maximum at 5 for the first shell and no limitation for the second shell.

Proteins that were pulled down using Fc alone were subtracted from proteins pulled down by Fc-glucagon to obtain the profile of proteins that specifically interact with glucagon.

2.3.6 Immunoprecipitation-immunoblotting of proteins associated with glucagon

To validate the interaction of glucagon with either GRP78 or histone H4 within secretory granules we first purified Fc-glucagon or Fc (as control) from the secretory granule preparation by incubating the secretory granule lysate with Protein A-Sepharose beads overnight at 4°C with rotation. The Fc or Fc-glucagon complex was eluted from the beads with 0.1 M glycine buffer (pH 2.8). The eluate was concentrated 50 times using a speed vac, run on a 10% Bis-Tris NuPAGE gel (Supplementary Table 1) and proteins were transferred onto a PVDF membrane. After an overnight incubation with primary antibodies against GRP78 or histone H4, bands were visualized with HRP-conjugated goat anti-rabbit secondary antibody and Clarity Western ECL substrate (Supplementary Table 1). Images were acquired on a BioRad ChemiDoc Imaging System.

2.3.7 Histone H4 assay

Enriched secretory granule fractions were prepared, resuspended in 0.2 N HCl, passed 10 times through a 30G needle, and kept at 4°C overnight. The reaction was stopped by addition of 0.2 volumes of 1N NaOH. The supernatant was collected after centrifugation at 6,500 × g at 4°C for 10 min. Protein levels were determined by BCA assay, and 100 ng of protein was used for measuring total histone H4 (Histone H4 Modification Multiplex ELISA-like format Kit, Supplementary Table 1), as per the manufacturer's instructions. The nuclear fraction was also assayed for histone H4 as a positive control.

2.3.8 Immunofluorescence microscopy

To validate the presence of GRP78 and histone H4 in glucagon-positive secretory granules, α-TC1-6 cells were cultured on collagen1-coated coverslips (three per experiment), and processed for immunofluorescence microscopy as described previously (18). Briefly, cells were fixed in 4% paraformaldehyde and permeabilized in 0.1% saponin in 0.5% BSA for 1 h. After blocking in 10% goat serum, cells were incubated with primary antibodies (mouse anti-glucagon and rabbit anti-GRP78 or rabbit anti-histone H4) overnight. Coverslips were washed in PBS and incubated with goat anti-

mouse Alexa Fluor IgG 488 and goat anti-rabbit Alexa Fluor 594 (Supplementary Table 1) for 3 h in the dark at room temperature, then mounted using ProLong Gold Antifade Mountant. Images were acquired on a Nikon A1R Confocal microscope with a 60x Nikon Plan-Apochromat oil differential interference contrast objective lens using NIS-Elements, software. To show secretory granule co-localization, images were post-processed by 2D deconvolution. To measure the degree of co-localization, regions of interest were manually drawn around distinct single or multicell bodies, positive for Fc-glucagon and either GRP78 or histone H4 and cropped for analysis. Co-localization of the pixels from each pseudo-colored image were used to calculate Pearson's correlation coefficient (PCC), as we described previously (19).

2.3.9 siRNA-mediated depletion of targeted proteins

After treatment of α-TC1-6 cells with GABA and/or insulin in media containing 25 mM glucose as described above, the proteomes were tabulated, and Venn diagram analysis revealed 27 metabolic/regulatory/secretory proteins and 36 histone/cytoskeletal/ribosomal proteins that were common between the groups treated with GABA and insulin. We selected 11 of these proteins (based on availability of the pre-designed siRNA) for siRNA-mediated depletion: Peroxiredoxin-2 (PRDX2), Malate dehydrogenase 1 (MDH1), Aconitate hydratase, mitochondrial (ACO2), 14-3-3 protein zeta/delta (KCIP-1), ELKS/Rab6-interacting/CAST family member 1 (ERC1), Alpha-tubulin 2 (AT2), ATP synthase F1 subunit alpha (ATP5F1A), Histone H4, GRP78, FXYD domain-containing ion transport regulator 2 (FXYD2), and Protein disulfide-isomerase (PDI), (Silencer siRNA, Thermo Fisher Scientific Inc. MA, USA).

Gene silencing was based on a published protocol (28). Briefly, α-TC1-6 cells were cultured to 60% confluency and transfected with final concentrations of 50 nM of pooled siRNAs (three siRNAs for each target) or control scrambled siRNA using Lipofectamine2000. Cells were incubated for 48 h, after which media were removed and replaced. After 24 h, expression levels of the targeted proteins were evaluated by immunoblotting using primary antibodies against each protein (Supplementary Table 1). Meanwhile, siRNA mediated knockdown of the proglucagon gene was shown as a

positive control using real-time PCR (Quant Studio Design and Analysis Real-Time PCR Detection System) (Supplementary Figure 2-1).

2.3.10 Glucagon measurement

To measure cellular and secreted glucagon levels after siRNA-mediated gene silencing, cell lysates or media were acidified in HCl-ethanol (92:2 v/v) in a 1:3 ratio, kept at −20°C overnight, then centrifuged at 13,000 × g for 15 min at 4°C. The supernatant was then mixed 1:1 with 20 mM Tris, pH 7.5 26 and glucagon levels were measured by ELISA (Thermo Fisher Scientific, Supplementary Table 1) according to the manufacturer's instructions. To measure Fc-glucagon, samples were diluted to reach an OD at the linear part of the standard curve.

2.3.11 Glucagon secretion and cell glucagon content in response to nutritional and paracrine effectors

α-TC1-6 cells cultured and kept under chronic exposure to 25 mM glucose and at confluency rate of ~70% were plated out into six-well plates. After 24 h, two sets of experiments were designed. In one set, medium was replaced by fresh 25 mM glucose-containing medium and in the other set medium was replaced by fresh medium containing 5.5 mM glucose. In both sets, cells were treated by GABA (25 μM), insulin (100 pM), or GABA (25 μM) + insulin (100 pM), and incubated for 24 h in serum free medium containing 0.5% BSA. At the end of incubation, plates were placed on ice and media were collected, centrifuged at 16,000 × g for 5 min, and supernatant was removed for glucagon measurement. The cells were washed three times with ice-cold PBS and scraped in Glycine-BSA buffer (100 mM glycine, 0.25% BSA, cOmplete Mini Protease Inhibitor Cocktail, 5 μg/mL Aprotinin, pH 8.8). The scraped cells were lysed by sonication (12 s at 30% amplitude on ice), and centrifuged at 16,000 × g for 45 min, from which the supernatant was collected for analysis. The protein concentration of the cell lysate was measured using BCA assay. To measure glucagon levels, the cell lysate or medium was mixed in an ethanol-acid solution (96% ethanol containing 0.18 M HCl) in a 1:3 ratio, kept at −20°C overnight, then centrifuged at 16,000 × g for 15 min at 4°C. The

supernatant was then mixed with 20 mM Tris buffer, pH 7.5, and glucagon measurements were conducted by ELISA.

2.3.12 Statistical analysis

Experiments were done in three biological replicates (three batches of newly thawed α-cells), each of which had two technical replicates (on passaged cells following three weeks adaptation to high glucose condition). Values were compared among treatment groups by one-way ANOVA (Bonferroni post-hoc test) using Sigma Stat 3.5 software ($\alpha = 0.05$). For image analysis, co-localization of channels in the merged images was calculated by PCC using NIS-Elements software (Nikon, Canada).

2.4 Results

Our method for purification of proteins that associate with glucagon within the α cell secretory granules consisted of two sequential steps. First, we modified and used a previously published method (27) for enrichment of the secretory granule fraction. Second, we used Fc-glucagon for affinity purification to pull down proteins associated with glucagon within the secretory granules.

2.4.1 Secretory granule enrichment

Immunoblotting for organelle-specific markers confirmed enrichment of secretory granules (Supplementary Figures 2- 2A–D). The final granule fraction was positive for the secretory granule marker, VAMP2. In contrast, the granule fraction did not contain the trans-Golgi marker TGN46, the nuclear envelope marker LaminB1, or the endoplasmic reticulum marker Calreticulin. As a positive control, the general cell lysate contained all four markers.

2.4.2 Confirmation of the enriched secretory granules

Secretory granules in α-cells have been previously studied using transmission electron microscopy and their average sizes have been reported to be in the range of 180–240 nm (29–31). Accordingly, we confirmed the presence of secretory granules using nano-scale

flow cytometry with Fc-glucagon as an exclusive marker for α-cell secretory granules (32, 33). We used beads in the range of 110–880 nm for calibration in the range of the reported sizes for secretory granules (Supplementary Figure 2- 3A). Fc-glucagon+ secretory granules distributed mostly to the gated regions of 179 and 235 nm (Supplementary Figures 2- 3B, C), confirming enrichment of secretory granules from α-TC1-6 cells.

2.4.3 Proteomic analysis of proteins that are associated with glucagon within α-cell secretory granules

Fc or Fc-glucagon was purified from the granule lysate by affinity purification, and proteins that interact with either Fc alone or Fc-glucagon were identified with LC-MS/MS. Proteins that were pulled down by Fc alone in both 25 mM glucose (Supplementary Table 2) and 5.5 mM glucose (Supplementary Table 3) conditions were subtracted from the list of proteins identified using Fc-glucagon, thus identifying proteins that specifically interact with glucagon, which we term the glucagon interactome. Proteins were assigned the following categories: metabolic-secretory-regulatory, histones, cytoskeletal, and ribosomal.

We identified 42 and 96 glucagon-interacting proteins within the category of metabolic-regulatory-secretory proteins when the cells were cultured in media containing 25 mM (Figure 2- 1A) and 5.5 mM glucose (Figure 2- 1B), respectively.

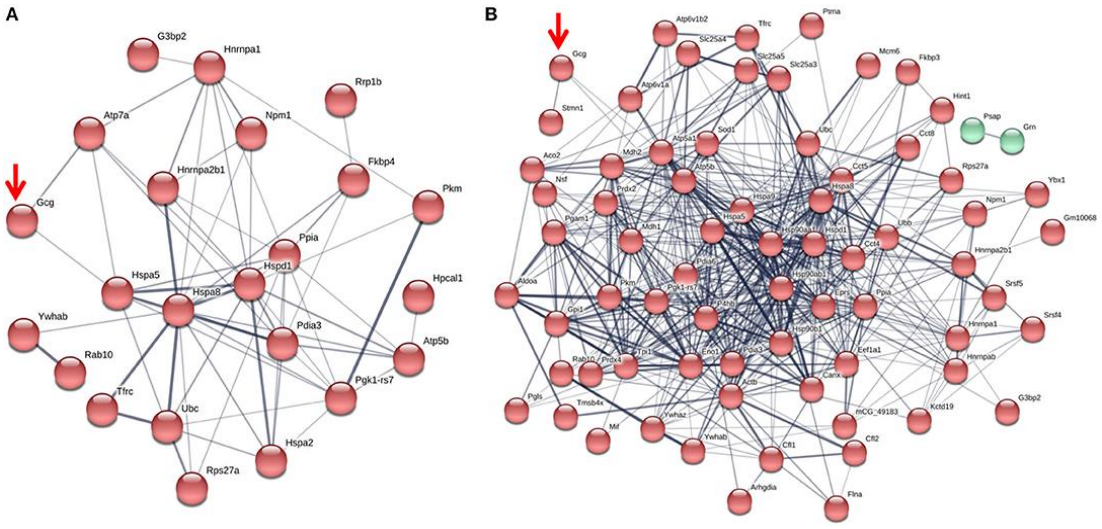

Figure 2-1. The glucagon interactome in secretory granules of α-TC1-6 cells. Cells were transfected with Fc-glucagon or Fc alone, and cultured in DMEM containing 25 mM or 5.5 mM glucose for 24h. Fc-glucagon was purified from enriched secretory granules and associated proteins were identified by LC-MS/MS. (A) Proteomic map of the metabolic-regulatory-secretory proteins that are predicted to associate with glucagon in the context of 25 mM glucose. Network clustering predicts direct interactions between glucagon and glucose regulated protein 78 KDa (Hspa5, also known as GRP78), and ATPase copper transporting alpha polypeptide (Atp7). (B) Proteomic map of the metabolic-regulatory-secretory proteins that are predicted to associate with glucagon in the context of 5.5 mM glucose. Network clustering predicts direct interactions between glucagon and GRP78, stathmin1 (Stmn1), and heat shock protein 90-alpha (Hsp90aa1). The thickness of the lines indicates the strength of the predicted protein-protein interaction.

In media containing 25 mM glucose, there was a predicted direct interaction of glucagon with glucose regulated protein 78 kDa (GRP78 or Hspa5), and ATPase copper transporting alpha polypeptide (Atp7a) (Figure 2- 1A), while in media containing 5.5 mM glucose, GRP78, Stathmin1 (Stmn1), and Heat shock protein 90- alpha (Hsp90aa1) were predicted to directly interact with glucagon (Figure 2- 1B). Under conditions of either 25 or 5.5 mM glucose, one common predicted interaction was that between glucagon and GRP78.

2.4.4 GRP78 interacts with glucagon and co-localizes to glucagon-positive secretory granules

Affinity purification of Fc-glucagon or Fc alone from the secretory granule lysate was followed by immunoblotting for GRP78. The presence of GRP78 immunoreactivity with Fc-glucagon, and not Fc alone, demonstrates a direct interaction with glucagon in the

enriched secretory granules (Figure 2- 2A). Immunofluorescence microscopy showed co-localization of GRP78 and endogenous glucagon within the secretory granules in α-TC1-6 cells (Figure 2- 2B). There was a strong positive correlation between glucagon and GRP78 immunoreactivities (PCC = 0.85 ± 0.08), indicating significant co-localization of GRP78 and glucagon.

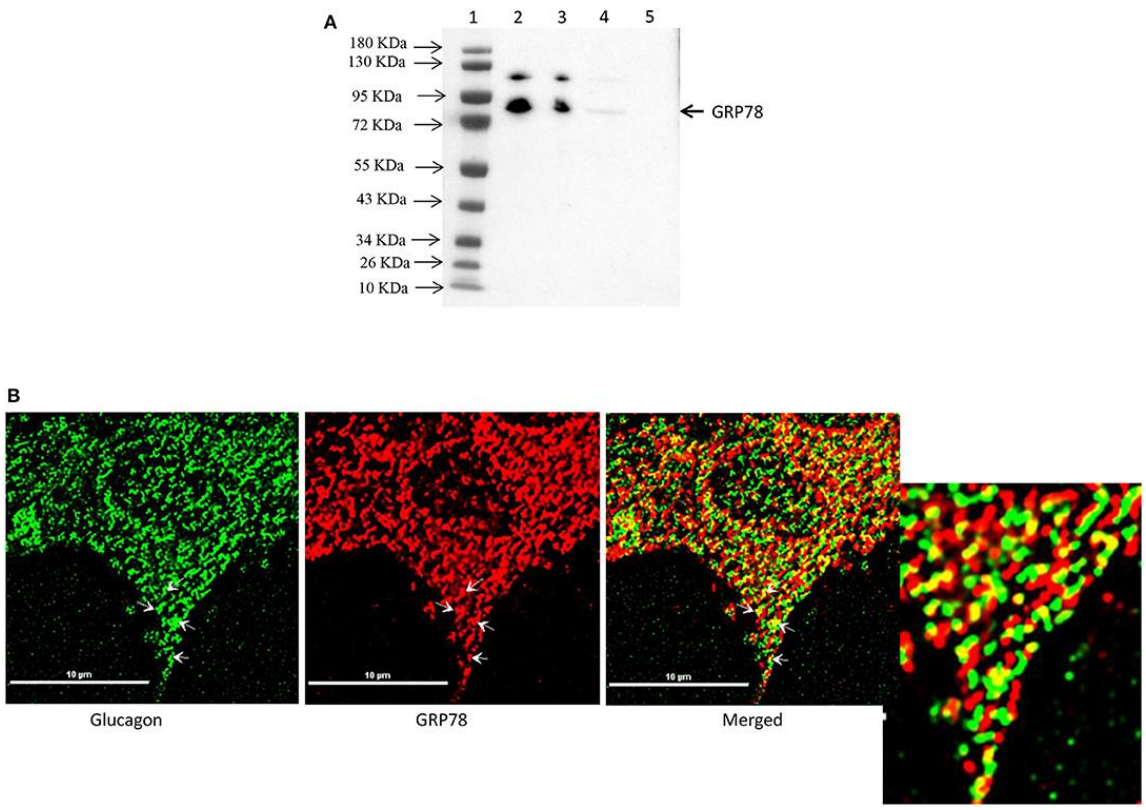

Figure 2-3. Glucagon and GRP78 directly interact and are localized within secretory granules in α-TC1-6 cells. (A) Western blot showing GRP78 immunoreactivity in: total cell extracts from untransfected (lane 2) and transfected (lane 3) cells; affinity-purified Fc-glucagon from isolated secretory granules (lane 4); and affinity-purified Fc alone from isolated secretory granules (lane 5). GRP78 binds to Fc-glucagon, but not Fc alone. (B) Immunofluorescence microscopy of glucagon (green), GRP78 (red) and both images merged. Cells were cultured on collagen-coated coverslips for 24h in DMEM containing 25 mM glucose. Images were acquired, 2D deconvoluted and analyzed with NIS software (Nikon, Canada). Pearson correlation coefficient (PCC) indicates strong correlation between GRP78 and glucagon (PCC = 0.85 ± 0.08). ROI shows areas of colocalization of GRP78 and glucagon within secretory granules.

2.4.5 GABA induces histone H4 interaction and co-localization with glucagon

Interestingly, proteomic analysis also revealed the presence of histone proteins, along with structural proteins and ribosomal proteins, within the secretory granules in α-TC1-6 cells (Supplementary Table 4). Histone H4 was predicted to interact with glucagon in cells incubated in medium containing 5.5 mM glucose. Therefore, we reasoned that this interaction was responsive to external effectors. We treated α-TC1-6 cells with GABA, a well-known modulator of glucagon secretion (21) and examined the interaction between histone and glucagon. Co-immunoprecipitation of granule lysates, histone H4 ELISA of granule lysates, and immunofluorescence microscopy all validated the interaction of histone H4 with glucagon and presence of histone H4 in secretory granules of α-TC1-6 cells after treatment with GABA (Figure 2- 3). Affinity purification of Fc-glucagon or Fc alone from the secretory granule lysate was followed by immunoblotting for histone H4

(Figure 2- 3A). The presence of histone H4 immunoreactivity with Fc-glucagon, and not Fc alone, demonstrates a direct interaction with glucagon in the enriched secretory granules (Figure 2- 3A). We then confirmed the presence of histone H4 in the enriched secretory granules of α-TC1-6 cells by ELISA (Figure 2- 3B). In cells treated with GABA in 25 mM glucose, there was a detectable amount of histone H4 in the granules. That this result was not due to contamination from the nuclear fraction was shown by the finding that histone H4 levels were undetectable in the secretory granules of cells not treated with GABA. As a positive control, the nuclear fraction showed high levels of histone H4. Finally, immunofluorescence microscopy showed the presence of histone H4 in glucagon-containing secretory granules (Figure 2- 3C), and there was significant co-localization with glucagon as assessed by Pearson's correlation coefficient (PCC = 0.78 ± 0.08).

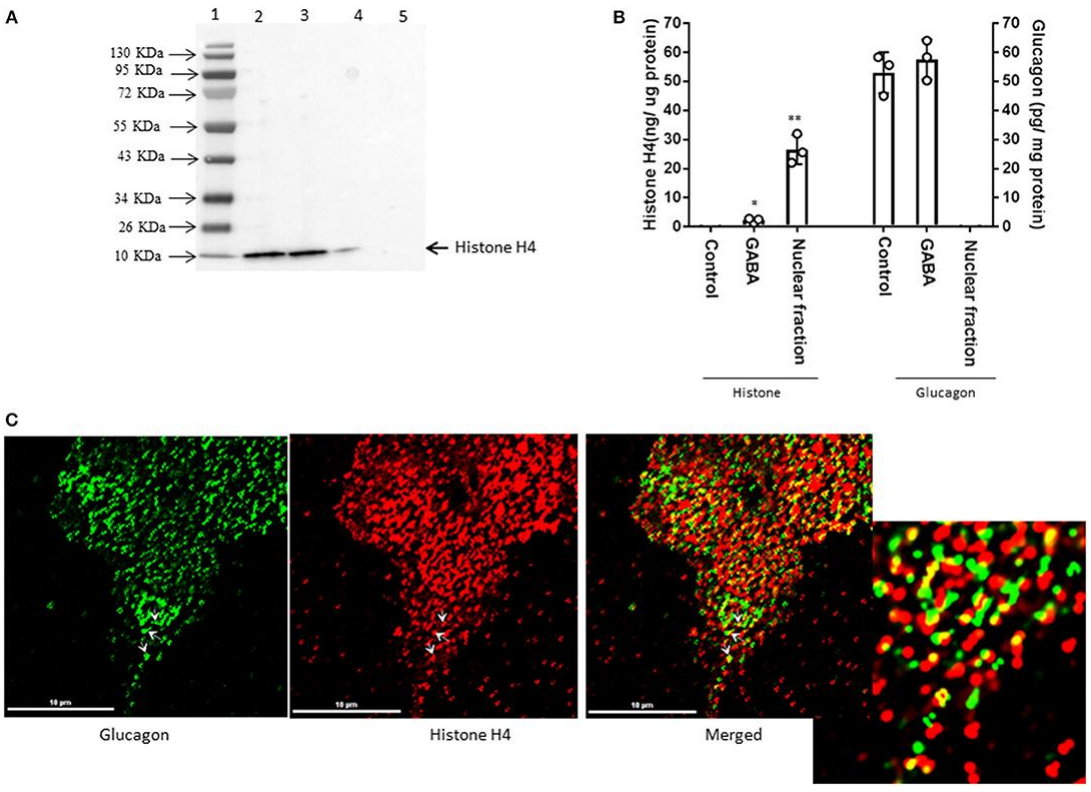

Figure 2-6. GABA induces direct interaction between glucagon and histone H4 within secretory granules in α-TC1-6 cells. (A) Western blot shows histone H4 immunoreactivity in: total cell extracts from untransfected (lane 2) and transfected (lane 3) cells; affinity-purified Fc-glucagon from isolated secretory granules (lane 4); and affinity-purified Fc alone from isolated secretory granules (lane 5). Histone H4 binds to Fc-glucagon, but not Fc alone. (B) Quantitative ELISA measurement of histone H4 (left Y axis) and glucagon (right Y axis) within the secretory granules (control GABA, insulin) and the nuclear fraction of α-TC1-6 cells. Values are expressed as mean ± SD and compared with 1-way ANOVA (α=0.05).*p<0.05; **p<0.001. (C) Immunofluorescence microscopy of glucagon (green), histone H4 (red) and both images merged. Cells were cultured on collagen-coated coverslips for 24h in DMEM containing 25 mM glucose. Images were acquired, 2D deconvoluted and analyzed with NIS software (Nikon, Canada). Pearson correlation coefficient (PCC) indicates strong correlation between histone H4 and glucagon (PCC = 0.78 ± 0.08). ROI shows areas of colocalization of histone H4 and glucagon within secretory granules.

2.4.6 The glucagon interactome changes in response to glucose, GABA and insulin

Since the interaction between histone H4 and glucagon was dependent on glucose levels and GABA, we determined the effects of the major α-cell paracrine effectors, GABA and insulin, on the glucagon interactome. The profiles of the metabolic-regulatory-secretory proteins that associate with glucagon within secretory granules were altered upon treatment with GABA, insulin or GABA + insulin, respectively, when α-TC1-6 cells

were cultured in medium containing 25 mM glucose (Figure 2- 4) and in 5.5 mM glucose (Figure 2- 5).

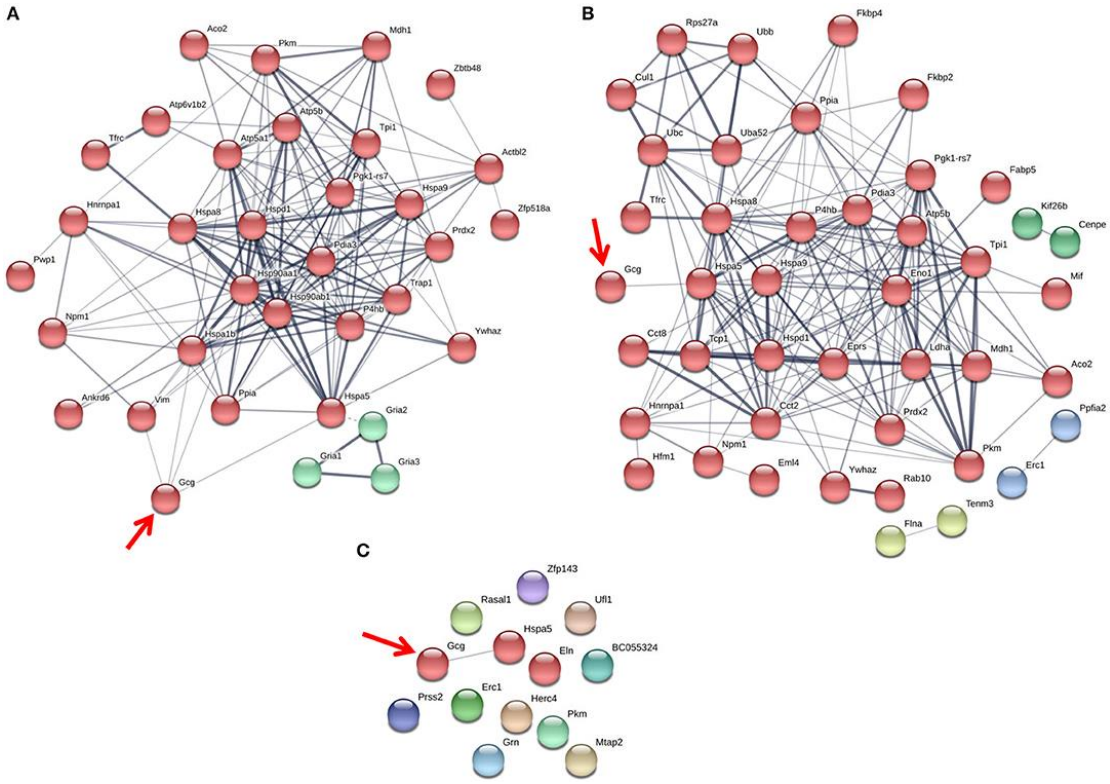

Figure 2-9. The glucagon interactome is altered in response to paracrine effectors in 25 mM glucose. α-TC1-6 cells were transfected with Fc-glucagon or Fc alone, and treated with GABA (25 µM), insulin (100 pM) or GABA (25 µM) plus insulin (100 pM) for 24h in DMEM containing 25 mM glucose. Fc-glucagon was purified from isolated secretory granules and associated proteins were identified by LC-MS/MS. (A) Proteomic map of metabolic-regulatory-secretory proteins that are associated with glucagon after treatment of α-TC1-6 cells with GABA shows direct interactions with 4 proteins: GRP78, Heat shock 70 kDa protein 1B (Hspa1b) Heat shock protein 90- alpha (Hsp90aa1), and Vimentin (Vim). (B) After treatment with insulin or (C) GABA+Insulin, glucagon is predicted to interact only with GRP78. Line thickness indicates the strength of data support.

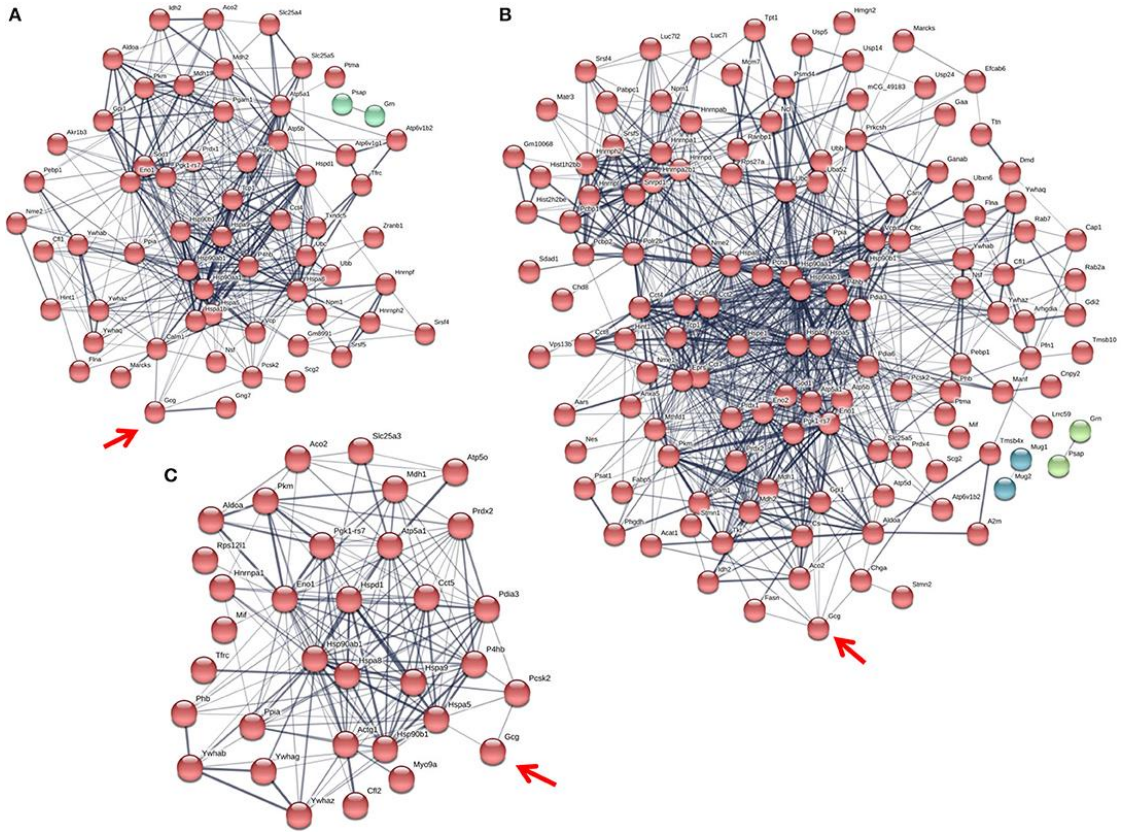
A
B
C
Aco2
Slc25a3
Atp5o
Mdh1
Pkm
Aldoa
Prdx2
Psk1-ps2
Atp5a1
Rps12l1
Hnrnpa1
Eno1
Hspd1
Cct5
Pdia3
Mif
Hspa9
P4hb
Tfrc
Hspa8
Pcsk2
Phb
Hspa5
Ppia
Actg1
Hsp90b1
Gcg
Ywhab
Ywhag
Myo9a
Ywhaz
Cfl2

Figure 2-12. The glucagon interactome is altered in response to paracrine effectors in 5.5 mM glucose. α-TC1-6 cells were transfected with Fc-glucagon or Fc alone, and treated with GABA (25 μM), insulin (100 pM) or GABA (25 μM) plus insulin (100 pM) for 24h in DMEM containing 5.5 mM glucose. Fc-glucagon was purified from isolated secretory granules and associated proteins were identified by LC-MS/MS. (A) Proteomic map of metabolic-regulatory-secretory proteins that are associated with glucagon after treatment of α-TC1-6 cells with GABA shows direct interactions with 6 proteins: GRP78, Heat shock protein 90- alpha (Hsp90aa1), Protein convertase subtilisin/kexin type2 (PCSK2), Heat shock 70 kDa protein 1B (Hspa1b), Calmodulin 1 (Calm1), Guanine nucleotide-binding protein G(I)/G(S)/G(O) subunit gamma-7 (Gng7). (B) After treatment with insulin, glucagon is predicted to directly interact with 7 proteins: GRP78, Heat shock protein 90-alpha, Annexin A5 (Anxa5), Stathmin1 (Stmn1), PCSK2, Fatty acid synthase (Fasn), and Chromogranin A (ChgA). (C) After treatment with GABA+Insulin, glucagon is predicted to directly interact with GRP78 and PCSK2. Line thickness indicates the strength of data support.

Additionally, we tabulated the profiles of histone, cytoskeletal, and ribosomal proteins in response to GABA, insulin and GABA + insulin in 25 mM glucose (Supplementary Tables 5A–C) or 5.5 mM glucose (Supplementary Tables 6A–C).

The glucagon interactomes were functionally classified into the following groups: Binding, Structural molecule, Catalytic, Receptor, Translation regulator, Transporter, Signal transducer, Antioxidant. The proportion of proteins in each category is shown in the context of 25 mM glucose (Supplementary Table 7) and 5.5 mM glucose (Supplementary Table 8).

The protein networks that are predicted to interact with glucagon within the secretory granules under conditions of 25 mM glucose are illustrated in Figure 2- 4. In cells treated with GABA, glucagon is predicted to directly interact with GRP78, HSP1B, HSP90, and

vimentin (Figure 2- 4A); however, in cells treated with insulin and GABA + insulin, glucagon interacts directly with only GRP78 (Figures 2- 4B,C). The clusters of metabolic-secretory-regulatory proteins that make up the rest of the glucagon interactomes change in composition in response to the different treatments. The numbers of proteins categorized as "structural molecule activities" decreased in response to GABA (~45%) or insulin (~38%) and increased in the GABA + insulin group (~16%) compared to the control (Supplementary Table 7). The numbers of cytoskeletal proteins increased in the GABA (29%), insulin (12%), and GABA + insulin (35%) groups, while the numbers of ribosomal proteins decreased in those groups by 51, 14, and 66%, respectively (Table 2-1. A).

Table 2-1. A- Sub-groups of proteins categorized as "structural molecules" in the glucagon interactome under conditions of 25 mM glucose. Panther GO-Slim Molecular Function analysis resulted in 3 sub-categories. The values represent protein hits as a percentage of the total number of hits within each sub-category when α-TC1-6 cells were cultured in media containing 25 mM glucose.

	Structural constituent of cytoskeleton	Structural constituent of ribosome	Extracellular matrix structural constituent
Control	66.7	29.2	4.2
GABA	85.7	14.3	-
Insulin	75	25	-
GABA+Insulin	90	10	-

Compared to cells incubated in medium containing 25 mM glucose, there were dramatic increases in the numbers of metabolic-regulatory-secretory proteins associated with glucagon after treatment with GABA, insulin or GABA + insulin in cells incubated in media containing 5.5 mM glucose (Figure 2- 5). In cells treated with GABA, glucagon is predicted to directly interact with the following proteins: GRP78 (Hspa5), HSP 90alpha

(Hsp90aa1), proprotein convertase subtilisin/kexin type 2 (PCSK2), heat shock 70 kDa protein 1B (Hsp1b), calmodulin 1(Calm1), and guanine nucleotide-binding protein G(I)/G(S)/G(O) subunit gamma-7 (Gng7) (Figure 2- 5A). Under insulin treatment, the following proteins were predicted to directly interact with glucagon: GRP78, HSP 90-alpha, annexin A5 (Anxa5), stathmin1 (Stmn1), fatty acid synthase (Fasn), and chromogranin A (ChgA) (Figure 2- 5B); and only two proteins, GRP78 and PCSK2, were predicted to directly interact with glucagon after treatment with GABA + insulin (Figure 2- 5C).

In the context of 5.5 mM glucose, the number of cytoskeletal proteins decreased, and the number of ribosomal proteins increased compared to cells treated with GABA, insulin and GABA + insulin in 25 mM glucose (Table 2-1. B). Interestingly, the total numbers of proteins classified as “structural molecule activities” did not change appreciably across treatments (Supplementary Table 8). However, differences became apparent when cytoskeletal and ribosomal proteins were compared separately. When compared to 5.5 mM glucose alone, there were decreases of ~24 and ~35%, respectively, in the numbers of cytoskeletal proteins when cells were treated with GABA or insulin alone, but a ~71% increase in response to GABA + Insulin. Conversely, the numbers of ribosomal proteins increased by ~26 and ~43% in response to GABA and insulin, respectively, and decreased by ~69% in response to GABA + Insulin (Table 2-1. B).

Table 2-1. B - Sub-groups of proteins categorized as "structural molecules" in the glucagon interactome under conditions of 5.5 mM glucose. Panther GO-Slim Molecular Function analysis resulted in 3 sub-categories. The values represent protein hits as a percentage of the total number of hits within each sub-category when α-TC1-6 cells were cultured in media containing 5.5 mM glucose.

	Structural constituent of cytoskeleton	Structural constituent of ribosome	Extracellular matrix structural constituent
Control	50	45.5	4.5
GABA	38.1	57.1	4.8
Insulin	32.4	64.9	2.7
GABA+Insulin	85.7	14.3	-

2.4.7 The dynamic glucagon interactome reveals novel proteins that regulate glucagon secretion

From our glucagon interactomes, we identified 11 proteins that interact with glucagon after treatment of α-TC1-6 cells with either GABA or insulin in media containing 25 mM glucose. To determine their effects on glucagon secretion, these proteins were depleted with siRNAs (Supplementary Figure 2-4) and glucagon secretion and cell content were measured.

Of these 11 proteins, knockdown of ELKS/Rab6-interacting/CAST family member 1 (ERC1) increased glucagon secretion ($p < 0.001$), while gene silencing of 14-3-3 zeta/delta (KCIP-1), cytosolic malate dehydrogenase (MDH1), FXYD domain-containing ion transport regulator 2 (FXYD2) and protein disulfide-isomerase (PDI) reduced glucagon secretion to the same statistically significant level ($p < 0.001$). As well,

knockdown of peroxiredoxin-2 (PRDX2), ATP synthase F1 subunit alpha (ATP5F1A), histone H4, and aconitate hydratase mitochondrial (ACO2) reduced glucagon secretion ($p < 0.01$), as did knockdown of alpha-tubulin 2 (AT2) ($p < 0.05$) (Figure 2- 6A). Gene silencing of MDH1, PRDX2, ATP5F1A, and FXYD2 reduced cellular glucagon content to a significance level of $p < 0.001$. Gene silencing of KCIP-1, ACO2, Histone H4 and PDI all reduced the levels of cellular glucagon content to a significance level of $p < 0.01$ and that for ERC1 at $p < 0.05$ (Figure 2- 6B). Gene silencing of GRP78 had no effect on glucagon secretion, and reduced cellular glucagon content ($p < 0.05$).

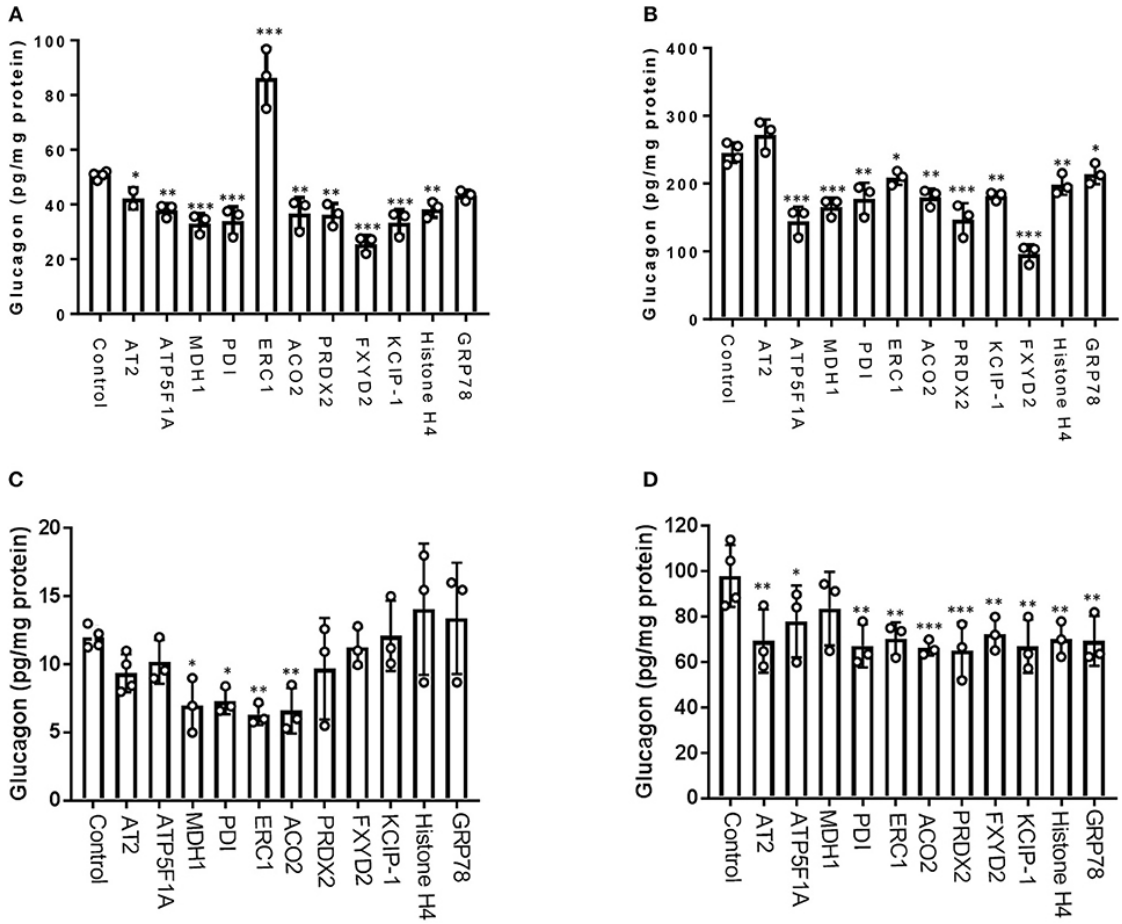

Figure 2-15. Glucagon secretion and cell content are regulated by a subset of interactome proteins. (A) Glucagon secretion and (B) cell content in the context of 25 mM glucose, and (C) glucagon secretion and (D) cell content in the context of 5.5 mM glucose were assessed after siRNA-mediated gene silencing of the following proteins: Alpha-tubulin 2 (AT2), ATP synthase F1 subunit alpha (ATP5F1A) , Malate dehydrogenase 1 (MDH1), Protein disulfide-isomerase (PDI), ELKS/Rab6-interacting/CAST family member 1 (ERC1), Aconitate hydratase mitochondrial (ACO2), Peroxiredoxin-2 (PRDX2), 14-3-3 protein zeta/delta (KCIP-1), FXYD domain-containing ion transport regulator 2 (FXYD2), histone H4, and GRP78 using pre-designed siRNAs for the mouse genome. After siRNA transfection, α-TC1-6 cells were cultured in DMEM containing 25 mM or 5.5 mM glucose for 24h and glucagon levels were measured using ELISA. Values are expressed as mean ± SD (α=0.05; n=3-4). *p<0.05; **p<0.01; ***p<0.001.

In the context of 5.5 mM glucose, significant reduction of glucagon secretion occurred by depletion of MDH1 ($p < 0.05$), PDI($p < 0.05$), ERC1($p < 0.01$), and ACO2 ($p < 0.01$). However, silencing of the other abovementioned genes did not significantly alter glucagon secretion (Figure 2- 6C). Cellular glucagon content was significantly decreased by silencing of ATP5F1A ($p < 0.05$), AT2, PDI, ERC1, FXYD2, KCIP-1, histone H4, GRP78 ($p < 0.01$), ACO2, and PRDX2 ($p < 0.001$) (Figure 2- 6D).

2.4.8 Alterations in glucagon secretion and cell glucagon content in response to nutritional and paracrine effectors

α-TC1-6 cells were cultured under high glucose conditions (25 mM) and then treated with paracrine effectors (GABA, insulin or GABA + insulin). The profiles of cumulative glucagon secretion and cellular glucagon content in 25 mM glucose was different from

that in 5.5 mM glucose. While neither GABA nor insulin affected glucagon secretion in 5.5 mM glucose, they suppressed glucagon secretion in 25 mM glucose (Supplementary Figure 2- 5A). In the context of 25 mM glucose, GABA reduced cellular glucagon content, while insulin increased cellular glucagon content (Supplementary Figure 2- 5B); in contrast, neither GABA nor insulin alone affected cellular glucagon content, but in combination, they decreased cellular glucagon content.

2.5 Discussion

We have identified a dynamic "glucagon interactome" within secretory granules of α-cells that is altered in response to glucose levels and the paracrine effectors GABA and insulin. We used a tagged glucagon construct, Fc-glucagon, to bring down proteins within secretory granules. We validated enrichment of the secretory granules by nano-scale flow cytometry and immunoblotting with compartment-specific markers. We identified a network of 392 proteins within the secretory granules that interact with glucagon and showed a direct interaction with GRP78 and Histone H4. Components of the interactome played a role in glucagon secretion, thus revealing a role for the interactome in the regulation of glucagon secretion in α-TC1-6 cells.

We have previously shown that α-TC1-6 cells have elevated levels of both proglucagon mRNA and glucagon secretion in response to 25 mM glucose (17), and other groups have shown the same effect in isolated mouse islets (3), clonal hamster InR1G9 glucagon-releasing cells (3, 34), and perfused rat pancreas (35). We also showed that this paradoxical glucagon release is accompanied by an up-regulation of components of the regulated secretory pathway, particularly in the active forms of PC1/3 and PC2 that post-translationally process proglucagon to glucagon, and in SNARE proteins that mediate vesicle exocytosis (17). Under conditions of 5.5 mM glucose, the up-regulation in RNA-binding proteins that modulate biosynthesis of islet secretory granule proteins, along with chaperonins, may indicate an increase in protein synthesis (36, 37). Chaperonins, as key components of the cellular chaperone machinery, are involved in maturation of newly-synthesized proteins in an ATP dependent manner (36). As ATP-generating proteins, such as ATP5F1A, MDH1, and glucose metabolic proteins, were also increased, we

speculate that 5.5 mM glucose induced a stress response that resulted in increased protein translation. This hypothesis is strengthened by the identification of cold shock protein, peroxiredoxin, thiol-disulfide isomerase and thioredoxin within the glucagon interactome at 5.5 mM glucose, all of which are up-regulated in pancreatic islets in response to stress (37).

One protein that was consistently predicted as interacting directly with glucagon was the ER stress protein and molecular chaperone GRP78. Previous proteomic studies have identified GRP78 in islets and β-cells (38, 39). Its presence in α-cell secretory granules may not be surprising, as it has previously been found in non-ER compartments such as the nucleus and lysosomes. Our data suggest that GRP78 may be a novel sorting receptor for glucagon in the regulated secretory pathway of α-cells. We have previously shown a potential role of chromogranin A as a sorting receptor for glucagon in both α-TC1-6 cells and PC12 cells (19), but unlike GRP78, we did not demonstrate any direct interactions with glucagon. While knockdown of GRP78 did not reduce glucagon secretion, it did reduce cell content, indicating a potential role in intracellular trafficking, but not exocytosis, of glucagon.

Interestingly, we identified histone proteins as a functional part of the glucagon interactome. The discovery of histone proteins within α-cell secretory granules is novel, and supported by the findings that the cytosolic fraction of pooled islets from multiple human donors had abundant amounts of the histone H2A (40). As well, quantitative proteomics of both α-TC1 and ßTC3 cells revealed the presence of histones H4, H3, H2A, H2B, and H1 (41). Our data indicate that one of these histones, H4, may directly bind to glucagon and regulate its basal level of secretion, perhaps under conditions of stress. Oxidative stress contributes to the pathogenesis of diabetes by disrupting the balance between reactive oxygen species and antioxidant proteins (42). Such an imbalance could target chromatin and globally alter profiles of gene expression, especially those encoding histone and DNA-binding proteins (42, 43). Thus, we speculate that the presence of histone H4 in the secretory granules could reflect a response to microenvironmental stress. Furthermore, it has been suggested that histones contained within secretory granules in neutrophils could function as a defense mechanism,

interacting with the plasma membrane to generate extracellular traps in response to bacterial infections (44). Thus, it is possible that histone proteins in the glucagon interactome take a role in the fusion step of granule exocytosis. Additionally, secretion of histones and other nuclear proteins has been associated with an inflammatory or senescent secretory phenotype (45, 46).

The α-cell paracrine effectors, GABA and insulin, remodeled the glucagon interactome in α-TC1-6 cells in a manner that was dependent on glucose levels. Compared to the respective control groups, GABA altered >70 and >80% of the metabolic-regulatory-secretory proteins within the glucagon interactome in the context of 25 and 5.5 mM glucose, respectively. One potentially novel GABA-regulated protein that may function in glucagon secretion in 25 mM glucose is ERC1, which has a role in the formation of the cytomatrix active zone and insulin exocytosis from β-cells (47), and we show for the first time a potential inhibitory effect of ERC1 on glucagon secretion that may be dependent on GABA. Ohara-Imaizumi et al. showed that ERC1 depletion in MIN6 cells and rat pancreatic β-cells suppressed glucose stimulated insulin secretion (47). When pancreatic β-cells were exposed to high glucose conditions, ERC1 takes a role in the process of granule docking and fusion toward insulin exocytosis. Here, by showing that depletion of ERC1 increased glucagon secretion at 25 mM glucose and reduced it at 5.5 mM glucose, it is tempting to speculate that ERC1 is a part of the granule exocytosis machinery in α-cells and plays a potential role in controlling glucagon exocytosis under diabetic conditions. Another potentially novel player in GABA-regulated glucagon secretion is KCIP-1, associated with β-cell survival (48). Furthermore, our proteomics findings suggest that GABA may enhance glucose uptake and glucose tolerance through leucine-rich repeat proteins. These proteins bind to the insulin receptor to promote glucose uptake in β-cells (49), and thus may be a new paracrine, or even autocrine, regulator of α-cell function. Interestingly, in the context of 5.5 mM glucose, GABA recruited PCSK2 and secretogranin 2, known α- cell granule proteins that function in proglucagon processing (19). Although our previous work showed no changes in PCSK2 in response to 5.5 mM glucose (17), we now show that plasticity in PCSK2 expression may be due to GABA under these glucose concentrations.

In the context of 25 mM glucose, insulin treatment increased the number of biosynthetic proteins, consistent with its role in cellular growth. Kinesin-like proteins also increased, suggesting a potential role in α-cell secretory granule synthesis and glucose homeostasis, as has been documented in β-cells (50). In the context of 5.5 mM glucose, insulin up-regulated nucleoside diphosphate kinases A and B, proposed regulators of insulin secretion (51). We also identified the small G proteins SAR1, Rab2A, and RhoA, present in INS-1E cell secretory granules (52); however, their functions are not known.

Interestingly, treatment of the α-TC1-6 cells with GABA + insulin in 25 mM glucose caused a dramatic decrease in the overall numbers of proteins within the glucagon interactome. Interaction with GRP78 remained preserved, while a new protein, microtubule-associated protein 2, appeared in the glucagon interactome. This protein may have a potential role in glucose homeostasis, as it is down-regulated in isolated diabetic rat islets exposed to low glucose conditions (53). In the context of 5.5 mM glucose, the combination of GABA and insulin again predicted the presence of PCSK2 in the glucagon interactome, as seen with GABA treatment alone and invites revisiting the question of PCSK2 acting as a sorting receptor for glucagon (19).

The design of our experiments was to mimic blood glucose volatility in diabetes in particular, and not in normal physiology, to investigate potential dynamic alterations in the glucagon interactome (54). Here, we have identified the glucagon interactome in α-TC1-6 cells after chronic exposure to extremely high glucose (25 mM), which, in diabetes, paradoxically increases glucagon secretion from pancreatic α-cells (3, 5). We further showed remodeling of this interactome by replacing that extremely high glucose condition (25 mM) with a relatively low glucose (5.5 mM) medium, which mimic conditions that represent glucose volatility in diabetes. However, we did not examine changes in the glucagon interactome throughout a range of high and low glucose conditions, which could be a limitation for the current study. Also, we used our negative control, Fc alone, only in the two glucose conditions and not in treatments with GABA and insulin, which may affect the interpretation of the interactome under these conditions.

It is well-established that, under normal physiological conditions, glucagon secretion is suppressed by high glucose (21). However, chronic hyperglycemia disrupts this fine regulation and results in elevated glucagon secretion (34, 55). It has been documented that chronic exposure to 25 mM glucose stimulates glucagon secretion in α-TC1-6 cells (17), thus mimicking the α-cell response to glucose in the diabetic, and not normal, condition.

While we presented a novel glucagon interactome within enriched secretory granules of α-TC1-6 cells and its alterations due to nutritional or paracrine effectors, direct comparisons to primary α-cells may be limited. When we compared our described glucagon interactome with the transcriptomic profile of mouse α-cells (56), and human α-cells (57), there were some differences in the protein profiles. Additionally, Lawlor et al. (58) compared gene expression profiles of α-TC1 cells with their primary mouse and human counterparts and showed a high level of discrepancy between them. One possibility for this discrepancy may be changes in gene expression in primary cells while cultured *in vitro* (17, 59). However, we feel that the findings we are reporting generally show that: (1) networks of proteins can interact with glucagon within the secretory granule compartment of the pancreatic α-cell; (2) this interactome is remodeled according to the micro-environmental milieu; and (3) some proteins within the interactome can regulate glucagon secretion. The next step will be to use our data to guide the identification of glucagon-interacting proteins that may regulate glucagon secretion within primary α-cells.

Under normal physiological conditions, GABA and insulin suppress glucagon secretion in pancreatic α-cells (21, 60). This response to GABA and insulin may differ depending on the cell line and experimental conditions used. Piro et al. (61) showed that with short-term treatment, insulin significantly suppressed glucagon secretion in α-TC1-6 cells without affecting cellular glucagon content. In INR1G cells, Kawamori et al. (62) showed that silencing of the insulin receptor significantly increased glucagon secretion, indicating that insulin receptor signaling is required for suppression of glucagon secretion. Here, we show that treatment with insulin suppresses the long-term cumulative secretion of glucagon when α-TC1-6 cells were cultured and chronically kept in 25 mM glucose.

Interestingly, under these conditions, cellular glucagon content increased, perhaps due to excess glucagon in the medium and its potential abolishing effect on insulin action (63). In addition, this increase could be due to an autocrine effect of glucagon on proglucagon gene expression, a notion that has been argued by Leibiger et al. for short-term effect of glucagon on proglucagon gene expression in non-cumulative culturing (26). As well, it is known that GABA inhibits glucagon secretion under high glucose conditions (64). Importantly, our findings show reductions in both glucagon secretion and content. Surprisingly, the combination of GABA and insulin did not suppress glucagon secretion, leading to questions on the mechanism of the interactions between these two signaling pathways.

In conclusion, we have described a novel and dynamic glucagon interactome in α-TC1-6 cells that is remodeled in response to glucose and the α-cell paracrine effectors, GABA and insulin. Our proteomics approach has revealed a number of novel secretory granule proteins that function in the regulation of glucagon secretion and illustrates the plasticity in the protein components of the α-cell secretory granules. These findings provide an important proteomics resource for further data mining of the α-cell secretory granules and targeting diabetes treatment.

Author contribution: FA and SD designed the experiments, wrote, and prepared the manuscript text and figures, and reviewed the manuscript prior to submission.

Funding: This work has been financially supported by a Discovery Grant from the Natural Sciences and Engineering Research Council of Canada to SD, and by a Dean's Award Scholarship to FA.

Conflict of Interest Statement: The authors declare that the research was conducted in the absence of any commercial or financial relationships that could be construed as a potential conflict of interest.

Acknowledgements: We would like to thank Paula Pittock at the Siebens-Drake Research Institute, University of Western Ontario for assistance in LC-MS/MS analysis and Dr. Hon Leong lab members for assistance with nanoflow cytometry. This

manuscript has been released by the preprint server for biology, bioRXiv (https://www.biorxiv.org/content/early/2018/07/20/373118) (65).

2.6 References

Cryer PE. Minireview: Glucagon in the pathogenesis of hypoglycemia and hyperglycemia in diabetes. Endocrinology (2012) 153:1039–48. doi: 10.1210/en.2011-1499

2. Lee YH, Wang MY, Yu XX, Unger RH. Glucagon is the key factor in the development of diabetes. Diabetologia (2016) 59:1372–5. doi: 10.1007/s00125-016-3965-9

3. Salehi A, Vieira E, Gylfe E. Paradoxical stimulation of glucagon secretion by high glucose concentrations. Diabetes (2006) 55:2318–23. doi: 10.2337/db06-0080

4. Unger RH, Cherrington AD. Glucagonocentric restructuring of diabetes: A pathophysiologic and therapeutic makeover. J Clin Invest (2012) 122:4–12. doi: 10.1172/JCI60016

5. Wewer Albrechtsen NJ, Kuhre RE, Pedersen J, Knop FK, Holst JJ. The biology of glucagon and the consequences of hyperglucagonemia. Biomark Med (2016) 10:1141–51. doi: 10.2217/bmm-2016-0090

6. Kim J, Okamoto H, Huang ZJ, Anguiano G, Chen S, Liu Q, et al. Amino acid transporter Slc38a5 controls glucagon receptor inhibition-induced pancreatic α cell hyperplasia in mice. Cell Metab (2017) 25:1348–61.e8. doi: 10.1016/j.cmet.2017.05.006

7. D'alessio D. The role of dysregulated glucagon secretion in type 2 diabetes. Diabetes, Obes Metab (2011) 13:126–32. doi: 10.1111/j.1463-1326.2011.01449.x

8. Scheen AJ, Paquot N, Lefèbvre PJ. Investigational glucagon receptor antagonists in Phase I and II clinical trials for diabetes. Expert Opin Investig Drugs (2017) 26:1373–89. doi: 10.1080/13543784.2017.1395020

9. Gelling RW, Vuguin PM, Du XQ, Cui L, Rømer J, Pederson RA, et al. Pancreatic β-cell overexpression of the glucagon receptor gene results in enhanced β-cell function and mass. Am J Physiol Meta (2009) 297:E695–707. doi: 10.1152/ajpendo.00082.2009

10. Wang M-Y, Yan H, Shi Z, Evans MR, Yu X, Lee Y, et al. Glucagon receptor antibody completely suppresses type 1 diabetes phenotype without insulin by disrupting a novel diabetogenic pathway. Proc Natl Acad Sci (2015) 112:2503–8. doi: 10.1073/pnas.1424934112

11. Walker JN, Ramracheya R, Zhang Q, Johnson PR V, Braun M, Rorsman P. Regulation of glucagon secretion by glucose: Paracrine, intrinsic or both? Diabetes, Obes Metab (2011) 13:95–105. doi: 10.1111/j.1463-1326.2011.01450.x

12. Müller TD, Finan B, Clemmensen C, DiMarchi RD, Tschöp MH. The new biology and pharmacology of glucagon. Physiol Rev (2017) 97:721–66. doi: 10.1152/physrev.00025.2016

13. Wendt A, Birnir B, Buschard K, Gromada J, Salehi A, Sewing S, et al. Glucose inhibition of glucagon secretion from rat α-cells is mediated by GABA released from neighboring β-cells. Diabetes (2004) 53:1038–45. doi: 10.2337/diabetes.53.4.1038

14. Xu E, Kumar M, Zhang Y, Ju W, Obata T, Zhang N, et al. Intra-islet insulin suppresses glucagon release via GABA-GABAA receptor system. Cell Metab (2006) 3:47–58. doi: 10.1016/j.cmet.2005.11.015

15. Briant L, Salehi A, Vergari E, Zhang Q, Rorsman P. Glucagon secretion from pancreatic α-cells. Ups J Med Sci (2016) 121:113–9. doi: 10.3109/03009734.2016.1156789

16. Li H, Liu T, Lim J, Gounko N V., Hong W, Han W. Increased biogenesis of glucagon-containing secretory granules and glucagon secretion in BIG3-knockout mice. Mol Metab (2015) 4:246–242. doi: 10.1016/j.molmet.2015.01.001

17. McGirr R, Ejbick CE, Carter DE, Andrews JD, Nie Y, Friedman TC, et al. Glucose dependence of the regulated secretory pathway in αTC1-6 cells. Endocrinology (2005) 146:4514–23. doi: 10.1210/en.2005-0402

18. McGirr R, Guizzetti L, Dhanvantari S. The sorting of proglucagon to secretory granules is mediated by carboxypeptidase E and intrinsic sorting signals. J Endocrinol (2013) 217:229–40. doi: 10.1530/JOE-12-0468

19. Guizzetti L, McGirr R, Dhanvantari S. Two dipolar alpha-helices within hormone-encoding regions of proglucagon are sorting signals to the regulated secretory pathway. J Biol Chem (2014) 289:14968–80. doi: 10.1074/jbc.M114.563684

20. Hayashi M, Yamada H, Uehara S, Morimoto R, Muroyama A, Yatsushiro S, et al. Secretory granule-mediated co-secretion of L-glutamate and glucagon triggers glutamatergic signal transmission in islets of Langerhans. J Biol Chem (2003) 278:1966–74. doi: 10.1074/jbc.M206758200

21. Quesada I, Tudurí E, Ripoll C, Nadal Á. Physiology of the pancreatic α-cell and glucagon secretion: Role in glucose homeostasis and diabetes. J Endocrinol (2008) 199:5–19. 10.1677/JOE-08-0290

22. Rouille Y, Westermark G, Martin SK, Steiner DF. Proglucagon is processed to glucagon by prohormone convertase PC2 in alpha TC1-6 cells. Proc Natl Acad Sci (1994) 91:3242–6. doi: 10.1073/pnas.91.8.3242

23. Sancho V, Daniele G, Lucchesi D, Lupi R, Ciccarone A, Penno G, et al. Metabolic regulation of GLP-1 and PC1/3 in pancreatic α-cell line. PLoS One (2017) 12:1–12. doi: 10.1371/journal.pone.0187836

24. Stamenkovic JA, Andersson LE, Adriaenssens AE, Bagge A, Sharoyko VV, Gribble F, et al. Inhibition of the malate–aspartate shuttle in mouse pancreatic islets

abolishes glucagon secretion without affecting insulin secretion. Biochem J (2015) 468:49–63. doi: 10.1042/BJ20140697

25. Ma X, Zhang Y, Gromada J, Sewing S, Berggren P-O, Buschard K, et al. Glucagon Stimulates Exocytosis in Mouse and Rat Pancreatic α-Cells by Binding to Glucagon Receptors. Mol Endocrinol (2005) 19:198–212. doi: 10.1210/me.2004-0059

26. Leibiger B, Moede T, Muhandiramlage TP, Kaiser D, Vaca Sanchez P, Leibiger IB, et al. Glucagon regulates its own synthesis by autocrine signaling. Proc Natl Acad Sci (2012) 109:20925–30. doi: 10.1073/pnas.1212870110

27. Bogan, J.S., Xu, X., Hao M. Cholesterol accumulation increases insulin granule size and impairs membrane trafficking. Traffic (2012) 13:1466–80. doi: 10.1111/j.1600-0854.2012.01407.x

28. Mossë YP, Laudenslager M, Longo L, Cole K a, Wood A, Attiyeh EF, et al. Identification of ALK as the major familial neuroblastoma predisposition gene. Nature (2008) 455:930–5. doi: 10.1038/nature07261

29. Pfeifer CR, Shomorony A, Aronova MA, Zhang G, Cai T, Xu H, et al. Quantitative analysis of mouse pancreatic islet architecture by serial block-face SEM. J Struct Biol (2015) 189:44–52. doi: 10.1016/j.jsb.2014.10.013

30. Huang YC, Rupnik MS, Karimian N, Herrera PL, Gilon P, Feng ZP, et al. In situ electrophysiological examination of pancreatic α cells in the streptozotocin-induced diabetes model, revealing the cellular basis of glucagon hypersecretion. Diabetes (2013) 62:519–30. doi: 10.2337/db11-0786

31. Olofsson CS, Salehi A, Göpel SO, Holm C, Rorsman P. Palmitate stimulation of glucagon secretion in mouse pancreatic alpha-cells results from activation of L-type calcium channels and elevation of cytoplasmic calcium. Diabetes (2004) 53:2836–43. doi: 10.2337/diabetes.53.11.2836

32. von Kolontaj K, Horvath GL, Latz E, Büscher M. Automated nanoscale flow cytometry for assessing protein–protein interactions. Cytom Part A (2016) 89:835–43. doi: 10.1002/cyto.a.22937

33. Biggs CN, Siddiqui KM, Al-Zahrani AA, Pardhan S, Brett SI, Guo QQ, et al. Prostate extracellular vesicles in patient plasma as a liquid biopsy platform for prostate cancer using nanoscale flow cytometry. Oncotarget (2016) 7:8839–49. doi: 10.18632/oncotarget.6983

34. Katsura T, Kawamori D, Aida E, Matsuoka TA, Shimomura I. Glucotoxicity induces abnormal glucagon secretion through impaired insulin signaling in InR1G cells. PLoS One (2017) 12. doi: 10.1371/journal.pone.0176271

35. Mokuda, O, Shibata, M, Ooka, H, Okazaki, R, Sakamoto Y. Glucagon is paradoxically secreted at high concentrations of glucose in rat pancreas perfused with diazoxide. Diabetes Nutr Metab (2002) 15:260–4.

36. Magro MG, Solimena M. Regulation of β-cell function by RNA-binding proteins. Mol Metab (2013) 2:348–55. doi: 10.1016/j.molmet.2013.09.003

37. Ahmed M, Bergsten P. Glucose-induced changes of multiple mouse islet proteins analysed by two-dimensional gel electrophoresis and mass spectrometry. Diabetologia (2005) 48:477–85. doi: 10.1007/s00125-004-1661-7

38. Spiess C, Meyer AS, Reissmann S, Frydman J. Mechanism of the eukaryotic chaperonin: Protein folding in the chamber of secrets. Trends Cell Biol (2004) 14:598–604. doi: 10.1016/j.tcb.2004.09.015

39. Sundsten T, Ortsäter H. Proteomics in diabetes research. Mol Cell Endocrinol (2009) 297:93–103. doi: 10.1016/j.mce.2008.06.018

40. Schrimpe-rutledge AC, Fontès G, Gritsenko MA, Angela D, Poitout V, Metz TO. Discovery of novel glucose-regulated proteins in isolated human pancreatic islets using LC-MS/MS-based proteomics. J Proteome Res (2013) 11:3520–32. doi: 10.1021/pr3002996

41. Choudhary A, He KH, Mertins P, Udeshi ND, Dančík V, Fomina-Yadlin D, et al. Quantitative-proteomic comparison of alpha and beta cells to uncover novel targets for lineage reprogramming. PLoS One (2014) 9. doi: 10.1371/journal.pone.0095194

42. Pacifici F, Arriga R, Sorice GP, Capuani B, Scioli MG, Pastore D, et al. Peroxiredoxin 6, a novel player in the pathogenesis of diabetes. Diabetes (2014) 63:3210–20. doi: 10.2337/db14-0144

43. Kreuz S, Fischle W. Oxidative stress signaling to chromatin in health and disease. Epigenomics (2016) 8:843–62. doi: 10.2217/epi-2016-0002

44. Brinkmann V, Reichard U, Goosmann C, Fauler B, Weiss DS, Weinrauch Y, et al. Neutrophil extracellular traps kill bacteria. Science (2004) 303:1532–5. doi: 10.1126/science.1092385

45. Hoeksema M, Van Eijk M, Haagsman HP, Hartshorn KL. Histones as mediators of host defense, inflammation and thrombosis. Futur Microbiol (2016) 11:441–53. doi: 10.2217/fmb.15.151

46. Davalos AR, Coppe JP, Campisi J, Desprez PY. Senescent cells as a source of inflammatory factors for tumor progression. Cancer Metastasis Rev (2010) 29:273–83. doi: 10.1007/s10555-010-9220-9

47. Ohara-Imaizumi M, Ohtsuka T, Matsushima S, Akimoto Y, Nishiwaki C, Nakamichi Y, et al. ELKS, a protein structurally related to the active zone-associated protein CAST, is expressed in pancreatic beta cells and functions in insulin exocytosis: interaction of ELKS with exocytotic machinery analyzed by total internal reflection fluorescence microscopy. Mol Biol Cell (2005) 16:1–13. doi: 10.1091/mbc.e04-09-0816

48. Lim GE, Piske M, Johnson JD. 14-3-3 proteins are essential signalling hubs for beta cell survival. Diabetologia (2013) 56:825–37. doi: 10.1007/s00125-012-2820-x

49. Lo HY, Ho TY, Li CC, Chen JC, Liu JJ HC. A novel insulin receptor-binding protein from Momordica charantia enhances glucose uptake and glucose clearance in

vitro and in vivo through triggering insulin receptor signaling pathway. J Agric Food Chem (2014) 62:8952–61. doi: 10.1021/jf5002099

50. Cui J, Wang Z, Cheng Q, Lin R, Zhang XM, Leung PS, et al. Targeted inactivation of Kinesin-1 in pancreatic β-cells in vivo leads to insulin secretory deficiency. Diabetes (2011) 60:320–30. doi: 10.2337/db09-1078

51. Kowluru A. Defective protein histidine phosphorylation in islets from the Goto-Kakizaki diabetic rat. Am J Physiol Endocrinol Metab (2003) 285:E498-503. doi: 10.1152/ajpendo.00121.2003

52. Brunner Y, Coute Y, Iezzi M, Foti M, Fukuda M, Hochstrasser DF, et al. Proteomics analysis of insulin secretory granules. Mol Cell Proteomics (2007) 6:1007–17. doi: 10.1074/mcp.M600443-MCP200

53. Ghanaat-Pour H, Huang Z, Lehtihet M, Sjöholm Å. Global expression profiling of glucose-regulated genes in pancreatic islets od spontaneously diabetic Goto-Kakizaki rats. J Mol Endocrinol (2007) 39:135–50. doi: 10.1677/JME-07-0002

54. Whitelaw BC, Choudhary P HD. Evaluating rate of change as an index of glycemic variability, using continuous glucose monitoring data. Diabetes Technol Ther (2011) 13:631–6. doi: 10.1089/dia.2010.0215

55. Gylfe E, Gilon P. Glucose regulation of glucagon secretion. Diabetes Res Clin Pract (2014) 103:1–10. doi: 10.1016/j.diabres.2013.11.019

56. Adriaenssens AE, Svendsen B, Lam BYH, Yeo GSH, Holst JJ, Reimann F, et al. Transcriptomic profiling of pancreatic alpha, beta and delta cell populations identifies delta cells as a principal target for ghrelin in mouse islets. Diabetologia (2016) 59:2156–65. doi: 10.1007/s00125-016-4033-1

57. Dominguez Gutierrez G, Xin Y, Okamoto H, Kim J, Lee A-H, Ni M, et al. Gene Signature of Proliferating Human Pancreatic α-Cells. Endocrinology (2018) 159:3177–86. doi: 10.1210/en.2018-00469

58. Lawlor N, Youn A, Kursawe R, Ucar D, Stitzel ML. Alpha TC1 and Beta-TC-6 genomic profiling uncovers both shared and distinct transcriptional regulatory features with their primary islet counterparts. Sci Rep (2017) 7:1–14. doi: 0.1038/s41598-017-12335-1

59. Brereton MF, Iberl M, Shimomura K, Zhang Q, Adriaenssens AE, Proks P, et al. Reversible changes in pancreatic islet structure and function produced by elevated blood glucose. Nat Commun (2014) 5:1–11. doi: 10.1038/ncomms5639

60. Ben-Othman N, Vieira A, Courtney M, Record F, Gjernes E, Avolio F, et al. Long-term GABA administration induces alpha cell-mediated beta-like cell neogenesis. Cell (2017) 168:73–85.e11. doi: 10.1016/j.cell.2016.11.002

61. Piro S, Mascali LG, Urbano F, Filippello A, Malaguarnera R, Calanna S, et al. Chronic exposure to GLP-1 increases GLP-1 synthesis and release in a pancreatic alpha cell line (a-TC1): Evidence of a direct effect of GLP-1 on pancreatic alpha cells. PLoS One (2014) 9. doi: 10.1371/journal.pone.0090093

62. Kawamori D, Kulkarni RN. Insulin modulation of glucagon secretion: the role of insulin and other factors in the regulation of glucagon secretion. Islets (2009) 1:276–9. doi: 10.4161/isl.1.3.9967

63. Li J1, Casteels T1, Frogne T2, Ingvorsen C2, Honoré C2, Courtney M. Artemisinins target GABAA receptor signaling and impair α cell identity. Cell (2017) 168:86–100.e15.doi: 10.1016/j.cell.2016.11.010

64. Rorsman P, Berggren PO, Bokvist K, Ericson H, Möhler H, Ostenson CG SP. Glucose-inhibition of glucagon secretion involves activation of GABAA-receptor chloride channels. Nature (1989) 341:233–6. doi: 10.1038/341233a0

65. Asadi F. DS. Plasticity in the glucagon interactome reveals novel proteins that regulate glucagon secretion in alpha TC1-6 cells. bioRxiv (2018). doi: 10.1101/373118

2.7 Supplementary Figures

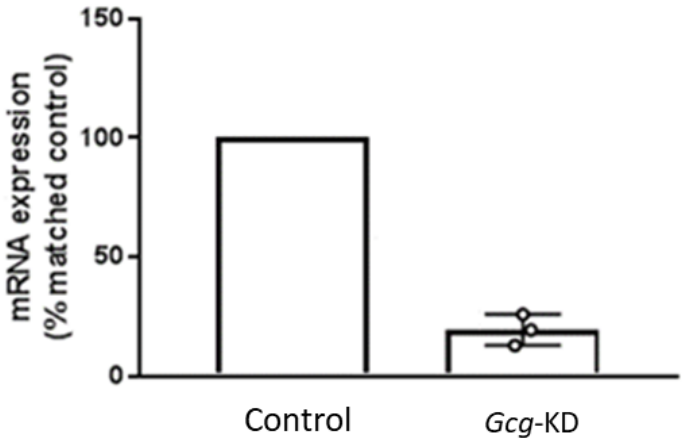

Supplementary Figure 2-1. Proglucagon gene knock down in α-TC1-6 cells. cDNA synthesis was performed using total extracted RNA. Quantitative PCR was achieved using Quant Studio Design and Analysis Real-Time PCR Detection System in conjunction with the Maxima SYBR Green qPCR Master Mix. The glucagon gene (*Gcg*) expression was determined in the transfected cells with scrambled siRNA (control) or *Gcg*-KD. Glucagon gene expression level was normalized to that of the internal control β-Actin. The normalized level of transcripts in protein depleted cells was shown relative to that of the negative control. Gene expression levels show >70% reduction in the glucagon depleted group compare to the control.

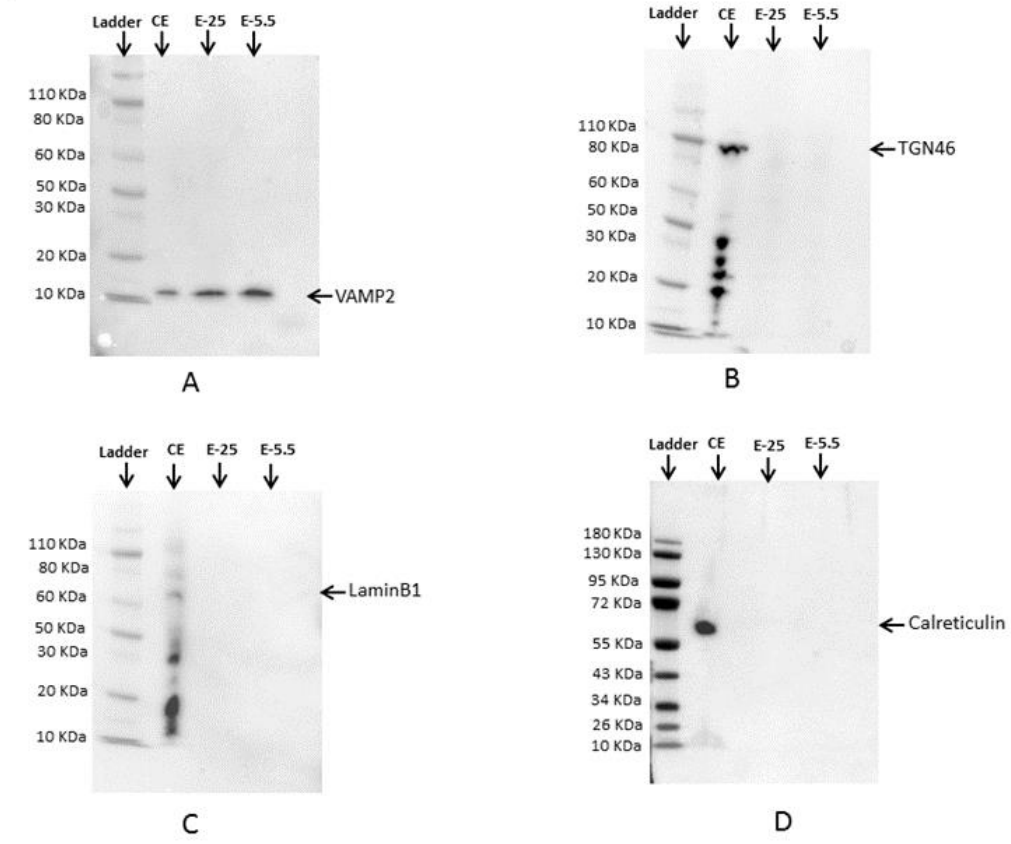

Supplementary Figure 2-3. Immunoblotting assessment of enrichment in the extracted secretory granules. Western blot analyses of the cell extract (CE), extract of the secretory granules in media containing 25 mM glucose (E-25) and 5.5 mM glucose (E-5.5). Proteins were resolved on 4-12% SDS-PAGE gel (NuPAGE), transferred to PVDF membrane and probed with antibodies to identify (A) vesicle-associated membrane protein 2 (VAMP2) for mature secretory granules; (B) TGN46 for the trans-Golgi network; (C) Lamin B1 for the nuclear envelope; and (D) Calreticulin for the endoplasmic reticulum. The immunoreactive bands were visualized using HRP-conjugated goat anti-rabbit secondary antibody and Clarity Western ECL substrate.

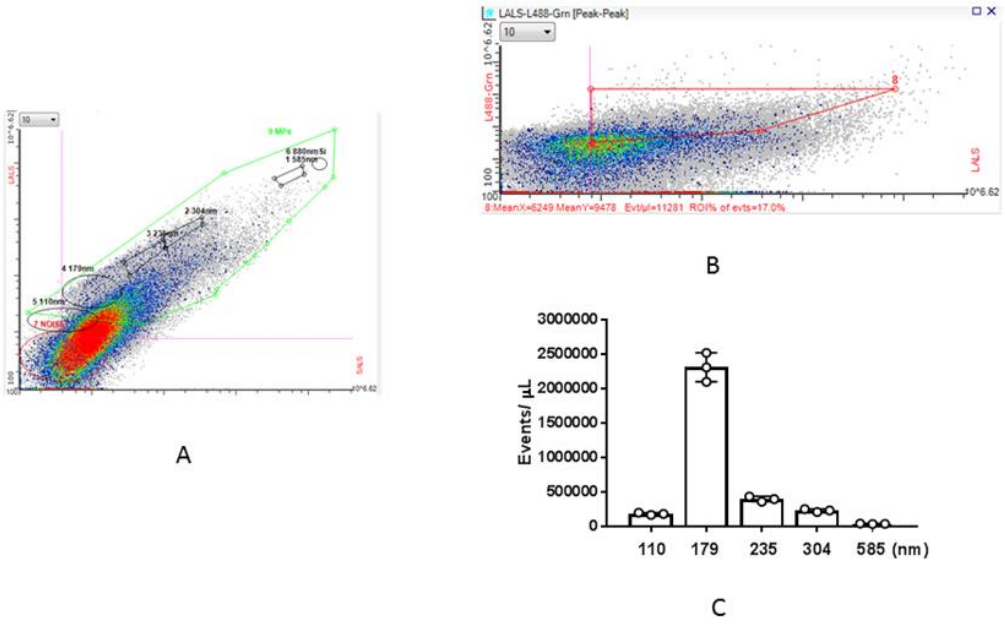

Supplementary Figure 2-4. Nano-scale flow cytometry of the enriched secretory granules. (A) Calibrating nano flow cytometer for size distribution of the enriched secretory granules using ApogeeMix beads. Circles indicate bead sizes of 110, 179, 235, 304, 585 and 880 nm. (B) Gating the glucagon+ secretory granules (L488) using FITC secondary antibody against the Fc segment of Fc-glucagon. (C) Size distribution of the secretory granules within the gate containing glucagon+ secretory granules.

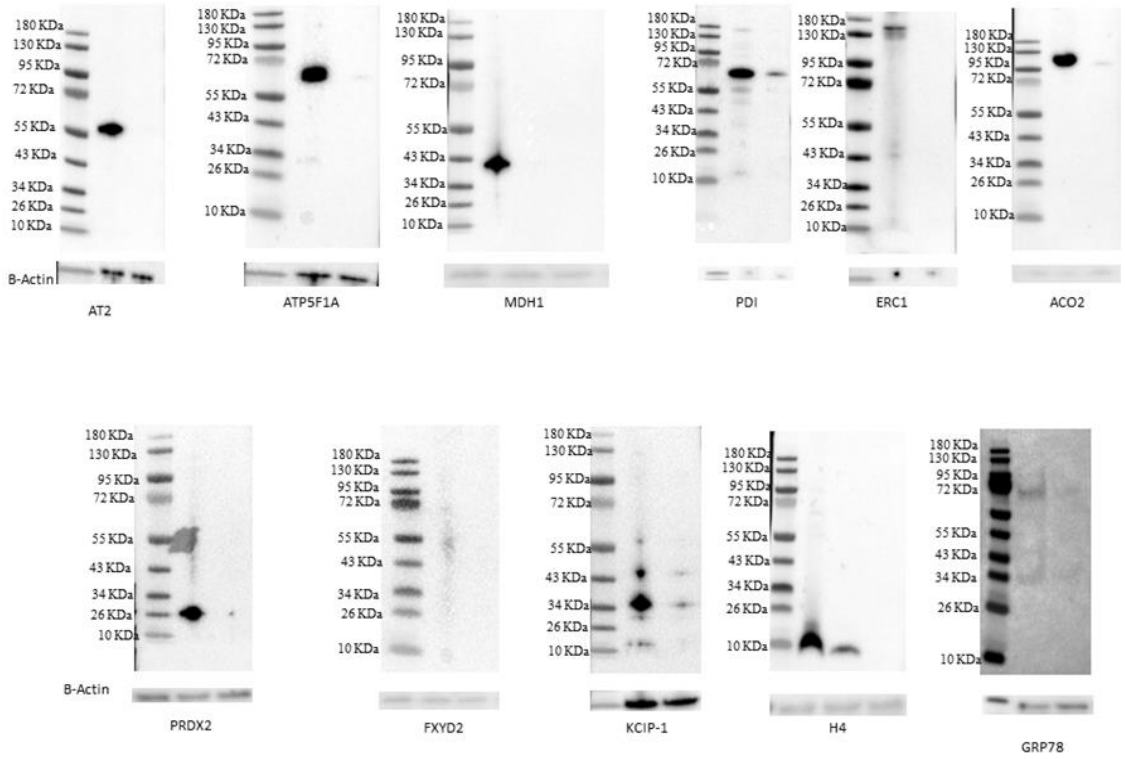

Supplementary Figure 2-6. siRNA mediated gene silencing of target proteins in the secretory granules. α-TC1-6 cells were transfected with 50 nM pooled of 3 predesigned siRNAs. Cell extract subjected to Western blot to follow expression of the following target proteins. For each protein, band intensity of the expressed protein was determined using ImageJ software. Values of ≥ 70% reduction in protein expression levels were considered as successful protein depletion. Alpha-tubulin 2 (AT2), ATP synthase F1 subunit alpha (ATP5F1A), cytosolic malate dehydrogenase (MDH1), Protein disulfide-isomerase (PDI), ELKS/Rab6-interacting/CAST family member 1 (ERC1), Aconitate hydratase mitochondrial (ACO2), peroxiredoxin-2 (PRDX2), FXYD domain-containing ion transport regulator 2 (FXYD2), 14-3-3 zeta/delta (KCIP-1), Histone H4 and Glucose regulated protein 78 KDa (GRP78).

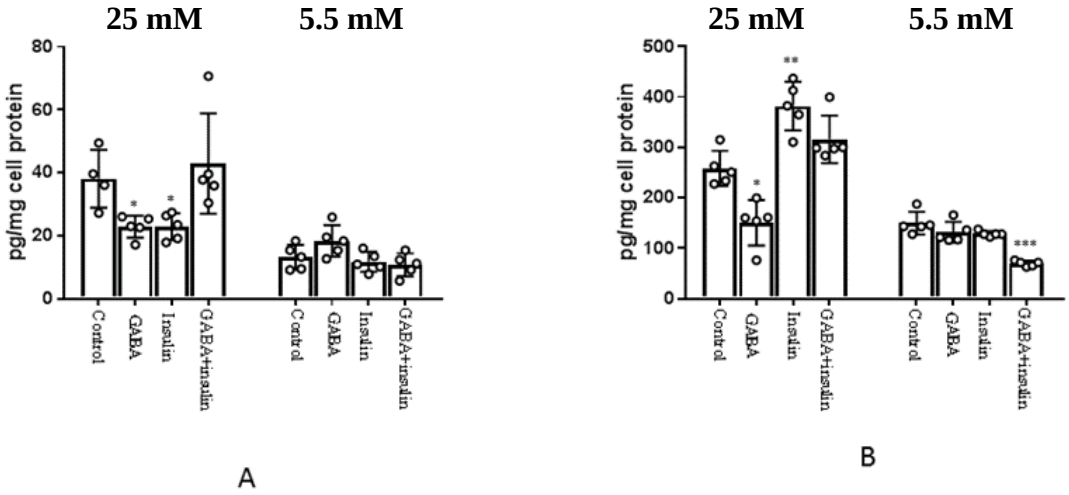

Supplementary Figure 2-8. Alterations in glucagon secretion and cell glucagon content of α-TC1-6 cells in response to nutritional and paracrine effectors. α-TC1-6 cells were cultured and kept under high glucose (25 mM) condition for a long-term. These chronically exposed cells to high glucose condition were treated with GABA (25 µM), insulin (100 pM) or GABA (25 µM) + insulin (100 pM) for 24h in 25 mM or 5.5 mM glucose containing media. At the end if incubation, glucagon levels were measured in the media and cell extract. Values were expressed as mean ± SD (n=4-5) and compared among groups using one-Way ANOVA (α=0.05).*p<0.05, **p<0.01. ***p<0.001.

2.8 Supplementary Tables

Supplementary Table 2-1. Reagents and resources.

REAGENT or RESOURCE	**SOURCE**	**IDENTIFIER**	**Research Resource Identification number**
GABA	Sigma	Cat # A2129	
Insulin	Sigma	Cat # 105-16	
ApogeeMix beads	Apogee FlowSystems Inc.	Cat # 1493	
Lipofectamine 2000	Invitrogen	Cat # 11668-027	
Acetonitrile	BDH	Cat # 83639.100E	
Formic acid	Optima	Cat # A117-50	
Dithiotreitol	Fisher Scientific	Cat # BP172-5	
Iodoacetamide	Alfa Aesar	Cat # A14715	
Protein A Sepharose CL-4B	GE Healthcare Life Science	Cat # 71-7090-00 AF	
HYPERSEP C18 column	ThermoFisher Scientific	Cat # 60108-303	
Mini Protease Inhibitor Cocktail	Sigma-Aldrich	Cat # 11836153001	

Trypsin	Promega	Cat # V5111	

Supplementary Table 2-1 (Continued)

REAGENT or RESOURCE	**SOURCE**	**IDENTIFIER**	**Research Resource Identification number**
Collagen type 1	Sigma	Cat # C3867	
NuPAGE	Invitrogen	Cat # NP0335Box	
iBlot Gel Transfer stacks, PVDF	Invitrogen	Cat # IB401001	
Anti-GRP78 Bip (HSPA5) antibody	Abcam	Cat # Ab21685	
Anti-VAMP2 antibody	Abcam	Cat # ab181869	AB_ 2721005
Anti-TGN46 antibody	Abcam	Cat # 1605	AB_443307
Anti-LaminB1 antibody	Abcam	Cat # ab16048	AB_ 443298
Anti-Histone H4 antibody (ChIP grade)	Abcam	Cat # ab10158	AB_ 296888
Anti-Glucagon antibody	Abcam	Cat # Ab10988	AB_ 297642

ProLong Gold antifade reagent with DAPI	Molecular Probes	Cat # P36935	

Supplementary Table 2-1 (Continued)

REAGENT or RESOURCE	**SOURCE**	**IDENTIFIER**	**Research Resource Identification number**
AlexaFluor 488 goat anti-mouse IgG	Molecular Probes	Cat # A-11001	AB_ 2534069
AlexaFluor 488 goat anti-rabbit IgG	Molecular Probes	Cat # A-11012	AB_ 2534079
Fc-specific FITC antibody	Sigma	Cat # F4143	AB_ 259587
Anti-ERC1 antibody	Abcam	Cat # ab 180507	
Anti- MDH1 antibody	Abcam	Cat # ab 180152	
Anti-ATP5A antibody	Abcam	Cat # ab 176569	
Anti-Aconitase 2 antibody	Abcam	Cat # ab 129105	
Anti-peroxiredoxin2 antibody	Abcam	Cat # ab 109367	

Anti-TUBA1B antibody	Abcam	Cat # ab 108629	
Anti-14-3-3zeta antibody	Abcam	Cat # ab 51129	

Supplementary Table 2-1 (Continued)

REAGENT or RESOURCE	**SOURCE**	**IDENTIFIER**	**Research Resource Identification number**
Anti Na/K ATPase antibody	Thermo Fisher Scientific	Cat# PA5-75640	
Anti-PDI antibody	Abcam	Cat # ab 3672	
Anti-Calreticulin antibody	Abcam	Cat # ab 2907	
Anti-Histone H4 antibody	Abcam	Cat # ab 10158	
Software and Algorithms			
Panther Classification System		http://Pantherdb.org	SCR_015893

ExPASY Bioinformatics Resource Portal		http://string-db.org	SCR_015894
UniportKB		http://uniport.org	SCR_004426
STRING		https://string-db.org	SCR_005223
Experimental model: cell line			
α-TC1-6 cell		mouse pancreatic α-cell line	

Supplementary Table 2-1 (Continued)

REAGENT or RESOURCE	**SOURCE**	**IDENTIFIER**	**Research Resource Identification number**
Recombinant DNA			
FC_pcDNA3.1(+)		http://www.genscript.com	
FC-glucagon_pcDNA3.1(+)		http://www.genscript.com	
Commercial assays			
Glucagon assay kit	ThermoFisher Scientific	Cat # EHGCG	

BCA protein assay kit	Biovision Incorporated	Cat # K813-2500	
Histone H4 Modification Multiplex Assay Kit	Abcam	Cat # Ab185914	
RNeasy extraction kit	Qiagen	Cat # 74104	
SuperScript III First Strand Synthesis Supermix	Thermo Fisher Scientific	Cat # 11752050	
Maxima SYBR Green qPCR Master Mix	Thermo Fisher Scientific	Cat # K0221	
Maxima SYBR Green qPCR Master Mix	Thermo Fisher Scientific	Cat # K0221	
siRNA			
14-3-3 zeta/delta	Thermo Fisher Scientific	Cat # S76190 Cat # S76191 Cat # S76189	
Aconitase	Thermo Fisher Scientific	Cat # S61847 Cat # S61845 Cat # S61846	

Supplementary Table 2-1 (Continued)

REAGENT or RESOURCE	**SOURCE**	**IDENTIFIER**	**Research Resource Identification number**
Sodium-Potassium transporting subunit gamma	Thermo Fisher Scientific	Cat # S62726 Cat # S201066 Cat # S62725	
Protein disulfide-isomerase	Thermo Fisher Scientific	Cat # S71205 Cat # S71206	
Peroxiredoxin-2	Thermo Fisher Scientific	Cat # S204749 Cat # S232273 Cat # S232272	
Malate dehydrogenase cytoplasmic	Thermo Fisher Scientific	Cat # S69980 Cat # S69981 Cat # S69979	
Aconitate hydratase mitochondrial	Thermo Fisher Scientific	Cat # S61847 Cat # S61845 Cat # S61846	
ELKS/Rab6-interacting/CAST family member 1	Thermo Fisher Scientific	Cat # S200972 Cat # S99972 Cat # S99973	

Supplementary Table 2-1 (Continued)

REAGENT or RESOURCE	**SOURCE**	**IDENTIFIER**	**Research Resource Identification number**
Tubulin alpha-1B chain	Thermo Fisher Scientific	Cat # S202331 Cat # S202330 Cat # S75582	
ATP synthase subunit alpha mitochondrial	Thermo Fisher Scientific	Cat # S62742 Cat # S62744 Cat # S62743	
Histone H4	Thermo Fisher Scientific	Cat # S234377 Cat # S234480 Cat # S234061	
GCG (PPG)	Thermo Fisher Scientific	Cat# s66523 Cat# s66522 Cat# s66524	
β-Actin	Thermo Fisher Scientific	Cat# s61899 Cat# s200989 Cat# s200988	
Mission siRNA Universal Negative Control #1	Sigma	SIC001	

Supplementary Table 2-2. List of proteins that interact the with Fc segment alone under conditions of 25 mM glucose.

Associated proteins with Fc segment in 25 mM glucose containing medium
Endoplasmin, Protein disulfide-isomerase A6, Leucine zipper protein 1, Eukaryotic initiation factor 4A-II, DnaJ homolog subfamily C member 12, UPF0565 protein C2orf69 homolog, Obg-like ATPase 1, Catenin beta-1, Nascent polypeptide-associated complex subunit alpha, muscle-specific form, Protein scribble homolog, AP2-associated protein kinase 1, Drebrin-like protein, Sorting nexin-2, Nucleoporin NUP53, Transient receptor potential cation channel subfamily M member 6, Transcription elongation factor A protein-like 3, Tyrosine-protein phosphatase non-receptor type 23, Protein phosphatase 1G, T-complex protein 1 subunit zeta, Malate dehydrogenase, mitochondrial, Protein CutA, Transaldolase, Dihydropyrimidinase-related protein 2, 60S ribosomal protein L10-like, Probable cation-transporting ATPase 13A1, 40S ribosomal protein S30, Phosphatidylethanolamine-binding protein 1, RNA-binding protein 14, Synaptosomal-associated protein 25, 60S ribosomal protein L8, Phosphatidylinositol-binding clathrin assembly protein, Importin subunit beta-1, T-complex protein 1 subunit delta, Proliferating cell nuclear antigen, Zyxin, Non-histone chromosomal protein HMG-17, Aldose reductase, T-complex protein 1 subunit eta, Sulfated glycoprotein 1, Stress-induced-phosphoprotein 1, Peroxiredoxin-1, 40S ribosomal protein S6, Ataxin-2-like protein, C-1-tetrahydrofolate synthase, cytoplasmic, Endophilin-B1, ProSAAS, Histidine triad nucleotide-binding protein 1, Transitional endoplasmic reticulum ATPase, Desmoplakin, Myosin-10, Clathrin light chain A, 26S protease regulatory subunit 6A, Rab GDP dissociation inhibitor alpha, Eukaryotic translation initiation factor 4 gamma 1, N-acetylglucosamine-6-sulfatase, Histone H3.3C, Eukaryotic initiation factor 4A-I, Transketolase, 60S ribosomal protein L22, Glucosidase 2 subunit beta, Dolichyl-diphosphooligosaccharide--protein glycosyltransferase 48 kDa subunit, Nuclear transport factor 2, Golgin subfamily A member 4, Tryptophan--tRNA ligase, cytoplasmic, Eukaryotic translation initiation

factor 4B, Tripeptidyl-peptidase 2, Ubinuclein-2, V-type proton ATPase subunit G 1, Peroxiredoxin-4, Aminoacyl tRNA synthase complex-interacting multifunctional protein 1, Potassium voltage-gated channel subfamily C member 3, Afadin, Nuclear autoantigenic sperm protein, 60S ribosomal protein L19, Histone H3.1, Vacuolar protein sorting-associated protein VTA1 homolog, Coatomer subunit alpha, COP9 signalosome complex subunit 3, Thioredoxin domain-containing protein 17, Serine/threonine-protein kinase PAK 2, Rho-associated protein kinase 2, G protein-regulated inducer of neurite outgrowth 1, Pleckstrin homology domain-containing family G member 5, F-actin-capping protein subunit beta, Histone H1.3, Microtubule-associated protein 4, Septin-9, Stromal membrane-associated protein 2, Trifunctional purine biosynthetic protein adenosine-3, Eukaryotic initiation factor 4A-III, Creatine kinase B-type, Chromatin target of PRMT1 protein,

Supplementary Table 2-3. List of proteins that interact the with Fc segment alone under conditions of 5.5 mM glucose.

Succinyl-CoA:3-ketoacid coenzyme A transferase 1, mitochondrial, Histone-lysine N-methyltransferase SETD1B, Importin subunit beta-1, Aldose reductase, Tumor-associated calcium signal transducer 2, Heterogeneous nuclear ribonucleoprotein A3, Elongation factor 1-gamma, 60S ribosomal protein L22, Calmodulin, Ubiquitin-conjugating enzyme E2 N, Actin, alpha skeletal muscle, Peptidyl-prolyl cis-trans isomerase FKBP2, V-type proton ATPase catalytic subunit A, Ubiquitin-like modifier-activating enzyme 1, Nascent polypeptide-associated complex subunit alpha, L-lactate dehydrogenase B chain, Farnesyl pyrophosphate synthase, Protein FAM171A2, Msx2-interacting protein, T-complex protein 1 subunit gamma, Calreticulin, Electron transfer flavoprotein subunit alpha, mitochondrial, ER membrane protein complex subunit 2, 40S ribosomal protein S2, L-lactate dehydrogenase A chain, Acyl-CoA-binding protein, Serine/threonine-protein phosphatase 2A 65 kDa regulatory subunit A alpha isoform, L-lactate dehydrogenase C chain, Alpha-actinin-4, Nuclease-sensitive element-binding protein 1, Chromogranin-A, Prefoldin subunit 2, Protein FAM117B, Stromal interaction molecule 2, ATP-dependent RNA helicase DDX3X, Nucleosome assembly protein 1-like 4, 60S ribosomal protein L5, Protein SET, Neurofilament light polypeptide, Transgelin-2

Supplementary Table 2-4. Profile of the histone, cytoskeletal and ribosomal proteins contained within the glucagon interactome when α-TC1-6 cells were incubated for 24h in media containing 25 mM or 5.5 mM glucose.

25 mM glucose containing medium	5.5 mM glucose containing medium
Histone H2A type 1, Histone H2A type 1-F, Histone H2A type 1-F, Histone H2A type 1-H, Histone H2A type 1-K, Histone H2A type 2-A, Histone H2A type 2-B, Histone H2A type 2-C, Histone H2A type 3, Histone H2A.J, Histone H2AX, Histone H2B type 1-B, Histone H2B type 1-C/E/G, Histone H2B type 1-F/J/L, Histone H2B type 1-H, Histone H2B type 1-K, Histone H2B type 1-M, Histone H2B type 1-P, Histone H2B type 2-B, Histone H2B type 2-E, Histone H2B type 3-A, Histone H2B type 3-B	Histone H2A type 3, Histone H2A type 1-F, Histone H2B type 1-B, Histone H1.3, Histone H2A type 2-A, Histone H2B type 1-H, Histone H2B type 3-A, Histone H4, Histone H3.3, Histone H3.3C, Histone H2A.J, Histone H2A type 1-K, Histone H3.1, Histone H2A type 2-C, Histone H2A type 1, Histone H2B type 1-K, Histone H3.2, Histone H2B type 1-M, Histone H1.2, Histone H2B type 3-B, Histone H2B type 2-B, Histone H2B type 2-E, Histone H2B type 1-C/E/G, Histone H2A type 1-H, Histone H1.5, Histone H2B type 1-P, Histone H1.1, Histone H2A type 2-B, Histone H2A type 1-F, Histone H2B type 1-B, Histone H2AX, Histone H2B type 1-F/J/L
Actin cytoplasmic 2, Actin cytoplasmic 1, Actin alpha skeletal muscle, Actin aortic smooth muscle, Actin alpha cardiac muscle 1, Actin gamma-enteric smooth muscle, Beta-actin-like protein 2, Tubulin beta-4B chain, Tubulin alpha-1C chain, Tubulin alpha-1A chain, Tubulin alpha-1B chain, Tubulin beta-5 chain, Tubulin beta-2B chain, Tubulin beta-4A chain,	Actin, cytoplasmic 1, Actin, cytoplasmic 2, Tubulin beta-4B chain, Tubulin beta-4A chain, Tubulin beta-5 chain, Tubulin alpha-1C chain, Tubulin beta-3 chain, Tubulin alpha-1A chain, Tubulin alpha-1B chain

Tubulin beta-3 chain, Tubulin beta-2A chain 60S ribosomal protein L13, 40S ribosomal protein S14, 60S ribosomal protein L23a, 60S ribosomal protein L11, 60S acidic ribosomal protein P1, Elongation factor 1-delta, Elongation factor 1-alpha 2, Eukaryotic translation initiation factor 5A-1, Elongation factor 1-alpha 1	40S ribosomal protein S15a, 60S ribosomal protein L23a, 40S ribosomal protein S7, 40S ribosomal protein S25, 60S ribosomal protein L13, 40S ribosomal protein S14, 40S ribosomal protein S12, Elongation factor 1-alpha 2, 60S acidic ribosomal protein P1, 60S ribosomal protein L11, 60S ribosomal protein L18, 60S acidic ribosomal protein P2, Elongation factor 2, Ubiquitin-60S ribosomal protein L40, Eukaryotic translation initiation factor 4B

Supplementary Table 2-5. Profile of the histone, cytoskeletal and ribosomal proteins within the glucagon interactome. α-TC1-6 cells were cultured in media containing 25 mM glucose and treated with GABA (Table S5-A), insulin (Table S5-B) and GABA+ insulin (Table S5-C). Proteins were identified using LC-MS/MS.

Table-S5-A

GABA + 25 mM glucose
Histone H2A type 1, Histone H2A type 1-F, Histone H2A type 1-F, Histone H2A type 1-H, Histone H2A type 1-K, Histone H2A type 2-A, Histone H2A type 2-B, Histone H2A type 2-C, Histone H2A type 3, Histone H2A.J, Histone H2AX, Histone H2B type 1-B, Histone H2B type 1-C/E/G, Histone H2B type 1-F/J/L, Histone H2B type 1-H, Histone H2B type 1-K, Histone H2B type 1-M, Histone H2B type 1-P, Histone H2B type 2-B, Histone H2B type 2-E, Histone H2B type 3-A, Histone H2B type 3-B, Histone H4
Actin cytoplasmic 1, Actin cytoplasmic 2, Anionic trypsin-2, Tubulin alpha-1A chain, Tubulin alpha-1B chain, Tubulin alpha-1C chain, Tubulin beta-2A chain, Tubulin beta-2B chain, Tubulin beta-3 chain, Tubulin beta-4A chain, Tubulin beta-4B chain, Tubulin beta-5 chain
60S acidic ribosomal protein P1, 60S ribosomal protein L11, Elongation factor 1-alpha 1, Eukaryotic translation initiation factor 4E

S5-B

Insulin + 25 mM glucose
Histone H1.5, Histone H1t, Histone H2A type 1, Histone H2A type 1-F, Histone H2A type 1-F, Histone H2A type 1-H, Histone H2A type 1-K, Histone H2A type 2-A, Histone H2A type 2-B, Histone H2A type 2-C, Histone H2A type 3, Histone H2A.J, Histone H2AX, Histone H2B type 1-B, Histone H2B type 1-C/E/G, Histone H2B type 1-F/J/L, Histone H2B type 1-H, Histone H2B type 1-K, Histone H2B type 1-M, Histone H2B type 1-P, Histone H2B type 2-B, Histone H2B type 2-E, Histone H2B type 3-A, Histone H2B type 3-B, Histone H4 Actin alpha cardiac muscle 1, Actin alpha skeletal muscle, Actin aortic smooth muscle, Actin cytoplasmic 1, Actin cytoplasmic 2, Actin gamma-enteric smooth muscle, Tubulin alpha-1A chain, Tubulin alpha-1B chain, Tubulin alpha-1C chain, Tubulin beta-2A chain, Tubulin beta-2B chain, Tubulin beta-3 chain, Tubulin beta-4A chain, Tubulin beta-4B chain, Tubulin beta-5 chain 40S ribosomal protein S14, 60 kDa heat shock protein mitochondrial, 60S acidic ribosomal protein P1, 60S ribosomal protein L11, Elongation factor 1-alpha 1, Elongation factor 1-alpha 2, Eukaryotic translation initiation factor 5A-1

S5-C

GABA+ insulin + 25 mM glucose
Histone H2B type 1-B, Histone H2B type 1-B, Histone H2B type 1-C/E/G, Histone H2B type 1-F/J/L, Histone H2B type 1-H, Histone H2B type 1-K, Histone H2B type 1-M, Histone H2B type 1-P, Histone H2B type 2-B, Histone H2B type 2-B, Histone H2B type 2-E, Histone H2B type 3-A, Histone H2B type 3-B Actin alpha cardiac muscle 1, Actin alpha skeletal muscle, Actin aortic smooth muscle, Actin cytoplasmic 1, Actin cytoplasmic 1, Actin gamma-enteric smooth muscle, Tubulin alpha-1A chain, Tubulin alpha-1A chain, Tubulin alpha-1B chain, Tubulin alpha-1C chain, Tubulin alpha-1C chain 60S ribosomal protein L23a

Supplementary Table 2-6. Profile of the histone, cytoskeletal and ribosomal proteins within the glucagon interactome. α-TC1-6 cells were cultured in media containing 5.5 mM glucose and treated with GABA (Table S6-A), insulin (Table S6-B) and GABA+insulin (Table S6-C). Proteins were identified using LC-MS/MS.

Table S6-A

GABA + 5.5 mM glucose
Histone H1.3, Histone H1.5, Histone H2A type 1, Histone H2A type 1-F, Histone H2A type 1-H, Histone H2A type 1-K, Histone H2A type 2-A, Histone H2A type 2-C, Histone H2A type 3, Histone H2A.J, Histone H2B type 1-B, Histone H2B type 1-C/E/G, Histone H2B type 1-F/J/L, Histone H2B type 1-H, Histone H2B type 1-K, Histone H2B type 1-P, Histone H2B type 2-B, Histone H2B type 2-E, Histone H2B type 3-A, Histone H2B type 3-B, Histone H3.1, Histone H3.3, Histone H3.3C, Histone H4, Histone H1.2, Histone H2B type 1-B, Histone H2B type 1-M, Histone H3.2
Actin cytoplasmic 1, Actin cytoplasmic 2, Tubulin alpha-1A chain, Tubulin alpha-1B chain, Tubulin alpha-1C chain, Tubulin beta-3 chain, Tubulin beta-5 chain
40S ribosomal protein S14, 40S ribosomal protein S15, 40S ribosomal protein S25, 40S ribosomal protein S5, 40S ribosomal protein SA, 60S acidic ribosomal protein P1, 60S acidic ribosomal protein P2, 60S ribosomal protein L11, 60S ribosomal protein L15, 60S ribosomal protein L18, 60S ribosomal protein L7a, 60S ribosomal protein L7a, Ubiquitin-60S ribosomal protein L40, Eukaryotic initiation factor 4A-I, Eukaryotic initiation factor 4A-II, Eukaryotic initiation factor 4A-III, Elongation factor 1-alpha 1, Elongation factor 2

Table S6-B

Insulin + 5.5 mM glucose
Histone H1.1, Histone H1.2, Histone H1.3, Histone H1.4, Histone H1.5, Histone H1t, Histone H2A type 1, Histone H2A type 1-F, Histone H2A type 1-H, Histone H2A type 1-K, Histone H2A type 2-A, Histone H2A type 2-C, Histone H2A type 3, Histone H2A.J, Histone H2B type 1-B, Histone H2B type 1-C/E/G, Histone H2B type 1-F/J/L, Histone H2B type 1-H, Histone H2B type 1-K, Histone H2B type 1-M, Histone H2B type 1-P, Histone H2B type 2-B, Histone H2B type 3-A, Histone H2B type 3-B, Histone H3.1, Histone H3.2, Histone H3.3, Histone H3.3C, Histone H4 Actin alpha cardiac muscle 1, Actin alpha skeletal muscle, Actin aortic smooth muscle, Actin cytoplasmic 1, Actin cytoplasmic 2, Actin gamma-enteric smooth muscle, Tubulin alpha-1A chain, Tubulin alpha-1B chain, Tubulin alpha-3 chain, Tubulin alpha-4A chain, Tubulin beta-5 chain, Tubulin-specific chaperone A 40S ribosomal protein S12, 40S ribosomal protein S14, 40S ribosomal protein S15a, 40S ribosomal protein S18, 40S ribosomal protein S19, 40S ribosomal protein S20, 40S ribosomal protein S25, 40S ribosomal protein S3, 40S ribosomal protein S3, 40S ribosomal protein S3a, 40S ribosomal protein S8, 40S ribosomal protein SA, 60 kDa heat shock protein mitochondrial, 60S acidic ribosomal protein P1, 60S acidic ribosomal protein P2, 60S ribosomal protein L11, 60S ribosomal protein L12, 60S ribosomal protein L13, 60S ribosomal protein L15, 60S ribosomal protein L18, 60S ribosomal protein L23a, 60S ribosomal protein L26, 60S ribosomal protein L27, 60S ribosomal protein L7, 60S ribosomal protein L7, 60S ribosomal protein L9, Elongation factor 1-alpha 1, Elongation factor 1-alpha 2, Elongation factor 1-beta, Elongation factor 1-delta, Elongation factor 2, Eukaryotic initiation factor 4A-I, Eukaryotic initiation factor 4A-II, Eukaryotic initiation factor 4A-III, Transcription elongation factor A protein-like 3, Transcription elongation factor A protein-like 3, Transcription elongation factor A protein-like 5, Transcription factor SOX-1,

Table S6-C

GABA+ insulin + 5.5 mM glucose
Histone H1.5, Histone H2A type 1, Histone H2A type 1-F, Histone H2A type 1-H, Histone H2A type 1-K, Histone H2A type 2-A, Histone H2A type 2-C, Histone H2A type 3, Histone H2A.J, Histone H2AX, Histone H2B type 1-B, Histone H2B type 1-C/E/G, Histone H2B type 1-H, Histone H2B type 1-M, Histone H2B type 1-P, Histone H2B type 2-B, Histone H2B type 3-A, Histone H2B type 3-B, Histone H4, Histone H2A type 2-B, Histone H2B type 1-F/J/L Actin cytoplasmic 1, Tubulin alpha-1A chain, Tubulin alpha-1B chain, Tubulin alpha-1C chain, Tubulin beta-2A chain, Tubulin beta-2B chain, Tubulin beta-3 chain, Tubulin beta-4A chain, Tubulin beta-4B chain, Tubulin beta-5 chain 60S ribosomal protein L11, Elongation factor 1-alpha 1, Elongation factor 2

Supplementary Table 2-7. Functional categories of the proteins within the glucagon interactome in the context of 25 mM glucose. Proteins were functionally categorized using Panther GO-Slim Molecular Function analysis. Values show protein hits as percentage of the total number of hits within each category when α-TC1-6 cells were cultured in media containing 25 mM glucose.

	Control	GABA	Insulin	GABA+ insulin
Binding	47.4	46.1	48.5	51.4
Structural molecule activity	24.7	13.7	15.4	28.6
Catalytic activity	19.6	22.5	26.2	17.1
Receptor activity	1	5.9	2.3	-
Translation regulator activity	4.1	1	2.3	-
Transporter activity	3.1	6.9	4.6	2.9
Signal transducer activity	-	2.9	-	-
Antioxidant activity	-	1	0.8	-

Supplementary Table 2-8. Functional categories of proteins within the glucagon interactome in the context of 5.5 mM glucose. Proteins were functionally categorized using Panther GO-Slim Molecular Function analysis. Each value shows protein hit as percentage of the total number of hits within each category when α-TC1-6 cells were cultured in media containing 5.5 mM glucose.

	Control	GABA	Insulin	GABA+ insulin
Binding	48.4	43.8	43.5	50.6
Structural molecule activity	15	11.4	14.9	17.6
Catalytic activity	25.5	28.6	31	22.4
Receptor activity	2	1.6	1.2	1.2
Translation regulator activity	2.6	1.1	2	2.4
Transporter activity	3.9	4.9	4.3	4.7
Antioxidant activity	2	1.6	1.6	1.2

Channel regulator activity	-	0.5	-	-
Signal transducer activity	-	6.5	1.6	-

Chapter 3

This chapter was reformatted from its original published paper in Frontiers in Endocrinology under the license of Creative Commons Attribution 4.0 International License (https://creativecommons.org/licenses/by/4.0/).

The citation for its original work is as follows:

Asadi F, Dhanvantari S. (2020) Stathmin-2 Mediates Glucagon Secretion From Pancreatic α-Cells. Front Endocrinol (Lausanne). 11:29. doi: 10.3389/fendo.2020.00029. eCollection 2020.

3. Stathmin-2 Mediates Glucagon Secretion from Pancreatic α-cells

3.1 Abstract

Inhibition of glucagon hypersecretion from pancreatic α-cells is an appealing strategy for the treatment of diabetes. Our hypothesis is that proteins that associate with glucagon within α-cell secretory granules will regulate glucagon secretion, and may provide druggable targets for controlling abnormal glucagon secretion in diabetes. Recently, we identified a dynamic glucagon interactome within the secretory granules of the α cell line, α-TC1-6, and showed that select proteins within the interactome could modulate glucagon secretion. In the present study, we show that one of these interactome proteins, the neuronal protein stathmin-2, is expressed in α-TC1-6 cells and in mouse pancreatic α-cells, and is a novel regulator of glucagon secretion. The secretion of both glucagon and Stmn2 was significantly enhanced in response to 55 mM K^+, and immunofluorescence confocal microscopy showed co-localization of stathmin-2 with glucagon and the secretory granule markers chromogranin A and VAMP-2 in α-TC1-6 cells. In mouse pancreatic islets, Stathmin-2 co-localized with glucagon, but not with insulin, and co-localized with secretory pathway markers. To show a function for stathmin-2 in regulating glucagon secretion, we showed that siRNA—mediated depletion of stathmin-2 in α-TC1-6 cells caused glucagon secretion to become constitutive without any effect on proglucagon mRNA levels, while overexpression of stathmin-2 completely abolished both basal and K^+-stimulated glucagon secretion. Overexpression of stathmin-2 increased the localization of glucagon into the endosomal-lysosomal compartment, while depletion of stathmin-2 reduced the endosomal localization of glucagon. Therefore, we describe stathmin-2 as having a novel role as an α-cell secretory granule protein that modulates glucagon secretion via trafficking through the endosomal-lysosomal system. These findings describe a potential new pathway for the regulation of glucagon secretion, and may have implications for controlling glucagon hypersecretion in diabetes.

Keywords: glucagon, α-cell, glucagon hypersecretion, glucagon interactome, stathmin-2

3.2 Introduction

Hyperglucagonemia is a characteristic sign of diabetes, causing fasting hyperglycemia and glycemic volatility. Clinically, glycemic variability contributes to the development of diabetes complications (1). Persistent hyperglucagonemia may exacerbate abnormal glucose metabolism in patients with type 2 diabetes and lead to metabolic disturbances in obese and prediabetic individuals (2). Further complicating glucose homeostasis in diabetes is the direct effect of glucose on the α-cells; while glucagon secretion is maximally suppressed at plasma glucose concentrations of 5–10 mM, it increases at glucose levels above 10 mM, thus exacerbating hyperglycemia (3–6). Therefore, controlling excess glucagon secretion may be a potential therapeutic strategy for diabetes (7) so that glycemia and glucose metabolism may be better regulated. Such an approach has been suggested as a priority for the treatment of diabetes (1).

Combating hyperglucagonemia could be theoretically achieved by (i) inhibition of glucagon action at target organs by blocking the glucagon receptor, or (ii) inhibition of glucagon secretion from the pancreatic α cells. While in the short-term the former could be an effective therapeutic strategy, it can lead to α cell hyperplasia and hyperglucagonemia over a long-term period (8), along with a risk of hypoglycemia (9) and disturbances in lipid metabolism (10). Therefore, inhibiting glucagon secretion, rather than blocking the glucagon receptor, may be a more appropriate therapeutic approach for the treatment of hyperglucagonemia of diabetes (11).

It has been documented that suppression of glucagon secretion can be mediated at the systemic, paracrine or intrinsic level (12). As a systemic modulator, GLP-1 inhibits glucagon secretion; however, there are controversies as to whether GLP-1 directly inhibits glucagon secretion from α cells by signaling through the α-cell GLP-1R (13–15), or indirectly by increasing inter-islet somatostatin or insulin secretion (13, 16). Glucagon secretion is also suppressed by paracrine signaling through the insulin, somatostatin and GABAA receptors on the α cell (16–18) At an intrinsic level, glucose directly or indirectly inhibits glucagon secretion from the α cell (19–22) by altering downstream activities of Ca^{2+} channels, K_{ATP} channels (23), and trafficking of secretory granules (24).

We are pursuing the hypothesis that glucagon secretion can also be controlled by proteins within the secretory granule that associate with glucagon. By conducting secretory granule proteomics in α-TC1-6 cells, we have recently described a dynamic glucagon interactome, and shown that components of this interactome can play a role in modulating glucagon secretion (25). Of these components, a protein of particular interest is Stathmin-2 (Stmn2 or SCG10), a member of the stathmin family of Golgi proteins (26) that may play a role in the regulation of neuroendocrine secretion (27). In the human islet, Stmn2 expression may be unique to α-cells, as shown by genome-wide RNA-Seq analysis (28) and single cell transcriptomics (23), and α-cell Stmn2 mRNA expression is differentially regulated in type 2 diabetes (29). These studies, together with our proteomics findings, led us to hypothesize that Stmn2 may function in α cells to modulate glucagon secretion. In the present study, we show that Stmn2 is co-localized with glucagon in secretory granules of α-TC1-6 cells and controls glucagon secretion by trafficking through the endosomal/lysosomal system.

3.3 Materials and methods

3.3.1 Cell culture

α-TC1-6 cells (a kind gift from C. Bruce Verchere, University of British Columbia, Vancouver, BC, Canada) were cultured in regular DMEM medium containing 5.6 mM glucose (Cat# 12320032, Thermo Fisher Scientific) supplemented with 15% horse serum (Cat# 26050088, Thermo Fisher Scientific), 2.5% FBS (Cat# 16000044, Thermo Fisher Scientific), L-glutamine and sodium pyruvate. For secretion experiments, cells were plated in 6 –well plates and for all experiments, a low passage number (up to P6) was used. Twenty-four hours prior to secretion experiments, media were removed and replaced with DMEM without supplements. To evaluate (25) the regulated secretion of glucagon, cells were washed twice with HBSS, pre-incubated for 2 h in DMEM without supplements, then incubated for 15 min with or without KCl (55 mM). These media were collected into tubes containing protease inhibitor (PMSF, 45 mM) and phosphatase inhibitors (sodium orthovanadate, 1 mM; and sodium fluoride 5 mM) while tubes were kept on ice. After collection, media were centrifuged at 13,000× g for 5 min at 4°C, and the supernatant was collected into new microfuge tubes and immediately kept at −80°C

until analysis. After media were removed, cells were washed using ice-cold PBS (pH 7.4) and lysed in RIPA buffer (Cat# 89900, Thermo Fisher Scientific) containing abovementioned protease and phosphatase inhibitors. The lysed cells were centrifuged at 13,000× g for 5 min at 4°C and the supernatant was kept at −80°C for protein assays.

3.3.2 Gene construct and plasmid preparation

To generate the expression plasmid for Stmn2, the Kozak sequence (GCCACC), signal peptide sequence and coding sequence of mouse Stmn2 (https://www.uniprot.org/uniprot/P55821) were ligated into the NheI and ApaI restriction sites of pcDNA3.1(+) MAr. The construct was synthesized by GENEART GmbH, Life Technologies (GeneArt project 2018AAEGRC, Thermo Fisher Scientific). Then, Max Efficiency DH5α competent cells (Thermo Fisher Scientific, Cat# 18258012) were transformed according to the manufacturer's protocol. Plasmids were then extracted and purified using the PureLink HiPure Plasmid Maxiprep Kit (Thermo Fisher Scientific, Cat# K210006) for downstream experiments. Correct assembly of the final construct was verified by gene sequencing at the London Regional Genomics Facility, Western University. For Stmn2 overexpression studies, α-TC1-6 cells were transiently transfected by pcDNA3.1 (+) MAr-stmn2 construct or empty vector (negative control). All transfections were done using Lipofectamine 2000 (Cat#11668-027, Invitrogen). To monitor normal cell growth and morphology, cells were checked daily by the EVOS cell imaging system (Thermo Fisher Scientific). The efficiency of transfection was determined in a preliminary study at >70% through co-transfection with pEGFP.

3.3.3 Gene silencing experiments

siRNA-mediated depletion of stathmin-2

Functional analysis of Stmn2 was done by gene silencing experiments. siRNAs targeting three regions within the Stmn2 mRNA (Cat# s73356, s73354, s73355) were chosen from pre-designed mouse siRNAs (Silencer siRNA, Thermo Fisher Scientific). The control group was treated with Mission siRNA Universal Negative Control # 1 (Cat# SIC001, Sigma-Aldrich). Gene silencing was done based on a previously published protocol (30) and as we have done previously with some modifications (25). Briefly, α-TC1-6 cells

were cultured in regular DMEM to 60% confluency. Media were removed and replaced with 2 mL Opti-MEM (Cat# 31985-070, Gibco) containing 50 nM pooled siRNAs with Lipofectamine 2000. After 8 h, media were changed to regular DMEM without sera (FBS and horse serum) and cultured for 72 h. Then, media were refreshed and cells were cultured for 15 min in the absence or presence of 55 mM KCl as described above. Gene silencing was confirmed by analyzing mRNA expression levels of Stmn2. After removing media, cells were washed by cold PBS (pH 7.4) and total RNA was extracted (RNeasy extraction kit; Cat # 74104, Qiagen). cDNA synthesis was performed using the SuperScript III First Strand Synthesis Supermix for qRT-PCR (Cat # 11752050, Thermo Fisher Scientific), according to the supplier's protocol. Real-time PCR was performed using Quant Studio Design and Analysis Real-Time PCR Detection System in conjunction with the Maxima SYBR Green qPCR Master Mix (Cat # K0221, Thermo Fisher Scientific) using specific primers for Stmn2: forward, 5′-GCAATGGCCTACAAGGAAAA-3′; reverse, 5′-GGTGGCTTCAAGATCAGCTC-3′; and β-Actin; forward, 5′-AGCCATGTACGTAGCCATCC-3′; reverse, 5′-CTCTCAGCTGTGGTGGTGAA-3′. Gene expression levels for stathmin-2 were normalized to that of β-Actin. The normalized level of transcripts in the depleted cells was shown relative to that of the non-targeting negative control. Relative expression levels were determined as percent of alterations compared to the control. Statistical analysis was performed using t-test at $\alpha = 0.05$.

Proglucagon gene expression levels following Stmn2 depletion

After siRNA treatments, proglucagon gene expression levels were measured by real-time PCR as described above using proglucagon-specific primers (forward: 5′-CAGAGGAGAACCCCAGATCA-3′, reverse: 5′-TGACGTTTGGCAATGTTGTT-3′).

3.3.4 Immunoblotting

To test for effects of siRNA transfection on levels of Stmn2, α-TC1-6 cells were lysed using non-ionic lysis buffer (50 mM Tris pH 7.4, 150mM NaCl, 1% Triton X-100 plus cOmplete Mini Protease Inhibitor Cocktail and 5 μg/mL Aprotinin). Proteins were resolved by 4-12% NuPAGE gel (Cat # NP0335Box, Invitrogen), transferred to a PVDF

membrane (Cat # IB401001, Invitrogen) and probed with primary antibodies (Stmn2, Cat# 720178, Thermo Fisher Scientific; 1:1000; beta actin, Cat# ab8227, Abcam, 1:1000) overnight. Immunoreactive bands were visualized using HRP-conjugated goat anti-rabbit secondary antibody (Cat# 31460, Invitrogen; 1:1000) and Clarity Western ECL substrate (Cat# 170-5061, Bio-Rad). Images were acquired on a BioRad ChemiDoc Imaging System. Total cell extracts from control cells were used as positive control.

3.3.5 Immunofluorescence confocal microscopy

α-TC1-6 cells

To determine if Stmn2 and glucagon could be co-localized to the same intracellular compartments, we used immunofluorescence confocal microscopy. Wild type α-TC1-6 cells were seeded on collagen (type I)-coated coverslips and grown in regular DMEM, then incubated in non-supplemented DMEM for 24 h. At the end of incubation, cells were washed once with PBS, fixed in 2% paraformaldehyde (in PBS) for 30 min, permeabilized with 0.25% Triton X-100 (in PBS) for 5 min and washed with PBS. After 1 h incubation with blocking buffer (10% goat serum in 1% BSA/PBS), coverslips were incubated with primary antibodies against glucagon (mouse anti- glucagon antibody, Cat # ab10988, Abcam; 1:1000), Stathmin-2 (goat anti-SCG10 antibody, Cat # ab115513, Abcam; 1:1000), secretory granule marker, chromogranin A (mouse anti-ChgA antibody, Cat# MAB319, Sigma; 1:1000), secretory granule marker, VAMP2 (rabbit anti-VAMP2, Cat# ab215721, Abcam; 1:1000), early endosome marker, EEA1 (rabbit antiEEA1, Cat # ab 2900, Abcam; 1:500) or the lysosomal marker, Lamp2A (rabbit anti-Lamp2A, Cat# ab18528, Abcam; 1:500) overnight. After washing with PBS, coverslips were incubated with the following secondary antibodies as appropriate: goat anti-mouse IgG Alexa Fluor 488 (Cat# A-11001, Molecular Probes; 1:500), goat anti-rabbit IgG Alexa Fluor 594 (Cat# A11037, Invitrogen; 1:500) or donkey anti-goat IgG Alexa Fluor 555 (Cat# ab150130, Abcam; 1:500) Invitrogen) for 2 h in the dark at room temperature. Then, coverslips were washed with PBS and mounted on glass slides using DAPI containing ProLong antifade mountant (Cat # P36935, Molecular Probes) for image analysis by confocal immunofluorescence microscopy (Nikon A1R, Mississauga, Canada). Coverslip

preparation was done at least four different times with freshly thawed cells. Each thawed batch of the cell was cultured and passaged three times.

Mouse pancreatic islets

All mice were treated in accordance with the guidelines set out by the Animal Use Subcommittee of the Canadian Council on Animal Care at Western University based on the approved Animal Use Protocol AUP 2012-020. Six to eight-week old male C57BL/6 mice (n = 7) were sacrificed by cervical dislocation under anesthesia with inhalant isoflurane. Pancreata were collected and fixed in 10% buffered formalin for 3 days and treated with 70% ethanol for 1 day before paraffin embedding at the Molecular Pathology Core Facility, Robarts Research Institute, Western University. The paraffin-embedded blocks were longitudinally sectioned in 5 μm slices and fixed onto glass microscope slides. The samples were de-paraffinized by graded washes using xylene, ethanol and PBS. Background Sniper (Cat# BS966H, Biocare Medical) was used to reduce non-specific background staining. Samples were incubated with primary antibodies against glucagon (1:500), Stmn2 (1:250), insulin (Cat# ab7842, Abcam; 1:250) and TGN46 (Cat# ab16059, Abcam; 1:200) and followed by secondary antibodies of goat anti-mouse IgG Alexa Fluor 488 (1:500), donkey anti-goat IgG Alexa Fluor 555 (1:500), and goat anti-guinea pig IgG Alexa Fluor 647 (Cat# A21450, Invitrogen; 1:500). Nuclei were stained with DAPI (1:1000), and tissues were mounted in Prolong Antifade mountant (Cat# P36982, Thermo Fisher Scientific). As a background control for Stmn2, islet staining for Stmn2 was done using only the secondary antibody.

Image acquisition

High-resolution images were acquired through a Nikon A1R Confocal microscope with a ×60 NA plan-Apochromat oil differential interference contrast objective and NIS-Elements software (Nikon, Mississauga, Canada) using a pinhole of 1 Airy unit. Images were sampled according to Nyquist criteria, and images of the Nyquist-cropped areas were captured at 1,024 × 1,024 pixel resolution, and deconvoluted by the 2D-deconvolution algorithm of the NIS-Elements software, thereby optimizing images for accurate co-localization of fluorescent signals.

Image Analysis

For cell image analysis, we prepared three coverslips for each group. Image analysis was performed by NIS-Elements software (Nikon, Mississauga, Canada), using the co-localization option and Pearson's correlation coefficient (PCC). Regions of interest (ROI) were manually drawn around distinct single or multicellular bodies, and merged values of glucagon and Stmn2 were taken for analysis. Colocalization of the pixels from each pseudo-colored image was used to calculate Pearson's correlation coefficient, as we described previously (25, 31).

For mouse pancreatic islets, images were captured using four channels of green (glucagon), red (Stmn2), purple (insulin) and blue (nucleus; DAPI). To calculate the extent of co-localization between glucagon and stathmin-2 (glucagon+, Stmn2+), images of 15 islets per pancreas were captured and analyzed by Pearson's correlation coefficient (PCC). To this end, we manually drew ROIs around each islet and then defined PCC values for colocalization between Stmn2 and glucagon or insulin using the colocalization option of the NIS-Elements software. To predict expression levels of Stmn2 in α or β-cells of the pancreatic islets we have performed binary analysis using M-Thresholding algorithm of NIS-Elements software, followed by regression analysis of Stmn2 vs. glucagon or insulin using GraphPad Prism 7.

3.3.6 Immunoelectron microscopy

Double immunogold transmission electron microscopy was done based on the protocol by Aida et al. (32) with some modifications. Briefly, pieces of mouse pancreata were cut and immediately placed into McDowell Trump's fixative (Cat# 18030-10; Electron Microscopy Sciences) for 1h. Then, after washing with PBS, samples were dehydrated in increasing concentrations of ethanol (10, 20, 30, 50, 70, 90, 100, and 100%) at 30 min per concentration. We followed the following protocol for LR White embedding and incubation: Incubation in ethanol-LR White mixture (3:1, v/v; 2 h), ethanol-LR White (1:1, v/v; 8 h), ethanol-LR White mixture (1:3, v/v; 12 h), pure LR White mixture (12 h), pure LR White (12 h) and pure LR White (12 h). The sample was then placed into a beem capsule, filled with pure LR White and incubated at 50°C for 24 h. Semi-thin sections

(500 nm) were cut from the embedded sample for Toluidin blue staining (1% Toluidin blue for 2 min). By defining the position of the islets, ultra-thin sections (70 nm) were prepared using a diamond microtome. The sections were mounted on formvar-carbon coated nickel grid (300 meshes) (Cat# FCF300-NI, Electron Microscopy Sciences). Then, slices were washed with Tris-buffered saline (Tris 1M, NaCl 5M pH 8) containing 0.05% Tween 20 (TBS-T) and incubated in blocking buffer (2% BSA in PBS plus 0.05% Tween 20) for 30 min at room temperature. Slices were incubated with primary antibodies (1:10 in blocking buffer) against glucagon (Cat# ab92517; Abcam) and Stmn2 (Cat# ab115513; Abcam) at 4°C overnight. After washing with TBS-T, slices were incubated with gold conjugated secondary antibodies (1:50 in blocking buffer) of donkey anti-goat IgG (18 nm; cat# ab105270, Abcam) and goat anti-rabbit IgG (10 nm; Cat# ab27244; Abcam) for 2 h at room temperature. After washing with TBS-T and staining with Uranyless (Cat# 22409, Electron Microscopy Sciences), transmission electron microscopy was conducted at the Biotron Experimental Research Center, Western University, London, ON, Canada.

3.3.7 Primary islet culture

Islet preparation and culture

Islet preparation and culture was done according to the Li et al. (33) protocol with some modifications. Male C57BL/6 mice (n = 5–6) were euthanized by CO2. The abdominal cavity was opened and 3 mL of 1.87 mg/mL collagenase V (Cat# C9263, Sigma;) in Hanks' Balanced Salt Solution was injected into the common bile duct. The pancreas was then removed, placed into a Falcon tube containing 2 mL of the ice-cold collagenase V solution and incubated for 12 min at 37°C with occasional shaking. Digestion was stopped by adding 1mM $CaCl_2$ and the cell suspension was washed twice in the $CaCl_2$ solution. Islets were collected into a sterile petri dish using a 70 μm cell strainer with RPMI1640 containing 11 mM glucose plus 20 mM glutamine, 10% FBS and penicillin (110 U/mL) and streptomycin (100 μg/mL). 180 islets were handpicked into the medium under a stereomicroscope and incubated for 2 h in the cell culture incubator. The medium was then changed to RPMI1640 containing 11 mM glucose plus 10% FBS and penicillin (110 U/mL) and streptomycin (100 μg/mL) and cultured overnight at 37°C.

Islet glucagon secretion experiments

Glucagon secretion from islets was measured based on the protocol by Suckow et al. (34). Briefly, islets were washed three times using Krebs-Ringer bicarbonate (KRB) buffer (135 mM NaCl, 3.6 mM KCl, 5 mM $NaHCO_3$, 0.5 mM NaH_2PO_4, 0.5 mM $MgCl_2$, 1.5 mM $CaCl_2$, 10 mM HEPES; pH 7.4) containing 11 mM glucose, and then pre-incubated in this buffer for 1 h. Glucagon secretion was tested by incubating islets in KRB containing 1 mM glucose in the presence or absence of arginine (25 mM) for 20 min. Media were collected into microcentrifuge tubes containing enzyme inhibitors (PMSF, 45 mM; Aprotinin, 5 μg/mL and sodium orthovanadate, 1 mM). Samples were centrifuged at 14,000 × g for 5 min at 4°C and the supernatant was collected and kept at −80°C until analysis.

Measurement of glucagon and stathmin-2

Glucagon levels in the media were determined by ELISA (Cat # EHGCG, Thermo Fisher Scientific) according to the manufacturer's instructions. Stmn2 levels in the media were measured using mouse stathmin-2 ELISA kit (Cat# MBS7223765, MyBioSource) according to the manufacturer's instruction. For each measurement, the values were compared between groups by t-test and among groups by 1-Way ANOVA and Bonferroni post-hoc test ($\alpha = 0.05$). Cell protein levels were determined using BCA assay and used for normalization of the glucagon or Stmn2 levels.

3.3.8 Statistical analysis

Values were compared among treatment groups by one-way ANOVA or between groups by unpaired t-test using Sigma Stat 3.5 software ($\alpha = 0.05$). For image analysis, co-localization of channels in the merged images was calculated by Pearson's correlation coefficient (PCC) using NIS-Elements software (Nikon, Canada).

3.4 Results

Immunostaining of glucagon and Stmn2 in α-TC1-6 cells revealed significant co-localization, as shown in Figure 3-1A and by a positive Pearson's correlation coefficient

(0.74 ± 0.05) between endogenously expressed glucagon and Stmn2. Linear regression of binary intensities showed a sensitive and significant relationship between colocalization of glucagon and Stmn2 (Figure 3- 1B). The secretion of both glucagon and Stmn2 was significantly enhanced in response to 55 mM K^+ (Figure 3- 1C), with corresponding decreases in cell contents (Figure 3- 1D). To further confirm the presence of stathmin-2 in secretory granules, α-TC1-6 cells were immunostained for stathmin-2 and the secretory granule markers chromogranin A (Figure 3- 1E) and VAMP2 (Figure 3-1F). There was moderate colocalization (35) between Stmn2 and chromogranin A (PCC 0.58 ± 0.07) or VAMP2 (PCC 0.56 ± 0.09) (Figure 3-1G), indicating that Stmn2 is partially localized to the secretory granule compartment in α-TC1-6 cells.

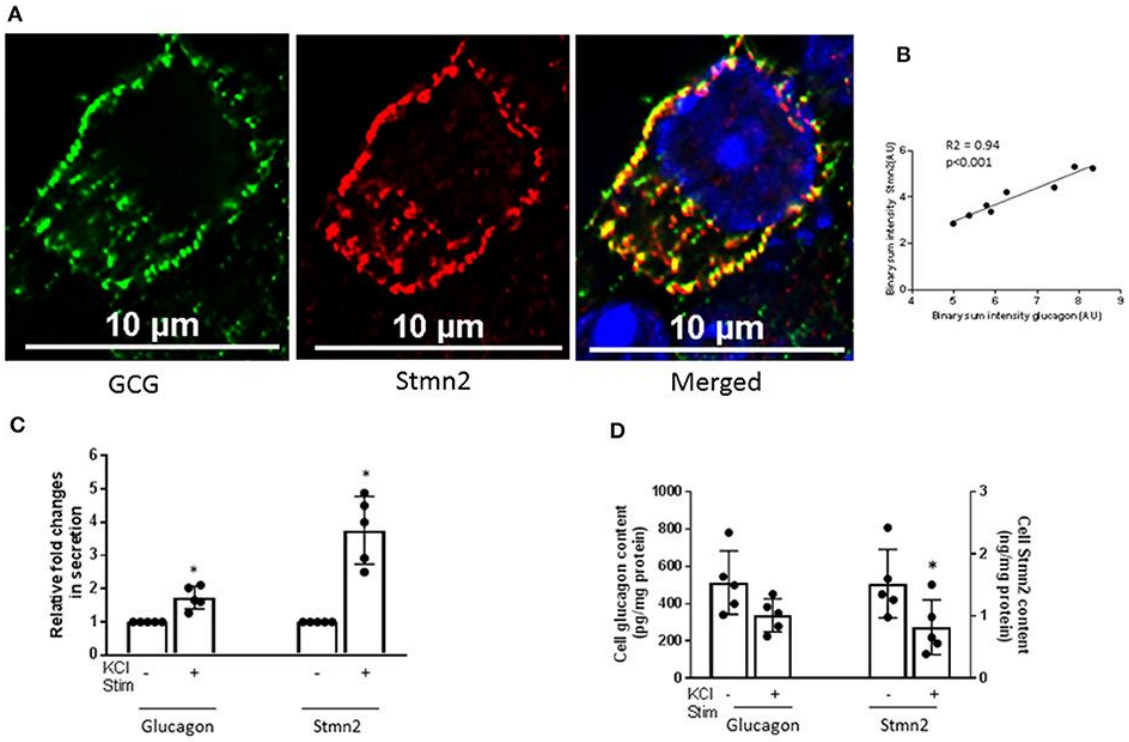

E

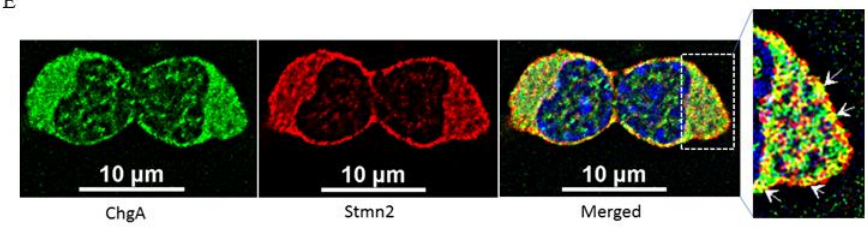
10 µm
10 µm
10 µm
ChgA
Stmn2
Merged

F

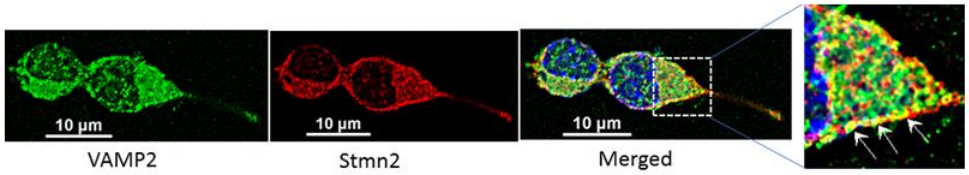
10 µm
10 µm
10 µm
VAMP2
Stmn2
Merged

G

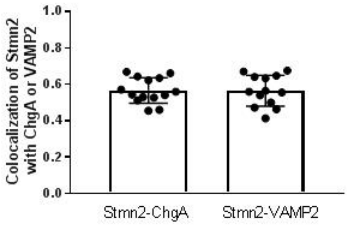
Colocalization of Stmn2 with ChgA or VAMP2
1.0
0.8
0.6
0.4
0.2
0.0
Stmn2-ChgA
Stmn2-VAMP2

Figure 3-1. Stathmin-2 localizes to secretory granules in α-TC1-6 cells. α-TC1-6 cells were immunostained using primary antibodies against glucagon (GCG, green) and stathmin-2 (Stmn2, red). DAPI (blue) indicates the nucleus in the merged image. Resolution of the images was extended by applying Nyquist XY scan and then 2D- Deconvolution in NIS Elements image analysis software. Images are representative of four biological replicates with 3 technical replicates each. (A) Areas of yellow in the merged image show colocalization of glucagon and Stmn2. (B) Linear regression analysis of binary intensities of glucagon and Stmn2 predicts a significant ($p<0.001$) correlation. Each value represents mean intensities of 5-7 cells. The secretion of both glucagon and Stmn2 (C) was significantly increased after KCl stimulation (KCl Stim)for 15 min. Cell Stmn2 and glucagon levels show reduction following KCl stimulation (KCl Stim) (D). Values are expressed as mean ± SEM (n=5). *$p<0.05$. Stmn2 colocalizes with the secretory granule proteins ChgA (E) and VAMP2 (F), as indicated by yellow punctate staining. (G) The extent of colocalization was analyzed by Pearson correlation coefficient for Stmn2 with ChgA or with VAMP2. Dots represent all biological and technical replicates.

3.4.1 Stathmin-2 localizes to the α-cell secretory pathway in mouse pancreatic islets

Immunostaining of mouse pancreatic islets showed a pattern of Stmn2 immunofluorescence similar to that of glucagon, and not insulin (Figure 3- 2A). Analysis by Pearson correlation showed a strong colocalization between glucagon and Stmn2 in the islets (PCC = 0.77 ± 0.02), but not between insulin and Stmn2 (Figure 3-2B). Linear regression analysis of the binary intensities revealed a very strong and significant relationship between Stmn2 and glucagon immunofluorescence (Figure 3- 2C), while there was no significant relationship between Stmn2 and insulin (Figure 3- 2D). There was also a strong relationship between Stmn2 and the trans Golgi marker, TGN46 (PCC = 0.72 ± 0.09) in both islet clusters (Figure 3- 2E) and mature islets (Figure 3- 2F).

A

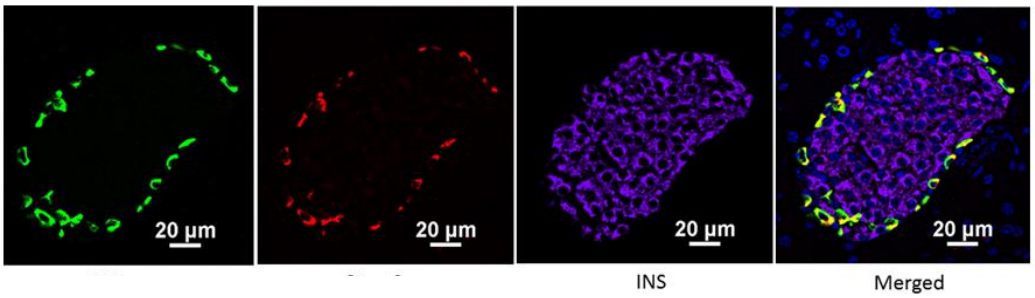
20 µm
20 µm
20 µm
20 µm
INS
Merged

B

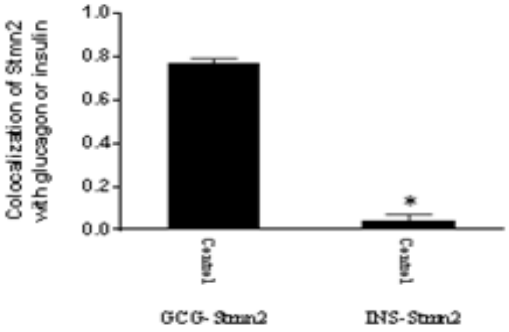
Colocalization of Stmn2 with glucagon or insulin
1.0
0.8
0.6
0.4
0.2
0.0
*
GCG- Stmn2
INS-Stmn2

C

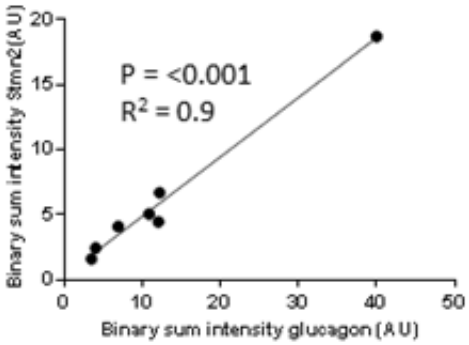
P = <0.001
R2 = 0.9
Binary sum intensity Stmn2(AU)
Binary sum intensity glucagon (AU)

D

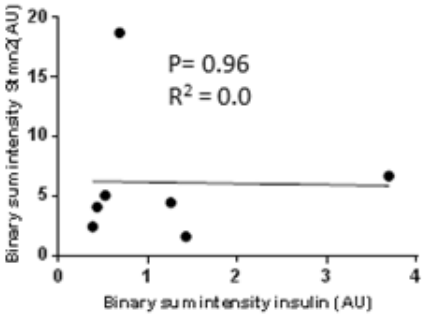
P= 0.96
R2 = 0.0
Binary sum intensity Stmn2(AU)
Binary sum intensity insulin (AU)

E

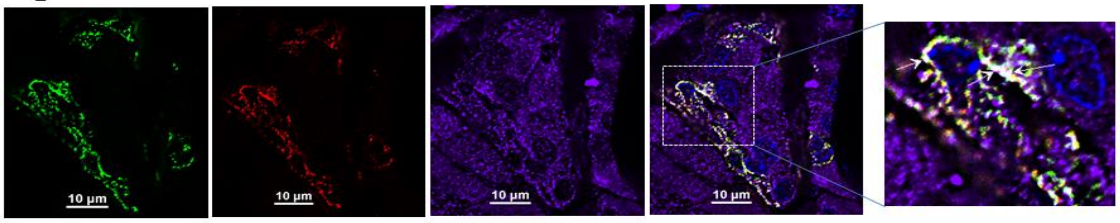
10 µm
10 µm
10 µm
10 µm
GCG
Stmn2
TGN46
Merged

F

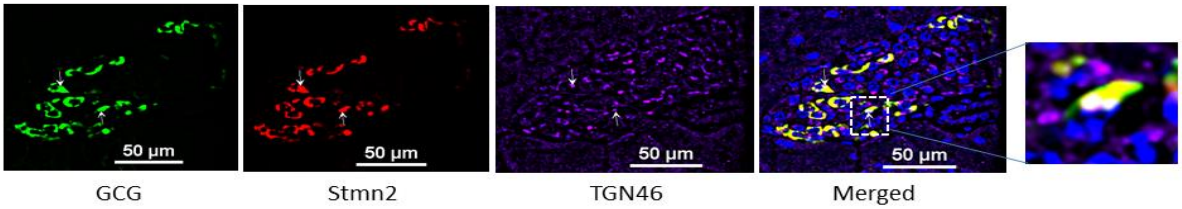
50 µm
50 µm
50 µm
50 µm
GCG
Stmn2
TGN46
Merged

Figure 3-4. Stathmin-2 is present in α-cells, but not β-cells, in murine pancreatic islets. Pancreata of C57BL/6 mice (n=7; 5µm sections) were immunostained for against glucagon (GCG), stathmin-2 (Stmn2) and insulin (INS). Images were acquired and analysed for co-localization as described in Figure 1. (A) Both glucagon and Stmn2 localize to the mantle of the islets, and areas of yellow in the merged image demonstrate dual positive α-cells (glucagon+ and Stmn2+). (B) Pearson's correlation coefficient for colocalization of Stmn2 and glucagon or insulin. (C) Linear regression analysis predicts a strong positive correlation between the binary intensities of glucagon and Stmn2 ($p<0.001$). (D) There is no correlation between the binary intensities of insulin and Stmn2. (E, F) Colocalization of Stmn2 and the trans-Golgi marker TGN46 in murine pancreatic islets. Areas of white (arrows in the magnified panel) indicate co-localization of glucagon, Stmn2 and TGN46 in islet clusters (E) and a single islet (F).

In addition, double immunogold-labeling TEM revealed the presence of both glucagon and Stmn2 within secretory granules of pancreatic α-cells. The co-localization of glucagon (10 nm particles; white arrows) and Stmn2 (18 nm particles; black arrows) was mostly within the core area of the secretory granules (Figure 3- 3A). Finally, 25 mM Arg significantly enhanced the secretion of both glucagon and Stmn2 from isolated islets (Figure 3- 3B). These results indicate that Stmn2 is localized to the secretory pathway of α cells in mouse pancreatic islets. Our approach was based on qualitatively showing the presence of Stmn2 within the secretory granules.

A

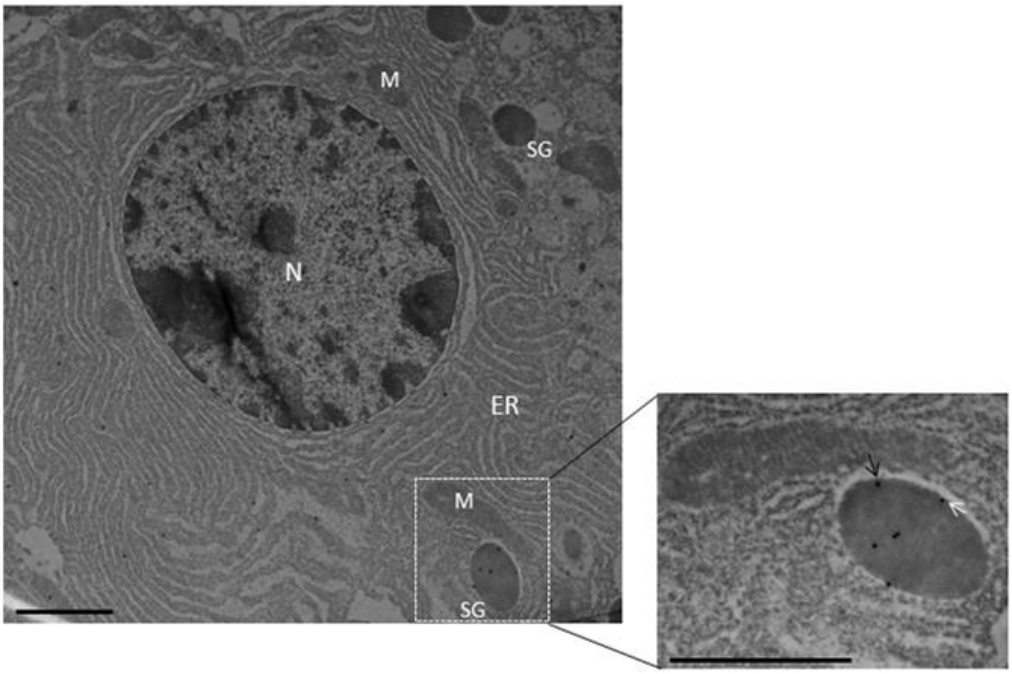
M
SG
N
ER
M
SG

B

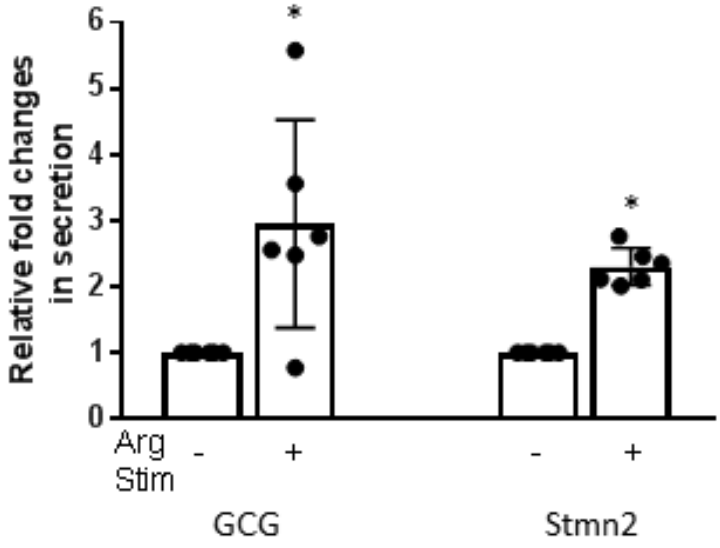
Relative fold changes in secretion
6
5
4
3
2
1
0
*
*
Arg
Stim
-
+
-
+
GCG
Stmn2

Figure 3-7. Glucagon and Stmn2 are present within secretory granules of pancreatic α-cells. (A) Immunogold labels for both glucagon (10 nm; white arrows) and Stmn2 (18 nm; black arrows) are localized within secretory granules. The low magnification image (25000×, scale bar = 1 μm) shows the ultrastructure of one α-cell. N (nucleus); M (mitochondria); ER (endoplasmic reticulum); SG (secretory granule). The magnified image (41000×, scale bar = 0.6 μm) highlights the presence of immunogold labels within a single secretory granule. (B) Isolated mouse islets were incubated in the presence or absence of 25 mM Arg for 20 min. Both glucagon and Stmn2 secretion from murine islets is stimulated by arginine. Values were normalized to the non-stimulated condition and expressed as mean ± SEM (n=5-6). *p<0.01.

3.4.2 Effects of depletion and overexpression of Stmn2 on glucagon secretion

In order to determine if Stmn2 had any functional effects in α-cells, we manipulated levels of Stmn2 and measured K^+-stimulated glucagon secretion. Following siRNA-mediated knockdown of Stmn2 in α-TC1-6 cells, basal secretion of glucagon was increased ~4.5-fold, and was not significantly different from K^+-stimulated secretion (Figure 3- 4A), indicating increased constitutive secretion. Efficacy of siRNA-mediated depletion of Stmn2 was shown by a significant reduction ($p < 0.01$) in Stmn2 mRNA levels (Figure 3- 4B) and the Stmn2 immunoreactive band by western blot (Figure 3- 4C). As well, silencing of Stmn2 did not affect proglucagon gene expression levels (Figure 3- 4D), indicating that the effects of Stmn2 depletion were on glucagon secretion alone. Conversely, overexpression of Stmn2 dramatically reduced both basal and stimulated glucagon secretion compared to the corresponding control groups (Figure 3- 4E; $p < 0.001$). These findings suggest that Stmn2 levels may control the regulated secretion of glucagon from α-TC1-6 cells.

A (glucagon secretion)

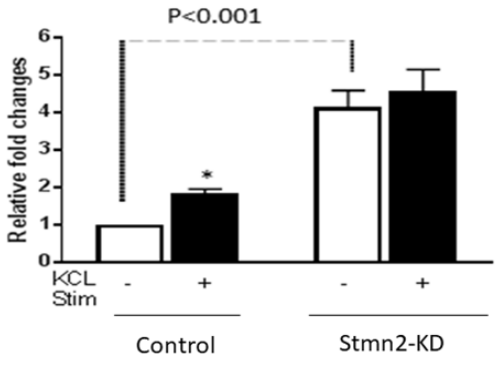

B (Stmn2 expression)

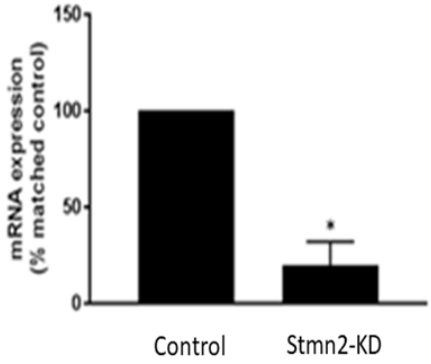

C (Silencing Stmn2-WB)

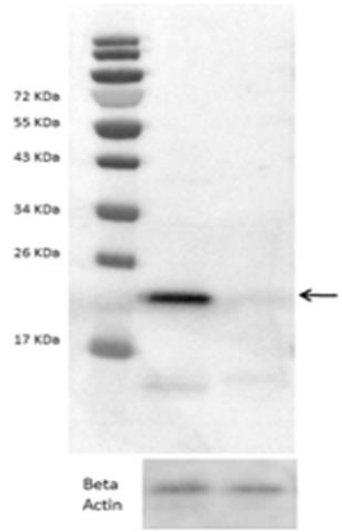

D (*Gcg* gene expression)

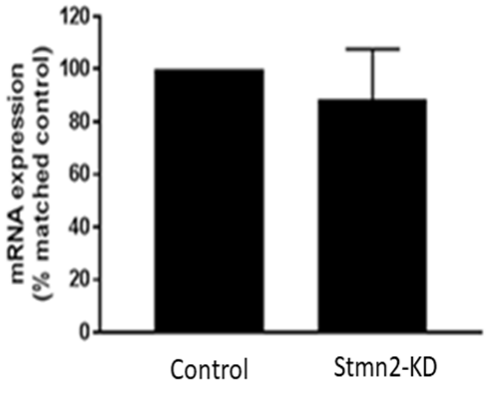

E (glucagon secretion)

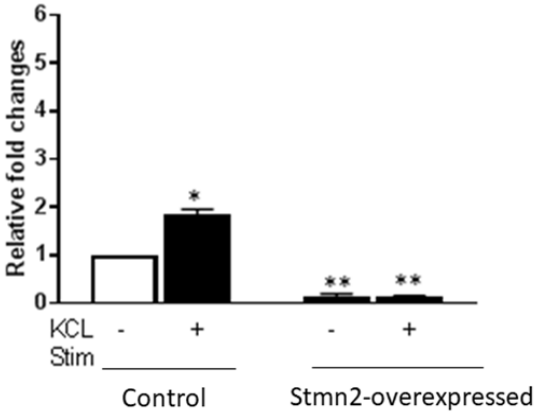

Figure 3-10. Silencing Stathmin-2 increased glucagon secretion and overexpression of stathmin-2 suppressed glucagon secretion in α-TC1-6 cells. Wild type (wt; control) and stathmin-2 depleted (Stmn2-KD) α-TC1-6 cells were preincubated 2h in serum- free medium and then incubated with or without KCl (55 mM) for 15 min. (A) Glucagon secretion is significantly stimulated by KCl in wt cells, while in Stmn2-KD cells, basal glucagon secretion is increased and does not respond to KCl. * $p<0.01$ compared to basal secretion in wt cells. (B) Stmn2 mRNA levels are decreased by about 70% after siRNA-mediated depletion in α-TC1-6 cells. Values are means ± SEM (n=5), * $p<0.01$. (C) siRNA-mediated silencing of Stmn2, shutdown expression of Stmn2.Western blot (WB) shows a faint band for Stmn2 after siRNA-mediated depletion of Stmn2 in α-TC1-6 cells. (D) Proglucagon mRNA levels are not affected by siRNA- mediated depletion of stathmin-2. (E) Glucagon secretion is inhibited by overexpression of Stmn2. α-TC1-6 cells were transfected with pcDNA3.1 (+) MAr-stmn2 construct or empty vector (control). Both basal ($p<0.001$) and K^+-stimulated ($p<0.001$) (KCl stimulation; KCl Stim) glucagon secretion were inhibited by overexpression of Stmn2. Values are means ± SEM (n=4).

3.4.3 Stmn2 directs glucagon into early endosomes

In wild type α-TC1-6 cells, there was weak co-localization between glucagon and the early endosome marker EEA1 (Figure 3- 5A) (PCC = 0.15 ± 0.02). When Stmn2 was overexpressed (Figure 3- 5B), the extent of colocalization between glucagon and EEA1 increased markedly (PCC = 0.53±0.08). Depletion of Stmn2 (Figure 3- 5C) drastically reduced the extent of colocalization (PCC = 0.05) between glucagon and EEA1. Pearson's correlation coefficient of co-localization between glucagon and Stmn2 showed a significant increase when Stmn2 was overexpressed ($p < 0.001$) and a significant reduction when Stmn2 was knocked down ($p < 0.05$) compared to the control (Figure 3-

5D). These findings suggest that Stmn2 plays a role in directing glucagon toward early endosomes.

Figure 5

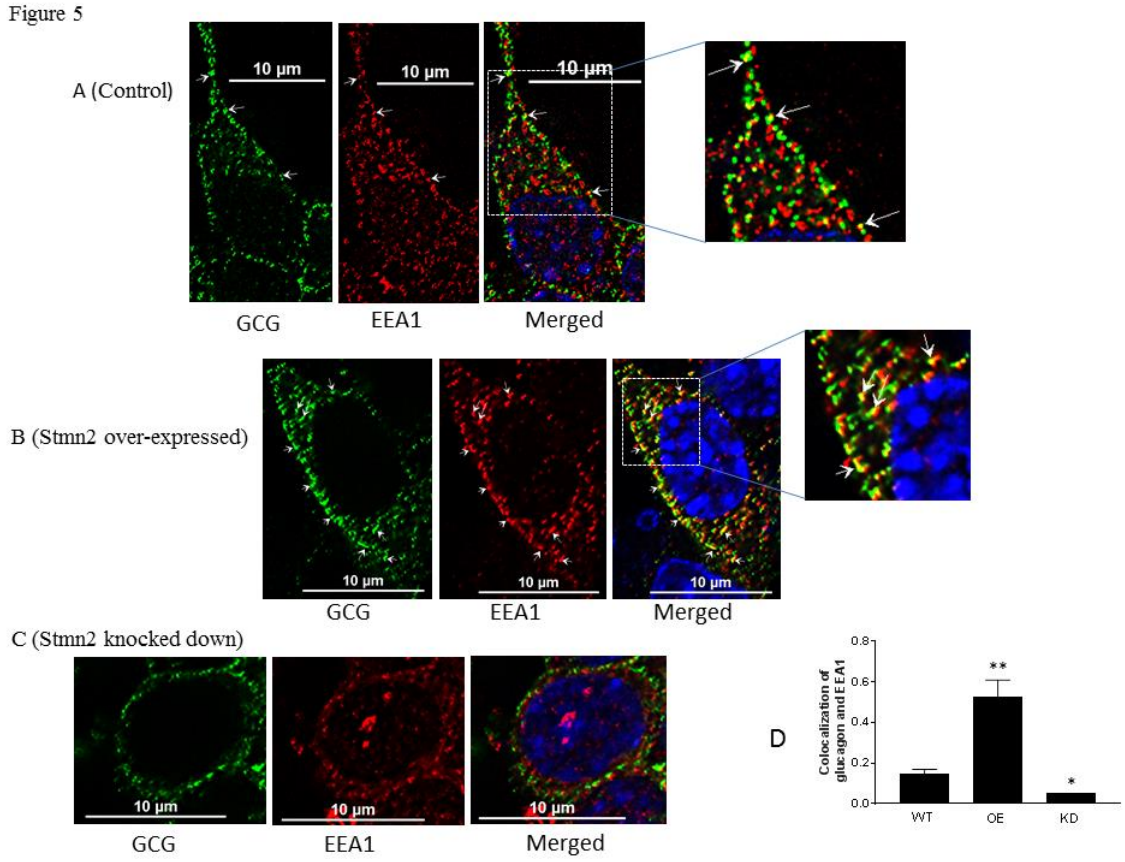

Figure 3-13. Stathmin-2 modulates glucagon trafficking through early endosomes. After transfection with either empty vector (A), vector encoding Stmn2 (B) or siRNAs against Stmn2 (C), α-TC1-6 cells were immunostained using primary antibodies against glucagon and the early endosome marker EEA1. Images were acquired and analysed for co-localization as described in Figure 1. Colocalization of glucagon and EEA1 (yellow puncta) are indicated by arrows in wt cells (A) or arrowheads in cells overexpressing Stmn2 (B). (D) Level of colocalization between glucagon and EEA1 was determined by Pearson's correlation coefficient in wt cells, cells in which Stmn2 was overexpressed (OE) and in which Stmn2 was knocked down by siRNA (KD). Values were expressed as mean ± SEM (n=5) and compared by 1-Way ANOVA. *p<0.05; **<0.001 compared to wt.

3.4.4 Stmn2 overexpression increases glucagon presence in the late endosome/lysosome compartment

Similar to our findings in early endosomes, there was a weak correlation between glucagon and the late endosome-lysosome marker, Lamp2A (PCC = 0.2 ± 0.02) in wild type α-TC1-6 cells (Figures 3- 6A,D). Following overexpression of Stmn2, the levels of colocalization between glucagon and Lamp2A were significantly increased (PCC = 0.89 ± 0.05, $p < 0.001$) (Figures 3- 6B,D). Depletion of Stmn2 significantly reduced the extent of colocalization between glucagon and Lamp2A compared to wild type cells (PCC = 0.001, $p < 0.01$) (Figures 3- 6C,D). Interestingly, the signal intensity of the endo-lysosomal marker, Lamp2A, was significantly increased ($p < 0.01$) upon overexpression of Stmn2, but did not change upon depletion of Stmn2 (Figure 3- 6E).

Figure 6

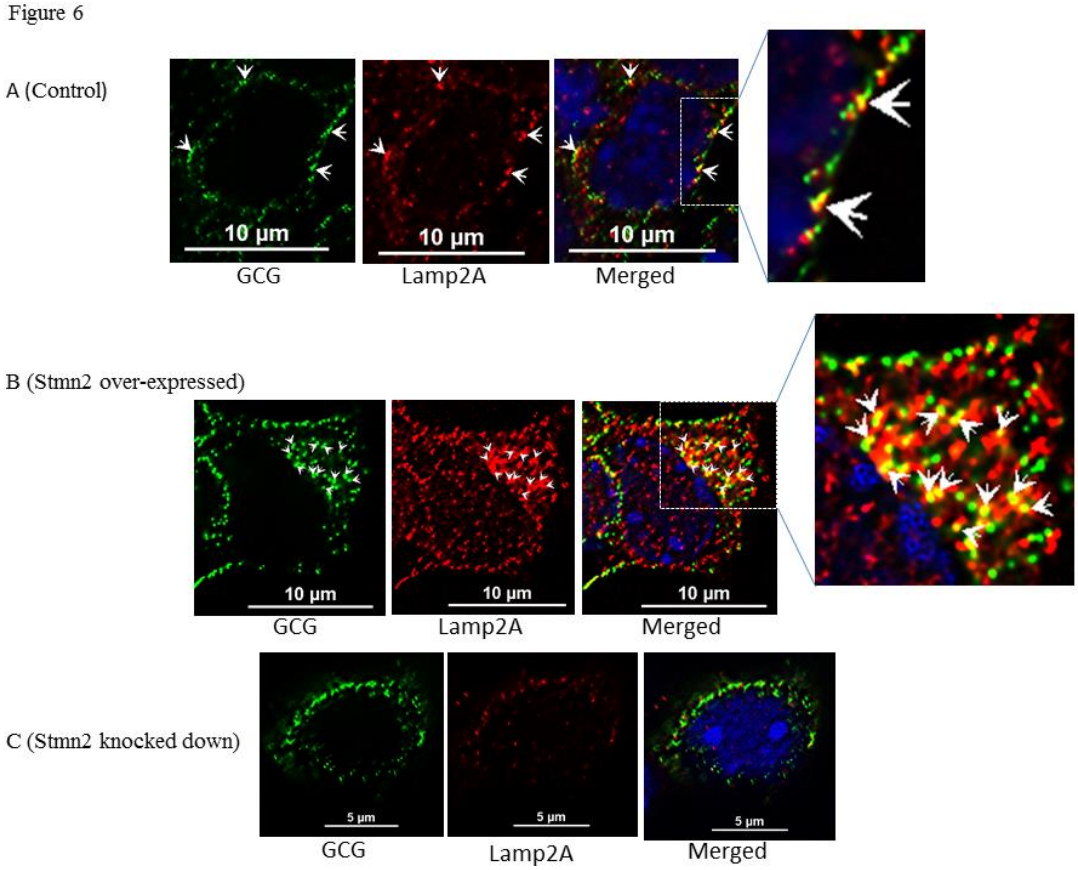

Figure 6

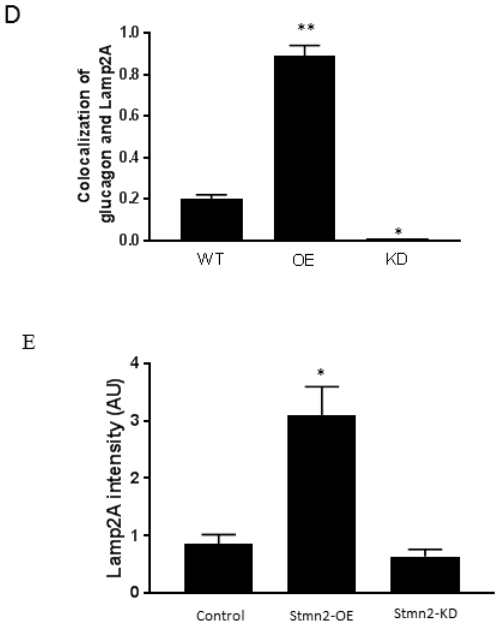

Figure 3-16. Overexpression of Stathmin-2 increases the presence of glucagon in late endosomes. After transfection with either empty vector (A), vector encoding Stmn2 (B) or siRNAs against Stmn2 (C), α-TC1-6 cells were immunostained using primary antibodies against glucagon and the late endosome-lysosome marker LAMP2A. Images were acquired and analysed for co-localization as described in Figure 1. (A) In wt cells, glucagon and LAMP2 show some co-localization at the plasma membrane (arrowheads). (B) In cells overexpressing Stmn2, there is colocalization of glucagon and LAMP2A in the cell body (arrowheads) and at the plasma membrane (arrows). (C) In cells in which Stmn2 levels are depleted, there is almost no detectable co-localization of glucagon and LAMP2A. (D) Level of colocalization between glucagon and LAMP2A was determined by Pearson's correlation coefficient in wt cells, cells in which Stmn2 was overexpressed (OE) and in which Stmn2 was knocked down by siRNA (KD). (E) Fluorescence intensity of Lamp2A in wt cells, and following overexpression (Stmn2-OE) or knockdown (Stmn2-KD) of Stmn2. Values are expressed as mean ± SD and compared by 1-Way ANOVA. *p<0.01; **<0.001 compared to wt.

Glucagon secretion is governed by systemic, paracrine and intrinsic factors. Our work has focused on the regulation of glucagon secretion by proteins that associate with glucagon within α-cell secretory granules. To this end, we have shown that a neuronal protein, Stmn2, which we have previously identified as part of the glucagon interactome (25), can be localized to the secretory granules of α-TC1-6 cells. We validated this association in mouse pancreatic islets, and through silencing and overexpression experiments, we showed that Stmn2 can play a role in glucagon secretion by trafficking through the endosomal-lysosomal pathway.

We have previously identified Stmn2 as part of a network of proteins that associate with glucagon within the secretory granules of α-TC1-6 cells (25). Data in the current study show that Stmn2 is localized to the secretory granule and Golgi compartments in α-TC1-6 cells and mouse pancreatic α-cells, respectively. Stathmin-2 is part of a family of

neuronal phosphoproteins that associates with intracellular membranes, notably the Golgi and vesicle transporters, in neurons (36). Although Stmn2 has been identified as a neuron-specific protein that functions in differentiation and development, its presence in pancreatic α-cells is not surprising, as several types of neuronal proteins, such as SNARE proteins, neurotransmitters and granins, are also expressed in endocrine cells (37–39). The expression of neuronal proteins such as Stmn2 in α-cells may be due to the absence of the transcriptional repressor RE-1 silencing transcription factor (REST) in mature endocrine cells (40, 41). The absence of Stmn2 in mouse pancreatic β-cells suggests that transcriptional silencing programs may operate in a cell-specific manner.

Our results indicate that Stmn2 is localized largely to punctate structures within α-TC1-6 cells, notably at the plasma membrane. Its colocalization with glucagon, ChgA and VAMP2 at the plasma membrane suggests that it is efficiently sorted from the Golgi to plasma membrane-associated secretory granules. Double immunogold labeling TEM confirmed the presence of glucagon and Stmn2 within secretory granules of α-cells in mouse pancreatic islets. The presence of Stmn2 within the dense core of the granule suggests that it is part of the soluble granule cargo along with glucagon. These results are consistent with our secretory granule proteomics, which predicted the presence of both glucagon and Stmn2 in secretory granules of α-TC1-6 cells (25). Our model also predicted that the complement of proteins within α-cell secretory granules differs in response to microenvironmental inputs, so it possible that Stmn2 is present only in a subpopulation of secretory granules. The trafficking of Stmn2 to secretory granules in α-TC1-6 cells may occur through specific molecular domains within its sequence. The subcellular trafficking pattern of Stmn2 in neurons and neuroendocrine cells is determined by its N-terminal extension, which contains a Golgi localization domain and a membrane anchoring domain that contains two conserved Cys residues as sites for palmitoylation (36). This lipid modification occurs in the Golgi (42) and is sufficient and necessary for the association of Stmn2 with Golgi membranes, and its sorting to post-Golgi vesicles (42, 43). While we have not directly shown that palmitoylation of these Cys residues is required for localization in secretory granules in α-TC1-6 cells, it is likely that this is a conserved sorting mechanism in neuroendocrine cells.

Consistent with its localization within secretory granules, the secretion of both glucagon and Stmn2 was significantly enhanced in response to 55 mM K^+. Although there was a statistically significant response to KCl, α-TC1-6 cells as a rule do not show robust secretory responses to KCl, glucose or other secretagogues. In general, α-TC1-6 cells differ in their complement of transcriptional and epigenetic factors from mouse primary α-cells, which may explain the relatively blunted secretory response seen in this cell line (44). The reduced response to glucose in particular could be due to a low efficiency in coupling between the glycolytic and TCA pathways, as has been shown in pancreatic islets (45). We have not shown alterations in glucagon secretion in response to physiological secretagogues such as glucose, which could be a limitation for our current study. Nonetheless, we were able to show similar secretory behavior of glucagon and Stmn2 in isolated mouse islets, thus confirming their localization within the releasable pool of secretory granules in pancreatic α-cells. While Stmn2 is a membrane–bound protein, it is also present in normal human blood as determined by serum ELISA (46) and plasma proteomics (47) and therefore can be also secreted. There is some evidence of a lower molecular weight form of Stmn2 that may correspond to a cleaved, soluble form (43, 48). In our model, it may be that a portion of Stmn2 becomes cleaved within the secretory granule, thus becoming part of the soluble cargo that is released.

By manipulating the expression of Stmn2, we were able to demonstrate a role in the control of glucagon secretion. There is precedence for a role for Stmn2 in the regulation of neuroendocrine secretion that has some interesting parallels with our results. While we showed that silencing of Stmn2 increased the constitutive secretion of glucagon, one study showed that silencing Stmn2 in PC12 cells decreased both basal and stimulated secretion of chromogranin A (27). In that study, it was shown that Stmn2 interacted directly with ChgA and its depletion reduced the buoyant density of chromaffin granules, suggesting that Stmn2 may participate in secretory granule formation, perhaps in partnership with ChgA (42) and thus promote regulated secretion. Although we could not demonstrate a direct interaction between Stmn2 and glucagon (data not shown), our results align with the idea that Stmn2 may be a sorting partner for glucagon, perhaps indirectly by interacting with other granule proteins such as ChgA or carboxypeptidase E (31), in the regulated secretory pathway of α-cells.

Overexpression of Stmn2 resulted in an almost complete shutdown of glucagon secretion and an increase in the localization of glucagon in early endosomes and lysosomes. These results may suggest induction of ER stress. However, overexpression of Stmn2 in Neuro2A cells, another cell line commonly used to examine regulated secretion, had the opposite effect and enhanced trafficking of post-Golgi carriers to the plasma membrane (49). There are only a few reports on how ER stress in α-cells is manifest; in one report, palmitate-induced ER stress in isolated rat α-cells resulted in an increase in glucagon secretion, not inhibition, even though the traditional markers of ER stress [DNA damage-inducible transcript 3 protein (Ddit3; Chop), X-box-binding protein (1Xbp1s), Endoplasmic reticulum chaperone BiP (Hspa5; BiP)] were elevated (50). Another study showed that *in vivo* depletion of Xbp1, which plays a crucial role in the unfolded protein response, induced dysfunctional glucagon secretion that was not fully suppressed by insulin (51). Therefore, the suppression of glucagon secretion by Stmn2 overexpression is not consistent with the phenotype of ER stress in the α-cell. Instead, these results, together with the increased the presence of glucagon in the lysosomal compartment, suggest that Stmn2 overexpression causes alterations in glucagon trafficking independent of ER stress.

We believe that the overexpression experiments suggest a mechanism whereby an increase in Stmn2 in the α-cell inhibits glucagon secretion by targeting glucagon secretory granules for degradation in the endosome-lysosome pathway, perhaps in a manner similar to that of insulin secretory granules in Type 2 diabetes (52). Very recently, it has been shown that insulin secretion can be inhibited by the targeting of proinsulin for lysosomal degradation by Rab7-interacting lysosomal protein (RILP) (53). The proposed mechanism of action was through interactions between RILP and an insulin secretory granule membrane protein, Rab26. It is tempting to speculate that Stmn2 could have a similar mechanism of action in α-cells. The increase in LAMP2A fluorescence intensity upon Stmn2 overexpression further suggests a role for Stmn2 in modulating glucagon secretion through increased lysosome function or biogenesis. We are currently investigating this mechanism of control of glucagon secretion in mouse islets.

In conclusion, we propose that Stmn2, a protein that is associated with glucagon in secretory granules, modulates glucagon secretion in α-cells by playing a role in its intracellular trafficking. Under conditions that decrease Stmn2 levels, constitutive secretion of glucagon is increased; and under conditions that increase levels of Stmn2, glucagon is targeted to the endolysosomal system, presumably for degradation (Figure 3-7). Our findings, which are mainly based on the clonal α-cell line α-TC1-6, represent a potentially novel intracellular pathway for the control of glucagon secretion, and may lead to new mechanistic insights in the dysregulation of glucagon secretion in diabetes.

Figure 7

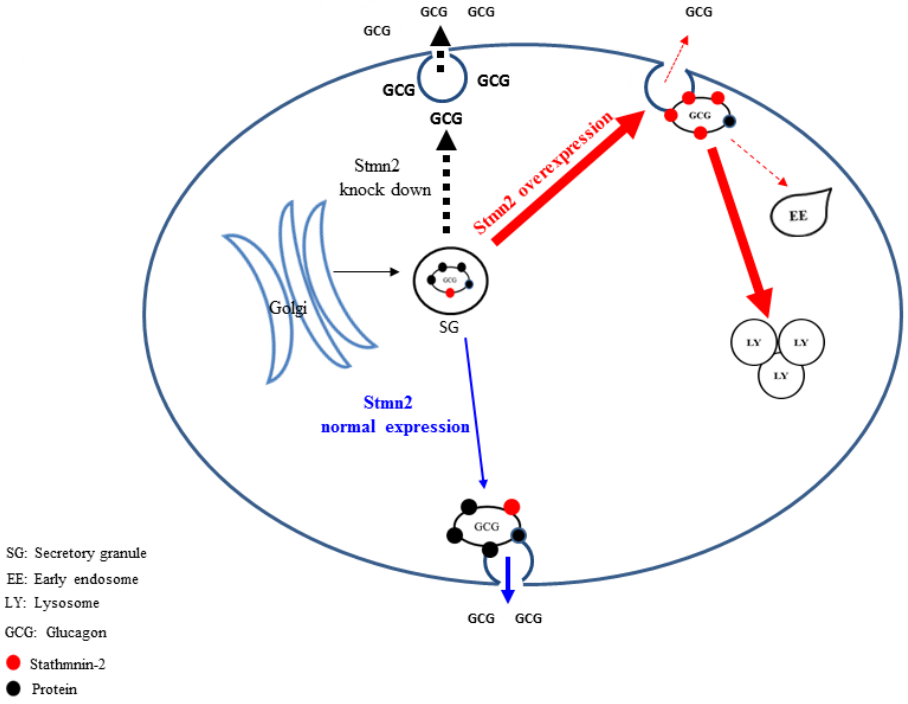

Figure 3-19. Proposed pathways by which stathmin-2 modulates glucagon secretion from α-TC1-6 cells. The model denotes status of glucagon secretion from α-TC1-6 cells in normal physiology or in the event of Stmn2- depletion or overexpression. Blue arrows indicate the normal trafficking of glucagon, together with Stmn2, to secretory granules, where they are stored until their release is triggered by a stimulus. Stmn2 overexpression (red arrows) reduces the amount of glucagon available for secretion by diverting secretory granules to lysosomes. Stmn2 depletion (black arrows) reduces the trafficking of glucagon into secretory granules and promotes the constitutive release of glucagon.

Data Availability Statement: All datasets generated for this study are included in the article/supplementary material.

Ethics Statement: The animal study was reviewed and approved by Animal Use Subcommittee of the Canadian Council on Animal Care at Western University, Animal Use Protocol AUP 2012-020.

Author Contributions: Designing the experiments, writing the manuscript, preparing the figures and reviewing the manuscript prior to submission were done by FA and SD.

Funding: This work has been financially supported by a Discovery Grant from the Natural Sciences and Engineering Research Council of Canada to SD, and by a Dean's Award Scholarship to FA.

Conflict of Interest: The authors declare that the research was conducted in the absence of any commercial or financial relationships that could be construed as a potential conflict of interest.

Acknowledgments: We would like to sincerely thank Dr. Jens Juul Holst (Department of Biomedical Sciences, University of Copenhagen, Denmark) for reviewing the manuscript and providing constructive suggestions; Ms. Karen Nygard and Mr. Reza Khazaee for assistance with electron microscopy; and Ms. Caroline O'Neil for tissue sample sectioning.

3.6 References

Ceriello A, Kilpatrick ES. Glycemic variability: Both sides of the story. Diabetes Care (2013) 36:S272-275. doi:10.2337/dcS13-2030

2. Demant M, Bagger J, Suppli M, Lund A, Gyldenløve M, Hansen K et al. Determinants of fasting hyperglucagonemia in patients with type 2 diabetes and nondiabetic control subjects. Metab Syndr Relat Disord (2018) 16:530–536. doi:10.1089/met.2018.0066

3. Salehi A, Vieira E, Gylfe E. Paradoxical stimulation of glucagon secretion by high glucose concentrations. Diabetes (2006) 55:2318–2323. doi:10.2337/db06-0080

4. Vieira E, Salehi A, Gylfe E. Glucose inhibits glucagon secretion by a direct effect on mouse pancreatic alpha cells. Diabetologia (2007) 50:370–379. doi:10.1007/s00125-006-0511-1

5. Gylfe E, Gilon P. Glucose regulation of glucagon secretion. Diabetes Res Clin Pract (2014) 103:1–10. doi:10.1016/j.diabres.2013.11.019

6. Gylfe E. Glucose control of glucagon secretion—'There's a brand-new gimmick every year.' Ups J Med Sci (2016) 9734:1–13. doi:10.3109/03009734.2016.1154905

7. Brand C, Rolin B, JØrgensen P, Svendsen I, JS et al K. Immunoneutralization of endogenous glucagon with monoclonal glucagon antibody normalizes hyperglycaemia in moderately streptozotocin-diabetic rats. Diabetologia (1994) 37:985–993.

8. Gelling RW, Du XQ, Dichmann DS, Romer J, Huang H, Cui L et al. Lower blood glucose, hyperglucagonemia, and pancreatic alpha cell hyperplasia in glucagon receptor knockout mice. Proc Natl Acad Sci U S A (2003) 100:1438–43. doi:10.1073/pnas.0237106100

9. Holst JJ, Albrechtsen NJW, Pedersen J, Knop FKG. Glucagon and amino acids are linked in a mutual feedback cycle: The liver-α-cell axis. Diabetes (2017) 66:235–240. doi:10.2337/db16-0994

10. Longuet C, Sinclair EM, Maida A, Baggio LL, Charron MJ, Drucker DJ. The glucagon receptor is required for the adaptive metabolic response to fasting. Cell Metab (2009) 8:359–371. doi:10.1016/j.cmet.2008.09.008

11. Unger RH, Cherrington AD. Glucagonocentric restructuring of diabetes: A pathophysiologic and therapeutic makeover. J Clin Invest (2012) 122:4–12. doi:10.1172/JCI60016

12. Gromada J, Chabosseau P, Rutter GA. The α-cell in diabetes mellitus. Nat Rev Endocrinol (2018) 14:694–704. doi:10.1038/s41574-018-0097-y

13. Ramracheya R, Chapman C, Chibalina M, Dou H, Miranda C, González A et al. GLP-1 suppresses glucagon secretion in human pancreatic alpha-cells by inhibition of P/Q-type Ca2+ channels. Physiol Rep (2018) 6:1–17. doi:10.14814/phy2.13852

14. Tornehave D, Kristensen P, Rømer J, Knudsen LB, Heller RS. Expression of the GLP-1 receptor in mouse, rat, and human pancreas. J Histochem Cytochem (2008) 56:841–851. doi:10.1369/jhc.2008.951319

15. Benner C, van der Meulen T, Cace´res E, Tigyi K, Donaldson CJ, Huising MO. The transcriptional landscape of mouse β-cells compared to human β-cells reveals notable species differences in long non-coding RNA and protein-coding gene expression. BMC Genomics (2014) 15:620. doi:10.1186/1471-2164-15-620

16. Ørgaard A, Holst JJ. The role of somatostatin in GLP-1-induced inhibition of glucagon secretion in mice. Diabetologia (2017) 60:1731–1739. doi:10.1007/s00125-017-4315-2

17. Kawamori D, Kulkarni RN. Insulin modulation of glucagon secretion: the role of insulin and other factors in the regulation of glucagon secretion. Islets (2009) 1:276–279. doi:10.4161/isl.1.3.9967

18. Rorsman P, Berggren P, Bokvist K, Ericson H, Möhler H, Ostenson C et al. Glucose-inhibition of glucagon secretion involves activation of GABAA-receptor chloride channels. Nature (1989) 341:233–236. doi:10.1038/341233a0

19. Basco D, Zhang Q, Salehi A, Tarasov A, Dolci W, Herrera P et al. α-cell glucokinase suppresses glucose-regulated glucagon secretion. Nat Commun (2018) 9:546. doi:10.1038/s41467-018-03034-0

20. Knudsen J, Hamilton A, Ramracheya R, Tarasov A, Brereton M, Haythorne E et al. Dysregulation of glucagon secretion by hyperglycemia-induced sodium-dependent reduction of ATP production. Cell Metab (2018)1–13. doi:10.1016/j.cmet.2018.10.003

21. González-Vélez V, Dupont G, Gil A, González A, Quesada I. Model for glucagon secretion by pancreatic α-cells. PLoS One (2012) 7:e32282. doi:10.1371/journal.pone.0032282

22. Wendt A, Birnir B, Buschard K, Gromada J, Salehi A, Sewing S et al. Glucose inhibition of glucagon secretion from rat α-cells is mediated by GABA released from neighboring β-cells. Diabetes (2004) 53:1038–1045. doi:10.2337/diabetes.53.4.1038

23. Rorsman P, Ashcroft FM. Pancreatic β-Cell electrical activity and insulin secretion: of mice and men. Physiol Rev (2018) 98:117–214. doi:10.1152/physrev.00008.2017

24. Le Marchand SJ, Piston DW. Glucose suppression of glucagon secretion: Metabolic and calcium responses from α-cells in intact mouse pancreatic islets. J Biol Chem (2010) 285:14389–14398. doi:10.1074/jbc.M109.069195

25. Asadi F, Dhanvantari S. Plasticity in the glucagon interactome reveals proteins that regulate glucagon secretion in alpha TC1-6 cells. Front Endocrinol (2019) 9:792. doi:10.3389/fendo.2018.00792

26. Charbaut E, Chauvin S, Enslen H, Zamaroczy S, Sobel A. Two separate motifs cooperate to target stathmin-related proteins to the Golgi complex. J Cell Sci (2005) 118:2313–2323. doi:10.1242/jcs.02349

27. Mahapatra NR, Taupenot L, Courel M, Mahata SK, O'Connor DT. The trans-golgi proteins SCLIP and SCG10 interact with chromogranin A to regulate neuroendocrine secretion. Biochemistry (2008) 47:7167–7178. doi:10.1021/bi7019996

28. Bramswig N, Everett L, Schug J, Dorrell C, Liu C, Luo Y et al. Epigenomic plasticity enables human pancreatic alpha to beta cell reprogramming. J Clin Invest (2013) 123:1275–1284. doi:10.1172/JCI66514

29. Lawlor N, George J, Bolisetty M, Kursawe R, Sun L, Sivakamasundari V et al. Single-cell transcriptomes identify human islet cell signatures and reveal cell-type – specific expression changes in type 2 diabetes. Genome Res (2017) 27:208–222. doi:10.1101/gr.212720.116.Freely

30. Mossé Y, Laudenslager M, Longo L, Cole K, Wood A, Attiyeh E et al. Identification of ALK as the major familial neuroblastoma predisposition gene. Nature (2009) 455:930–935. doi:10.1038/nature07261.Identification

31. Guizzetti L, McGirr R, Dhanvantari S. Two dipolar alpha-helices within hormone-encoding regions of proglucagon are sorting signals to the regulated secretory pathway. J Biol Chem (2014) 289:14968–14980. doi:10.1074/jbc.M114.563684

32. Aida K, Saitoh S, Nishida Y, Yokota S, Ohno S, Mao X et al. Distinct cell clusters touching islet cells induce islet cell replication in association with over-expression of Regenerating Gene (REG) protein in fulminant type 1 diabetes. PLoS One (2014) 9:1–11. doi:10.1371/journal.pone.0095110

33. Li DS, Yuan YH, Tu HJ, Liang Q Le, Dail LJ. A protocol for islet isolation from mouse pancreas. Nat Protoc (2009) 4:1649–1652. doi:10.1038/nprot.2009.150

34. Suckow AT, Polidori D, Yan W, Chon S, Ma JY, Leonard J, Briscoe CP. Alteration of the glucagon axis in GPR120 (FFAR4) knockout mice: A role for gpr120 in glucagon secretion. J Biol Chem (2014) 289:15751–15763. doi:10.1074/jbc.M114.568683

35. Zinchuk V, Wu Y, Grossenbacher-Zinchuk O. Bridging the gap between qualitative and quantitative colocalization results in fluorescence microscopy studies. Sci Rep (2013) 3:1–5. doi:10.1038/srep01365

36. Chauvin S, Sobel A. Neuronal stathmins: A family of phosphoproteins cooperating for neuronal development, plasticity and regeneration. Prog Neurobiol (2015) 126:1–18. doi:10.1016/j.pneurobio.2014.09.002

37. Franklin IK, Wollheim CB. GABA in the endocrine pancreas: its putative role as an islet cell paracrine-signalling molecule. J Gen Physiol (2004) 123:185–190. doi:10.1085/jgp.200409016

38. Daily NJ, Boswell KL, James DJ, Martin TFJ. Novel interactions of CAPS (Ca2+-dependent activator protein for secretion) with the three neuronal SNARE proteins required for vesicle fusion. J Biol Chem (2010) 285:35320–35329. doi:10.1074/jbc.M110.145169

39. Schafer MKH, Mahata SK, Stroth N, Eiden LE, Weihe E. Cellular distribution of chromogranin A in excitatory, inhibitory, aminergic and peptidergic neurons of the rodent central nervous system. Regul Pept (2010) 165:36–44. doi:10.1016/j.regpep.2009.11.021

40. Atouf F, Czernichow P, Scharfmann R. Expression of neuronal traits in pancreatic beta cells. J Biol Chem (1997) 272:1929–1934. doi:10.1074/jbc.272.3.1929

41. Martin D, Grapin-Botton A. The importance of REST for development and function of beta cells. Front Cell Dev Biol (2017) 5:1–13. doi:10.3389/fcell.2017.00012

42. Koshimizu H, Kim T, Cawley N, Loh Y. Chromogranin A: A new proposal for trafficking, processing and induction of granule biogenesis. Regul Pept (2010) 165:95–101. doi:doi:10.1016/j.regpep.2010.09.006

43. Lutjens R, Igarashi M, Pellier V, Blasey H, Di Paolo G, Ruchti E et al. Localization and targeting of SCG10 to the trans-Golgi apparatus and growth cone vesicles. Eur J Neurosci (2000) 12:2224–2234. doi:10.1046/j.1460-9568.2000.00112.x

44. Lawlor N, Youn A, Kursawe R, Ucar D, Stitzel ML. Alpha TC1 and Beta-TC-6 genomic profiling uncovers both shared and distinct transcriptional regulatory features with their primary islet counterparts. Sci Rep (2017) 7:1–14. doi:10.1038/s41598-017-12335-1

45. Stamenkovic JA, Andersson LE, Adriaenssens AE, Bagge A, Sharoyko V V., Gribble F et al. Inhibition of the malate–aspartate shuttle in mouse pancreatic islets abolishes glucagon secretion without affecting insulin secretion. Biochem J (2015) 468:49–63. doi:10.1042/BJ20140697

46. Kuttapitiya A, Assi L, Laing K, Hing C, Mitchell P, Whitley G et al. Microarray analysis of bone marrow lesions in osteoarthritis demonstrates upregulation of genes implicated in osteochondral turnover, neurogenesis and inflammation. Ann Rheum Dis (2017) 76:1764–1773. doi:10.1136/annrheumdis-2017-211396

47. Nanjappa V, Thomas J, Marimuthu A, Muthusamy B, Radhakrishnan A, Sharma R et al. Plasma proteome database as a resource for proteomics research: 2014 update. Nucleic Acids Res (2014) 42:959–965. doi:10.1093/nar/gkt1251

48. Levy A, Devignot V, Fukata Y, Fukata M, Sobel A, Chauvin S. Subcellular Golgi localization of stathmin family proteins is promoted by a specific set of DHHC palmitoyl transferases. Mol Biol Cell (2011) 22:1930–1942. doi:10.1091/mbc.E10-10-0824

49. Wang J, Shan C, Cao W, Zhang C, Teng J, Chen J. SCG10 promotes non-amyloidogenic processing of amyloid precursor protein by facilitating its trafficking to the cell surface. Hum Mol Genet (2013) 22:4888–4900. doi:10.1093/hmg/ddt339

50. Marroqui L, Masini M, Merino B, Grieco FA, Millard I, Dubois C et al. Pancreatic α cells are resistant to metabolic stress-induced apoptosis in type 2 diabetes. EBioMedicine (2015) 2:378–385. doi:10.1016/j.ebiom.2015.03.012

51. Akiyama M, Liew CW, Lu S, Hu J, Martinez R, Hambro B et al. X-Box binding protein 1 is essential for insulin regulation of pancreatic α-cell function. Diabetes (2013) 62:2439–2449. doi:10.2337/db12-1747

52. Pasquier A, Vivot K, Erbs E, Spiegelhalter C, Zhang Z, Aubert V et al. Lysosomal degradation of newly formed insulin granules contributes to β cell failure in diabetes. Nat Commun (2019) 10:1–14. doi:10.1038/s41467-019-11170-4

53. Yuxia Z, Zhiyu L, Shengmei Z, Ruijuan Z, Huiying L, Xiaoqing L et al. RILP restricts insulin secretion through mediating lysosomal degradation of proinsulin. Diabetes (2019) doi:10.2337/db19-0086

Chapter 4

4. Mediation of Glucagon Trafficking from the Endolysosomal System Towards the Secretory Pathway by Stathmin-2 in Diabetic α-Cells

Farzad Asadi[1], Savita Dhanvantari[1, 2, 3*]

[1]Department of Pathology and Laboratory Medicine, Schulich School of Medicine & Dentistry, Western University, London, ON, Canada

[2]Department of Medical Biophysics, Western University, London, ON, Canada

[3]Lawson Health Research Institute, London, ON, Canada

*Corresponding author (sdhanvan@lawsonimaging.ca)

Short running title: Diabetes, Stathmin-2 and glucagon trafficking

4.1 Abstract

Glucagon hypersecretion from the pancreatic α-cell is a characteristic sign of diabetes, which exacerbates fasting hyperglycemia. Thus, targeting glucagon secretion from α-cells may be a promising approach for combating hyperglucagonemia. We have recently shown that stathmin-2 (Stmn2), a protein that associates with glucagon in secretory granules, can regulate glucagon secretion by directing glucagon towards the endolysosomal system in α-cells. Here, we examined how Stmn2-mediated glucagon trafficking is affected in diabetes, and if such a mechanism could explain the hyperglucagonemia of diabetes. To this end, C57BL/6 mice were rendered diabetic by streptozotocin (STZ; 30 mg/kg i.p. for 5 days). Using confocal immunofluorescence microscopy, we showed strong colocalization between Stmn2 and glucagon in intact islets of both non-diabetic (PCC 0.77±0.02) and diabetic mice (PCC 0.83±0.06). Immunogold labeling transmission electron microscopy showed the presence of both glucagon and Stmn2 in the dense core portion of secretory granules in both control and diabetic mice. The secretion of both glucagon and Stmn2 from either normal or diabetic islets was significantly enhanced by arginine. In contrast, cell glucagon content was significantly increased in diabetic islets, ($p<0.001$), but Stmn2 levels were reduced ($p<0.01$). In islets from diabetic mice, there was an increase ($p<0.001$) in glucagon immunofluorescence that was concomitant with a decrease ($p<0.01$) in Stmn2 immunofluorescence, and expression of *Gcg* mRNA increased ~4.5 times, while *Stmn2* mRNA levels did not change. We then followed changes in glucagon and Stmn2 trafficking in diabetes. In islets from control mice, both glucagon and Stmn2 showed a moderate level of colocalization with the lysosomal marker, Lamp2A; however, this colocalization was dramatically reduced ($p<0.001$) in islets from diabetic mice. Interestingly, the co-localization of Stmn2 with the late endosome marker, Rab7, significantly ($p<0.01$) increased in islets from diabetic mice, while the co-localization between glucagon and Rab7 did not change. As well, there was a significant increase in the intensity of Rab7 in diabetic α-cells compared to control. Retrograde shuttling of glucagon towards early endosome or recycling endosome was not prominent in α-cells. Thus, we propose that the hyperglucagonemia of diabetes may be partially explained by a

decrease in the lysosomal trafficking of glucagon and Stmn2 associated with a relative decrease in cellular Stmn2 and re-routing of Stmn2 to late endosomes.

Keywords: diabetes, hyperglucagonemia, glucagon secretion, stathmin-2, lysosome, endosome

4.2 Introduction

In diabetes, glucagon secretion from the pancreatic α-cell becomes abnormally up-regulated, resulting in hyperglucagonemia. This paradoxical glucagon hypersecretion from α-cells then causes exacerbation of hyperglycemia (1–3). It has been suggested that, in order to fully control hyperglycemia in diabetes, glucagon secretion should be suppressed. Therefore, the mechanisms and pathways that underlie the abnormal secretion of glucagon must be elucidated, so that potential targets for suppressive therapy can be identified.

Studies have shown that glucagon secretion can be controlled by targeting mediators of intracellular signaling and exocytosis within the α-cell. Agonists of the glucagon-like peptide receptor (GLP-1R) inhibit glucagon secretion by directly acting on α-cells, or indirectly through releasing insulin, Zn^{2+}, and GABA from β-cells, or by releasing somatostatin from δ-cells (4). GABA receptor agonists also directly inhibit glucagon secretion through binding with $GABA_A$ receptor on α-cells, increasing Cl^- influx, and hyperpolarization of plasma membrane (5,6). Antagonists of the glucose-dependent insulinotropic peptide receptor (GIP-R) directly suppress the glucagonotropic effect of GIP on α-cells (7). Insulin itself suppresses glucagon secretion through binding its receptor on α-cells (8,9) or indirectly by increasing secretion of somatostatin from δ-cells (10). Amylin inhibits amino acid-dependent exaggerated glucagon secretion in patients with diabetes (11,12). Blockers of K_{ATP} channels inactivate ion channels, and reduce α-cell electrical activity, which result in suppression of glucagon secretion (13–15). n addition to blocking the effects of glucagon on hepatic glucose mobilization, anti-glucagon receptor antibodies may also block the autocrine effect of glucagon on glucagon secretion from α-cells (16,17).

All of the above mechanisms eventually converge on the α-cell secretory pathway by which glucagon is stored in and secreted from secretory granules. We hypothesize that elucidating the intracellular mechanisms of glucagon trafficking through the α-cell secretory pathway could also yield clues on possible mechanisms of the regulation of glucagon secretion. Using α-TC1-6 cells, we have shown that components of the

regulated secretory pathway are up-regulated after chronic exposure to high levels of glucose (18) and proposed that proteins that associated with glucagon within secretory granules (glucagon interactome) play a role in the regulation of glucagon secretion (19). We showed that the interactome was responsive to glucose, GABA and insulin, known modulators of glucagon secretion. In particular, treatment with insulin, which is a potent inhibitor of glucagon secretion at euglycemic and hypoglycemic conditions (8), appeared to recruit stathmin-2 (Stmn2 or SCG10) to the interactome, thus potentially identifying another inhibitor of glucagon secretion. In a subsequent study, we showed that Stmn2 is co-secreted in a regulated manner with glucagon, and when over-expressed, suppressed glucagon secretion by increasing its trafficking through the endolysosomal pathway in α-TC1-6-cells(20).

There is one report on the reuptake of glucagon by α-cells after secretion and trafficking to the endolysosomal system for degradation (21). Our previous study was the first to show that the endolysosomal system may figure prominently in the intracellular trafficking of glucagon as it is directed through the regulated secretory pathway(20). Interestingly, parallel findings in β-cells showed that there is a shuttling of insulin from secretory pathway towards the endolysosomal system for degradation, which may be an underlying mechanism for β-cell failure in type 2 diabetes (22). Therefore, the endolysosomal trafficking pathway may be a novel pathway for the dysregulation of both insulin and glucagon secretion in diabetes. We hypothesize that a disruption in the Stmn2-mediated trafficking of glucagon through the endolysosomal pathway might be a possible mechanism by which glucagon secretion becomes dysregulated in diabetes, resulting in glucagon hypersecretion and hyperglucagonemia.

In the present study, we show that there is a discordance in the levels of glucagon and Stmn2 in diabetic mouse islets. This discordance is associated with increased glucagon secretion, cell content and mRNA levels, and an inhibition of the trafficking of both glucagon and Stmn2 to the lysosome. There appears to be re-routing of Stmn2 to late endosomes which accompanies the increased secretion of glucagon. Therefore, we propose that the loss of the α-cell lysosomal trafficking pathway in diabetes could contribute to glucagon hypersecretion and hyperglucagonemia.

4.3 Materials and methods

4.3.1 Animals

C57BL/6 male mice (8 weeks old) were purchased from the Jackson Laboratory (Bar Harbor, Maine, United States). Mice were kept at 12h light/12h dark cycle and had free access to water and regular chow diet. All mice were treated and euthanized in accordance with the guidelines set out by the Animal Use Subcommittee of the Canadian Council on Animal Care at Western University based on the approved Animal Use Protocol AUP 2012-020. Mice were fasted 5h before blood collection or euthanasia.

Induction of diabetes: Streptozotocin (STZ; Cat# S0130, Sigma) was dissolved in freshly prepared 0.1 M sodium citrate buffer, pH 4.5, and immediately used. Mice (n=18) were intraperitoneally injected with 30 mg/kg STZ for 5 consecutive days and used for microscopic (total n=7; 7 out of 7 for immunofluorescent microscopy; 4 out of 7 for transmission electron microscopy), islet secretion (n=7) and gene expression (n=4) studies. Three days after the last STZ injection, blood was sampled by tail vein lancing and glucose levels were determined with the OneTouch Ultra glucometer. Values above 14 mmol/L were considered an indicator of diabetes onset (https://www.jax.org). Control mice (n=18) were injected with citrate buffer alone at the same regimen. Animals were euthanized 14 days after the last STZ injection by cervical dislocation under deep isoflurane anesthesia.

Blood collection: Prior to cervical dislocation and under isoflurane induced anesthesia, blood (1 mL) was collected by cardiac puncture into microcentrifuge tubes containing 15 µL of anticoagulant (15% Na_2-EDTA) and 15 µL of freshly prepared enzyme inhibitor cocktail (Cat# 4693159001 Millipore Sigma). Samples were kept on ice and then centrifuged at 1500 g for 15 min at 4°C. Plasma was collected and kept at -80°C until analysis.

4.3.2 Preparation of pancreas tissue sections for confocal immunofluorescence

Microscopy: Immediately after euthanasia, pancreata of STZ-treated (n=7) and vehicle-treated (n=7) mice were excised, fixed in 10% buffered formalin for 3 days and treated with 70% ethanol for one day before paraffin embedding. Paraffin-embedded tissue blocks were longitudinally sectioned in 5 µm slices and fixed on glass microscope slides. The tissue samples were de-paraffinized by graded washes using xylene, ethanol and PBS. Antigen retrieval was conducted in sodium citrate buffer (10 mM sodium citrate, 0.05% Tween 20, pH 6) with 20 min steam heating of slides in a steam cooker. After permeabilization with 0.1% Triton X-100 in PBS, Background Sniper (Cat# BS966H, Biocare Medical) was used to block non-specific background staining. Samples were incubated with primary antibodies against glucagon (Cat # ab10988 or Cat# ab92517, Abcam; 1:1000), Stmn2 (Cat # ab115513, Abcam; 1:250 or Cat# 720178, Thermo Fisher Scientific; 1:500), insulin (Cat# ab7842, Abcam; 1:500 or Cat# I2018, Sigma; 1:1000), late endosome marker, Rab7 (Cat# ab126712, Abcam; 1:500), lysosomal marker, Lamp2A (Cat# ab18528, Abcam; 1:1000), or recycling endosome markers Rab11A (Cat# ab180778, Abcam; 1:100) and Rab11B (Cat# ab 228954, Abcam;1:100). The corresponding secondary antibodies used were goat anti-mouse IgG Alexa Fluor 488 (Cat# A-11001, Molecular Probes; 1:500), donkey anti-goat IgG Alexa Fluor 555 (Cat# ab150130, Abcam; 1:500), goat anti-guinea pig IgG Alexa Fluor 647 (Cat# A21450, Invitrogen; 1:500), donkey anti-rabbit 488 (Cat#ab150073, Abcam; 1:500), donkey anti-mouse 555 (Cat# A-31570, Molecular Probes; 1:500) and goat anti-rabbit IgG Alexa Fluor 594 (Cat# A 11037, Invitrogen; 1:500). Nucleus counter-staining was done by DAPI and coverslips were mounted using Prolong Antifade mountant (Cat# P36982, Thermo Fisher Scientific). As a background control for Stmn2, islet staining for Stmn2 was done using only the secondary antibody.

Image acquisition: Images were acquired through Nikon A1R Confocal microscope with a ×60 NA plan-Apochromat oil differential interference contrast objective and NIS-Elements software (Nikon, Mississauga, Canada). Acquisition of high-resolution images

was done by selecting Nyquist XY scan area, 1024×1024-pixel size scanning of the selected area and 2D- Deconvolution of the captured images.

Image Analysis: Three adjacent longitudinal slices of pancreas were placed on each glass slide. In total, 10 slides were prepared from each pancreas. Image analysis was performed by NIS-Elements software (Nikon, Mississauga, Canada). To calculate colocalization values of endosomal and lysosomal markers with glucagon or Stmn2 within the same islet, channels were pseudocolored for Lamp2A, Rab7, Rab11A or Rab11B. Colocalization of pixels from each pseudocolored image was used to calculate Pearson's correlation coefficient (PCC), as we have done previously (23)(19). Regions of interest (ROIs) were manually drawn around each islet and then defined PCC values for colocalization between Stmn2 and target markers (glucagon, insulin, Lamp2A, Rab7, Rab11A, Rab11B) were calculated using the colocalization algorithm of NIS-Elements software. To show the relationships between expression levels of Stmn2 and the target markers (glucagon, insulin, Lamp2A, Rab7, Rab11A, Rab11B) in α or β- cells of the pancreatic islets, binary images were generated using M-Threshold algorithm of NIS-Elements software. ROIs were manually drawn around each binary arranged image of the islet and the fluorescence intensity of each marker was calculated. Levels of fluorescence intensities were normalized by dividing by the intensity of DAPI within each ROI. These values were used for linear regression analysis between Stmn2 and the target markers.

4.3.3 Double immunogold labeling transmission electron microscopy

Double immunogold labeling TEM was done based on the protocol of Aida et al (2014) with some modifications (24) as we have recently used (20). Briefly, in both non-diabetic (n=4) and diabetic (n=4) mice, pancreas was dissected, and a piece of pancreas in its long axis was cut, and immediately placed into McDowell Trump's fixative (Cat# 18030-10, Electron Microscopy Sciences) for 1h. Then, after washing with PBS, samples were cut into smaller pieces, and dehydrated in the increasing concentrations of ethanol (10%, 20%, 30%, 50%, 70%, 90%, 100% and 100%) at 30 min per concentration. Samples were sequentially embedded in LR White Resin (Cat# 14381, Electron Microscopy Sciences)

as follows: ethanol-LR White mixture A (3:1, v/v; 2h), ethanol-LR White mixture B (1:1, v/v; 8h), ethanol-LR White mixture C (1:3, v/v; 12h), and 3 × 12h in pure LR White. Samples were then placed into a beem capsule, filled with pure LR White and incubated at 50°C for 24h. Semi-thin sections (500 nm) were cut from embedded samples for Toluidin blue staining (1% Toluidin blue for 2 min). After defining the position of the islets within the pancreatic tissue, ultra-thin section slices (70 nm) were prepared using a diamond microtome. The sections were mounted on formvar-carbon coated nickel grid (300 meshes; Cat# FCF300-NI, Electron Microscopy Sciences). Afterwards, slices were washed with Tris-buffered saline, 0.1% Tween 20 (TBS-T) and incubated in blocking buffer (2% BSA in PBS plus 0.05% Tween 20) for 30 min at room temperature. Slices were incubated with primary antibodies (1:10 in blocking buffer) against glucagon (Cat# ab10988; Abcam) and Stmn2 (Cat# ab115513; Abcam) at 4°C overnight. After washing with TBS-T, slices were incubated with gold-conjugated secondary antibodies of donkey anti-goat (18 nm; cat# ab105270, Abcam; 1:50) and donkey anti-mouse (10nm; cat# ab39593, Abcam; 1:50) for 2h at room temperature. After washing with TBS-T and staining with Uranyless (Cat# 22409, Electron Microscopy Sciences), TEM was conducted at the Biotron Experimental Research Center, Western University, London, ON, Canada.

4.3.4 Proglucagon and stathmin-2 gene expression

Handpicked islets (~180) from control (n=4) and diabetic (n=4) mice were placed into 1 mL Trizol (Cat# 15596018, Ambion) and processed for RNA extraction, as described previously (25,26) . Islets were homogenized by being passed 10 times through a 25-gauge needle, and again through a 27-gauge needle. After centrifugation at 10000×g for 5 min at 4°C, the supernatant was mixed with chloroform, vortexed for 30 seconds and placed on ice for 2 min. After centrifugation at 12000×g for 15 min at 4°C, the aqueous layer was collected and mixed with 0.5 volumes of high salt solution (0.8 M Na-citrate containing 1.2 M NaCl). Isopropanol (0.5 volumes) was added, and the samples were mixed, incubated for 10 min at room temperature and centrifuged at 12000×g for 30 min at 4°C. The pellet was dissolved in 70% ethanol and RNA was purified by RNeasy kit (Cat # 74104, Qiagen) according to the supplier's protocol. cDNA synthesis was

performed using the SuperScript III First Strand Synthesis Supermix for qRT-PCR (Cat # 11752050, Thermo Fisher Scientific), according to the manufacturer's protocol. Real-time PCR was performed using Quant Studio Design and Analysis Real-Time PCR Detection System in conjunction with the Maxima SYBR Green qPCR Master Mix (Cat # K0221, Thermo Fisher Scientific) using specific primers for *Stmn2*: forward, 5'-GCAATGGCCTACAAGGAAAA-3'; reverse, 5'-GGTGGCTTCAAGATCAGCTC-3'; *Gcg*: forward, 5'-AACAACATTGCCAAACGTCA-3'; reverse, 5'-TGGTGCTCATCTCGTCAGAG-3' and *18S rRNA*: forward, 5'-ACGATGCCGACTGGCGATGC-3'; reverse, 5'-CCCACTCCTGGTGGTGCCCT-3'. Gene expression levels were normalized to that of *18S* rRNA. Gene expression in the diabetic condition was normalized to the corresponding control group and expressed as percent of matched control. Statistical analysis was performed using t-test at $\alpha = 0.05$.

4.3.5 Primary islet culture

Islets were isolated and cultured as we have done previously (20) using a modified protocol from Li et al. (27). Non-diabetic (n=7) or diabetic mice (n=7) were euthanized. The abdominal cavity was opened and 3 mL of 1.87 mg/mL collagenase V (Cat# C9263, Sigma;) in Hanks' Balanced Salt Solution was injected into the common bile duct. The pancreas was then removed, placed into a Falcon tube containing 2 mL of the ice-cold collagenase V solution and incubated for 12 min at 37°C with occasional shaking. Digestion was stopped by adding 1mM $CaCl_2$ and the cell suspension was washed twice in the $CaCl_2$ solution. Islets were collected into a sterile petri dish using a 70 µm cell strainer with RPMI1640 containing 11 mM glucose plus 20 mM glutamine, 10% FBS and penicillin (110U/mL) and streptomycin (100 µg/mL). A total of 180 islets were handpicked under a stereomicroscope and incubated for 2h at 37°C. The medium was then changed to RPMI1640 containing 11 mM glucose plus 10% FBS and penicillin (110U/mL) and streptomycin (100 µg/mL) and islets were cultured overnight at 37°C.

Glucagon secretion experiments: Glucagon secretion from islets was measured based on the protocol by Suckow et al (2014). Briefly, islets were washed three times using Krebs-Ringer bicarbonate (KRB) buffer (135 mM NaCl, 3.6 mM KCl, 5 mM $NaHCO_3$, 0.5 mM

NaH_2PO_4, 0.5 mM $MgCl_2$, 1.5 mM $CaCl_2$, 10 mM HEPES; pH 7.4) containing 11 mM glucose, and then pre-incubated in this KRB for 1h. Islets were then incubated in KRB containing 1mM glucose in the presence or absence of arginine (25 mM) for 20 min. Media were collected into microcentrifuge tubes containing enzyme inhibitors (PMSF, 45 mM; Aprotinin, 5 µg/mL and sodium orthovanadate, 1mM). Samples were centrifuged at 14000 × g for 5 min at 4°C and the supernatant was collected and kept at -80°C until analysis. Islets were lysed in lysis buffer (0.1 M citric acid, 1% Triton X-100 plus enzyme inhibitors) and homogenized by passing 10 times through a 25-gauge needle, and again through a 27-gauge needle. The extracts were centrifuged at 14000×g for 15 min at 4°C and the supernatant was collected and kept at -80°C until analysis (28).

Measurement of glucagon and stathmin-2: Glucagon levels in the media and islet extracts were determined by ELISA (Cat # EHGCG, Thermo Fisher Scientific) according to the manufacturer's instructions. Stmn2 levels in the media and islet extracts were measured using stathmin-2 ELISA kit (Cat# MBS7223765, MyBioSource) according to the supplier's instruction. For each measurement, the values were compared between groups by t-test and among groups by one-way ANOVA ($\alpha = 0.05$). Total cellular protein was determined using BCA assay and used to normalize cellular glucagon or Stmn2 per mg of cell protein. Then, alterations in values were expressed as percent changes compared to the baseline control. To this end, the Arg-stimulated secretion of glucagon or Stmn2 was normalized to the baseline level of glucagon and Stmn2, respectively, and expressed as relative fold changes.

Statistical analyses: Comparison of values among groups was done by one-way ANOVA (Bonferroni post-hoc test), and between groups by t-test using Sigma Stat 3.5 software at $\alpha=0.05$. For colocalization analysis of images, Pearson correlation coefficient values were extracted using NIS-Elements software and then values were compared between groups by t-test ($\alpha=0.05$).

4.4 Results

4.4.1 Induction of diabetes in C57BL/6 mice

Measuring blood glucose levels following STZ injection showed fasting hyperglycemia (>14 mmol/L), indicating onset of diabetes (Figure 4- 1A). Plasma levels of glucagon were significantly ($p<0.001$) higher and plasma levels of insulin were significantly reduced ($p<0.001$) in STZ-treated mice compared to the control group (Figure 4- 1B, C), and there was a significantly ($p<0.001$) higher glucagon: insulin ratio in STZ-treated mice compared to the control (Figure 4- 1D). These findings indicate development of a diabetic metabolic and hormonal profile following STZ administration.

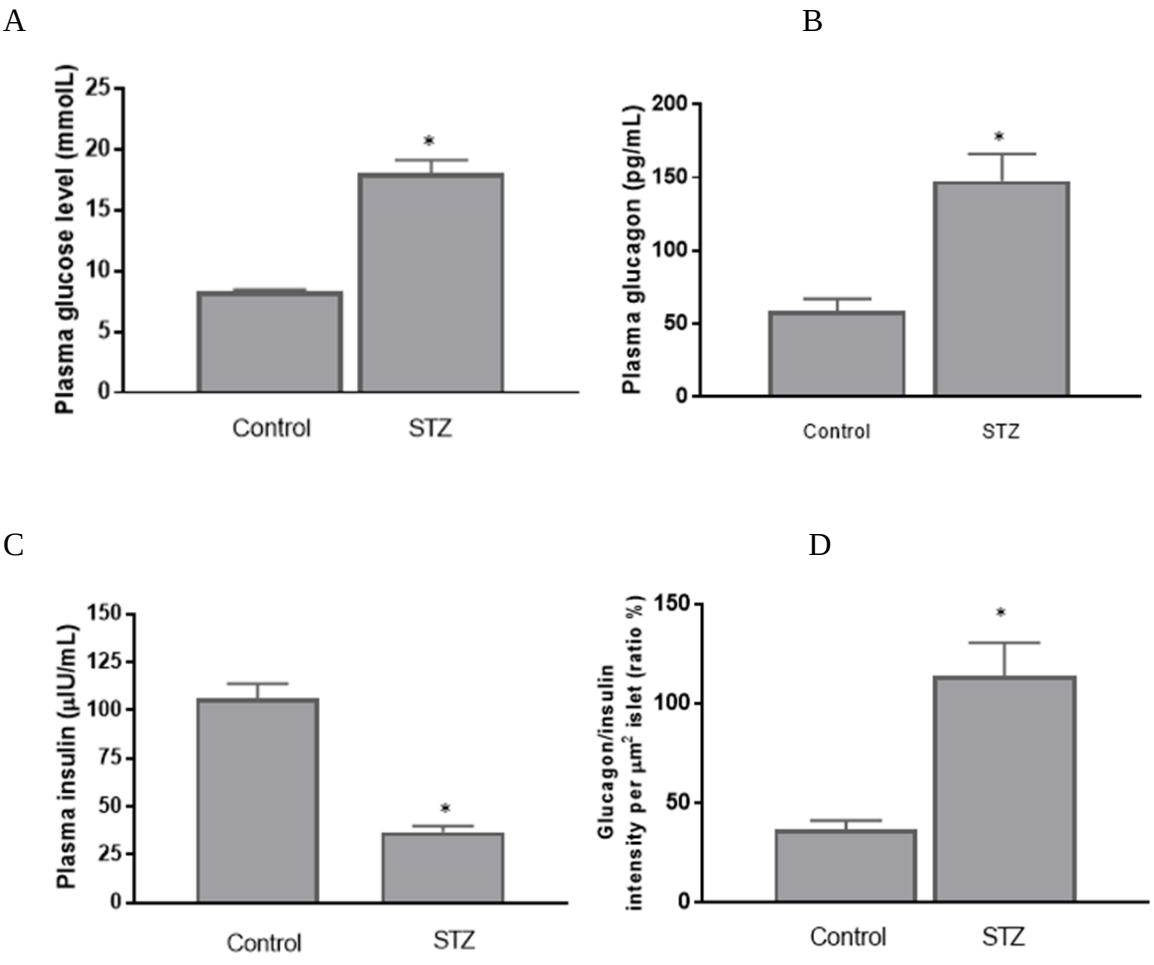

Figure 4-1. Streptozotocin (STZ) induced diabetes in C57BL/6 mice. (A) Plasma glucose, (B) plasma insulin, (C) plasma glucagon, and (D) glucagon: insulin ratio per µm2 of islet in STZ-induced diabetic mice. Values (mean± SD) were compared between diabetic (n=7) and control (n=7) mice by t-test. *p<0.001.

4.4.2 Glucagon and Stmn2 co-localize in islets of diabetic and non-diabetic mice

Confocal immunofluorescence microscopy studies on islets of non-diabetic mice (Figure 4- 2A) showed colocalization between glucagon and Stmn2 (Figure 4- 2B) but not between insulin and Stmn2 (Figure 4- 2C). This pattern of co-localization was conserved in islets from diabetic mice (Figures 4- 2D-F). Quantification and analysis (Figure 4- 2G) revealed strong colocalization between glucagon and Stmn2 in α-cells of both control (PCC 0.77± 0.02) and STZ-induced diabetic mice (PCC 0.83 ± 0.06). In contrast, there was almost no colocalization between insulin and Stmn2 in both control (PCC 0.04±0.03) and STZ-induced diabetic mice (PCC 0.03±0.06).

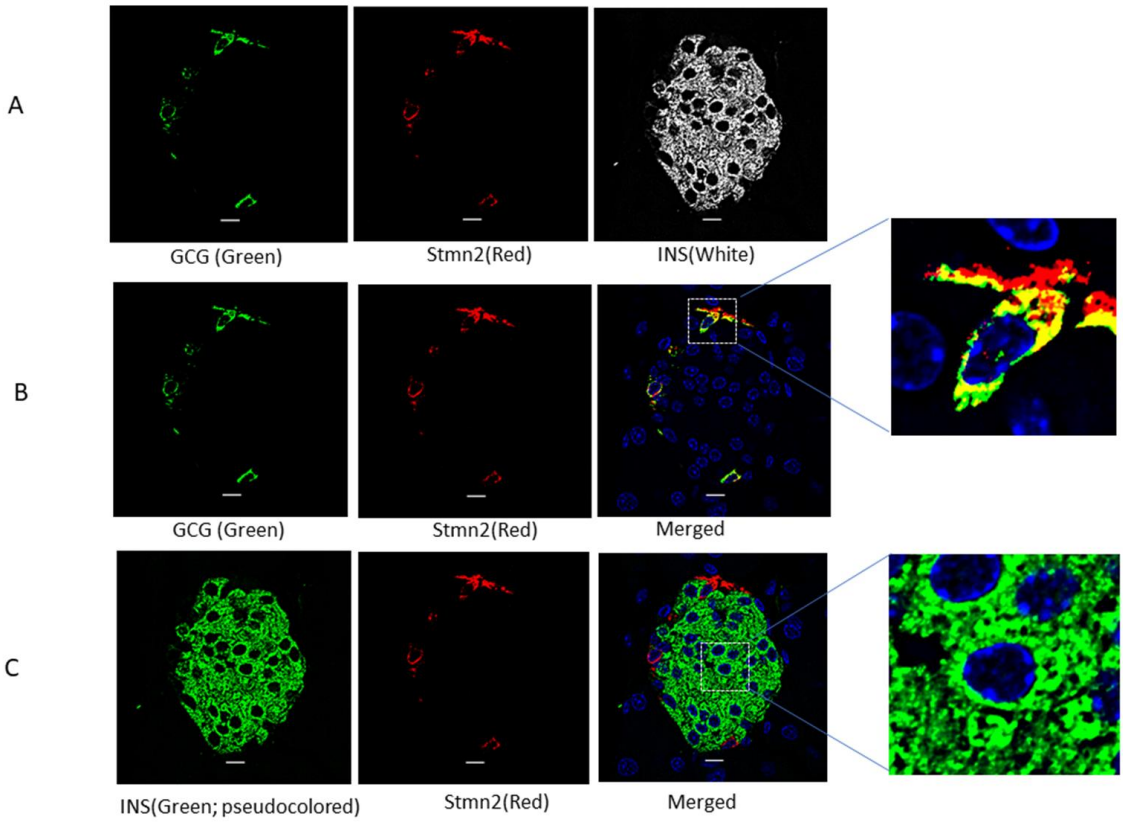
A
GCG (Green)
Stmn2(Red)
INS(White)
B
GCG (Green)
Stmn2(Red)
Merged
C
INS(Green; pseudocolored)
Stmn2(Red)
Merged

D

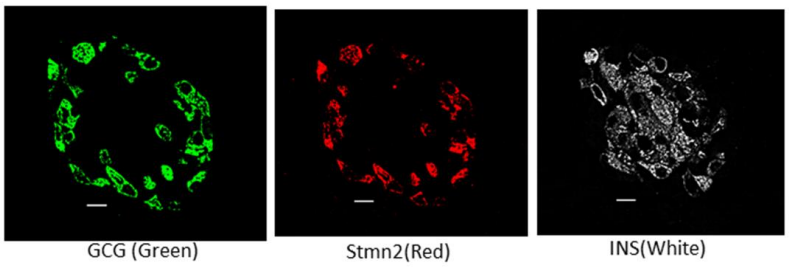
GCG (Green)
Stmn2(Red)
INS(White)

E

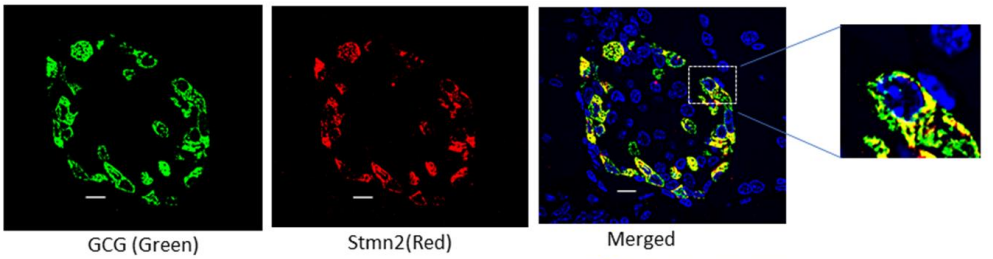
GCG (Green)
Stmn2(Red)
Merged

F

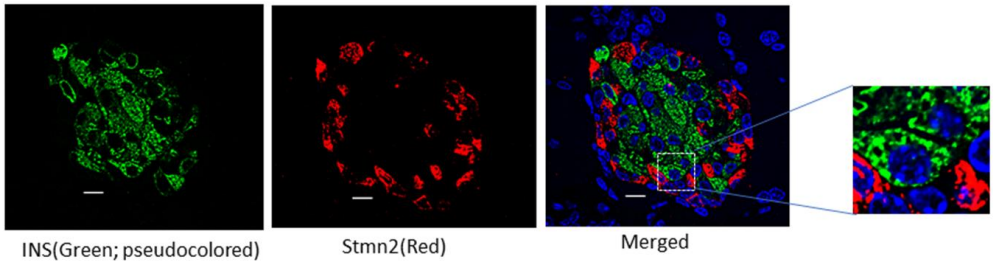
INS(Green; pseudocolored)
Stmn2(Red)
Merged

G

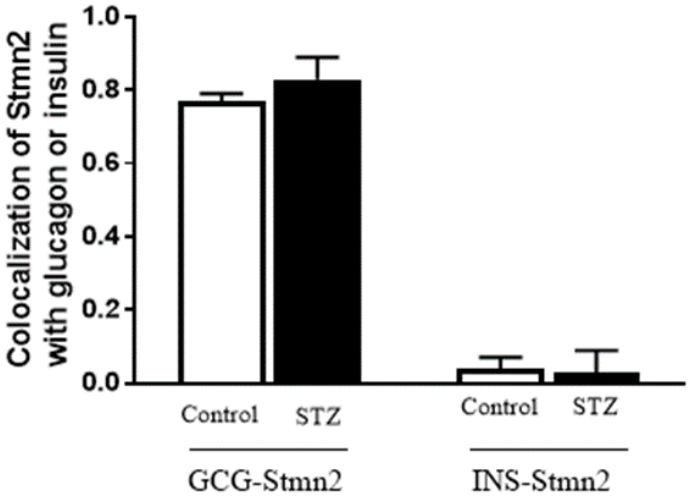
Colocalization of Stmn2 with glucagon or insulin
1.0
0.8
0.6
0.4
0.2
0.0
Control
STZ
Control
STZ
GCG-Stmn2
INS-Stmn2

Figure 4-4. Stathmin-2 colocalizes with glucagon but not insulin in both non-diabetic and STZ-induced diabetic mice. (A) Islets of non-diabetic mice (n=7) were immunostained for glucagon (GCG), insulin (INS) and stathmin-2 (Stmn2); (B) after removing INS channel, colocalization was determined between GCG and Stmn2; (C) after removing GCG channel, and pseudocoloring of INS channel to green, colocalization was determined between Stmn2 and INS. (D) Islets of diabetic mice (n=7) were immunostained for GCG, INS and Stmn2; (E) after removing INS channel, colocalization was determined between GCG and Stmn2; (F) after removing GCG channel and pseudocoloring of INS channel to green, colocalization was determined between Stmn2 and INS. In each panel, marked area by square was magnified to show a typical individual cell. (G) Correlation between GCG and Stmn2 or INS and Stmn2 was determined by Pearson's correlation coefficient (PCC) using NIS-Elements software. Images were acquired by Nikon A1R confocal microscope.

4.4.3 STZ-induced diabetes increases glucagon levels and reduces Stmn2 levels in α-cells

Analysis of fluorescence intensities revealed increased cellular levels of glucagon ($p<0.001$) and reduced levels of Stmn2 ($p<0.01$) in islets of STZ-induced diabetic mice (Figure 4- 3A). As a consequence, the ratio of glucagon: Stmn2 in α-cells of STZ-induced diabetic mice significantly increased ($p<0.01$) compared to the non-diabetic controls (Figure 4- 3B). Linear regression analysis of binary sum intensities showed a strong positive correlation between expression of Stmn2 and glucagon in α-cells of non-diabetic mice ($R^2 = 0.9$, $p<0.001$) that was disrupted in STZ-induced diabetic mice ($R^2 = 0.07$, $p >0.05$) (Figure 4- 3C).

A

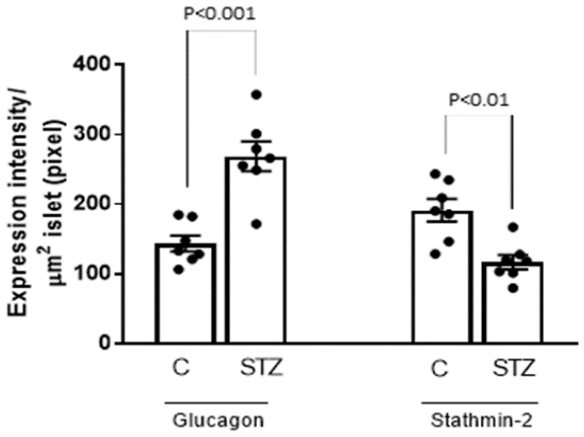
P<0.001
P<0.01
Expression intensity/ µm² islet (pixel)
400
300
200
100
0
C
STZ
C
STZ
Glucagon
Stathmin-2

B

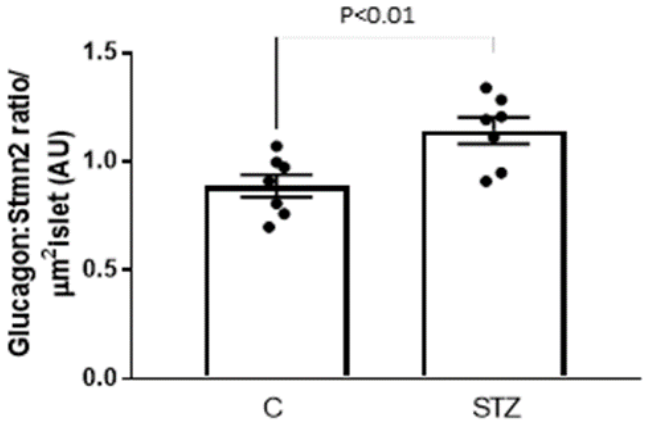
P<0.01
Glucagon:Stmn2 ratio/ µm²Islet (AU)
1.5
1.0
0.5
0.0
C
STZ

C

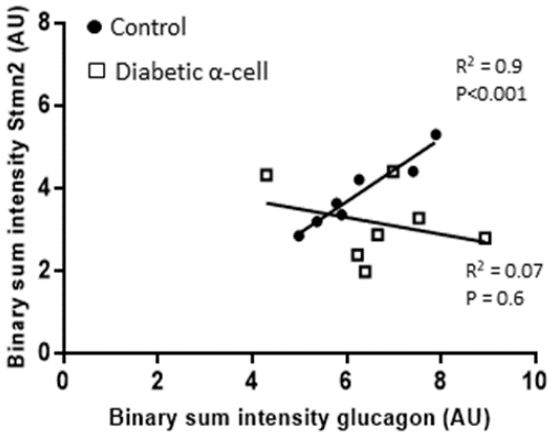
Control
Diabetic α-cell
R² = 0.9
P<0.001
R² = 0.07
P = 0.6
Binary sum intensity Stmn2 (AU)
Binary sum intensity glucagon (AU)
0
2
4
6
8
10

Figure 4-7. Imbalanced ratios of stathmin-2 and glucagon in islets of STZ-induced diabetic mice. Islets were immunostained for stathmin-2 (Stmn2) and glucagon and images were acquired by A1R confocal microscope. (A) Expression of glucagon and Stmn2 were determined in islets of non-diabetic and diabetic mice by immunofluorescence intensity analysis . (B) Ratios of glucagon: Stmn2 levels were calculated per µm2 of islets in non-diabetic and diabetic mice. (C) Linear regression analysis on binary image intensities of the Stmn2 and glucagon. Filled circles and open squares demonstrate values in non-diabetic and diabetic islets, respectively.

This increase in cellular glucagon was paralleled by a ~ 4.5 times increase in the levels of *Gcg* mRNA, while there was no effect on *Stmn2* mRNA levels (Figure 4- 4).

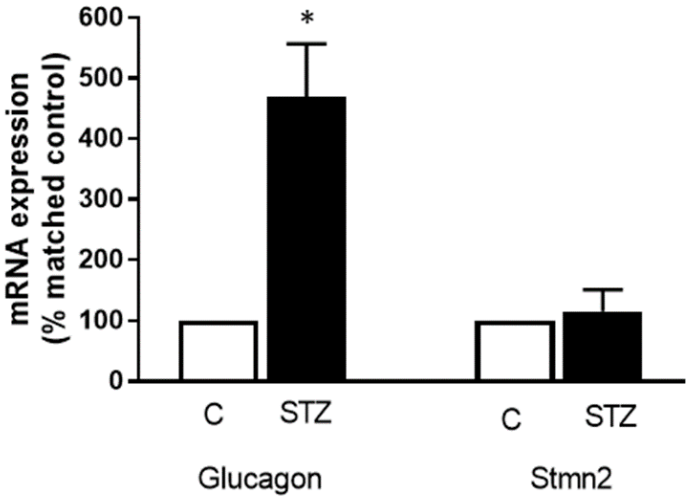

Figure 4-10. Expression of Stmn2 and Gcg mRNA levels were determined in islets of non-diabetic (n=4) and diabetic (n=4) mice by RT-qPCR. Gene expression levels were normalized to that of 18S rRNA. For each gene alterations in diabetic condition was normalized by the corresponding control group and expressed as matched control percent. Comparison between control and diabetic ones was done by t-test, α=0.05.

4.4.4 Both glucagon and Stmn2 are localized within secretory granules of α-cells

Double immunogold-labeling transmission electron microscopy revealed co-localization of glucagon and Stmn2 within the secretory granules of mouse islet α-cells. Glucagon (10 nm particles; white arrows) and Stmn2 (18 nm particles; black arrows) were co-localized within the dense core of secretory granules in both non-diabetic (Figure 4- 5A) and diabetic (Figure 4- 5B) mice.

A

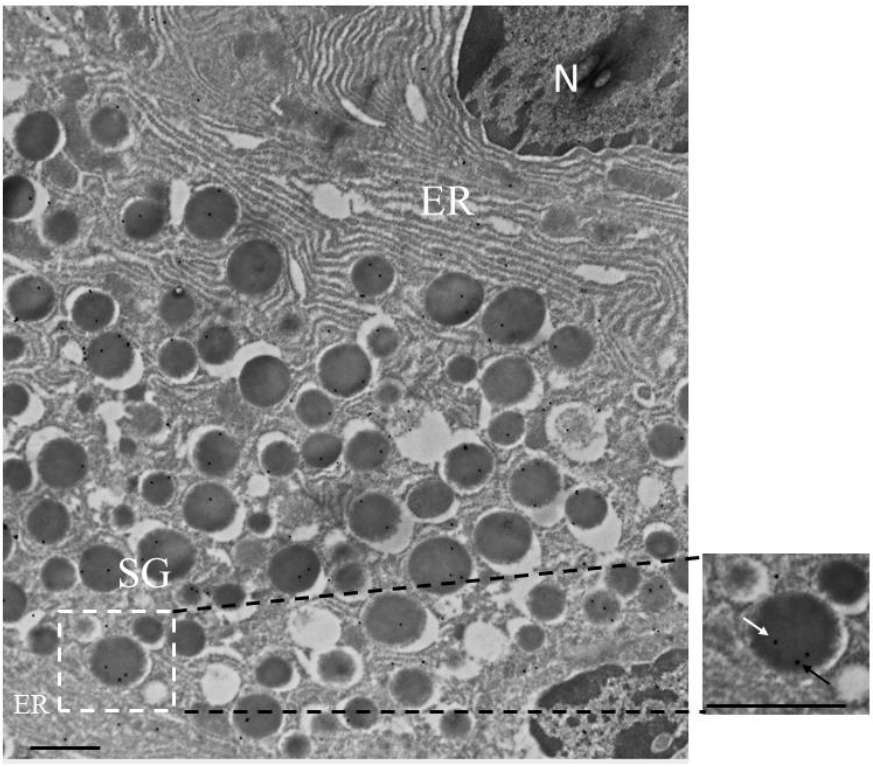

B

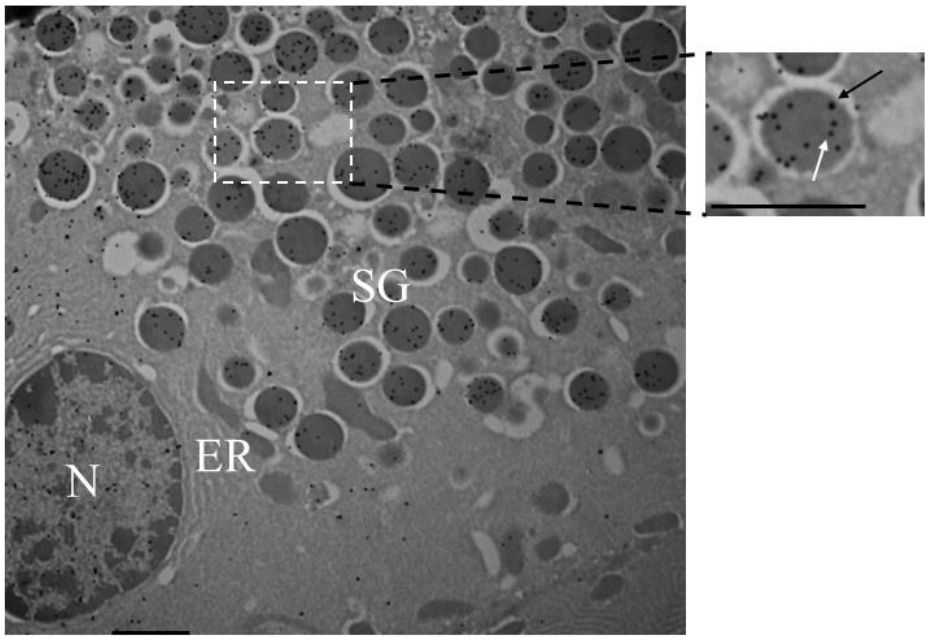

Figure 4-13. The presence of stathmin-2 and glucagon within secretory granules of α-cells. (A) Double immunogold labelling transmission electron microscopy of islets in non-diabetic and (B) STZ-induced diabetic mice was done by antibody against glucagon (10 nm gold, white arrows in the magnified section) and stathmin-2 (18 nm gold, black arrows in the magnified section). The low magnification images (19000×, scale bar = 1 µm) show the ultrastructure of one α-cell. N (nucleus); ER (endoplasmic reticulum); SG (secretory granule); PM (plasma membrane). The magnified images (21000×, scale bar = 0.6 µm) highlight the presence of immunogold labels within a single secretory granule.

4.4.5 Arginine stimulates parallel increases in glucagon and Stmn2 secretion

In line with our recent findings (20), there was an increase in the secretion of both glucagon (~2.9 times) and Stmn2 (~2.3 times) from isolated islets in response to 25 mM Arg. In islets from diabetic mice, the glucagon secretory response was exaggerated, with increased basal and Arg-stimulated secretion (Figure 4- 6A). There was also a small but significant increase in basal Stmn2 secretion and a significant increase in response to Arg in diabetic islets (Figure 4- 6B). There was a concomitant reduction in cell glucagon content of non-diabetic islets in response to Arg (Figure 4- 6A). In contrast, cell glucagon content of diabetic islets was elevated in the absence of Arg, and remained elevated after Arg stimulation (Figure 4- 6A), consistent with the diabetic phenotype of glucagon production. In parallel with the pattern of cell glucagon content in non-diabetic islets, cell Stmn2 content also decreased in response to Arg (Figure 4- 6B). Interestingly, cell Stmn2 content was reduced in islets of diabetic mice, and further reduced after Arg stimulation (Figure 4- 6B), thereby showing a different profile from that of glucagon in diabetes.

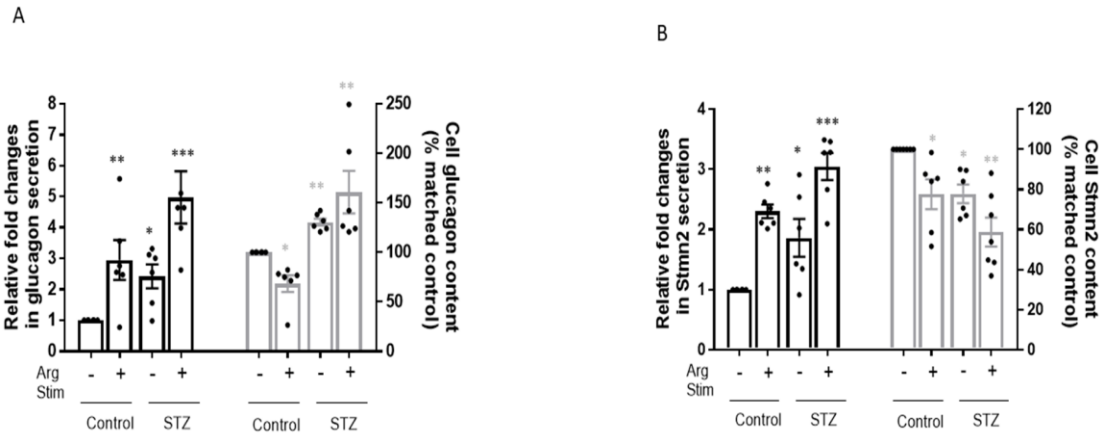

Figure 4-16. Parallel alterations in secretion of glucagon and Stmn2 from α-cells in both non-diabetic and diabetic mice. (A) Secretion of glucagon and islet glucagon content in isolated islets of non-diabetic (C; n=7) and diabetic mice (STZ; n=7) at the presence or absence of Arginine (25 mM, 20 min). Secretion values were normalized by baseline control secretion and expressed as fold changes. Glucagon contents were normalized by baseline control and expressed as percent changes. (B) Secretion of Stmn2 and islet Stmn2 content in isolated islets of non-diabetic (C; n=7) and diabetic mice (STZ; n=7) at the presence or absence of Arginine (25 mM, 20 min). Secretion values were normalized by baseline secretion in control and expressed as fold changes. Glucagon contents were normalized by baseline content in control and expressed as percent changes. Values were expressed as mean ± SEM and compared among groups by 1-Way ANOVA at α=0.05. *p<0.05; **p<0.01; ***p<0.001.

4.4.6 Trafficking of glucagon and Stmn2 to the lysosome is inhibited in islets from STZ-induced diabetic mice:

Based on our recent study that indicated a role for Stmn2 in regulating glucagon secretion by trafficking through the endolysosomal compartment in α-TC1-6 cells [187], we were interested to determine if the diabetes-induced alterations in the levels of Stmn2 and glucagon in mouse islets were due to changes in the pattern of intracellular trafficking through the endolysosomal system. We therefore determined the presence of glucagon and Stmn2 in all four compartments of the endolysosomal pathway (the recycling endosome, early endosome, late endosome and lysosome) in normal and diabetic mouse islets.

Using confocal immunofluorescence microscopy (Figure 4- 7A), we identified individual α-cells in which Lamp2A colocalized with either glucagon (Figure 4- 7B) or Stmn2

(Figure 4- 7C) in normal mouse islets. In contrast, Lamp2A did not colocalize with either glucagon or Stmn2 in individual α-cells in islets of STZ-induced diabetic mice (Figures 4- 7D-F). Quantification and analysis of colocalization showed a moderate level of colocalization between Lamp2A and glucagon (PCC 0.48±0.08) and between Lamp2A and Stmn2 (PCC 0.52±0.09) in the control group (Figure 4- 7G). In contrast, STZ - induced diabetes significantly reduced levels of colocalization between glucagon and Lamp2A (PCC 0.14±0.03; $p<0.01$) and also between Stmn2 and Lamp2A (PCC 0.15±0.03; $p<0.01$) (Figure 4- 7G).

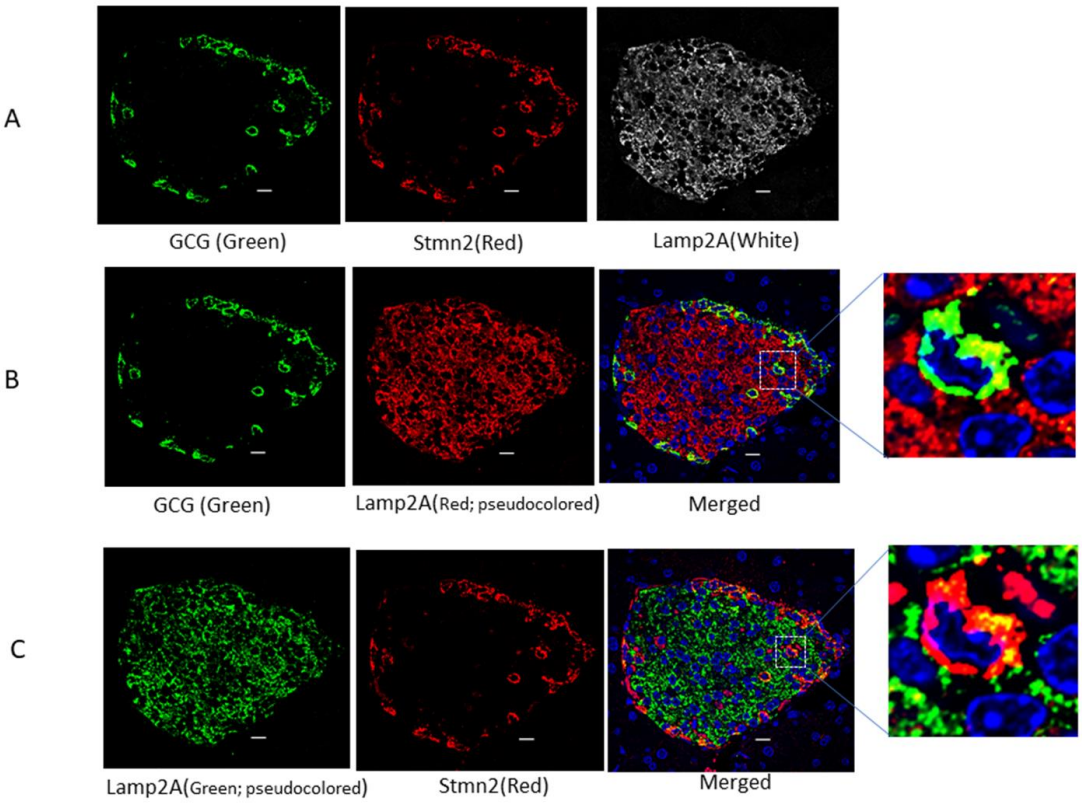

D

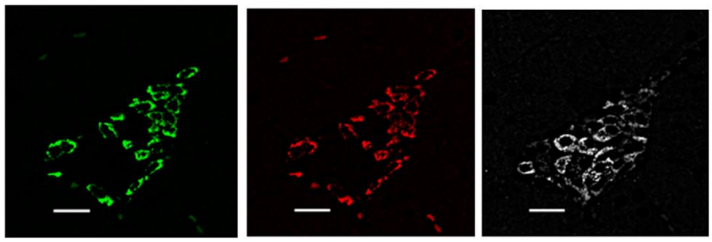
GCG (Green)
Stmn2(Red)
Lamp2A(White)

E

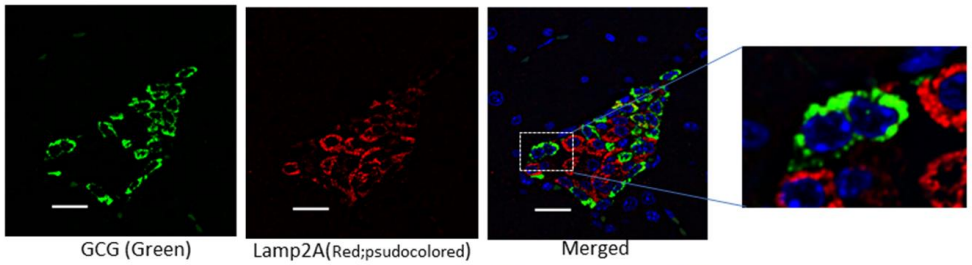
GCG (Green)
Lamp2A(Red;psudocolored)
Merged

F

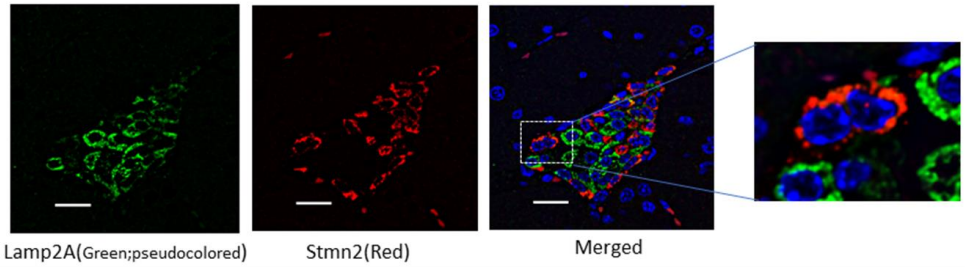
Lamp2A(Green;pseudocolored)
Stmn2(Red)
Merged

G

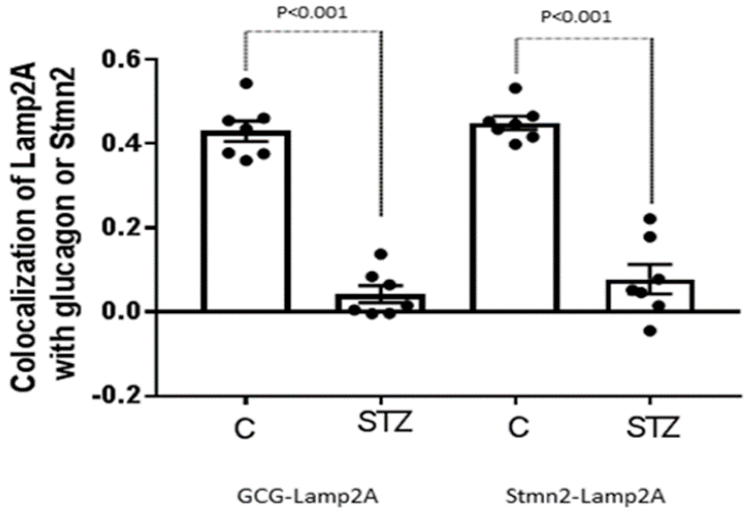
P<0.001
P<0.001
Colocalization of Lamp2A with glucagon or Stmn2
0.6
0.4
0.2
0.0
-0.2
C
STZ
C
STZ
GCG-Lamp2A
Stmn2-Lamp2A

Figure 4-19. The localization of Stmn2 and glucagon in lysosomes of α-cells is inhibited in diabetes. (A) Islets from non-diabetic mice (n=7) were immunostained with antibodies against glucagon (GCG), stathmin-2 (Stmn2) and the lysosomal marker, Lamp2A. Representative images are shown. (B) Colocalization of glucagon and Lamp2A. The Lamp2A image was pseudocoloured red for visualization of co-localization in the merged image and inset. (C) Colocalization of Stmn2 and Lamp2A. The Lamp2A image was pseudocoloured green for visualization of co-localization in the merged image and inset. (D) Islets of diabetic mice (n=7) were immunostained for glucagon, Stmn2 and Lamp2A. (E) Colocalization of glucagon and Lamp2A. The Lamp2A image was pseudocoloured red for visualization of co-localization in the merged image and inset. (F) Colocalization of Stmn2 and Lamp2A. The Lamp2A image was pseudocoloured green for visualization of co-localization in the merged image and inset. All images were acquired and post-processed as described in Methods. In each merged panel, selected areas (white square) were magnified to show individual cells within islets. (G) Analysis of colocalization of glucagon and LAMP2A, and Stmm2 and LAMP2A in normal and diabetic (STZ) islets. Pearson's correlation coefficient (PCC) values are shown as means ± SEM. Each dot represents a mean of 9-15 images per mouse.

4.4.7 STZ-induced diabetes increased the localization of Stmn2 in late endosomes

The late endosome marker, Rab7, colocalized with glucagon (Figure 4- 8B), but did not appear to colocalize with Stmn2 (Figure 4- 8C). However, following induction of diabetes, Rab7 did appear to colocalize with Stmn2 (Figure 4- 8F) and maintained

colocalization with glucagon (Figure 4- 8E). Quantification and analysis showed a moderate level of colocalization between glucagon and Rab7 in both control (PCC 0.42±0.1) and STZ-induced diabetic (PCC 0.48±0.1) mice (Figure 4- 8G). Colocalization between Stmn2 and Rab7 in the control group was weak (PCC 0.29±0.12), but significantly increased (PCC 0.48±0.09, $p<0.01$) in islets from STZ-induced diabetic mice. In addition, the fluorescence intensity of Rab7 itself increased in α cells from islets of diabetic mice (Figures 4- 8H, I), and quantification demonstrated that this increase was significant ($p<0.001$) (Figure 4- 8J). Importantly, quantification and analysis demonstrated (Figure 4- 8J) similar levels of Rab7 fluorescence intensity in α and β-cells of control mice. However, following induction of diabetes, Rab7 intensity significantly increased ($p < 0.001$) in α-cells, but not in β-cells.

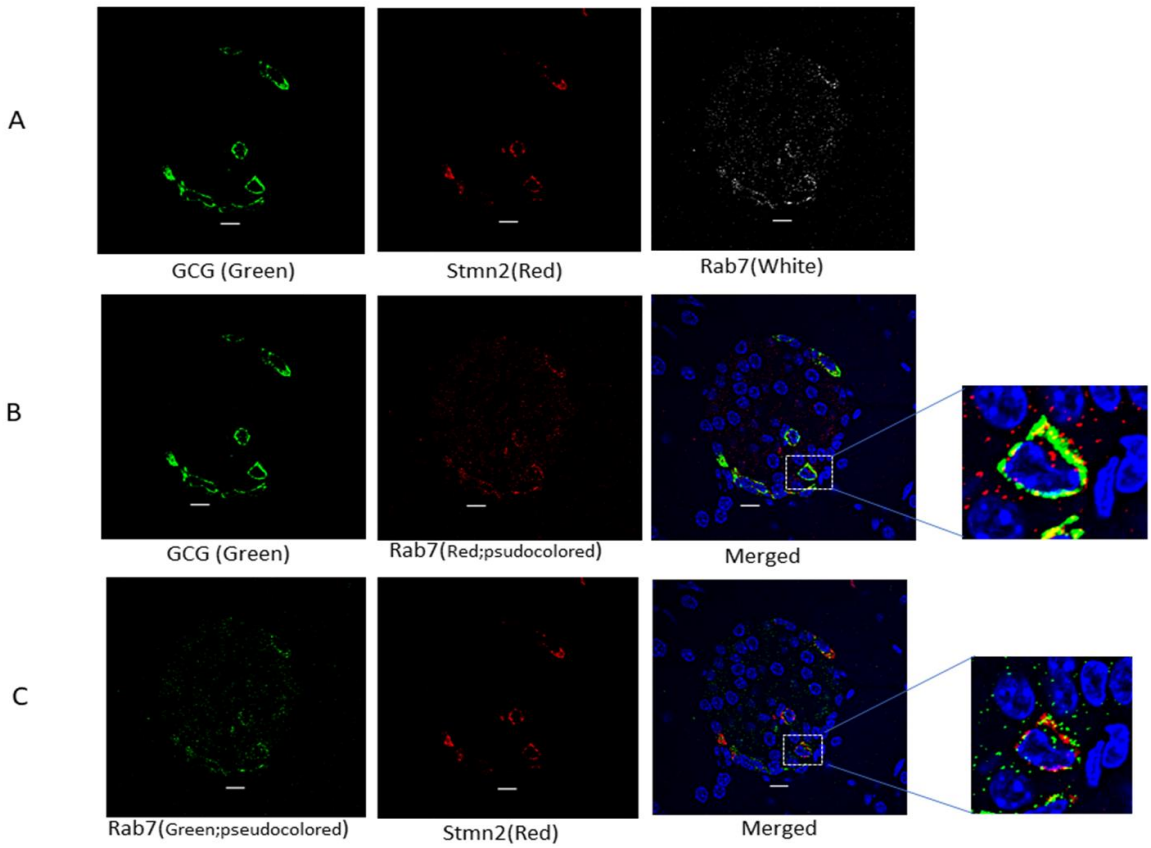

D

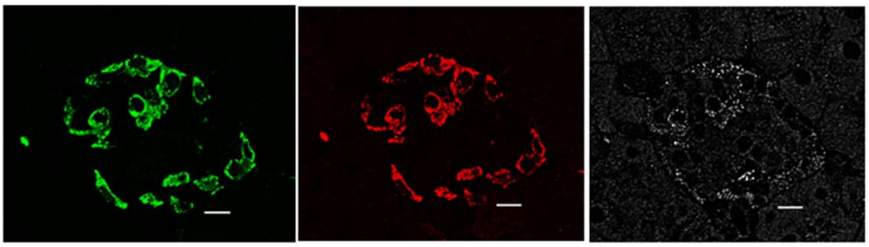
GCG (Green)
Stmn2(Red)
Rab7(White)

E

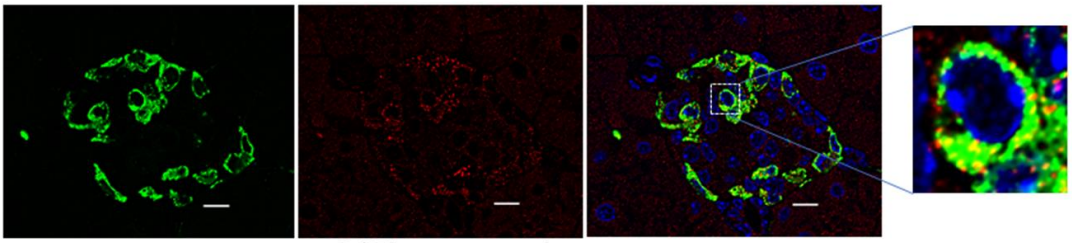
GCG (Green)
Rab7(Red;psudocolored)
Merged

F

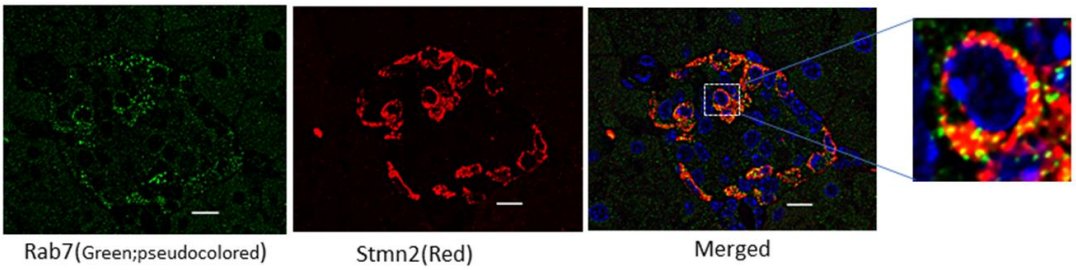
Rab7(Green;pseudocolored)
Stmn2(Red)
Merged

G

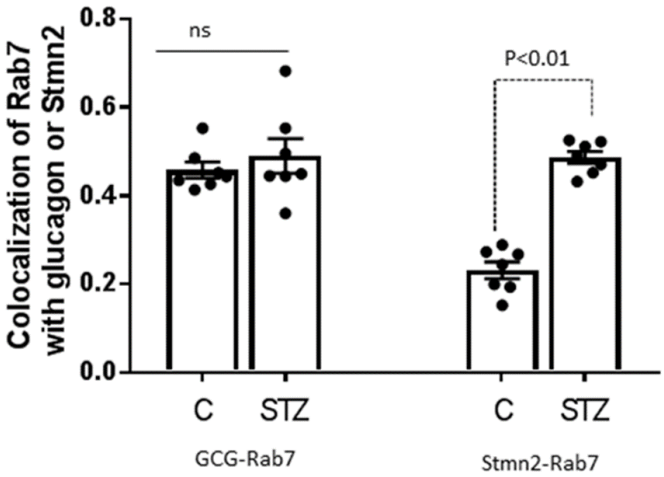
Colocalization of Rab7 with glucagon or Stmn2
0.8
0.6
0.4
0.2
0.0
ns
P<0.01
C
STZ
C
STZ
GCG-Rab7
Stmn2-Rab7

H

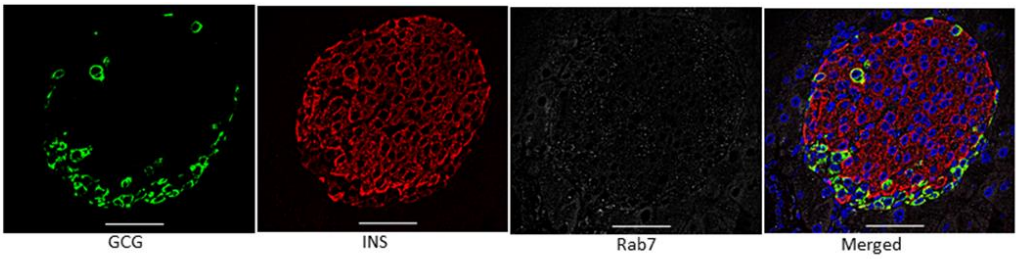
GCG
INS
Rab7
Merged

I

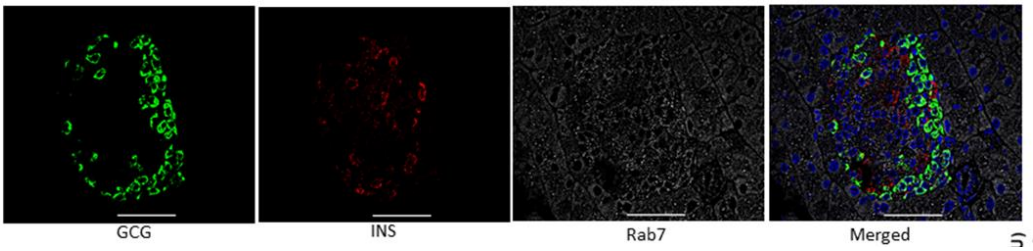
GCG
INS
Rab7
Merged

J

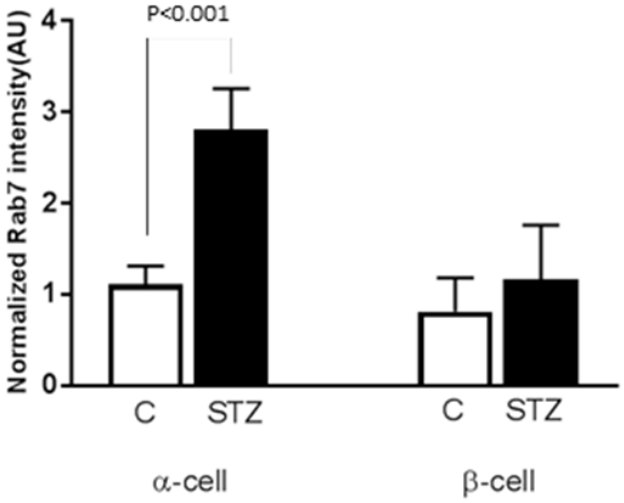
P<0.001
Normalized Rab7 intensity(AU)
0
1
2
3
4
C
STZ
C
STZ
α-cell
β-cell

Figure 4-22. Diabetes enhanced colocalization of Stmn2 with late endosome in α-cells. (A) Islets from non-diabetic mice (n=7) were immunostained with antibodies against glucagon (GCG), stathmin-2 (Stmn2) and the late endosome marker, Rab7. Representative images are shown. (B) Colocalization of glucagon and Rab7. The Rab7 image was pseudocoloured red for visualization of colocalization in the merged image and inset. (C) Colocalization of Stmn2 and Rab7. The Rab7 image was pseudocoloured green for visualization of colocalization in the merged image and inset. (D) Islets from diabetic mice (n=7) were immunostained for glucagon, Stmn2 and Rab7; (E) Colocalization of glucagon and Rab7. The Rab7 image was pseudocoloured red for visualization of colocalization in the merged image and inset. (F) Colocalization of Stmn2 and Rab7. The Rab7 image was pseudocoloured green for visualization of colocalization in the merged image and inset. All images were acquired and post-processed as described in Methods. In each merged panel, selected areas (white square) were magnified to show individual cells within islets. (G) Analysis of colocalization of glucagon and Rab7, and Stmm2 and Rab7 in normal and diabetic (STZ) islets. Pearson's correlation coefficient (PCC) values are shown as means ± SEM. Each dot represents a mean of 15 images per mouse. (H) Fluorescent intensities of glucagon, insulin (INS) and Rab7 were shown in islets from non-diabetic and (I) diabetic mice. (J) Analysis of fluorescent intensities of Rab7 in α and β-cells. Intensities of DAPI- stained nuclei were used to normalize Rab7 intensities.

4.4.8 Glucagon and Stmn2 do not localize within the early endosome

The early endosome marker, EEA1, appeared to be localized strongly to the core of the islet (Figure 4- 9A). As shown by the magnified images, EEA1 did not colocalize with either glucagon (Figure 4- 9B) or Stmn2 (Figure 4- 9C). These patterns of colocalization remained unchanged in diabetes (Figures 4- 9D-F). Quantification and analysis showed a very weak colocalization of EEA1 with glucagon (PCC 0.07±0.05) or Stmn2 (PCC 0.07±0.04) in the control group. Following induction of diabetes, colocalization of EEA1 with glucagon (PCC 0.03±0.07) or Stmn2 (PCC 0.04±0.07) still remained very weak.

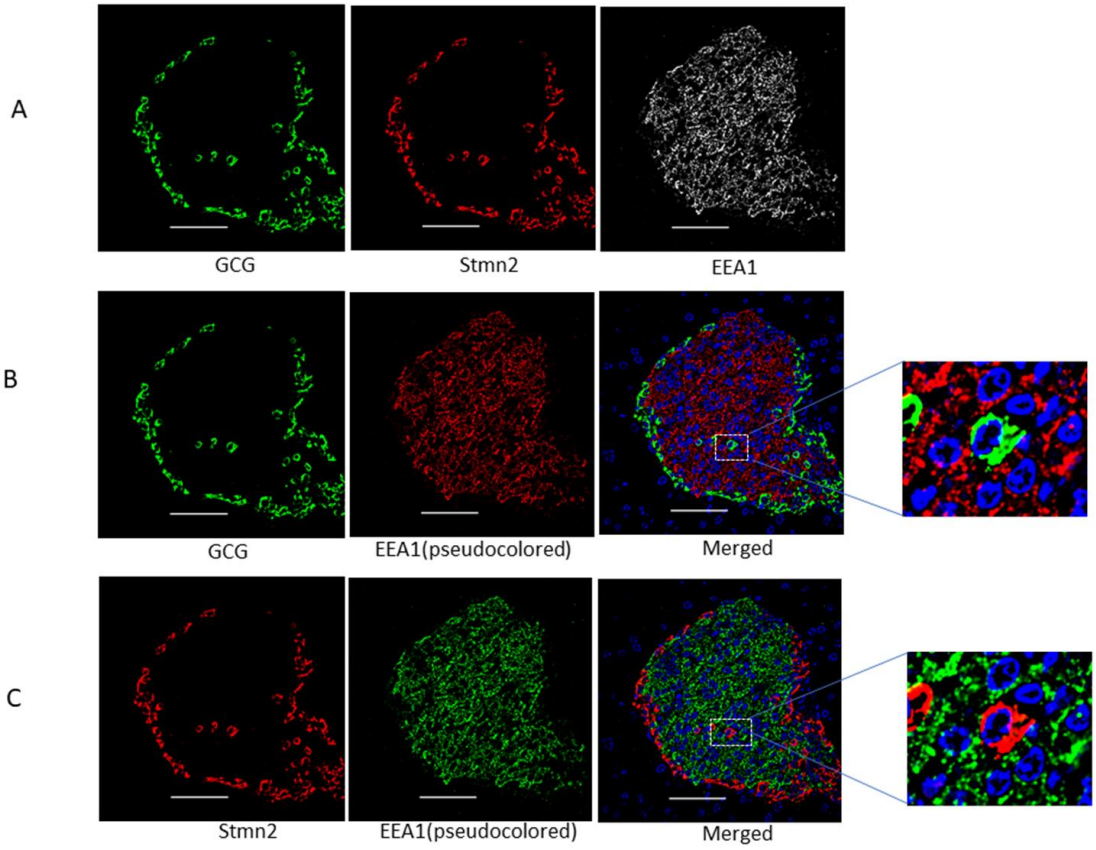

D

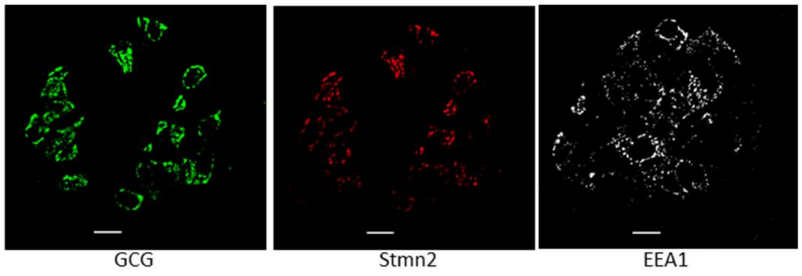
GCG
Stmn2
EEA1

E

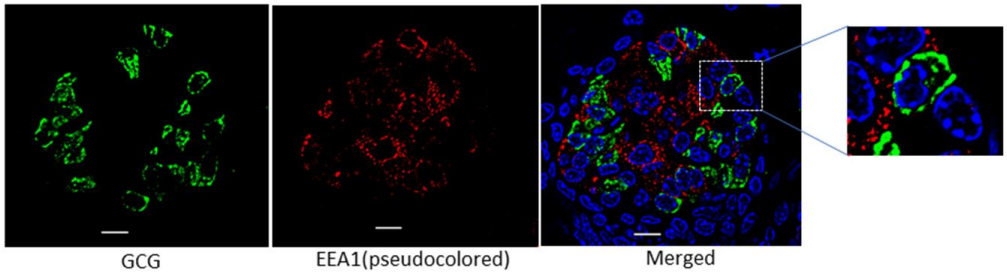
GCG
EEA1(pseudocolored)
Merged

F

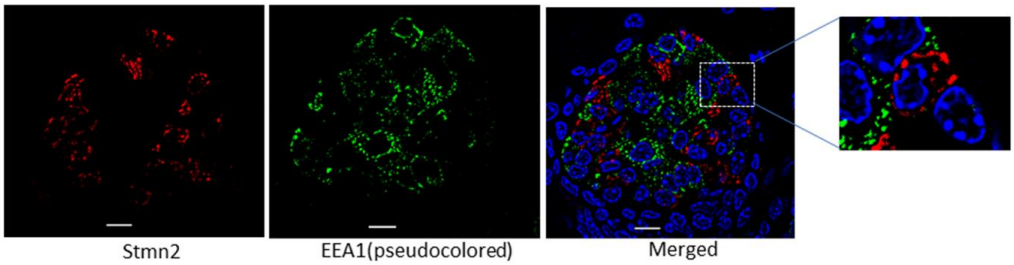
Stmn2
EEA1(pseudocolored)
Merged

G

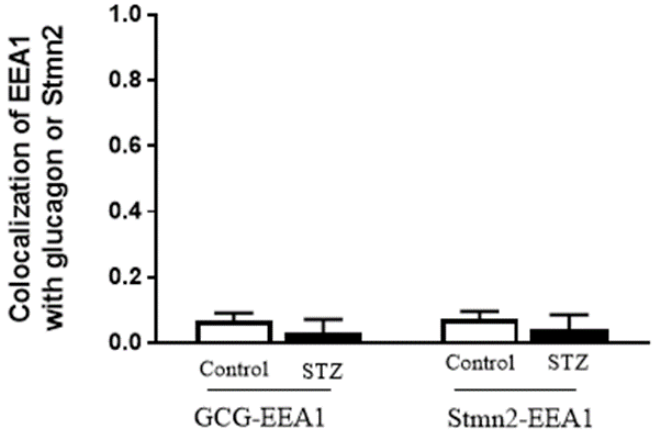
Colocalization of EEA1 with glucagon or Stmn2
1.0
0.8
0.6
0.4
0.2
0.0
Control
STZ
Control
STZ
GCG-EEA1
Stmn2-EEA1

Figure 4-25. Glucagon and stathmin-2 are not localized in early endosomes in α-cells. (A) Islets from non-diabetic mice (n=7) were immunostained with antibodies against glucagon (GCG), stathmin-2 (Stmn2) and the early endosome marker, EEA1. Representative images are shown. (B) Colocalization of glucagon and EEA1. The EEA1 image was pseudocoloured red for visualization of colocalization in the merged image and inset. (C) Colocalization of Stmn2 and EEA1. The EEA1 image was pseudocoloured green for visualization of colocalization in the merged image and inset. (D) Islets from diabetic mice (n=7) were immunostained for glucagon, Stmn2 and EEA1. (E) Colocalization of glucagon and EEA1. The EEA1 image was pseudocoloured red for visualization of colocalization in the merged image and inset. (F) Colocalization of Stmn2 and EEA1. The EEA1 image was pseudocoloured green for visualization of colocalization in the merged image and inset. All images were acquired and post-processed as described in Methods. In each merged panel, selected areas (white square) were magnified to show individual cells within islets. (G) Analysis of colocalization of glucagon and EEA1, and Stmm2 and EEA1 in normal and diabetic (STZ) islets. Pearson's correlation coefficient (PCC) values are shown as means ± SEM. Each dot represents a mean of 9-15 images per mouse.

4.4.9 Glucagon is not present in recycling endosome

The immunofluorescence signal of the recycling endosome marker, Rab11A, also appeared to be quite strong in the core of the islet (Figure 4- 10A), and did not colocalize with glucagon (Figure 4- 10B), but colocalized with insulin (Figure 4- 10C). As well, STZ-induced diabetes did not alter the pattern of distribution between Rab11A and glucagon (Figure 4- 10D), but did decrease the colocalization between insulin and Rab11A (Figures 4- 10D-F). In addition, another recycling endosome marker, Rab11B, showed a similar distribution within the islet (Figure 4- 10 G); it also did not colocalize with glucagon (Figure 4- 10H) but colocalized with insulin (Figure 4- 10I); this pattern remained unchanged in diabetes (Figures 4- 10K, L). Quantification and analysis (Figure

4- 10M) confirmed the weak colocalization between glucagon and Rab11A (PCC 0.13±0.05) or Rab11B (PCC 0.13±0.04) in non-diabetic mice, and in diabetic mice (colocalization of glucagon with Rab11A, PCC 0.13±0.04 or Rab11B, PCC 0.13±0.03). In contrast, insulin showed a strong colocalization with Rab11A (PCC 0.63±0.09) or Rab11B (PCC 0.61±0.06), which significantly decreased ($p<0.001$) following induction of diabetes (colocalization of insulin with Rab11A, PCC 0.35±0.5) or Rab11B, PCC 0.38±0.07).

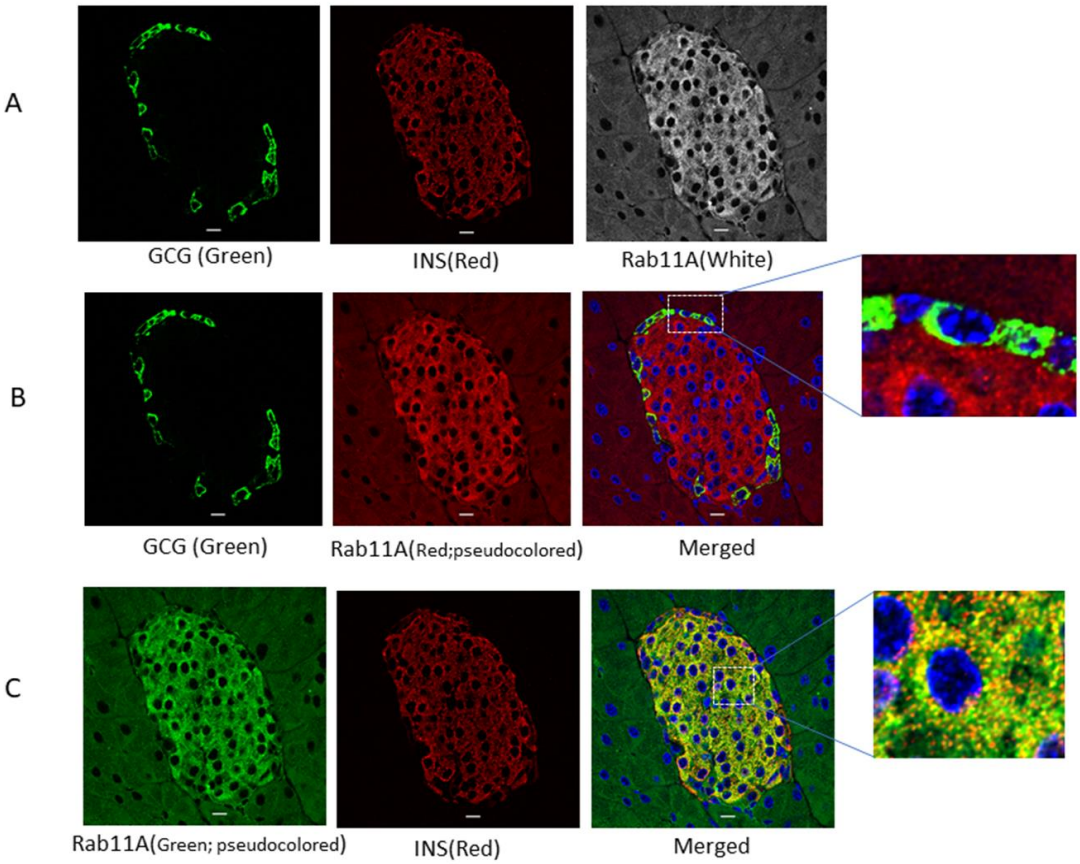

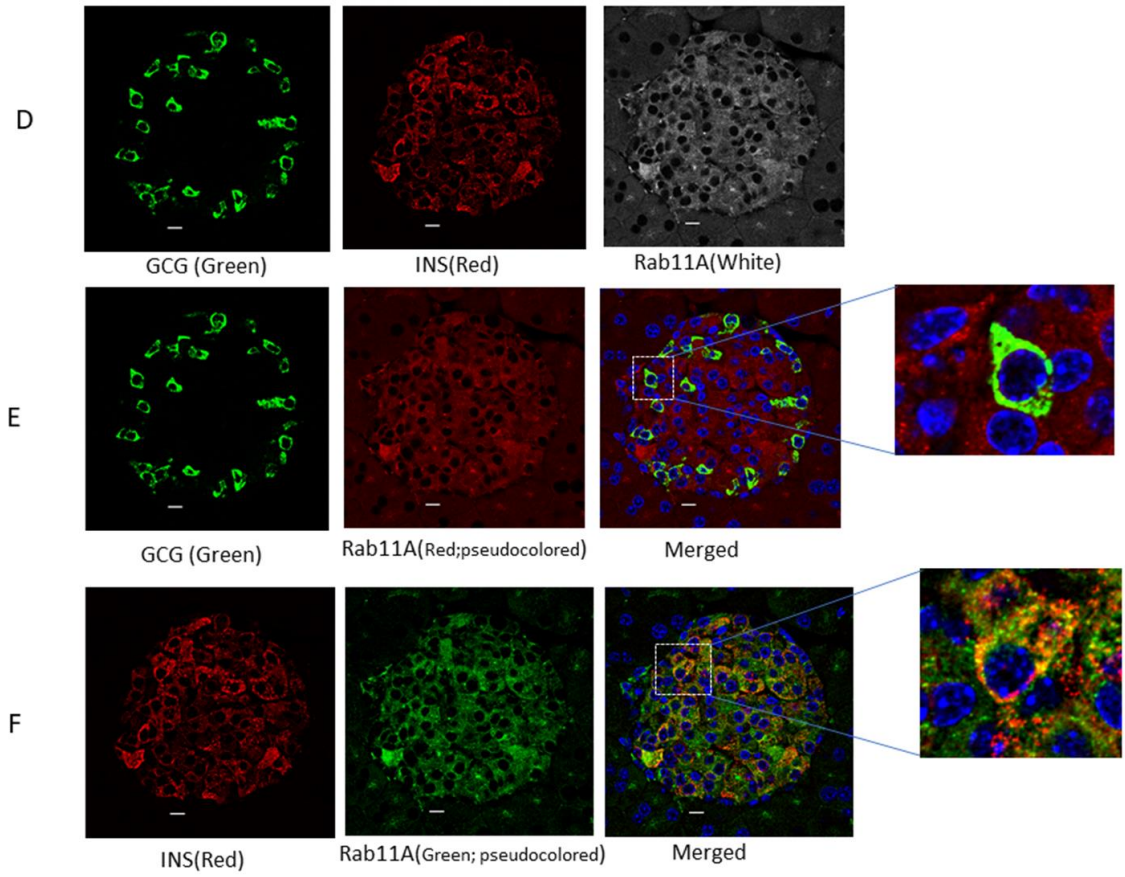
D
GCG (Green)
INS(Red)
Rab11A(White)
E
GCG (Green)
Rab11A(Red;pseudocolored)
Merged
F
INS(Red)
Rab11A(Green; pseudocolored)
Merged

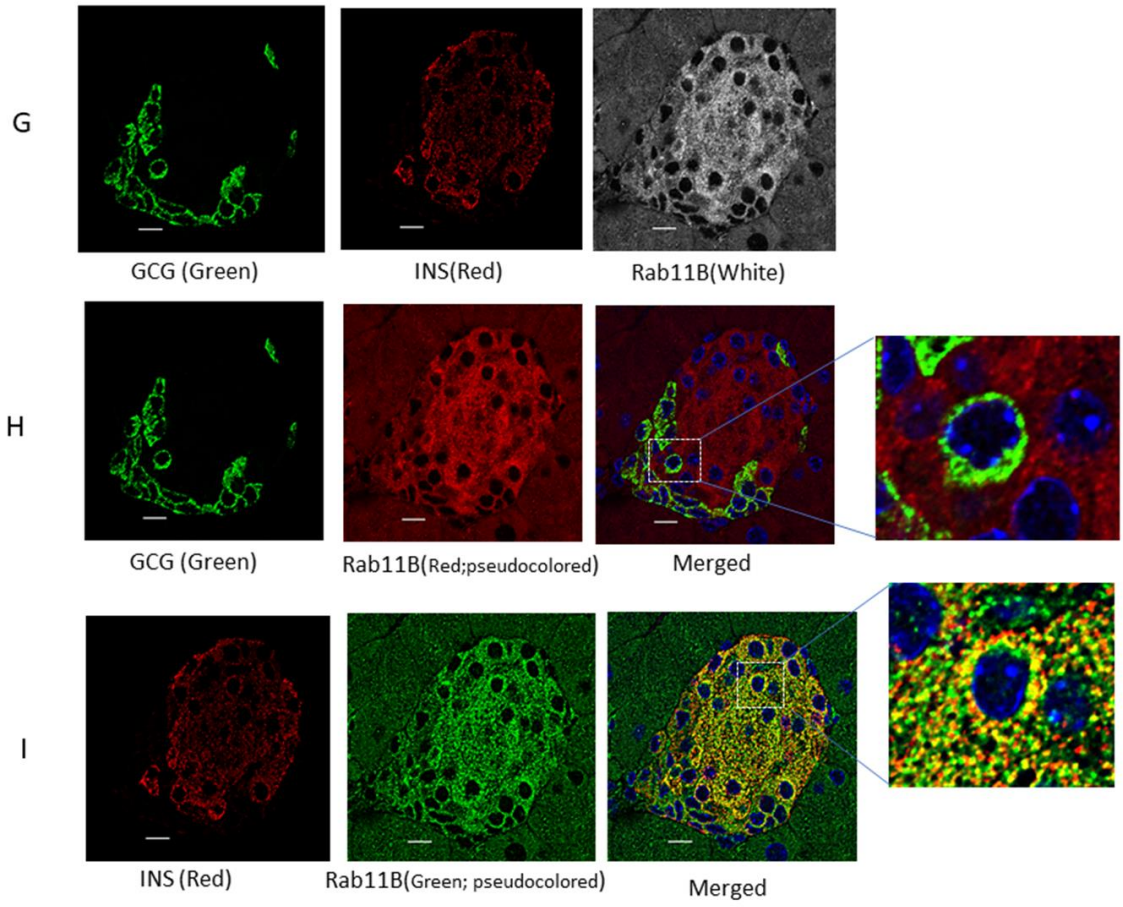
G
GCG (Green)
INS(Red)
Rab11B(White)
H
GCG (Green)
Rab11B(Red;pseudocolored)
Merged
I
INS (Red)
Rab11B(Green; pseudocolored)
Merged

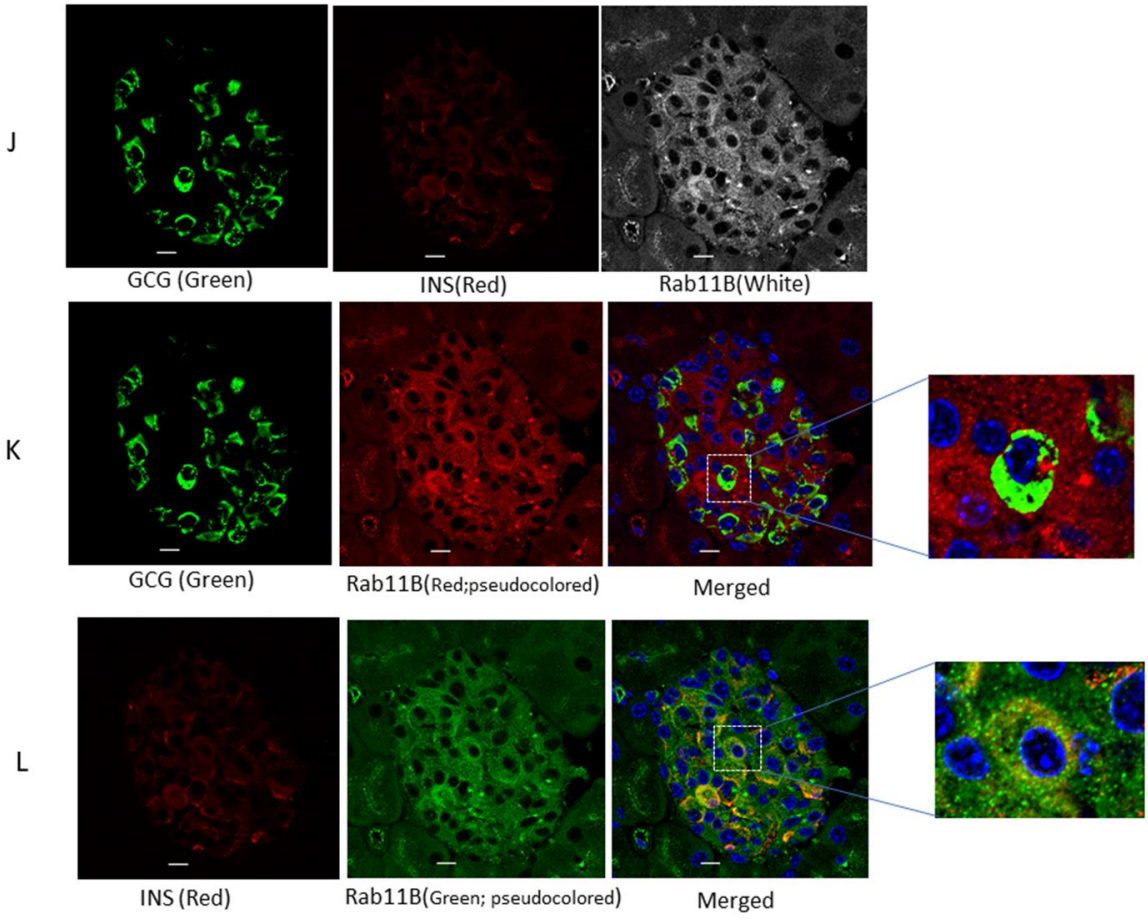
J
GCG (Green)
INS(Red)
Rab11B(White)
K
GCG (Green)
Rab11B(Red;pseudocolored)
Merged
L
INS (Red)
Rab11B(Green; pseudocolored)
Merged

M

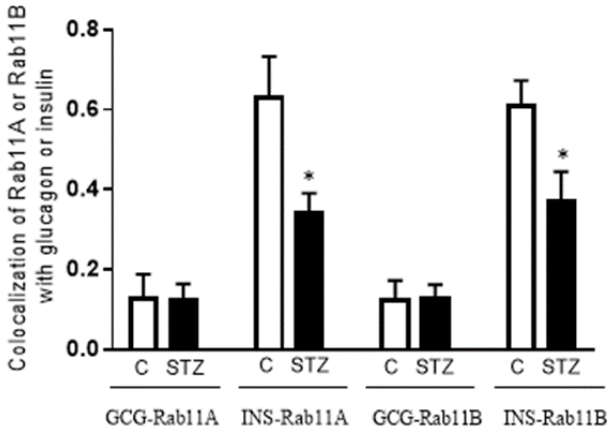
Colocalization of Rab11A or Rab11B with glucagon or insulin
0.8
0.6
0.4
0.2
0.0
C STZ
C STZ
C STZ
C STZ
GCG-Rab11A
INS-Rab11A
GCG-Rab11B
INS-Rab11B

Figure 4-28. Glucagon is not localized in recycling endosome of α-cells. (A) Islets from non-diabetic mice (n=7) were immunostained with antibodies against glucagon (GCG), insulin (INS) and the recycling endosome marker, Rab11A. (B) Colocalization of glucagon and Rab11A. The Rab11A image was pseudocoloured red for visualization of colocalization in the merged image and inset. (C) Colocalization of insulin and Rab11A. The Rab11A image was pseudocoloured green for visualization of colocalization in the merged image and inset. (D) Islets from diabetic mice (n=7) were immunostained for glucagon, insulin and Rab11A. (E) Colocalization of glucagon and Rab11A. The Rab11A image was pseudocoloured red for visualization of colocalization in the merged image and inset. (F) Colocalization of insulin and Rab11A. The Rab11A image was pseudocoloured green for visualization of colocalization in the merged image and inset. (G) Islets from non-diabetic mice were immunostained for glucagon, insulin and Rab11B. (H) Colocalization of glucagon and Rab11B. The Rab11B image was pseudocoloured red for visualization of colocalization in the merged image and inset. (I) Colocalization of insulin and Rab11B. The Rab11B image was pseudocoloured green for visualization of colocalization in the merged image and inset. (J) Islets from diabetic mice were immunostained for glucagon, insulin and Rab11B. (K) Colocalization of glucagon and Rab11B. The Rab11B image was pseudocoloured red for visualization of colocalization in the merged image and inset. (L) Colocalization of insulin and Rab11B. The Rab11B image was pseudocoloured green for visualization of colocalization in the merged image and inset. All images were acquired and post-processed as described in Methods. In each merged panel, selected areas (white square) were magnified to show individual cells within islets. (M) Analysis of colocalization of glucagon and Rab11A or Rab11B, and Stmm2 and Rab11A or Rab11B in normal and diabetic (STZ) islets. Pearson's correlation coefficient (PCC) values are shown as means ± SEM. Each dot represents a mean of 9-15 images per mouse.

4.5 Discussion

Diabetes is always accompanied by a degree of hyperglucagonemia, which reflects dysregulated glucagon secretion from α-cells. We have recently proposed that protein components of glucagon interactome within secretory granules of α-cells may regulate glucagon secretion (19) and one of these proteins, Stmn2, may mediate glucagon secretion through the endolysosomal system in α-TC1-6 cells and islets from non-diabetic mice (20). In the present study, we show that in diabetes, there is a disruption in the ratio of glucagon:Stmn2 together with hyperglucagonemia. These phenomena were accompanied by a sharp reduction in the trafficking of both glucagon and Stmn2 into the lysosome, and increased localization of Stmn2 within the late endosome, but not in the early or recycling endosomal compartment. We propose that, in diabetic α-cells, glucagon hypersecretion may result from a loss of Stmn2-mediated trafficking of glucagon to the lysosomal pathway.

In non-diabetic α-cells, glucagon secretion is regulated by several factors (29) mainly nutritional elements, such as glucose, amino acids and free fatty acids (2,12,30–33), neuronal effectors, such as norepinephrine and acetylcholine (12,34), and hormonal stimuli, particularly through paracrine regulation by insulin and somatostatin, and autocrine regulation by glucagon itself) (12,35–39). Diabetes disrupts this fine regulation, resulting in glucagon hypersecretion and aggravation of hyperglycemia. Most notably, alterations in the paracrine control of glucagon secretion by insulin results in an abnormal α-cell response to high glucose concentrations, either through insulin deficiency (40,41) or α cell insulin resistance(41,42). Additionally, impairments in hepatic amino acid turnover increases glucagon secretion from α-cells through the liver-α-cell axis (43,44). As well, higher secreted glucagon and concomitantly co-secreted glutamate from diabetic α-cells exacerbate glucagon hypersecretion in an autocrine manner (45).

The search for novel regulators of glucagon secretion has revealed that proteins associated with the α-cell secretory pathway may also comprise mechanisms that underlie hyperglucagonemia. Exposure of α-TC1-6 cells to chronically high glucose concentrations resulted in an up-regulation of several secretory granule proteins,

including processing enzymes, chromogranins and exocytotic proteins (18), indicating that many components of the α-cell secretory pathway play a role in glucagon hypersecretion in diabetes. Secretory granule proteomics in α-TC1-6 cells revealed several proteins predicted to associate with glucagon as possible mediators of glucagon secretion (19), and our recent work has shown that Stmn2 may be one such novel regulator (20). Knockdown of Stmn2 enhanced glucagon secretion from α-TC1-6 cells, indicating that Stmn2 could be a negative regulator of glucagon secretion. Our present results demonstrating a reduction in Stmn2 cell content in diabetes concomitantly with glucagon hypersecretion are consistent with these results. A similar database search has shown that another granule protein, brefeldin A-inhibited guanine nucleotide exchange protein 3 or BIG3, also regulated glucagon secretion from mouse pancreatic islets, and its depletion *in vivo* resulted in glucagon hypersecretion (46), possibly through promoting secretory granule biogenesis or maturation. Therefore, proteins within the α-cell secretory pathway are emerging as prominent regulators of glucagon secretion by mediating the intracellular trafficking of glucagon, and may explain dysregulated glucagon hypersecretion in diabetes.

In the present study, we observed that the relationship between glucagon and Stmn2 was disrupted, indicated by increased glucagon and decreased Stmn2 cell content. Proglucagon gene transcription, glucagon synthesis and secretion are all highly responsive to prevailing glucose concentrations (18,47–49), reflecting the hyperglucagonemic state of diabetes. However, it appears that Stmn2 mRNA and protein levels show a different profile. A BLAST search of the promoter region of the *Stmn2* gene (GeneBank: AH000817 ; mouse *Stmn2* complete cds) against sequence of the glucose response element in the mouse glucagon receptor gene (50) (GeneBank: AF229079.1; mouse *Gcgr* complete cds), did not reveal any sequence homology. Thus, the enhanced secretion of Stmn2 in diabetes may reflect its localization in secretory granules, which may be elevated in number and exocytotic activity in hyperglucagonemia (48), or an increase in α-cell mass(5,51).

The altered balance between glucagon and Stmn2 has also been found in islets from patients with diabetes. By means of α-cell RNA sequencing analysis, Lawlor et al (2017)

showed a higher *Gcg*: *Stmn2* gene expression ratio in islets of people with type 2 diabetes compared to healthy controls (52). Since there are many other metabolic disturbances in diabetes as described above, those results, along with ours, suggest that Stmn2 gene and protein expression levels within α-cells do not show parallel behavior with glucagon over chronic disruptions in metabolism.

Since Stmn2 within the α-cell appears to persist within secretory granules in diabetes, and does not show the same dynamics as glucagon in diabetes, we reasoned that changes in its intracellular trafficking may be a mechanism of glucagon hypersecretion. In our previous study, we showed that overexpression of Stmn2 in α-TC1-6 cells suppressed glucagon secretion by increasing its trafficking through the endolysosomal pathway (20). Conversely, knockdown of Stmn2 increased glucagon secretion and decreased its localization in endosomes and lysosomes. In the present study, we explored the dynamics of glucagon and Stmn2 trafficking in the endolysosomal pathway as a possible mechanism of glucagon hypersecretion in diabetes.

The endolysosomal system is comprised of lysosomes, late endosomes, early endosomes and recycling endosomes (53). In the context of dynamic movements of cargos within the endolysosomal system, late endosome cargos can be transported to the lysosome (anterograde) or the plasma membrane (retrograde). Retrograde transport can occur in two ways: *1)* to the early endosome, recycling endosome and then the plasma membrane, or *2)* to the Golgi apparatus and through the secretory pathway (54,55). The dramatic decrease in localization of glucagon and Stmn2 in lysosomes and increased localization of Stmn2 in the late endosomal compartment, together with Rab7, in diabetes suggest that glucagon and Stmn2 are re-routed from anterograde transport to the lysosome to retrograde transport to the late endosome and the secretory pathway. This pathway is further confirmed by the lack of glucagon and Stmn2 localization in early endosomes and recycling endosomes, suggesting that retrograde transport from the late endosome towards the early endosome-recycling endosome is not prominent in α-cells. Therefore, increased retrograde trafficking of glucagon from the late endosome to the secretory pathway may be a potential new pathway of glucagon hypersecretion in diabetes. Although a mechanism has not been investigated in this study, it is possible that Rab7, a

member of the Rab family of GTPase endosomal trafficking proteins, interacts with the retromer complex in this retrograde transport in α-cells (56–58). Retrograde transport of proteins from endosomes to the TGN has been documented for some proteins such as the acid hydrolase cathespsin D and its sorting receptor, mannose-6-phosphate receptor (M6PR), transmembrane enzymes and SNAREs (59,60). It has been suggested that Rab7 may act as a master regulator of multiple endosomal processes, functioning in retrograde transport throughout the process of endosome maturation(61) Our findings showing higher fluorescence intensity of Rab7 together with increased co-localization with Stmn2 in diabetic α-cells suggests increased recruitment of Stmn2 a potential sorting protein, into the late endosome to facilitate movement of glucagon towards TGN and secretory pathway for glucagon hypersecretion.

It is well documented that Rab proteins can impact the regulated secretory pathway through direct effects on secretory granules. The early endosomal protein Rab5 regulates homotypic fusion of mast cell secretory granules prior to compound exocytosis (62) and transports CD63 from early endosomes to secretory granules to promote granule maturation (63). A more recent study has shown that trafficking proteins from early endosomes are required for secretory granule maturation in Drosophila larval salivary gland cells (64). However, our study did not reveal a role for early endosomes in diabetes-induced glucagon hypersecretion; rather, we suggest that there is a possible role for late endosomes in the transport of glucagon to the secretory pathway. Interestingly, it has been found that, in pancreatic β-cells, there is an increase in insulin trafficking to the lysosome in diabetic *ob/ob* mice (22), and a very recent study has determined a role for the Rab7-interacting lysosomal protein RILP in the transport of insulin from secretory granules to late endosomes and lysosomes for degradation in diabetes (65). Therefore, it is tempting to speculate that, in diabetes, insulin is directed to lysosomes from granules for degradation and glucagon is transported from late endosomes to granules for enhanced secretion via the action of endosomal trafficking proteins.

In conclusion, our findings suggest that Stmn2 as an α-cell protein plays a potential role in the abnormal intracellular glucagon trafficking in diabetes. We propose that there is a switch from anterograde transport of glucagon and Stmn2 from endosomes to lysosomes,

to retrograde transport of glucagon from late endosomes to the secretory pathway. These findings suggest a potentially novel pathway that could account for the hyperglucagonemia of diabetes.

Acknowledgement: We would like to thank Ms. Karen Nygard and Mr. Reza Khazaee at Biotron Experimental Research Center, Western University for assistance with electron microscopy; Ms. Caroline O'Neil at Robarts Research Institute, Western University for tissue sample sectioning.

4.6 References

1. Unger RH, Cherrington AD. Glucagonocentric restructuring of diabetes: A pathophysiologic and therapeutic makeover. *J Clin Invest* (2012) **122**:4–12. doi:10.1172/JCI60016

2. Salehi A, Vieira E, Gylfe E. Paradoxical stimulation of glucagon secretion by high glucose concentrations. *Diabetes* (2006) **55**:2318–2323. doi:10.2337/db06-0080

3. Honzawa N, Fujimoto K, Kitamura T. Cell autonomous dysfunction and insulin resistance in pancreatic α cells. *Int J Mol Sci* (2019) **20**: doi:10.3390/ijms20153699

4. DJ Drucker. Mechanisms of action and therapeutic application of glucagon-like peptide-1. *Cell Metab* (2018) **27**:740–456. doi:10.1016/j.cmet.2018.03.001

5. Feng AL, Xiang Y, Gui L, Kaltsidis G, Feng Q, Lu W. Paracrine GABA and insulin regulate pancreatic alpha cell proliferation in a mouse model of type 1 diabetes. *Diabetologia* (2017) **60**:1033–1042. doi:10.1007/s00125-017-4239-x

6. Rorsman P, Berggren P, Bokvist K, Ericson H, Möhler H, Ostenson C, et al. Glucose-inhibition of glucagon secretion involves activation of GABAA-receptor chloride channels. *Nature* (1989) **341**:233–236. doi:10.1038/341233a0

7. Gasbjerg LS, Gabe MBN, Hartmann B, Christensen MB, Knop FK, Holst JJ,

Rosenkilde MM. Glucose-dependent insulinotropic polypeptide (GIP) receptor antagonists as anti-diabetic agents. *Peptides* (2018) **100**:173–181. doi:10.1016/j.peptides.2017.11.021

8. Kawamori D, Kurpad AJ, Hu J, Liew CW, Shih JL, Ford EL, et al. Insulin signaling in α-cells modulates glucagon secretion in vivo. *Cell Metab* (2009) **9**:350–361. doi:10.1016/j.cmet.2009.02.007.Insulin

9. Kawamori D, Kulkarni RN. Insulin modulation of glucagon secretion: the role of insulin and other factors in the regulation of glucagon secretion. *Islets* (2009) **1**:276–279. doi:10.4161/isl.1.3.9967

10. Vergari E, Knudsen JG, Ramracheya R, Salehi A, Zhang Q, Adam J, et al. Insulin inhibits glucagon release by SGLT2-induced stimulation of somatostatin secretion. *Nat Commun* (2019) **10**:1–11. doi:10.1038/s41467-018-08193-8

11. Young A. Inhibition of glucagon secretion. *Adv Pharmacol* (2005) **52**:151–71. doi:10.1016/S1054-3589(05)52008-8

12. Quesada I, Tudurí E, Ripoll C, Nadal A. Physiology of the pancreatic alpha-cell and glucagon secretion: role in glucose homeostasis and diabetes. *J Endocrinol* (2008) **199**:5–19. doi:10.1677/JOE-08-0290

13. Zhang Q, Ramracheya R, Lahmann C, Tarasov A, Bengtsson M, Braha O, et al. Role of KATP channels in glucose-regulated glucagon secretion and impaired counterregulation in type 2 diabetes. *Cell Metab* (2013) **18**:871–882. doi:10.1016/j.cmet.2013.10.014

14. Olsen HL, Theander S, Bokvist K, Buschard K, Wollheim CB, Gromada J. Glucose stimulates glucagon release in single rat α-cells by mechanisms that mirror the stimulus-secretion coupling in β-cells. *Endocrinology* (2005) **146**:4861–4870. doi:10.1210/en.2005-0800

15. MacDonald PE, De Marinis YZ, Ramracheya R, Salehi A, Ma X, Johnson PR V. A KATP channel-dependent pathway within α cells regulates glucagon release

from both rodent and human islets of langerhans. *PLoS Biol* (2007) **5**:1236–1247. doi:10.1371/journal.pbio.0050143

16. Lee YH, Wang MY, Yu XX, Unger RH. Glucagon is the key factor in the development of diabetes. *Diabetologia* (2016) **59**:1372–1375. doi:10.1007/s00125-016-3965-9

17. Wang MY, Yan H, Shi Z, Evans MR, Yu X, Lee Y, et al. Glucagon receptor antibody completely suppresses type 1 diabetes phenotype without insulin by disrupting a novel diabetogenic pathway. *Proc Natl Acad Sci U S A* (2015) **112**:2503–2508. doi:10.1073/pnas.1424934112

18. McGirr R, Ejbick CE, Carter DE, Andrews JD, Nie Y, Friedman TC, et al. Glucose dependence of the regulated secretory pathway in αTC1-6 cells. *Endocrinology* (2005) **146**:4514–4523. doi:10.1210/en.2005-0402

19. Asadi F, Dhanvantari S. Plasticity in the glucagon interactome reveals proteins that regulate glucagon secretion in alpha TC1-6 cells. *Front Endocrinol* (2019) **9**:792. doi:10.3389/fendo.2018.00792

20. Asadi F, Dhanvantari S. Stathmin-2 mediates glucagon secretion from pancreatic α-cells. *Front Endocrinol* (2020) **11**: doi:10.3389/fendo.2020.00029

21. Amherdt M, Patel YC, Orci L. Binding and internalization of somatostatin, insulin, and glucagon by cultured rat islet cells. *J Clin Invest* (1989) **84**:412–417. doi:10.1172/JCI114181

22. Pasquier A, Vivot K, Erbs E, Spiegelhalter C, Zhang Z, Aubert V, et al. Lysosomal degradation of newly formed insulin granules contributes to β cell failure in diabetes. *Nat Commun* (2019) **10**:1–14. doi:10.1038/s41467-019-11170-4

23. Guizzetti L, McGirr R, Dhanvantari S. Two dipolar alpha-helices within hormone-encoding regions of proglucagon are sorting signals to the regulated secretory pathway. *J Biol Chem* (2014) **289**:14968–14980. doi:10.1074/jbc.M114.563684

24. Aida K, Saitoh S, Nishida Y, Yokota S, Ohno S, Mao X, et al. Distinct cell clusters touching islet cells induce islet cell replication in association with over-expression of Regenerating Gene (REG) protein in fulminant type 1 diabetes. *PLoS One* (2014) **9**:1–11. doi:10.1371/journal.pone.0095110

25. Augereau C, Lemaigre FP, Jacquemin P. Extraction of high-quality RNA from pancreatic tissues for gene expression studies. *Anal Biochem* (2016) **500**:60–62. doi:10.1016/j.ab.2016.02.008

26. Li W, Zhao R, Liu J, Tian M, Lu Y, He T, Cheng M, Liang K, Li X, Wang X, et al. Small islets transplantation superiority to large ones: Implications from islet microcirculation and revascularization. *J Diabetes Res* (2014) **2014**: doi:10.1155/2014/192093

27. Li DS, Yuan YH, Tu HJ, Liang Q Le, Dail LJ. A protocol for islet isolation from mouse pancreas. *Nat Protoc* (2009) **4**:1649–1652. doi:10.1038/nprot.2009.150

28. Pisania A, Papas KK, Powers DE, Rappel MJ, Omer A, Bonner-Weir S, et al. Enumeration of islets by nuclei counting and light microscopic analysis. *Lab Investig* (2010) **90**:1676–1686. doi:10.1038/labinvest.2010.125

29. Gromada J, Franklin I, Wollheim CB. Alpha-cells of the endocrine pancreas: 35 years of research but the enigma remains. *Endocr Rev* (2007) **28**:84–116. doi:10.1210/er.2006-0007

30. Gylfe E, Gilon P. Glucose regulation of glucagon secretion. *Diabetes Res Clin Pract* (2014) **103**:1–10. doi:10.1016/j.diabres.2013.11.019

31. Ravier MA, Rutter GA. Glucose or insulin, but not zinc ions, inhibit glucagon secretion from mouse pancreatic [alpha]-cells. *Diabetes* (2005) **54**:1789–1797. doi:10.2337/diabetes.54.6.1789

32. Harp JB, Yancopoulos GD, Gromada J. Glucagon orchestrates stress-induced hyperglycaemia. *Diabetes, Obes Metab* (2016) **18**:648–653. doi:10.1111/dom.12668

33. Gromada J, Ma X, Høy M, Bokvist K, Salehi A, Berggren P, et al. ATP-sensitive K+ channel–dependent regulation of glucagon release and electrical activity by glucose in wild-type and SUR1-/- mouse alpha cells. *Diabetes* (2004) **53**:S181-189.

34. Cryer PE. Minireview: Glucagon in the pathogenesis of hypoglycemia and hyperglycemia in diabetes. *Endocrinology* (2012) **153**:1039–1048. doi:10.1210/en.2011-1499

35. Rodriguez-diaz R, Tamayo A, Hara M, Caicedo A. The local paracrine actions of the pancreatic alpha-cell. *Diabetes* (2020) **69**:550–558.

36. Briant L, Salehi A, Vergari E, Zhang Q, Rorsman P. Glucagon secretion from pancreatic α-cells. *Ups J Med Sci* (2016) **121**:113–9. doi:10.3109/03009734.2016.1156789

37. Walker JN, Ramracheya R, Zhang Q, Johnson PR V, Braun M, Rorsman P. Regulation of glucagon secretion by glucose: Paracrine, intrinsic or both? *Diabetes, Obes Metab* (2011) **13**:95–105. doi:10.1111/j.1463-1326.2011.01450.x

38. Watts M, Ha J, Kimchi O, Sherman A. Paracrine regulation of glucagon secretion : the β/α/δ model model. *Am J Physiol Endocrinol Metab* (2016) **310**:E597–E611. doi:10.1152/ajpendo.00415.2015

39. Brereton MF, Vergari E, Zhang Q, Clark A. Alpha-, Delta- and PP-cells. *J Histochem Cytochem* (2015) **63**:575–591. doi:10.1369/0022155415583535

40. Lee Y, Berglund ED, Wang M, Fu X, Yu X, Charron MJ, et al. Metabolic manifestations of insulin deficiency do not occur without glucagon action. *PNAS* (2012) **109**:14972–14976. doi:10.1073/pnas.1205983109/-/DCSupplemental.www.pnas.org/cgi/doi/10.1073/pnas.1205983109

41. Gilon P. The role of alpha-cells in islet function and glucose homeostasis in health and type 2 diabetes. *J Mol Biol* (2020) **432**:1367–1394. doi:10.1016/j.jmb.2020.01.004

42. Lee Y, Berglund ED, Yu X, Wang M, Evans MR, Scherer PE. Hyperglycemia in rodent models of type 2 diabetes requires insulin-resistant alpha cells. *PNAS* (2014) **111**:13217–13222. doi:10.1073/pnas.1409638111

43. Janah L, Kjeldsen S, Galsgaard KD, Winther-Sørensen M, Stojanovska E, Pedersen J, et al. Glucagon receptor signaling and glucagon resistance. *Int J Mol Sci* (2019) **20**: doi:10.3390/ijms20133314

44. Adeva-andany MM, Funcasta-calderón R, Fernández-fernández C, Castro-quintela E, Carneiro-freire N. Metabolic effects of glucagon in humans. *J Clin Transl Endocrinol* (2019) **15**:45–53. doi:10.1016/j.jcte.2018.12.005

45. Gaisano HY, MacDonald PE, Vranic M. Glucagon secretion and signaling in the development of diabetes. *Front Physiol* (2012) **3 SEP**:1–12. doi:10.3389/fphys.2012.00349

46. Li H, Liu T, Lim J, Gounko N V., Hong W, Han W. Increased biogenesis of glucagon-containing secretory granules and glucagon secretion in BIG3-knockout mice. *Mol Metab* (2015) **4**:246–242. doi:10.1016/j.molmet.2015.01.001

47. Wewer Albrechtsen NJ, Kuhre RE, Hornburg D, Jensen CZ, Hornum M, Dirksen C, et al. Circulating glucagon 1-61 regulates blood glucose by increasing insulin secretion and hepatic glucose production. *Cell Rep* (2017) **21**:1452–1460. doi:10.1016/j.celrep.2017.10.034

48. Huang YC, Rupnik MS, Karimian N, Herrera PL, Gilon P, Feng ZP, et al. In situ electrophysiological examination of pancreatic alpha cells in the streptozotocin-induced diabetes model, revealing the cellular basis of glucagon hypersecretion. *Diabetes* (2013) **62**:519–530. doi:10.2337/db11-0786

49. Dusaulcy R, Handgraaf S, Heddad-masson M, Visentin F, Vesin C, Reimann F, et al. Alpha-cell dysfunctions and molecular alterations in male insulinopenic diabetic mice are not completely corrected by insulin. *Endocrinology* (2016) **157**:536–547. doi:10.1210/en.2015-1725

50. Portois L, Maget B, Tastenoy M, Perret J, Svoboda M. Identification of a glucose response element in the promoter of the rat glucagon receptor gene. *J Biol Chem* (1999) **274**:8181–8190. doi:10.1074/jbc.274.12.8181

51. Bru-tari E, Cobo-vuilleumier N, Alonso-magdalena P, Dos RS, Marroqui L, Nada A. Pancreatic alpha-cell mass in the early-onset and advanced stage of a mouse model of experimental autoimmune diabetes. *Sci Rep* (2019) **9**:9515. doi:10.1038/s41598-019-45853-1

52. Lawlor N, George J, Bolisetty M, Kursawe R, Sun L, Sivakamasundari V et al. Single-cell transcriptomes identify human islet cell signatures and reveal cell-type – specific expression changes in type 2 diabetes. *Genome Res* (2017) **27**:208–222. doi:10.1101/gr.212720.116.Freely

53. Hu Y, Dammer EB, Ren R, Wang G. The endosomal-lysosomal system : from acidification and cargo sorting to neurodegeneration. *Transl Neurodegener* (2015) **4**:18. doi:10.1186/s40035-015-0041-1

54. Hsu VW, Bai M, Li J. Getting active: Protein sorting in endocytic recycling. *Nat Rev Mol Cell Biol* (2012) **13**:323–328. doi:10.1038/nrm3332

55. Seto ES, Bellen HJ, Lloyd TE. When cell biology meets development: Endocytic regulation of signaling pathways. *Genes Dev* (2002) **16**:1314–1336. doi:10.1101/gad.989602

56. Progida C, Bakke O. Bidirectional traffic between the Golgi and the endosomes – machineries and regulation. *J Cell Sci* (2016) **129**:3971–3982. doi:10.1242/jcs.185702

57. Pfeffer SR. Multiple routes of protein transport from endosomes to the trans Golgi network. *FEBS Lett* (2009) **583**:3811–3816. doi:10.1016/j.febslet.2009.10.075.Multiple

58. Johannes L, Popoff V. Tracing the retrograde route in protein trafficking. *Cell* (2008) **5**:1175–1187. doi:10.1016/j.cell.2008.12.009

59. Guerra F, Bucci C. Multiple Roles of the Small GTPase Rab7. *Cells* (2016) **5**:1–28. doi:10.3390/cells5030034

60. Bonifacino JS, Rojas R. Retrograde transport from endosomes to the trans -Golgi network. *Nat Rev Mol Cell Biol* (2006) **7**:568–580. doi:10.1038/nrm1985

61. Rojas R, Vlijmen T Van, Mardones GA, Prabhu Y, Rojas AL, Mohammed S, Heck AJR, Sluijs P Van Der, Bonifacino JS. Regulation of retromer recruitment to endosomes by sequential action of Rab5 and Rab7. *J Cell Biol* (2007) **183**:513–526. doi:10.1083/jcb.200804048

62. Klein O, Roded A, Zur N, Azouz NP, Pasternak O, Hirschberg K, Hammel I, Roche PA, Yatsu A, Fukuda M, et al. Rab5 is critical for SNAP23 regulated granule-granule fusion during compound exocytosis. *Sci Rep* (2017) **7**:1–14. doi:10.1038/s41598-017-15047-8

63. Azouz NP, Zur N, Efergan A, Ohbayashi N, Fukuda M, Amihai D, et al. Rab5 is a novel regulator of mast cell secretory granules: Impact on size, cargo, and exocytosis. *J Immunol* (2014) **192**:4043–4053. doi:10.4049/jimmunol.1302196

64. Ma CJ, Yang Y, Kim T, Chen CH, Polevoy G, Vissa M, et al. An early endosome – derived retrograde trafficking pathway promotes secretory granule maturation. *J Cell Biol* (2020) **219**:e201808017.

65. Zhou Y, Liu Z, Zhang S, Zhuang R, Liu H, Liu X, et al. RILP restricts insulin secretion through mediating lysosomal degradation of proinsulin. *Diabetes* (2020) **69**:67–82. doi:10.2337/db19-0086

Chapter 5

5. Discussion and Future Directions

5.1 Glucagon interactome in secretory granules of α-cells and its plasticity

It is well known that under normal physiological conditions, glucagon secretion is suppressed by high glucose, GABA and insulin (1–5). However, chronic hyperglycemia disrupts this fine regulation and results in elevated glucagon secretion (6–10). In Chapter 2, my results confirmed that chronic exposure of α-TC1-6 cells to high glucose increases both glucagon production and secretion. My proteomics findings, together with related functional studies, reflect a relationship between components of the glucagon interactome and glucagon secretion from α-cells. Changes in the microenvironmental conditions of α-cells alters the protein components of the glucagon interactome, which results in altered glucagon secretion. Proteomic analysis also revealed that the glucagon interactome contains two clusters of proteins: a histone core of proteins, previously unknown in α-cell granules, and a cytoplasmic cluster of proteins.

The protein components of the cytoplasmic cluster were altered in response to the paracrine inhibitors of glucagon secretion, GABA and insulin, and also to ambient glucose levels. These alterations were accompanied by changes in glucagon secretion. We propose that effects of either insulin or GABA, alone or in combination, on the α-cell secretory phenotype could be governed through their effects on the glucagon interactome within secretory granules.

Regarding the plasticity of cytoplasmic proteins within the glucagon interactome in response to intrinsic or paracrine effectors, our proposed mechanism expands our lab's model for sorting proglucagon into the secretory granule via sorting signals (11) and sorting receptors. To this end, several proteins were projected to have interactions with glucagon and among them some proteins are predicted to directly interact with glucagon in response to ambient glucose levels (5.5 mM or 25 mM) and presence of paracrine

effectors (GABA, INS or GABA+INS) (Figures 5- 1A-B). The formation of the glucagon interactome may begin within the immature secretory granule, and based on the "sorting by retention" theory, immature secretory granules transform into mature secretory granules. The maturation process is accompanied by protein condensation in the dense core portions of secretory granules, localization of integral proteins within the membrane of secretory granule, acidification of granule contents, and removal of some of their protein contents (12,13). This process could be accompanied by *i)* forming different types of secretory granules, which bring about plasticity in secretory granules, and *ii)* trafficking some proteins towards degradation machinery or exocytosis pathway. Currently, there is no published document to show α-cell granule subtypes or glucagon interactome in islets of animal models or humans to be able to make a matched comparison. However, in a parallel comparison with secretory granules of β-cells (14), some proteins of the glucagon interactome are well-known secretory granule proteins such as carboxypeptidase E, PC2, chromogranin A, secretogranin family, GTP-binding proteins, VAMP family, and Ras-related proteins of Rab family.

A

HGM	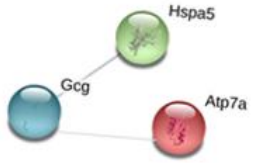
HGM+GABA	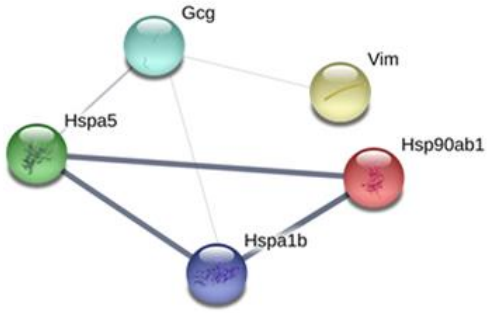
HGM+INS	
HGM+GABA+INS	

B

LGM	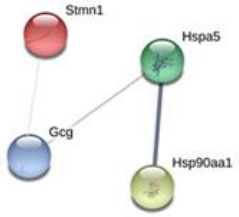
LGM+GABA	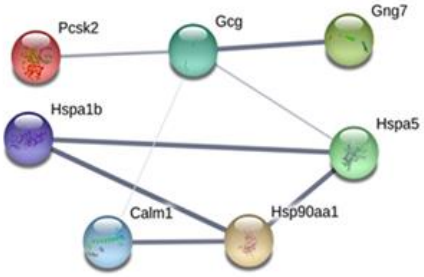
LGM+INS	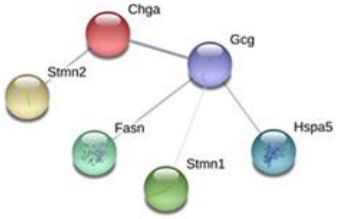
LGM+GABA+INS	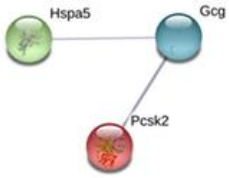

Figure 5-1. Predicted proteins in the first shell of interacting proteins with glucagon within the glucagon interactome. α-TC1-6 cells were cultured (A) in 25 mM glucose containing medium (HGM); or supplemented with GABA, insulin (INS) or GABA+INS. (B) α-TC1-6 cells were cultured (A) in 5.5 mM glucose containing medium (LGM); or supplemented with GABA, insulin (INS) or GABA+INS.

Treatment with insulin showed recruitment of ChgA into the first shell of the glucagon interactome (Figure 5- 1B). This finding supports sorting receptor role of ChgA towards secretory granule biogenesis in α-cells. Actually, special characteristics of ChgA in terms of its aggregation in low pH, and high Ca^{2+}microenvironment and also in response to catecholamine makes it a good sorting receptor candidate(15). ChgA is the main component of the secretory granules in neuroendocrine cells, and pancreatic α and β-cells (16,17). Depletion of ChgA in neuroendocrine cell line PC12 suppressed secretory granule biogenesis. In contrast, overexpression of ChgA in neuroendocrine cell line of 6T3 cells and in fibroblastic cell line of CV-1 cells, induced secretory granule biogenesis (18). It was shown that ablation of ChgA in the mouse model reduced granule size and number in the chromaffin cells of adrenal medulla (19). Anti-sense vector against ChgA in the mouse model, reduced secretory granule numbers in the chromaffin cell (20). Our lab already proposed that chromogranin A plays a potential sorting receptor for glucagon in both α-TC1-6 cells and PC12 cells (11). Thus, finding potential interaction between ChgA and Stmn2 could provide a novel protein network as a sorting receptor for granule biogenesis.

My findings showed that GRP78 (Hspa5) is present in the interactome regardless of glucose concentrations or presence of paracrine inhibitors, and co-localizes with and interacts directly with glucagon. Interestingly, its depletion suppressed cell glucagon content with no effect on glucagon secretion. This pattern reflects two potential roles for GRP78; *i)* enhancing glucagon synthesis, and *ii)* reducing glucagon degradation. Recently, it was shown that GRP78 is a component of the secretory granule in β-cells (21), which provides further evidence on presence of GRP78 within secretory granules, and its potential role in the secretory granule biogenesis, and trafficking. In terms of interaction between GRP78 and ChgA, it was shown that GRP78 interacted with a ChgA-derived peptide (pancreastatin) , which resulted in suppression of GRP78's ATPase activity. It was proposed that this interaction results in dysglycemia through increasing hepatic glycogenolysis (22). However, underlying mechanism of interaction between GRP78 and ChgA within the secretory granule of α-cells, and its physiological effect or pathological consequences remain to be elucidated.

My findings propose that plasticity in secretory granules of α-cells determine which granules can dock and fuse with the plasma membrane. It was already discussed that protein components of secretory granules play a vital role in the fusion and exocytosis of secretory granules (23). To this end, it was shown that some select proteins of secretory granules could be accelerator (such as Rabphilin3A) or inhibitor (such as Rab3A) for docking machinery of secretory granules and exocytosis (24,25). In the context of the pancreatic islet, it is well-known that all secretory granules are not functionally equivalent. About 10% of the total granule population will dock to the plasma membrane, and about 10% of those are in readily releasable pool (26,27). Granule properties are likely governed by other parameters, such as homotypic fusion (28), membrane composition (29) and composition of cargo proteins within the secretory granule. Since I found that the granule cargo is remodeled in response to glucose and paracrine effectors, it's likely that the membrane components can also be remodeled to govern exocytosis.

The proteomics analysis has also revealed a cluster of histone proteins within the glucagon interactome. Unlike the plasticity exhibited by the cytoplasmic core, the protein components of the histone cluster appeared to have small changes in treatment groups. The discovery of the histone cluster within α-cell secretory granules is novel, and supported by the finding that the cytosolic fraction in pooled islets from multiple human donors with 5 mM blood glucose had abundant amounts of the histone H2A (30). In this respect, we showed the histone H2 as the most abundant histone in secretory granules regardless of the prevailing glucose levels. We propose that the histone cluster within secretory granules in α-cells is a conserved part of the glucagon proteome in which small changes result in a significant effect on the α-cell response to different stimuli. As I have already discussed, the presence of histone proteins within secretory granules could be an adaptive mechanism in α-cells for responding to unfavorable microenvironmental conditions (31–34).

One limitation of the study in Chapter 2 was the use of the murine pancreatic islet cell line, α-TC1-6, for proteomics and glucagon secretion studies. Importantly, this well-differentiated cell line keeps normal endocrine properties of α-cells. It was shown that α-TC1 derived cell lines (α-TC1, α-TC1-6, α-TC1-9) correctly process proglucagon

towards production of matured glucagon and properly respond to stimuli especially in high glucose condition (35). This cell line has been extensively used by our lab (11,36,37) and others (38,39) for glucagon secretion studies and uncovering related molecular aspects. As well, proteomic analysis of this cell line has been used to uncover druggable targets in α-cells for clinical application (40) and its integrated proteomics-genomics has been well demonstrated (41). On the other hand, preparing sufficient amount of purified primary α-cells is a challenging subject, in a way that has been an obstacle for doing research on α-cells. Thus, this cell line has afforded advantages to perform molecular studies on several aspects of glucagon in a well-differentiated α-cell model. However, I acknowledge that using mouse primary islets or human primary islets would provide conditions closer to normal physiological conditions.

5.2 Stmn2 modulates glucagon secretion through the endolysosomal system in non-diabetic α-cells

Stathmin-2 is a neuronal protein that possesses a stathmin-like domain (SLD) and an N-terminal extension (Figure 5- 2) (42). The former contains four conserved sites for phosphorylation and the latter has three subdomains as follows; Golgi-specifying sub-domain (n), membrane anchoring subdomain (m) and a variable subdomain (c). Membrane anchoring is mediated by palmitoylation of two cysteine residues within “m” subdomain. SLD is a conserved domain, which has four phosphorylation sites and two tubule binding repeats. As a membrane-associated phosphoprotein it has been mostly found in cell membranes of Golgi and some vesicles (such as endosomes) in neuronal cells (43–45); a fact that has been recapitulated in current findings by showing localization of Stmn2 in the cell membrane and cytoplasmic organelles, Golgi and secretory granules. In terms of function, it has been shown that Stmn2 has a role in regulation of signal transduction, microtubule dynamics, and protein transport and secretion (46,47).

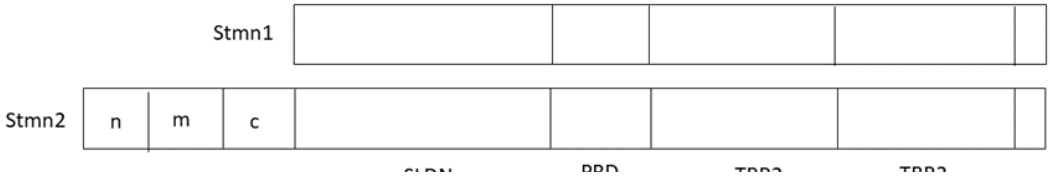

Figure 5-4. Schematic structure of Stmn2 in comparison with other members of the stathmin family. Both stathmin-1 (Stmn1) and stathmin-2 (Stmn2) contain a "stathmin-like domain" (SLD). This domain includes the following subdomains: tubulin binding repeats (TBR1 and TBR2), "Proline rich domain" (PRD), and N-terminal region of SLD (SLDN). Stmn2 contains an extra domain of N-terminal extension. This domain includes conserved Golgi-specifying subdomain "n", conserved membrane anchoring subdomain "m", and poorly conserved subdomain "c".

For the first time, my findings show the presence of Stmn2 within the α-cell secretory granule and its regulatory role in glucagon secretion. Co-presence of glucagon and Stmn2 within the secretory granule and their increased secretion in response to stimulation suggests α-cells use co-secreted secretory granule proteins as a strategy for regulation of glucagon secretion from α-cells. In this respect, co-storage and co-secretion of glucagon and glutamate have been shown in α-TC1-6 cells, rat isolated islets and mouse islets (23,48,49). It was shown that when α-cells are exposed to low glucose conditions, co-secreted glutamate plays an autocrine role in increasing glucagon secretion from α-cells (23). In addition, co-storage and co-secretion of glucagon with acetylcholine and a number of proglucagon-derived factors (such as un-processed proglucagon, proglucagon 1-61 and miniglucagon) have been reported (50–52).

Overexpression of Stmn2 in α-TC1-6 cells suppressed glucagon secretion and its depletion brought about an increase in glucagon secretion, suggesting that Stmn2 may be a tonic inhibitor of glucagon secretion. In a parallel study on β-cells, the concept of hormone-protein co-storage and co-secretion has been already documented for insulin. To this end, the regulatory role of insulin-interacting proteins [such as transmembrane protein 24

(TMEM24) carboxypeptidase E or chromogranin A] on insulin secretion has been shown in INS-1E cells, MIN6 cells and mouse pancreatic β cells (53–55). Furthermore, it was shown that co-secretion of the co-stored proteins with insulin (53,56)could be a mechanism to locally regulate insulin secretion from β-cells. For instance, ChgA or its cleaved product, betagranin, could inhibit glucose stimulated insulin secretion through binding K_{ATP} channel and keeping it in an opened state, which prevents β-cell depolarization and insulin secretion (56,57). I acknowledge that I used an immunostaining approach on fixed islets to study the subcellular status of Stmn2. To this end, making a knock-in of fluorescent reporter gene for Stmn2 in the mouse islet and its tracking using immunofluorescence confocal microscopy would uncover more details about role of Stmn2 in glucagon secretion in both normal and pathological condition.

5.3 Stmn2 plays a role in glucagon hypersecretion through intracellular glucagon trafficking towards endolysosomal system in diabetic α-cells

By tracking Stmn2 and glucagon, I have shown degradation of glucagon within the α-cell and disturbance of this pathway in the diabetic condition. My findings proposed that under normal physiological conditions, Stmn2 directs glucagon into the endolysosomal system for degradation; however, in case of diabetes it takes a role in glucagon hypersecretion from α-cells. To this end my findings propose that *1)* there is a basal level of degradation for glucagon within the endolysosomal system when there are coordinated levels of glucagon and Stmn2; *2)* this basal level of glucagon degradation will be compromised in diabetes due to discordance between glucagon and Stmn2 levels; *3)* the relatively lower Stmn2 levels reduce trafficking of glucagon and Stmn2 towards lysosome; *4)* As a consequence, the levels of glucagon and Stmn2 within the late endosome will be increased; *5)* in addition, there is an increased colocalization of Stmn2 and Rab7 within the late endosome, and 6*)* these phenomena direct glucagon towards secretory pathway, which results in higher glucagon secretion in diabetic α-cells. Thus, it can be proposed that Stmn2 could have a dual role in both the degradation and secretion of glucagon. In this context, Rab7 may interact with Stmn2 in directing glucagon towards the secretory pathway. Of note, such a dual role has been already proposed for Rab7 in β-cells (58). It has recently

been shown that insulin is degraded within the endolysosomal system of β-cells, which is mediated by interaction of Rab7 with Rab7 interacting lysosomal protein (RILP) (58). In fact, this finding highlights a previously proposed model for Rab7-mediated late endosome trafficking, in which Rab7 directs late endosome cargos towards perinuclear lysosomes for degradation or the plasma membrane for secretion (59,60)(Figure 5- 3).

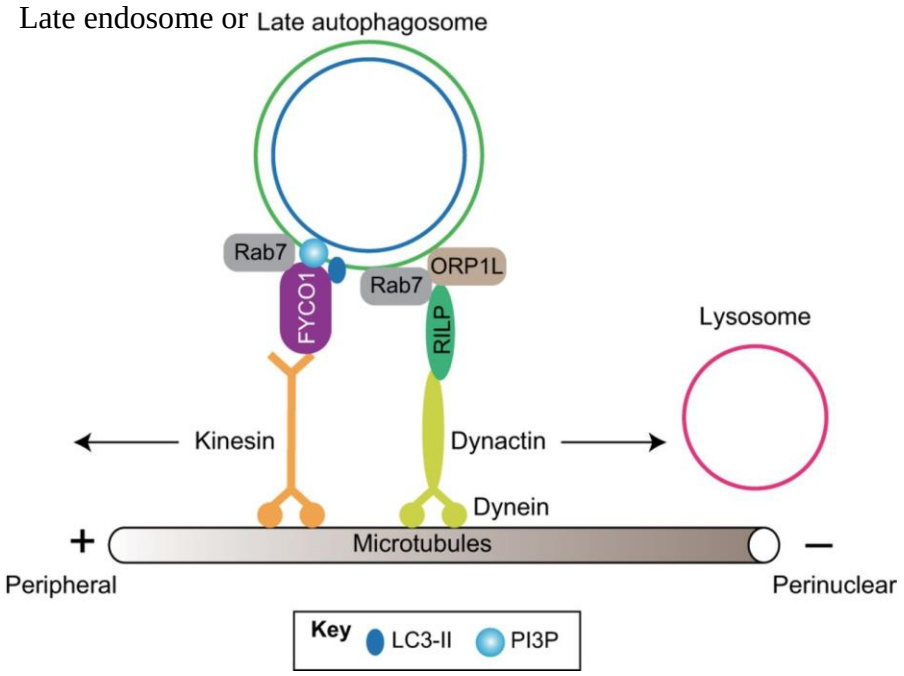

Figure 5-7. Rab7 mediates late endosomal cargos towards lysosome (for degradation) or plasma membrane (for secretion). The Figure was extracted from reference 60 according to the Creative Commons Attribution License (http://creativecommons.org/Licenses/by/4.0/).

5.4 Summary

My overall findings indicate that there is a glucagon interactome within the secretory granule that regulates glucagon secretion from α-cells. This glucagon interactome shows dynamic alterations in response to intrinsic and paracrine factors and may be a defense tactic for α-cells to cope with stressful conditions such as diabetes. In this context, recruitment of Stmn2 within the interactome could be α-cells' adaptive response to

variability in blood glucose levels. Recruitment of Stmn2 within the interactome occurred in the presence of glucagon secretion inhibitor, insulin, which was accompanied by reduced fractional glucagon secretion and cell glucagon content. It seems that Stmn2 should be considered as a regulator of glucagon secretion with bimodality roles, in a way that *1)* directing glucagon towards endolysosomal system for degradation in normal physiological condition when there is a balanced glucagon: Stmn2 ratio, and *2)* mediating glucagon hypersecretion in diabetic condition when the glucagon:Stmn2 ratio becomes imbalanced. In this respect, I suggest that coordination of Stmn2 and Rab7 plays a role in late endosomal re-routing of glucagon from lysosomal degradation towards secretory pathway (Figure 5- 4). My findings reflect that reduction in Stmn2: glucagon ratio increases glucagon secretion and an increase in this ratio suppresses glucagon secretion. In fact, it seems that α-cell contains limiting amounts of Stmn2 in the diabetic condition due to *1)* lack of response in *Stmn2* gene expression and Stmn2 synthesis to prevailing glucose levels and *2)* increased secretion of Stmn2 in diabetic condition. Thus, diabetic hyperglucagonemia may occur through increased trafficking of glucagon to the secretory pathway and decreased degradation through the lysosomal pathway mediated through an association between Stmn2 and Rab7 within the late endosome.

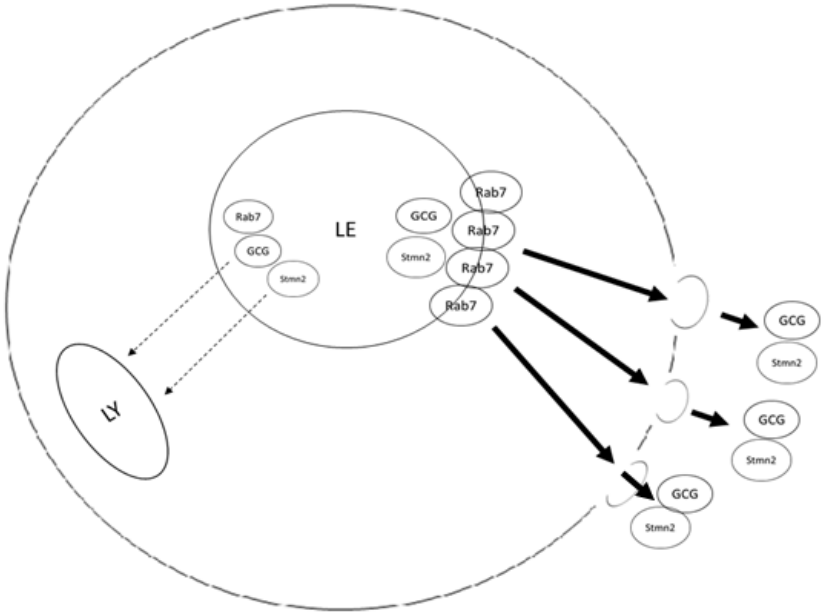

Figure 5-10. Late endosomal re-routing of glucagon and Stmn2 from lysosome towards secretory pathway in diabetic α-cells. Lysosomal degradation of glucagon and Stmn2 were suppressed. There is an enhanced Rab7 levels within the late endosome of diabetic α-cells.

5.5 Future Directions

In my thesis, I revealed a mediating role for Stmn2 in glucagon degradation through the endolysosomal system and its impairment in the diabetic condition. To further uncover role of Stmn2 in glucagon hypersecretion from diabetic α-cells the following future directions will be taken. By generating a transgenic mouse model with knock-out of Stmn2 in α-cells (for instance, through tissue specific Cre/lox system), and following glucagon secretion and intracellular glucagon trafficking in α-cells, it would complement our findings on knock down of Stmn2 in α-TC1-6 cells. In this context, by generating transgenic mouse model with knock-out of Rab7 in α-cells it would complement our findings on potential role of Rab7 in glucagon secretion. In addition, by knock- in of a fluorescent reporter gene for glucagon and inducing diabetes (through STZ injection) in the abovementioned models it would be an approach to dynamically study role of Stmn2 and Rab7 in glucagon hypersecretion. In all of the abovementioned animal models, performing glucose tolerance tests would provide more clinically related findings. As well, generating Stmn2 knock-out in a type 2 diabetic model animal and following glucagon intracellular tracking, glucagon secretion, and glucose tolerance tests would extend our knowledge on role of Stmn2 in type 2 diabetes- related glucagon hypersecretion. In addition, applying these approaches for testing potential role of other uncovered proteins in my study (ChgA or GRP78; proteins in the first shell of interaction with glucagon) could potentially introduce more candidate regulators for secretion of glucagon. As well, one option for all of abovementioned models would be studying related cell signaling pathways to Stmn2 through electrophysiological studies (patch clamp studies) on single primary α-cells. This approach would be helpful to find a key signaling pathway for Stmn2 and targeting its related elements for treatment of diabetes.

By confirming current findings through these approaches, designing a pharmacological agonist for Stmn2 would be a long-term goal to effectively reduce glucagon hypersecretion in α-cells as a potential treatment for hyperglucagonemia of diabetes.

5.6 References

1. Quesada I, Tudurí E, Ripoll C, Nadal Á. Physiology of the pancreatic α-cell and glucagon secretion: Role in glucose homeostasis and diabetes. *J Endocrinol* (2008) **199**:5–19. doi:10.1677/JOE-08-0290

2. Briant L, Salehi A, Vergari E, Zhang Q, Rorsman P. Glucagon secretion from pancreatic α-cells. *Ups J Med Sci* (2016) **121**:113–9. doi:10.3109/03009734.2016.1156789

3. Ben-Othman N, Vieira A, Courtney M, Record F, Gjernes E, Avolio F, et al. Long-term GABA administration induces alpha cell-mediated beta-like cell neogenesis. *Cell* (2017) **168**:73-85.e11. doi:10.1016/j.cell.2016.11.002

4. Walker JN, Ramracheya R, Zhang Q, Johnson PR V, Braun M, Rorsman P. Regulation of glucagon secretion by glucose: Paracrine, intrinsic or both? *Diabetes, Obes Metab* (2011) **13**:95–105. doi:10.1111/j.1463-1326.2011.01450.x

5. MacDonald PE, De Marinis YZ, Ramracheya R, Salehi A, Ma X, Johnson PR V, et al . A KATP channel-dependent pathway within α cells regulates glucagon release from both rodent and human islets of langerhans. *PLoS Biol* (2007) **5**:1236–1247. doi:10.1371/journal.pbio.0050143

6. Gromada J, Franklin I, Wollheim CB. Alpha-cells of the endocrine pancreas: 35 years of research but the enigma remains. *Endocr Rev* (2007) **28**:84–116. doi:10.1210/er.2006-0007

7. Gaisano HY, MacDonald PE, Vranic M. Glucagon secretion and signaling in the development of diabetes. *Front Physiol* (2012) **3 SEP**:1–12.

doi:10.3389/fphys.2012.00349

8. Salehi A, Vieira E, Gylfe E. Paradoxical stimulation of glucagon secretion by high glucose concentrations. *Diabetes* (2006) **55**:2318–2323. doi:10.2337/db06-0080

9. Katsura T, Kawamori D, Aida E, Matsuoka TA, Shimomura I. Glucotoxicity induces abnormal glucagon secretion through impaired insulin signaling in InR1G cells. *PLoS One* (2017) **12**: doi:10.1371/journal.pone.0176271

10. Gylfe E, Gilon P. Glucose regulation of glucagon secretion. *Diabetes Res Clin Pract* (2014) **103**:1–10. doi:10.1016/j.diabres.2013.11.019

11. Guizzetti L, McGirr R, Dhanvantari S. Two dipolar alpha-helices within hormone-encoding regions of proglucagon are sorting signals to the regulated secretory pathway. *J Biol Chem* (2014) **289**:14968–14980. doi:10.1074/jbc.M114.563684

12. Bonnemaison ML, Eipper BA, Mains RE. Role of adaptor proteins in secretory granule biogenesis and maturation. *Front Endocrinol (Lausanne)* (2013) **4**:1–17. doi:10.3389/fendo.2013.00101

13. Kuliawat R, Arvan P. Protein targeting via the "constitutive-like" secretory pathway in isolated pancreatic islets: passive sorting in the immature granule compartment. *J Cell Biol* (1992) **118**:521–529.

14. Li M, Du W, Zhou M, Zheng L, Song E, Hou J. Proteomic analysis of insulin secretory granules in INS-1 cells by protein correlation profiling. *Biophys Reports* (2018) **4**:329–338. doi:10.1007/s41048-018-0061-3

15. Morvan J, Tooze SA. Discovery and progress in our understanding of the regulated secretory pathway in neuroendocrine cells. *Histochem Cell Biol* (2008) **129**:243–252. doi:10.1007/s00418-008-0377-z

16. Stephens SB, Edwards RJ, Sadahiro M, Lin W, Jiang C, Salton SR, et al. The prohormone VGF regulates beta-cell function via insulin secretory granule biogenesis. *CellReports* (2017) **20**:2480–2489. doi:10.1016/j.celrep.2017.08.050

17. Lukinius A, Stridsberg M, Wilander E. Cellular expression and specific intragranular localization of chromogranin A , chromogranin B , and synaptophysin during ontogeny of pancreatic islet cells : An ultrastructural study. *Pancreas* (2003) **27**:38–46.

18. Kim T, Eiden LE, Loh YP. Chromogranin A , an " On / Off " switch controlling dense-core secretory granule biogenesis. *Cell* (2001) **106**:499–509.

19. Mahapatra NR, Connor DTO, Vaingankar SM, Hikim APS, Mahata M, Ray S, et al. Hypertension from targeted ablation of chromogranin A can be rescued by the human ortholog. *J Clin Invest* (2005) **115**:1942–1952. doi:10.1172/JCI24354.1942

20. Kim T, Zhang C, Sun Z, Wu H, Loh YP. Chromogranin A deficiency in transgenic mice leads to aberrant chromaffin granule biogenesis. *J Neurosci* (2005) **25**:6958–6961. doi:10.1523/JNEUROSCI.1058-05.2005

21. Vig S, Buitinga M, Rondas D, Crèvecoeur I, Van Zandvoort M, Waelkens E, et al. Cytokine-induced translocation of GRP78 to the plasma membrane triggers a pro-apoptotic feedback loop in pancreatic beta cells. *Cell Death Dis* (2019) **10**:309. doi:10.1038/s41419-019-1518-0

22. Biswas N, Friese RS, Gayen JR, Bandyopadhyay G, Mahata SK, Connor DTO. Discovery of a novel target for the dysglycemic chromogranin A fragment pancreastatin: interaction with the chaperone GRP78 to influence metabolism. *PLoS One* (2014) **9**:e84132. doi:10.1371/journal.pone.0084132

23. Cabrera O, Jacques-Silva MC, Speier S, Yang SN, Köhler M, Fachado A, et al. Glutamate is a positive autocrine signal for glucagon release. *Cell Metab* (2008) **503**:371–376. doi:10.1038/nature12598.DNMT1-interacting

24. Burgoyne RD, Morgan A. Secretory granule exocytosis. *Physiol Rev* (2003) **83**:581–632. doi:10.1152/physrev.00031.2002

25. Mizuno K, Fujita T, Gomi H, Izumi T. Granuphilin exclusively mediates functional granule docking to the plasma membrane. *Sci Rep* (2016) **6**:1–12.

doi:10.1038/srep23909

26. Weir GC, Bonner-Weir S. GABA signaling stimulates β- cell regeneration in diabetic mice. *Cell* (2017) **168**:7–9. doi:10.1016/j.cell.2016.12.006

27. Brereton MF, Vergari E, Zhang Q, Clark A. Alpha-, Delta- and PP-cells. *J Histochem Cytochem* (2015) **63**:575–591. doi:10.1369/0022155415583535

28. Wendler F, Page L, Urbe´S, Tooze SA. Homotypic fusion of immature secretory granules during maturation in a cell-free assay. *J Cell Biol* (1998) **143**:1831–1844. doi:10.1083/jcb.143.7.1831

29. Bogan, J.S., Xu, X., Hao M. Cholesterol accumulation increases insulin granule size and impairs membrane trafficking. *Traffic* (2012) **13**:1466–1480. doi:10.1111/j.1600-0854.2012.01407.x.Cholesterol

30. Schrimpe-Rutledge AC, Fontès G, Gritsenko MA, Norbeck AD, Anderson DJ, Waters KM, et al. Discovery of novel glucose-regulated proteins in isolated human pancreatic islets using LC-MS/MS-based proteomics. *J Proteome Res* (2012) **11**:3520–3532. doi:10.1021/pr3002996

31. Brinkmann V, Reichard U, Goosmann C, Fauler B, Weiss DS, Weinrauch Y, et al. Neutrophil extracellular traps kill bacteria. *Science (80-)* (2011) **303**:1532–1535.

32. Hoeksema M, Van Eijk M, Haagsman HP, Hartshorn KL. Histones as mediators of host defense, inflammation and thrombosis. *Futur Microbiol* (2016) **11**:441–453. doi:10.2217/fmb.15.151

33. Davalos AR, Coppe JP, Campisi J, Desprez PY. Senescent cells as a source of inflammatory factors for tumor progression. *Cancer Metastasis Rev* (2010) **29**:273–283. doi:10.1007/s10555-010-9220-9

34. Pacifici F, Arriga R, Sorice GP, Capuani B, Scioli MG, Pastore D, et al. Peroxiredoxin 6, a novel player in the pathogenesis of diabetes. *Diabetes* (2014) **63**:3210–3220. doi:10.2337/db14-0144

35. Powers AC, Efrat S, Mojsov S, Spector D, Habener JF, Hanahan D. Proglucagon processing similar to normal islets in pancreatic α-like cell line derived from transgenic mouse tumor. *Diabetes* (1990) **39**:406–414.

36. McGirr R, Ejbick CE, Carter DE, Andrews JD, Nie Y, Friedman TC, et al. Glucose dependence of the regulated secretory pathway in αTC1-6 cells. *Endocrinology* (2005) **146**:4514–4523. doi:10.1210/en.2005-0402

37. McGirr R, Guizzetti L, Dhanvantari S. The sorting of proglucagon to secretory granules is mediated by carboxypeptidase E and intrinsic sorting signals. *J Endocrinol* (2013) **217**:229–40. doi:10.1530/JOE-12-0468

38. Suga T, Kikuchi O, Kobayashi M, Matsui S, Yokota-Hashimoto H, Wada E, et al. SGLT1 in pancreatic α cells regulates glucagon secretion in mice, possibly explaining the distinct effects of SGLT2 inhibitors on plasma glucagon levels. *Mol Metab* (2018) doi:10.1016/j.molmet.2018.10.009

39. Sancho V, Daniele G, Lucchesi D, Lupi R, Ciccarone A, Penno G, et al. Metabolic regulation of GLP-1 and PC1/3 in pancreatic α-cell line. *PLoS One* (2017) **12**:1–12. doi:10.1371/journal.pone.0187836

40. Li J, Casteels T, Frogne T, Ingvorsen C, Honore C, Courtney M, et al. Artemisinins target GABAA receptor signaling and impair α cell identity. *Cell* (2017) **168**:86-100.e15. doi:10.1016/j.cell.2016.11.010

41. Maziarz M, Chungţ C, Drucker DJ, Emili A. Integrating global proteomic and genomic expression profiles generated from islet alpha cells: Opportunities and challenges to deriving reliable biological inferences *Mol Cell Proteomics* (2005)458–474. doi:10.1074/mcp.R500011-MCP200

42. Chauvin S, Sobel A. Neuronal stathmins: A family of phosphoproteins cooperating for neuronal development, plasticity and regeneration. *Prog Neurobiol* (2015) **126**:1–18. doi:10.1016/j.pneurobio.2014.09.002

43. Gavet O, Messari SE, Ozon S, Sobel A. Regulation and subcellular localization of

the microtubule-destabilizing stathmin family phosphoproteins in cortical neurons. *J Neurosci Res* (2002) **68**:535–550. doi:10.1002/jnr.10234

44. Gavet O, Ozon S, Manceau V, Lawler S, Curmi P, Sobel A. The stathmin phosphoprotein family: intracellular localization and effects on the microtubule network. *J Cell Sci* (1998) **111**:3333–3346.

45. Curmi PA, Gavet O, Charbaut E, Ozon S, Lachkar-Colmerauer S, Manceau V, et al. Stathmin and its phosphoprotein family: general properties, biochemical and functional interaction with tubulin. *Cell Struct Funct* (1999) **24**:345–57.

46. Wang J, Shan C, Cao W, Zhang C, Teng J, Chen J. SCG10 promotes non-amyloidogenic processing of amyloid precursor protein by facilitating its trafficking to the cell surface. *Hum Mol Genet* (2013) **22**:4888–4900. doi:10.1093/hmg/ddt339

47. Mahapatra NR, Taupenot L, Courel M, Mahata SK, O'Connor DT. The trans-golgi proteins SCLIP and SCG10 interact with chromogranin A to regulate neuroendocrine secretion. *Biochemistry* (2008) **47**:7167–7178. doi:10.1021/bi7019996

48. Hayashi M, Yamada H, Uehara S, Morimoto R, Muroyama A, Yatsushiro S, et al. Secretory granule-mediated co-secretion of L-glutamate and glucagon triggers glutamatergic signal transmission in islets of Langerhans. *J Biol Chem* (2003) **278**:1966–1974. doi:10.1074/jbc.M206758200

49. Jenstad M, Chaudhry FA. The amino acid transporters of the glutamate/GABA-glutamine cycle and their impact on insulin and glucagon secretion. *Front Endocrinol (Lausanne)* (2013) **4**:1–8. doi:10.3389/fendo.2013.00199

50. Furuta M, Carroll R, Martin S, Swift HH, Ravazzola M, Orci L, et al. Incomplete processing of proinsulin to insulin accompanied by elevation of Des-31,32 proinsulin intermediates in islets of mice lacking active PC2. *J Biol Chem* (1998) **273**:3431–3437. doi:10.1074/jbc.273.6.3431

51. Bataille D, Fontés G, Costes S, Longuet C, Dalle S. The glucagon-miniglucagon interplay: A new level in the metabolic regulation. *Ann N Y Acad Sci* (2006) **1070**:161–166. doi:10.1196/annals.1317.005

52. Wewer Albrechtsen NJ, Kuhre RE, Hornburg D, Jensen CZ, Hornum M, Dirksen C, et al. Circulating glucagon 1-61 regulates blood glucose by increasing insulin secretion and hepatic glucose production. *Cell Rep* (2017) **21**:1452–1460. doi:10.1016/j.celrep.2017.10.034

53. Pottekat A1, Becker S, Spencer KR, Yates JR 3rd, Manning G, Itkin-Ansari P BW. Insulin biosynthetic interaction network component, TMEM24, facilitates insulin reserve pool release. *Cell Rep* (2013) **4**:921–930. doi:10.1016/j.celrep.2013.07.050

54. Hutton JC. The insulin secretory granule. *Diabetologia* (1989) **32**:271–281.

55. Chu KY, Briggs MJL, Albrecht T, Drain PF, Johnson JD. Differential regulation and localization of carboxypeptidase D and carboxypeptidase E in human and mouse β-cells. *Islets* (2011) **3**:155–165. doi:10.4161/isl.3.4.15767

56. Bandyopadhyay GK, Mahata SK. Chromogranin A regulation of obesity and peripheral insulin sensitivity. *Front Endocrinol (Lausanne)* (2017) **8**:1–10. doi:10.3389/fendo.2017.00020

57. Schmid GM, Meda P, Caille D, Wargent E, O'Dowd J, Hochstrasser DF, et al. Inhibition of insulin secretion by betagranin, an N-terminal chromogranin A fragment. *J Biol Chem* (2007) **282**:12717–12724. doi:10.1074/jbc.M700788200

58. Zhou Y, Liu Z, Zhang S, Zhuang R, Liu H, Liu X, et al. RILP restricts insulin secretion through mediating lysosomal degradation of proinsulin. *Diabetes* (2020) **69**:67–82. doi:10.2337/db19-0086

59. Hyttinen JMT, Niittykoski M, Salminen A, Kaarniranta K. Maturation of autophagosomes and endosomes: A key role for Rab7. *Biochim Biophys Acta - Mol Cell Res* (2013) **1833**:503–510. doi:10.1016/j.bbamcr.2012.11.018

60. Nakamura S, Yoshimori T. New insights into autophagosome-lysosome fusion. *J Cell Sci* (2017) **130**:1209–1216. doi:10.1242/jcs.196352

6. Appendices

Western

AUP Number: 2012-020
PI Name: Dhanvantari, Savita
AUP Title: Pet Imaging Of Pancreatic Beta Cell Stress During The Progression Of Diabetes
Approval Date: 01/09/2017

Official Notice of Animal Use Subcommittee (AUS) Approval: Your new Animal Use Protocol (AUP) entitled "Pet Imaging Of Pancreatic Beta Cell Stress During The Progression Of Diabetes" has been APPROVED by the Animal Use Subcommittee of the University Council on Animal Care. This approval, although valid for four years, and is subject to annual Protocol Renewal.2012-020::5

1. This AUP number must be indicated when ordering animals for this project.
2. Animals for other projects may not be ordered under this AUP number.
3. Purchases of animals other than through this system must be cleared through the ACVS office. Health certificates will be required.

The holder of this Animal Use Protocol is responsible to ensure that all associated safety components (biosafety, radiation safety, general laboratory safety) comply with institutional safety standards and have received all necessary approvals. Please consult directly with your institutional safety officers.

7. Curriculum Vitae

Name: **Farzad Asadi Jomnani**

Post-secondary Education and Degrees:

1) **Doctor of Veterinary Medicine (DVM)**, Faculty of Veterinary Medicine, University of Tehran, Tehran, Iran (1996)
2) **Research Traineeship for completion of Ph.D program in Clinical Biochemistry**, Department of Experimental Medicine, Royal Victoria Hospital, McGill University, Montreal, Quebec, Canada (2003)
3) **Ph.D in Clinical Biochemistry**, Department of Clinical Biochemistry, School of Medicine, Tehran University of Medical Sciences, Tehran, Iran (2003)
4) **Ph.D in Pathology and Laboratory Medicine**, Department of Pathology and Laboratory Medicine, The University of Western Ontario, Ontario, Canada (2020)

Honours and Awards (Related to my current Ph.D program):

1) **Dean's Award of Excellence**, The University of Western Ontario (September 2016-August 2020), 100000 CAD (25000 CAD per year)
2) **Ontario Graduate Scholarship** (OGS), Ontario, Canada (May 2019-April 2020), 15000 CAD
3) Dr. Fredrick Winnett **Luney Graduate Scholarship**, The University of Western Ontario (March 2020), 5000 CAD
4) European Association for the Study of Diabetes **Travel Grant**, Barcelona, Spain (September 16-20, 2019), 1700 CAD
5) **Ontario Graduate Scholarship** (OGS), Ontario, Canada (September 2017-August 2018) 15000 CAD

6) European Association for the Study of Diabetes **Travel Grant**, Berlin, Germany (September 30-October 5, 2018), 1700 CAD
7) Molecular Imaging Graduate Program, The University of Western Ontario **Travel Award** (July 5, 2018), 400 CAD
8) **Best Basic Science Poster Presentation**, The University of Western Ontario (March 2017), 100 CAD
9) **Mitacs Funding**, Mitacs Canada, Currently eligible
10) **Co-Innovation,** Improved malondialdehyde (MDA) assay kit, under registration, The University of Western Ontario Innovation Park (March 2020)

Publications (related to my current Ph.D program):

1) **Asadi F.** & Dhanvantari S. 2020. Stathmin-2 mediates glucagon secretion from pancreatic α-cells. *Frontiers in Endocrinology*. 11:29, eCollection 2020
2) **Asadi F.** & Dhanvantari S. 2019. Plasticity in the glucagon interactome reveals novel proteins that regulate glucagon secretion in αTC1-6 cells. *Frontiers in Endocrinology*. 9:792, eCollection 2018
3) Taqui B. **Asadi F.** Capobianco E. Hardy DB. Jawerbaum A. & Arany E. 2020. Addition of olive oil during pregnancy in rats with mild diabetes impacts β-cell development in male adult offspring. *Journal of Endocrinology*. 246:175-187
4) **Asadi F.** & Dhanvantari S. 2020. Mediation of glucagon trafficking from the endolysosomal system towards the secretory pathway by stathmin-2 in diabetic α-cells. *Under submission*
5) **Asadi F.** & Dhanvantari S. 2019. Stathmin-2 modulate glucagon secretion from pancreatic alpha cells. EASD 55th Annual Meeting, *Barcelona, Spain*
6) **Asadi F.** & Dhanvantari S. 2018. Proteomics of secreted glucagon reveals heterogeneous complexes as novel mediators of alpha cell function. EASD 54th Annual Meeting, *Berlin, Germany*
7) **Asadi F.** & Dhanvantari S. 2018. Heterogenous glucagon-immunoreactive peptides as novel regulators of insulin secretion, London Health Research Day Conference; Pathology and Laboratory Research Day Conference. *London, Ontario, Canada*

8) **Asadi F.** & Dhanvantari S. 2017. A Novel Theory on Mechanisms of Glucagon Secretion from Pancreatic Alpha Cells, London Health Research Day Conference; Pathology and Laboratory Research Day Conference. *London, Ontario, Canada*

Related Work
Experience (related to my current Ph.D program)

1) Volunteer, **co-administrator of Confocal Microscopy** training and management, St. Joseph Hospital, London, Ontario, Canada, February 2018-2020
2) Volunteer, **scientific judge**, Thames Valley Science & Engineering Fair, London, Ontario, Canada, May 2020
3) Volunteer, **moderator of the Featured Platform Presentations**, London Health Research Day, London, Ontario, Canada, April 2019
4) Volunteer, Science RendezVous, London, Ontario, Canada, May 2019
5) Volunteer, **scientific judge**, Thames Valley Science & Engineering Fair, London, Ontario, Canada, March 2019